

**Tractor Operated Pneumatic No-Till Pulse Planter  
with Electronic Control System**

**by  
Amit Kumar  
(2020-28-005)**



**DEPARTMENT OF FARM MACHINERY AND POWER ENGINEERING  
KELAPPAJI COLLEGE OF AGRICULTURAL ENGINEERING AND  
FOOD TECHNOLOGY, TAVANUR - 679 573**

**KERALA, INDIA**

**2024**

**TRACTOR OPERATED PNEUMATIC NO-TILL PULSE PLANTER  
WITH ELECTRONIC CONTROL SYSTEM**

*by*

**Amit Kumar  
(2020-28-005)**

**THESIS**

**Submitted in partial fulfilment of the  
requirements for the degree of**

**DOCTOR OF PHILOSOPHY**

**IN**

**AGRICULTURAL ENGINEERING**

**(Farm Machinery and Power Engineering)**

**Faculty of Agricultural Engineering and Technology**

**Kerala Agricultural University**



**DEPARTMENT OF FARM MACHINERY AND POWER ENGINEERING**

**KELAPPAJI COLLEGE OF AGRICULTURAL ENGINEERING AND**

**FOOD TECHNOLOGY, TAVANUR - 679 573**

**KERALA, INDIA**

**2024**

## DEDICATION

*This thesis is dedicated to my beloved **Family** who sacrificed much to bring me up to this level, and to my major advisor **Dr. Jayan P. R.** for his unwavering support and invaluable guidance.*

## **DECLARATION**

I, hereby declare that this thesis entitled **“TRACTOR OPERATED PNEUMATIC NO- TILL PULSE PLANTER WITH ELECTRONIC CONTROL SYSTEM”** is a bonafide record of research work done by me during the course of research and the thesis has not previously formed the basis for the award to me of any degree, diploma, associateship, fellowship or other similar title, of any other University or Society.

Tavanur,

Amit Kumar  
(2020-28-005)

## **CERTIFICATE**

Certified that this thesis entitled “**TRACTOR OPERATED PNEUMATIC NO-TILL PULSE PLANTER WITH ELECTRONIC CONTROL SYSTEM**” is a record of research work done independently by **Er. Amit Kumar (2020-28-005)** under my guidance and supervision and that it has not previously formed the basis for the award of any degree, diploma, fellowship or associateship to him.

Tavanur,

**Dr. Jayan P. R.**

(Major Advisor, Advisory Committee)

Dean of Faculty (Agrl. Engg.)

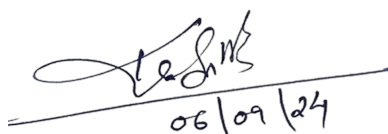
Prof. & Head (FMPE)

KCAEFT, Tavanur

## CERTIFICATE

We, the undersigned members of the advisory committee of **Er. Amit Kumar, (2020-28-005)**, a candidate for the degree of **Doctor of Philosophy** in Agricultural Engineering with major in Farm Machinery and Power Engineering, agree that the thesis entitled **“TRACTOR OPERATED PNEUMATIC NO- TILL PULSE PLANTER WITH ELECTRONIC CONTROL SYSTEM”** may be submitted by **Er. Amit Kumar**, in partial fulfilment of the requirement for the degree.

**Dr. Jayan P. R.**  
(Chairman, Advisory Committee)  
Dean of Faculty (Agrl. Engg.),  
Professor & Head (FMPE)  
KCAEFT, Tavanur

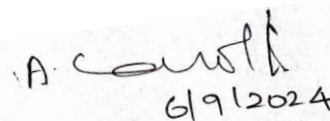


06/09/24

**Dr. Joby Bastian**  
(Member, Advisory Committee)  
Professor (FMPE)  
RRS, Moncompu

**Er. Sindhu Bhaskar**  
(Member, Advisory Committee)  
Asst. Professor, (FMPE)  
KCAEFT, Tavanur

**Ms. Roshini Vijayan**  
(Member, Advisory Committee)  
Asst. Professor,  
Division of Plant Breeding  
and Genetics, RARS Pattambi



6/9/2024

**Dr. Ahammed Muneer K.V.**  
(Member, Advisory Committee)  
Assoc. Professor,  
Dept. of Applied Electronics  
And Instrumentation Engg.,  
Govt. Engg. College, Kozhikode

**EXTERNAL EXAMINER**  
**Dr. A. Carolin Rathinakumari**  
Principal Scientist (Farm Machinery &  
Power)  
Division of Post Harvest Technology  
and Agrl. Engg.  
ICAR- Indian Institute of Horticulture  
Research,  
Hessaraghatta Lake (PO), Bengaluru-89

## **ACKNOWLEDGEMENT**

*It is with great pride and gratitude that I take this opportunity to express my sincere appreciation to my major advisor, **Dr. Jayan P. R.**, Dean of Faculty (Agrl. Engg.), Professor & Head (FMPE), KCAEFT, Tavanur. His insightful guidance, constructive suggestions, and unwavering encouragement have inspired and guided me throughout my research journey.*

*My sincerely thank my advisory committee members: **Dr. Joby Bastian**, Professor (FMPE), RARS, Kumarakom; **Er. Sindhu Bhaskar**, Asst. Professor (FMPE), KCAEFT, Tavanur; **Ms. Roshini Vijayan**, Asst. Professor, Division of Plant Breeding and Genetics, RARS Pattambi, and **Dr. Ahammed Muneer K.V.**, Assoc. Professor, Dept. of Applied Electronics and Instrumentation Engg., Govt. Engg. College, Kozhikode, for their invaluable counsel and cooperation during my research program.*

*My deeply thankful to **Dr. Manoj Mathew**, Retired Professor (FMPE), RRS, Moncompu, for his valuable advice and insightful suggestions. Special thanks go to **Dr. Dhalin D.**, Professor (FMPE), and **Er. Sanchu Sukumaran**, Assistant Professor (FMPE), KCAEFT, Tavanur, for their invaluable support and guidance.*

*My sincere appreciation also goes to **Dr. Prince M. V.**, Professor and Head, (P&FE), KCAEFT, Tavanur, for the facilities provided, and to **Dr. Edwin Benjamin**, **Dr. Rajesh**, **Dr. Dipak S. Khatwakar**, **Er. Vipin**, and **Er. Shamin M K**, Assistant Professors (Contract basis), Department of FMPE, KCAEFT, Tavanur, for their immense help and support in successfully completing the research.*

*I extend my deepest gratitude to **Dr. Abdul Jabbar P.K.**, Professor and Head of the Instructional Farm, KCAEFT, Tavanur, for his unwavering support and invaluable assistance throughout my research. His guidance at every step and his immense support were crucial in the successful completion of this project.*

*I extend my special thanks to workshop technicians **Danesh**, **Prasoon**, **Likesh**, **Shobith**, **Sudhir**, **Surjith**, and **Rahul** for their sincere assistance during my study.*

*Words cannot sufficiently express my gratitude to my dear family, including my mother, **Prem Lata**; father, **Bijender Singh**; brothers, **Sumit** and **Vineet**; sister-in-law, **Seerat**; and my lovely niece **Arzoo**, for their whole-hearted support, generosity, and guidance throughout this journey.*

*I also wish to express my heartfelt thanks to my friends: **Dr. Venkata Reddy**, **Dr. J. Srinivas**, **Dr. N. L. Kalyan Chakravarthi**, **Dr. Chandrasekhar**, **Dr. Aishwarya L.**, **Er. Chethan B. J.**, **Er. K. Venkata Sai**, **Er. Athira Prasad**, **Er. T. Mahesh Babu**, **Er. Siddharam**, **Er. Yeshubabu**, **Er. Sharanbasava**, **Er. A. Ajay**, **Er. Alankar**, **Er. Abhishek Govind Navale**, **Er. Anand Mohan Yadav**, **Er. Mohit Sharma** and **Er. Varun**, for their sincere help and support during my studies.*

*I also extend my sincere thanks to the **staff members of the library, KCAEFT Tavanur**, for their invaluable help in accessing research literature and their ever-willing cooperation. My sincere gratitude to all the **faculty members of KCAEFT, Tavanur**, and to **Kelappaji College of Agricultural Engineering & Food Technology** for providing me with the opportunity to pursue my PhD studies under the auspices of **Kerala Agricultural University**.*

*Amit Kumar*



# CONTENTS

---

Chapter No.	Title	Page No.
	LIST OF TABLES	i-ii
	LIST OF FIGURES	iii-v
	LIST OF PLATES	vi-vii
	LIST OF APPENDICES	viii
	SYMBOLS AND ABBREVIATIONS	ix-xi
I	INTRODUCTION	1-6
II	REVIEW OF LITERATURE	7-46
III	MATERIALS AND METHODS	47-129
IV	RESULTS AND DISCUSSION	130-206
V	SUMMARY AND CONCLUSION	207-214
	REFERENCES	215-236
	APPENDICES	237-266
	ABSTRACT	267-268

---

## LIST OF TABLES

<b>Table No.</b>	<b>Title</b>	<b>Page No.</b>
3.1	PoP, recommendations of KAU for planting of black gram and horse gram	57
3.2	Technical specifications of the stepper motor	70
3.3	Technical specifications of the micro-step drive	71
3.4	Technical specifications of the rotary encoder	74
3.5	Technical specifications of the proximity sensor	75
3.6	Technical specifications of the vacuum pressure sensor	76
3.7	Technical specifications of the ESP32	78
3.8	Technical specifications of the battery	79
3.9	Technical specifications of the charger	80
3.10	Technical specifications of the Vacuum blower	85
3.11	Details of the experiments	86
3.12	Plan of experiment for field evaluation	124
4.1	Specification of the developed tractor operated pneumatic planter with electronic controlled system	139-140
4.2	Analysis of variance for seed spacing of black gram in the laboratory testing	142
4.3	Analysis of variance for miss index of black gram in the laboratory testing	145
4.4	Analysis of variance for multiple index of black gram in the laboratory testing	148
4.5	Analysis of variance for quality of feed index of black gram in the laboratory testing	150
4.6	Analysis of variance for precision of black gram in the laboratory testing	153
4.7	Multi response numerical optimization constraints	155
4.8	Analysis of variance for seed spacing of horse gram in the laboratory testing	157
4.9	Analysis of variance for miss index of horse gram in the laboratory testing	160

4.10	Analysis of variance for multiple index of horse gram in the laboratory testing	162
4.11	Analysis of variance for quality of feed index of horse gram in the laboratory testing	165
4.12	Analysis of variance for precision of horse gram in the laboratory testing	167
4.13	Analysis of variance for seed spacing of black gram in the field testing	174
4.14	Analysis of variance for miss index of black gram in the field testing	176
4.15	Analysis of variance for multiple index of black gram in the field testing	177
4.16	Analysis of variance for quality feed index of black gram in the field testing	179
4.17	Analysis of variance for precision index of black gram in the field testing	181
4.18	Analysis of variance for germination of black gram in the field testing	183
4.19	Multi response numerical optimization constraints	185
4.20	Analysis of variance for seed spacing of horse gram in the field testing	188
4.21	Analysis of variance for miss index of horse gram in the field testing	190
4.22	Analysis of variance for multiple index of horse gram in the field testing	192
4.23	Analysis of variance for quality feed index of horse gram in the field testing	194
4.24	Analysis of variance for precision index of horse gram in the field testing	196
4.25	Analysis of variance for germination of horse gram in the field testing	198
4.26	Soil parameters	203
4.27	Field performance of developed pneumatic planter with electronic system	204

---

## LIST OF FIGURES

<b>Fig. No.</b>	<b>Title</b>	<b>Page No.</b>
3.1	Forces acting on seeds during pick-up stage	61
3.2	Forces acting on seeds during transport stage	64
3.3	Power flow diagram of the electronic control circuit	81
3.4	Block diagram of the electronic unit	82
3.5	Inverted t-type furrow opener	92
3.6	Shoe type furrow opener	95
3.7	Cross sectional view of seed box	98
3.8	Seed plate	102
3.9	Steel ground wheel	119
4.1	Effect on seed spacing of black gram	143
4.2	Interaction effect on seed spacing of black gram	144
4.3	Effect on miss index of black gram	146
4.4	Interaction effect on miss index of black gram	147
4.5	Effect on multiple index of black gram	149
4.6	Interaction effect on multiple index of black gram	149
4.7	Effect on quality of feed index of black gram	151
4.8	Interaction effect on quality of feed index of black gram	152
4.9	Effect on precision of spacing of black gram	154
4.10	Interaction effect on precision of spacing of black gram	154
4.11	Desirability index for lab model of vacuum metering mechanism with electronic control system for black gram	55
4.12	Optimum value for sensor, hole size, vacuum pressure and forward speed on performance parameters for black gram	156

4.13	Effect on seed spacing of horse gram	157
4.14	Interaction effect on seed spacing of horse gram	159
4.15	Effect on miss index of horse gram	161
4.16	Interaction effect on miss index of horse gram	161
4.17	Effect on multiple index of horse gram	163
4.18	Interaction effect on multiple index of horse gram	164
4.19	Effect on quality feed index of horse gram	166
4.20	Interaction effect on quality feed index of horse gram	166
4.21	Effect on precision of spacing of horse gram	168
4.22	Interaction effect on precision of spacing of horse gram	169
4.23	Desirability index for lab model of vacuum metering mechanism with electronic control system for horse gram	170
4.24	Optimum value for sensor, hole size, vacuum pressure and forward speed on performance parameters for horse gram	171
4.25	Effect of furrow opener and location of encoder on seed spacing for black gram	175
4.26	Effect of furrow opener and location of encoder on miss index for black gram	176
4.27	Effect of furrow opener and location of encoder on multiple index for black gram	178
4.28	Effect of furrow opener and location of encoder on QFI for black gram	180
4.29	Effect of furrow opener and location of encoder on precision index for black gram	182
4.30	Effect of furrow opener and location of encoder on germination for black gram	184
4.31	Desirability index for field testing of pneumatic planter with electronic control system for black gram	186
4.32	Optimum level of independent parameter on performance parameters for black gram	186
4.33	Effect of furrow opener and location of encoder on seed spacing for horse gram	189
4.34	Effect of furrow opener and location of encoder on miss index for horse gram	191

4.35	Effect of furrow opener and location of encoder on multiple index for horse gram	193
4.36	Effect of furrow opener and location of encoder on QFI for horse gram	195
4.37	Effect of furrow opener and location of encoder on precision index for horse gram	197
4.38	Effect of furrow opener and location of encoder on germination for horse gram	199
4.39	Desirability index for field testing of pneumatic planter with electronic control system for horse gram	200
4.40	Optimum level of independent parameter on performance parameters for horse gram	200

---

## LIST OF PLATES

<b>Plate No.</b>	<b>Title</b>	<b>Page No.</b>
3.1	Measurement of black gram (VBN-6) and horse gram (KS-2) seeds	49
3.2	Measurement of linear dimension of seeds	49
3.3	Measurement of coefficient of friction	49
3.4	Vacuum seed metering mechanism	59
3.5	Bevel gear in metering mechanism	68
3.6	Stepper motor	69
3.7	Micro-step driver DM556	71
3.8	PCB control board	72
3.9	Rotary encoder (2500 PPR)	74
3.10	Proximity sensor	75
3.11	Vacuum pressure sensor	76
3.12	ESP32	77
3.13	Lithium iron phosphate battery	78
3.14	Charger	80
3.15	Side channel vacuum pressure blower	85
3.16	Experimental setup for testing of seed metering mechanism with electronic control system	88
3.17	Aspirator blower	110
3.18	Four-bar parallelogram mechanism	111
3.19	Seed hopper	112
3.20	a) Electronic system in box b) Stepper motor fixed with metering mechanism c) Rotary encoder fixed at ground wheel	113
3.21	Complete electronic system	114

3.22	Stub type runner and seed covering device	117
3.23	a) pneumatic drive wheel, b) Compression wheel	118
3.24	Measurement of cone index of soil using proving ring cone penetrometer	122
3.25	Developed tractor operated pneumatic no-till pulse planter with electronic control system	123
3.26	Working of pneumatic planter with electronic control system	123
3.27	Measurement of seed to seed and plant to plant spacing	125
3.28	Draft measurement	126
3.29	Measurement of plant population	128

---



## LIST OF APPENDICES

Appendix No.	Title	Page No.
I	Physical properties of black gram (VBN-6) and horse gram (KS-2) seeds	237
II	Engineering properties of black gram (VBN-6) and horse gram (KS-2) seeds	239
III	Field performance evaluation of the developed planter	240-241
IV	Economic evaluation of developed pneumatic planter with electronic control system	242-245
V	Programming for the electronic control system	246-266

## SYMBOLS AND ABBREVIATIONS

Symbols	:	Abbreviations
$\pm$	:	Plus or minus
$\times$	:	Multiplication
$^{\circ}$	:	Degree
$^{\circ}\text{C}$	:	Degree centigrade
AC	:	Alternate Current
Amp	:	Ampere
bhp	:	Brake horsepower
$\text{cc rev}^{-1}$	:	Cubic centimetre per revolution
$\text{cc min}^{-1}$	:	Cubic centimetre per minute
cm	:	Centimeter
$\text{cm}^2$	:	Square centimeter
$\text{cm}^3$	:	Cubic centimeter
d.b.	:	Dry basis
<i>et al.</i>	:	and others
Fig.	:	Figure
FMPE	:	Farm Machinery and Power Engineering
g	:	Gram
$\text{g cm}^{-3}$	:	Gram per cubic centimeter
GI	:	Galvanized Iron
h	:	Hour
ha	:	Hectare
$\text{h}^{-1}$	:	Per hour
$\text{ha}^{-1}$	:	Per hectare
$\text{h ha}^{-1}$	:	Hour per hectare
$\text{h yr}^{-1}$	:	Hour per year
hp	:	Horsepower
Hz	:	Hertz
i.e.	:	that is

KCAEFT	:	Kelappaji College of Agricultural Engineering and Food Technology
kg	:	Kilogram
kg-cm	:	Kilogram centimeter
kg-mm	:	Kilogram millimeter
kg-m	:	Kilogram meter
kgf	:	Kilogram force
kN	:	Kilonewton
kPa	:	kilo Pascal
kW	:	Kilowatt
MC	:	Moisture content
m	:	Meter
m <sup>2</sup>	:	Square meter
m <sup>3</sup>	:	Cubic meter
mm	:	Millimeter
m s <sup>-1</sup>	:	Meter per second
MS	:	Mild steel
N	:	Newton
N cm <sup>-1</sup>	:	Newton per centimeter
N-m	:	Newton meter
N m <sup>-2</sup>	:	Newton per square meter
P.T.O	:	Power takeoff
rpm	:	Revolutions per minute
Rs. h <sup>-1</sup>	:	Rupees per hour
Rs. ha <sup>-1</sup>	:	Rupees per hectare
Rs. yr <sup>-1</sup>	:	Rupees per year
sec	:	Seconds
Sl. No.	:	Serial number
v	:	Volt

viz.,	:	Namely
W	:	Watt
yr	:	Year
$\alpha$	:	Alpha
$\delta$	:	Delta
$\gamma$	:	Gamma
$\mu$	:	Mue
$\pi$	:	Pi
$\phi$	:	Phi
$\rho$	:	Rho
$\sigma$	:	Sigma
$\theta$	:	Theta

---

## CHAPTER 1

### INTRODUCTION

#### 1.1 BACKGROUND

The world's population, having reached 8 billion in 2022, is projected to grow to 9.7 billion by 2050 and potentially peak at 10.4 billion in the mid-2080s (AA and Stover, 2023). This exponential growth, from just 2.5 billion in 1950, presents significant challenges for agriculture (Hemathilake and Gunathilake, 2022). With the global land area at 13,003 million hectares, of which 4,889 million hectares (37.6 %) are classified as agricultural land (FAO, 2013; Lahai *et al.*, 2022), the intensifying demand for food production is evident. Global hunger has been increasing since 2014, reversing previous trends of decline. The proportion of undernourished people increased from 10.6 % in 2015 to 11 % in 2016, with an estimated 821 million people affected in 2017 (FAO, 2018). This issue is particularly acute in developing regions, where agricultural challenges are compounded by soil degradation and climate change. In India, the scenario is stark, with only 42.67 % of the total geographical area being net sown, and the intensive cultivation of 2-3 crops per year in fertile regions deteriorating soil health (Molotoks *et al.*, 2021).

In response to the challenges posed by global population growth and increasing food demand, integrating pulses into agriculture emerges as a sustainable solution. Pulses not only enhance soil fertility but also contribute to resilient and productive ecosystems, addressing the pressing issues of food security and sustainable land use. Pulses, through biological nitrogen fixation and integration into crop rotations, play a pivotal role in restoring soil health by elevating nitrogen content and organic carbon concentration. This reduces reliance on chemical fertilizers, improving soil structure, fostering biological activity, enhancing aeration, and mitigating erosion—integral factors for establishing a sustainable and productive agricultural ecosystem. This makes pulses a vital component in sustainable intensification of agroecosystems, ensuring the nutritional needs of the current and future global population are met (Yuvaraj *et al.*, 2020; Kumar *et al.*, 2023; Nath *et al.*, 2023).

Over the decade from 2010-11 to 2020-21, India witnessed fluctuations in pulse production, showing a notable increase in 2016-17. Kerala, contributing a small fraction, maintained higher productivity than the national average, reaching 1133 kg h<sup>-1</sup> in 2015-16 (Directorate of Pulses Development, 2022). These trends highlight the significance of pulses in India's agriculture, with Kerala's productivity indicating potential for expansion and contributing to overall production, emphasizing the crop vital role in ensuring food security and nutritional requirements.

## 1.2 PROBLEM STATEMENT

### 1.2.1 Challenges faced in traditional pulse planting methods

Traditional pulse planting methods are often labor-intensive and can lead to reduced productivity due to reliance on human and animal labor (Siddique *et al.*, 2012). As of the financial year 2013-14, the farm power availability in India stood at 1.84 kW per hectare (Nag *et al.*, 2020). This figure saw an increase to 2.761 kW per hectare by the financial year 2020-21 (Singh and Singh, 2021). There are further ambitions to elevate this figure to 4.0 kW per hectare by the end of 2030, reflecting a continuous effort to enhance the mechanization and efficiency in agricultural sector of India (Shinde *et al.*, 2023). Despite this, many regions in the country still depend heavily on manual labor for farm operations, which is inefficient and limits potential yield (Dagar *et al.*, 2020). Mechanization serves as a crucial input in contemporary agriculture, enhancing productivity while reducing human drudgery and the overall cost of cultivation (Verma, 2006). There is a pressing need for the development of farm machines that are tailored to the pulse-producing states (Khura *et al.*, 2018).

In the cultivation of pulses, a suite of farm implements is integral to the execution of both primary and secondary tillage activities. The preparation of the pulses field typically involves the use of cultivators and disc harrows to plough the land. The sowing process employs a variety of drills, including standard seed drills, fertilizer-cum-seed drills, and zero-till seed drills, each designed to optimize the planting phase of pulse cultivation (Pandey, 2004). Traditionally, pulse crops are manually harvested using sickles or, in some cases, by machines when pods are ripe but unopened (Kaur *et al.*, 2023). This labor-intensive process, requiring 80-100 man-hours per hectare,

involves pulling up plants and sun-drying them (Nithiyanandham *et al.*, 2018). Mechanization, particularly through combine harvesters adapted from wheat, holds transformative potential for pulse harvesting. These efficient machines, with a capacity of 0.9 to 1.1 hectares per hour (Khura *et al.*, 2018), are effective but are mostly limited to large, level fields with uniformly maturing varieties.

Despite these advancements a specialized machine or equipment dedicated to the efficient harvesting of pulses remains notably absent from the current array of agricultural tools (Singh, 2013). To bridge this gap and foster the development of such harvesting equipment, the introduction of a compatible and effective planter for pulse crops is a prerequisite (Osadare and Manuwa, 2019). This planter would need to precisely sow seeds at the correct depth and spacing, ensuring optimal growth conditions and facilitating the subsequent harvesting process. For enhancing harvesting operation, it is essential to have a uniform crop with synchronized maturity (Kumar *et al.*, 2020). This uniformity begins at sowing; hence, the planter role is crucial. A planter capable of sowing pulses with high-variety seeds at fixed plant-to-plant distances which is pivotal for achieving the desired uniformity (Sani *et al.*, 2021).

### **1.2.2 Mechanization for pulse planting**

The introduction of a tractor-operated pneumatic no-till planter marks a significant advancement in pulse farming by tackling the limitations of traditional sowing methods. This sophisticated machinery ensures accurate and uniform seed placement, which is vital for consistent crop growth (Shearer and Pitla, 2013). Its no-till feature preserves the soil's structural integrity and moisture content, which is essential for maintaining the soil health benefits provided by pulse crops (Nunes *et al.*, 2018). This approach also markedly reduces the labor hours required for planting, diminishing physical exertion and operational costs. Additionally, the planter meticulous seed distribution curtails waste, augmenting resource efficiency and profitability. The uniform emergence and growth of plants make for a well-managed, productive crop, while the minimized soil disturbance helps to prevent soil erosion, thereby preserving soil health and enhancing moisture retention and nutrient availability (Meena *et al.*, 2016). In terms of environmental impact, the reduced need for tillage translates to lower greenhouse gas emissions, aligning with more sustainable farming

practices (Yanni *et al.*, 2021). The planter capability to operate at increased speeds offers greater coverage in less time, optimizing overall farm efficiency. It also boasts adaptability to various seed types and soil conditions, providing operational flexibility. By promoting better soil structure and nutrient cycling, it increases the efficiency of fertilizers and water use, and ultimately, by optimizing seed placement and soil conditions, it contributes to improved crop yields, offering a long-term profitability edge for farmers (Yasir *et al.*, 2012).

### **1.2.3 The need for an electronic control system in planters**

Electronic control system integrated into planters represent a significant advancement in agricultural technology, addressing the inherent inefficiencies of mechanical planters. These sophisticated systems ensure uniform seed distribution, critical for achieving consistent crop emergence and optimal growth (Cherubin *et al.*, 2022). Notably, they offer precision in seed spacing and can save seeds up to 12.04 % compared to their mechanical counterparts (Rajaiah *et al.*, 2020; Pradhan *et al.*, 2021). The automation of complex tasks, including seed metering and depth control, substantially reduces the workload on operators, enabling a greater concentration on the broader spectrum of the planting operation. Moreover, these systems facilitate comprehensive data collection, providing valuable insights for planting parameter optimization and strategic decision-making. The adaptability of electronic systems to a variety of planting conditions and seed types enhances the versatility of planters, making them indispensable tools for a wide range of pulse cultivation environments. Integration with other cutting-edge agricultural technologies, such as GPS and yield monitors, pushes the boundaries of precision farming, further streamlining the cultivation process. Additionally, the gentle handling of seeds by these systems minimizes damage, promoting successful germination and contributing to overall yield improvement (Wang *et al.*, 2022). Incorporating an electronic system into a pneumatic planter brings several advantages, including a reduction in the overall weight of the equipment. This lighter design results in decreased vibration during operation as there would be less mass contributing to inertia and oscillations. These improvements not only enhance the efficiency and ease of use of the planter but also contribute to better seed placement and reduced wear on the machinery. By optimizing planting operations



and reducing manual intervention, electronic control systems also improve fuel efficiency and reduce the environmental impact of farming, marking a step forward in the pursuit of sustainable agriculture.

#### **1.2.4 Pulses for research study**

In this research, a detailed analysis focuses on two specific pulses: Black gram (*Vigna mungo*) and Horse gram (*Macrotyloma uniflorum*), both of which hold a significant place in the agricultural landscape of Kerala.

##### **Black Gram**

Black gram, locally known as Uzhunnu, is a staple pulse integral to Kerala's cuisine. It is utilized in a variety of dishes, including thoran, sambar, payasam, and appam, showcasing its versatility in the culinary realm (Singh *et al.*, 2014). Nutritionally, it is lauded for its high protein, fiber, and essential mineral content. In Ayurveda, it's recognized for its "heating" properties within the body. Black gram is extensively cultivated across Kerala, making it widely available and a familiar ingredient in daily diets.

##### **Horse Gram**

Horse gram, locally referred to as Kollu, although less common than Black gram, is gradually gaining popularity (Krishna, 2010). Its culinary use extends to dishes like kootu curry, thoran, and payasam, and its flour is often used in making puttu. Horse gram is celebrated for its high protein, fiber, iron, and calcium content. From an Ayurvedic perspective, it is known for its "cooling" effect on the body and is believed to offer various health benefits. While its cultivation is less widespread compared to Black gram, Horse gram can be found in local markets and health food stores. Its increasing popularity is attributed to its robust nutritional profile and health benefits. Additionally, its drought resistance and ability to thrive in poor soil conditions make Horse gram a sustainable crop choice in the diverse agro-climatic zones of Kerala.

Both pulses play a significant role in the Kerala region's agricultural practices. Studying them will unveil insights into the intricacies of pulse cultivation in Kerala,

delving into the potential for agricultural sustainability within the state, particularly regarding the ease of sowing operations using a planter.

### 1.3 OBJECTIVES OF THE STUDY

The growing global population and the subsequent rise in food demand pose significant challenges for agriculture, particularly in densely populated region like India. Pulses, notably black gram and horse gram, play a crucial role in addressing these challenges due to their high nutritional value and soil health benefits. In India, the fluctuating pulse production and productivity underscore the need for improved agricultural practices. Traditional pulse planting methods, reliant on manual labor and inefficient tools, lead to reduced yields and increased costs.

To address these issues holistically and improve pulse cultivation, a study was proposed to develop a “Tractor Operated Pneumatic No-Till Pulse Planter with Electronic Control System” with following objectives:

- i. To study the physical and engineering properties of selected pulse seeds
- ii. To design and develop a pneumatic seed metering mechanism for the selected seeds
- iii. To design and develop an electronic control system suitable for pneumatic seed metering mechanism
- iv. To evaluate the performance of a tractor operated pneumatic no-till pulse planter with electronic control system

The introduction of a tractor-operated pneumatic no-till planter, integrated with an electronic control system, offers a promising solution. This advanced planter enhances seed distribution uniformity, reduces labor requirements, and minimizes soil disturbance, thereby preserving soil health and increasing crop yield potential. It also aligns with sustainable farming by reducing greenhouse gas emissions and optimizing resource utilization.

## CHAPTER 2

### REVIEW OF LITERATURE

This chapter illustrates the pulse cultivation and the challenges in planting, and to identify the gap in specialized planting technology. Accordingly, the exploration of pneumatic planters and the role in developing planting technologies are briefly explained. Further, it delves into integration of electronic systems, enhancing precision in these planters. The chapter is structured into various sections viz., seed properties, planter technology, pneumatic planter, electronic systems, and no-till planting, each dissecting critical aspects of planter design and agricultural innovation. This synthesis not only addresses past research but also paves the way for future advancements, creating a narrative that intertwines technological evolution with practical agricultural needs.

#### 2.1 ENGINEERING PROPERTIES OF SEEDS

The physical and mechanical properties of seeds relevant to planting technology aspects such as size, shape, density, moisture content, coefficient of friction and aerodynamic properties, which are also critical in the design of planting machinery are briefed below. The physical, gravimetric and aerodynamic properties of seeds like black gram and horse gram which are pertinent to the development of effective planting mechanisms are also explained.

Jayan and Kumar (2006) explored the impact of physical properties of seed towards the design of a planter for maize, red gram, and cotton seeds. They determined that the design of seed metering discs should account for the maximum breadth and length of seed, was focused on parameters of seeds like length, breadth, surface area, roundness, equivalent diameter, sphericity, weight, true density, angle of repose, and coefficient of restitution. They found out the roundness as of  $1.14 \pm 0.14$  for maize,  $1.15 \pm 0.10$  for red gram, and  $1.26 \pm 0.10$  for cotton, and sphericity at natural rest positions are  $0.621 \pm 0.065$ ,  $0.750 \pm 0.016$ , and  $0.550 \pm 0.016$ , respectively. The study revealed that the setting of the hopper slope at  $30^\circ$ , slightly higher than the angle of repose of the seed and lining the inner surfaces of the seed transfer cups with a 3 mm thick rubber sheet.

Lower coefficient of restitution was observed in rubber sheet as compared mild steel. This was significantly improved the seed flow and reduced the damage of the seed.

Liny *et al.* (2013) conducted an experimental study to ascertain the physical properties of black gram. The study, conducted at a moisture content of 11.11 %, assessed various characteristics of black gram seeds. They found out that the average dimensions were 3.53 mm in length, 2.22 mm in width, and 2.29 mm in thickness. The thousand grain weight was noted as 40.6 gram. Also observed that, the sphericity, aspect ratio, surface area, and volume were respectively as 74.35 %, 65.5 %, 21.59 mm<sup>2</sup> and 9.56 mm<sup>3</sup>. Additionally, they measured densities and porosity, with true density at 1335.08 kg m<sup>-3</sup>, bulk density 805.091 kg m<sup>-3</sup>, and porosity 39.7 per cent. These findings were necessary for the optimal design of various systems handling black gram.

Sonawane *et al.* (2014) explored the impact of moisture content on the physical properties of horse gram (*Macrotyloma uniflorum*). The experiment was conducted at the moisture content of 8.66 to 20.76 % (d.b.). They observed that a significant increment in grain dimensions with rising moisture levels viz., length by 9.01 %, width by 16.90 %, and thickness by 6.84 per cent. Concurrently, the thousand grain mass increased from 29.8 g to 34.10 g. However, the bulk density and true density were decreased with increased moisture content from 855 kg m<sup>-3</sup> to 689 kg m<sup>-3</sup> and 1237 kg m<sup>-3</sup> to 1102 kg m<sup>-3</sup>, respectively, while porosity linearly increased from 30.80 to 37.48 %. The study inferred that the terminal velocity and angle of repose of the grains raised from 8.45 m s<sup>-1</sup> to 10.52 m s<sup>-1</sup> and from 8.66° to 20.76°, respectively. Moreover, the static coefficient of friction against various materials varied significantly ranged from 0.190 to 0.532 at different moisture levels.

Theertha *et al.* (2014) studied the impact of varying moisture content levels ranging from 10.23 to 19.73 % (dry basis) on the physical and gravimetric properties of black gram (*Vigna mungo L.*). The bulk density decreased from 692.30 to 661.50 kg m<sup>-3</sup> with increased moisture, whereas the true density increased from 1012.34 to 1315.03 kg m<sup>-3</sup>, and porosity increased from 31.58 to 49.67 %. Additionally, the static coefficient of friction against surfaces like plywood and glass increased as moisture content increased, affecting handling and processing characteristics.

Bakhtiari (2015) conducted a comprehensive study on the physical and aerodynamic properties of garlic cloves, for the development of a pneumatic garlic clove metering system. The data was analyzed using a completely randomized design (CRD) with five replications by SAS program version 9.1 and Duncan multiple range test (DMRT) for mean comparison. The base measurement of the garlic cloves included length (32.0 mm), width (21.8 mm), thickness (20.9 mm), geometric mean diameter (24.4 mm), and arithmetic mean diameter (24.9 mm). As the moisture content increased from 35.8 to 60.5 % wet basis (w.b.), the corresponding surface area, (from 1718.3 to 2029.1 mm<sup>2</sup>), projected area, (from 546.6 to 644.3 mm<sup>2</sup>), one thousand kernel mass, (from 6783.0 to 8159.3 g), volume, (from 5916.5 to 7356.0 mm<sup>3</sup>), and bulk density, (from 476.3 to 567.4 kg/m<sup>3</sup>) increased respectively. Also observed that the terminal velocity was linearly increased from 15.6 to 16.7 ms<sup>-1</sup> of garlic cloves with increased of moisture content.

Sharon *et al.* (2015) conducted a study to evaluate the moisture-dependent physical properties of black gram. As the moisture content of the black gram increased from 8.69 to 21.95 % (dry basis), certain change were observed in its physical properties. The arithmetic and geometric mean diameters ranging from 3.73 ± 0.14 to 4.27 ± 0.14 mm and 3.79 ± 0.13 to 4.32 ± 0.13 mm, respectively. The thousand grain mass values were increased form 42.52 ± 1.03 g to 48.18 ± 0.45 g and sphericity increased from 79.69 to 82.82 % with increase in moisture content. Both the bulk and true density values decreased as moisture content increased for black gram. The porosity increased from 38.06 to 42.60 %, and the angle of repose increased from 28.4° to 32.2° as the moisture content increased from 8.69 % to 21.95 % d.b.

Qinghui *et al.* (2016) designed a vibrating feeding pneumatic disc seed-metering device by incorporating a metering plate, an air chamber, a frame, and a vibrating seed feeding mechanism. The performance of the machine was optimized using FLUENT software. An orthogonal test, considered experimental indices like the feed index, multiple index, missing index, and operating speed. Optimal result was obtained at 2.4 km h<sup>-1</sup> operating speed, 6.5 Hz vibration frequency, and 6 kPa negative pressure. Satisfactory performance indices were observed as feed index of 94.2, missing index of 1.7, and multiple index of 4.1 - aligning with China's technical specifications for quality evaluation, thus enhancing the efficiency of mini-tuber planting.

Manoharan (2018) conducted a comprehensive study on the physical and mechanical properties of black gram (variety *VBN-3*) and green gram (variety *CO-6*), focused on the application in designing an inclined seed metering mechanism for planters. The study aimed to optimize the structural parameters of the seed based on size and uniformity. Using a digital Vernier caliper, the major and minor axes of the seeds were found as 3.97 mm and 4.25 mm for black gram, and 3.60 mm and 3.92 mm for green gram. The mean angle of repose/coefficient of friction over surfaces like plywood, galvanized steel, mild steel, and rubber were also recorded. For black gram, these values were 28.64°/0.605, 35.55°/0.746, 24.26°/0.592, and 39.57°/0.706, respectively. The corresponding values for green gram were 26.3°/0.676, 32.6°/0.823, 26.8°/0.486, and 38.5°/0.865 respectively.

Harshvardhan *et al.* (2020) conducted a study on the physical and frictional properties of three varieties of black gram seeds (*VBN 6*, *ADT 5*, and *T9*) to design a seeder. The cell diameters and thickness of metering discs were decided on seed dimension. Both roundness and sphericity affected the seed flow through various components of the seeder. *VBN 6*, *ADT 5*, and *T9* varieties has roundness value of 0.52, 0.49, and 0.51 respectively and the sphericity was found out as  $0.85 \pm 0.05$ ,  $0.85 \pm 0.06$ , and  $0.85 \pm 0.04$ , respectively. The slope of the seed hopper was fixed at 30°, slightly higher than the average angle of repose, to ensure a free flow of seeds. Mild steel sheet (material grade Fe 410 and 18-gauge, 1.214 mm thickness) was chosen for the seed due to its coefficient of friction. A 3 mm thick rubber sheet was embedded on the inner hopper bottom to reduce the bouncing of the seed. This was due to its lower coefficient of restitution compared to a mild steel sheet of the same thickness at various heights.

Vashishth *et al.* (2020) studied the engineering properties of horse gram (*Macrotyloma uniflorum*) of three varieties viz., *GPM-6*, *PAYIUR-2*, and *BHK*. The moisture contents varied from 10 to 30 per cent. The study revealed that as the moisture content increased from 10.08 to 29.98 %, the average length, width, and thickness of the grains also increased from 5.43 to 6.53 mm, 3.96 to 4.48 mm, and 2.21 to 2.99 mm, respectively. Also observed that the porosity increased from 35.20 to 38.76 %, and the angle of repose from 22.72 to 29.86 degree. The volume, porosity and terminal velocity of the grains

increased linearly with moisture content. It was noted that positive correlation in the coefficient of friction against various surfaces for plywood.

Findura *et al.* (2023) conducted a laboratory study on the physical properties of sugar beet seeds and its impact on seeding mechanisms, following ISO 7256/1 standard. In the field study loamy-sandy soil, two sugar beet cultivars viz., Roxana and flair, were selected. The study compared the planting quality of two different sugar beet planters: one with an internal mechanism for gathering opening and another based on the vacuum principle. The result showed that the vacuum- based planter resulted a higher seed damage at higher working speeds with a damage rate of 5.4 per cent. Conversely, the mechanical system planter showed the most seed damage at forward working speeds of 1.0-1.5 ms<sup>-1</sup>.

## 2.2 PLANTER TECHNOLOGY: A FOUNDATION FOR GROWTH

This section of literature review delves into the technological advancements and research studies conducted to increase the efficiency and effectiveness of planting machinery, with a specific focus on precision planters. This segment of review shows how different planter designs and components have evolved to meet the varying needs of modern agriculture, from improving seed spacing accuracy to mitigate the environmental impacts.

Johnson *et al.* (1991) developed a planter test stand. They mounted four different row crop planter units on mobile stands with hydraulic motors to test a simulated field condition. Planter test stand with a variable speed conveyor belt allowed real-time observation of planter performance. Seed distributions were observed on the conveyor belt. Actual seed count and spacing were shown on a planter monitor console. This approach provided practical insights into the impact of various designs of planter and components on planting accuracy and efficiency.

Karayel and Özmerzi (2008) conducted a study to evaluate the effectiveness of three depth control components in precision planting of maize and watermelon seeds under various field conditions. They determined that the vertical and horizontal distribution of seeds inside the soil and the subsequent seedling emergence. They used runner and double-disc furrow opener with depth-control component. The findings showed that the

mean seed spacing for both maize and watermelon were unaffected by the depth-control component. The side gauge wheel emerged as the most effective, showed the least variation in seeding depth and distribution areas, which lead to a uniform vertical distribution of seeds and a higher emergence per centage. Conversely, the rear press wheel was deemed least effective, often sinking into loosened soil and causing more variable seeding depths.

Liu *et al.* (2018) developed an electric motor driven seed precise delivery mechanism with an electronic control system and tested its performance in a laboratory. They analyzed seed movement from the seed meter release point to the delivery cavity in the belt, by developing a mathematical model for precise seed delivery time analysis. A comparative experiment was conducted between the traditional seed tube delivery system and the new seed precise delivery mechanism. Results showed that the new mechanism had superior feed index qualities and lower coefficients of variation, especially notable at forward speeds of 10, 12, and 14 km h<sup>-1</sup>.

Foqué *et al.* (2018) investigated the environmental risks associated with sowing pesticide-treated seeds, especially concerning the expulsion of abraded pesticide laden seed particles by vacuum-based precision drills. This study was propelled by the connection between neonicotinoid laden dust particles and bee mortality. CREA-IT and ILVO are developed mitigation devices that minimized the adverse effects during sowing. The research compared these new technologies against a conventional vacuum-based precision drill and also evaluated it by using CREA-IT indoor dust drift setup. The findings indicated that both mitigation technologies significantly reduced dust drift, achieving reductions ranging from 44 to 90 %, compared to the conventional method using air deflectors.

Osadare and Manuwa (2019) developed a pulse planter specifically for conservation agriculture. The pulse planter structure includes a main frame, adjustable handle, seed hopper, seed metering device, adjustable furrow opener, furrow coverer, drive wheels, seed tube, and a disc coulter. All components, except for the rubber-made seed tube, were fabricated as of mild steel. A unique aspect of this planter is the inclusion of a coulter disc, designed to cut through residue and trash on the soil surface, for clear



sowing paths. The planter operated with a drive shaft that controlled the seed plate shaft through a bevel gear, facilitated efficient and precise seeding.

Soyoye (2020) tackled the prevalent issue of inconsistent seed spacing in precision planters, often caused by slippage in the driving wheel. He proposed an innovative solution by replacing the traditional metering wheel with a direct current (DC) motor, controlled by transistor-generated pulses, to drive the metering shaft. This novel approach offered enhanced control over seed distribution, effectively addressed the limitations posed by mechanical linkages in standard planters. Study demonstrated a clear relationship between the planter forward speed and the rotational speed of the metering shaft. Through the experiments, he established an optimal rotational speed of 45 rpm for the meter shaft at a forward speed of  $1.3 \text{ m s}^{-1}$ .

Kumar *et al.* (2020) improved the existing planter design for high-density cotton planting. They evaluated the performance of five different planters, along with manual sowing, in high-density planting scenarios, concentrated on intra-row spacing over 8-meter strips for each method. Another research identified two planters – the CIAE tractor-operated pneumatic planter and the CIAE inclined plate planter – as the most effective for high-density cotton planting. Notably, the inclined plate planter achieved an optimal planting depth of 45 mm, which was near the recommended depth of 50 mm. In terms of feed index, both the tractor drawn inclined plate planter and the pneumatic planter scored the highest at 0.75, compared to the lowest score of 0.21 with the tractor drawn seed-drill.

### 2.3 PNEUMATIC PLANTER MECHANISMS

Pneumatic planters represent a significant advancement in precision agriculture, offered enhanced seed placement accuracy and efficiency. These planters utilize air suction or pressure to handle seeds, allowed for precise metering and distribution, critical for achieving optimal planting outcomes. The following review of literature encapsulates various studies that were explored different aspects of pneumatic planter technology, ranged from design innovations to operational optimizations. These studies collectively contributed to understand the pneumatic planters that could be tailored to

meet the specific needs of different crops, soil conditions, and agricultural practices, ultimately lead to the improvements in crop yield and resource utilization.

Molin *et al.* (1998) developed and evaluated a punch planter in no-till condition with specific focus on corn crop. Punch planter prototype was integrated with commercial seed metering unit. The seed meter performance was meticulously analyzed for seed spacing, initially at a vertical orientation at 2.5 kPa vacuum and subsequently at an inclination of 22° with higher vacuum of 4.0 kPa. Results showed minimum variations in seed meter performance ranged from 1.0 to 3 m s<sup>-1</sup> velocity of rotation.

Kamel *et al.* (2003) studied the impact of operating factors on the uniformity of seed distribution in a pneumatic and mechanical seed drills for sowing wheat. The research focused on evaluating the drills performance at five different forward speeds at three levels of land preparation. Result showed that both longitudinal and lateral scattering of seeds increased with the forward speed of the drills. This pattern was consistent for both pneumatic and mechanical seed drills. Longitudinal scattering ranged from 1.54 to 5.69 cm, and lateral scattering ranged from 0.18 to 2.85 cm, when the forward speed varied from 0.56 m s<sup>-1</sup> to 2.34 m s<sup>-1</sup> at different land preparation conditions.

Barut and Özmerzi (2004) studied the dynamics of seed holding in pneumatic planters for maize (*Zea mays L.*) seeding, specifically focusing on a single seed metering unit. They developed an electronic counter to detect seedless plate holes in a vacuum-assisted vertical seed plate. The research meticulously examined various operational parameters including the shape of hole, peripheral velocities, vacuum pressure and the area of holes of the seed plate. The study showed that the shape of hole, peripheral velocity, vacuum pressure and hole area significantly influenced the seed holding ratio (SHR) at a significant level ( $P < 0.01$ ). Specifically, oblong-shaped holes emerged as the most effective for maize seeds. Notably, the SHR was inversely proportional to the peripheral velocity of the seed plate, whereas an increased vacuum pressure increased the SHR.

Karayel *et al.* (2004) optimized the vacuum pressure for a precision vacuum seeder. The study aimed to establish the relationship between various physical properties of seeds and the optimum vacuum pressure needed for effective seeding. The properties analyzed were one thousand kernel mass, projected area, sphericity, and kernel density

respectively. They determined the optimal vacuum pressures for each seed type. Results showed that maize required a vacuum pressure of 4.0 kPa, while cotton, soybean, and watermelon needed 3.0 kPa. Cucumber were the best seeded at 2.5 kPa, sugarbeet at 2.0 kPa, and onion seeds required the least pressure at 1.5 kPa. Moreover, they developed mathematical models to predict the vacuum pressure for the precision vacuum seeder. These models proved highly effective, demonstrated by a chi-square test of  $2.51 \times 10^{-3}$ , a root mean square error of  $2.74 \times 10^{-2}$ , and a modelling efficiency of 0.99.

Rahmati *et al.* (2005) designed and developed a tomato pneumatic planter for direct seeding. The developed pneumatic planter sealed the air system to prevent air loss and hence reduced the pressure drop inside the metering mechanism. The results indicated a high seed emergence (92.5 %), with high accuracy in seed placement and spacing (over 91 %). In comparison with the mechanical planter, which sowed seeds continuously like a seed drill, had a seed emergence rate of 94.6 per cent. Notably, the improved pneumatic planter reduced seed breakage to 1 %, compared to 8 % in the mechanical planter and significantly decreased the seed rate per hectare, which are 835 g ha<sup>-1</sup> for the pneumatic and 4500 g ha<sup>-1</sup> for the mechanical planter.

Maheshwari and Varma (2007) conducted a comprehensive study using a 6-row tractor drawn pneumatic precision planter for pea seeding. The study was conducted in sandy loam soil with a 16.3 % moisture content and 1.52 g cm<sup>-3</sup> bulk density. The results revealed that pneumatic planter had an seed rate of 60 kg ha<sup>-1</sup> as compared to 100 kg ha<sup>-1</sup> when operated with the conventional seed drill. A higher uniformity coefficient of 90.85 % was recorded against 82.28 % for the seed drill. Furthermore, the planter resulted a higher average plant population of 20.48 plants m<sup>-2</sup>, about 11 % higher than the seed drill, and required fewer man-hours per hectare, i.e. 6.1 man-h ha<sup>-1</sup> as compared to 9.0 man-h ha<sup>-1</sup> for the seed drill, indicated a higher labor efficiency.

Ismail (2008) conducted a study to enhance the performance of pneumatic planters for wheat and sorghum seeds. The study aimed to evaluate and improve various aspects such as spacing uniformity, seed volumetric rate, irregular depth of seeds in soil and seed speeds from the injection device nozzle to the soil. The study identified several factors viz., which influenced seed singulation and placement, including the injection mechanism speed, air pressure level, the shape and size of the orifice head, and the bulk

density. Also observed that the amount of volumetric flow rate (seed per second) was directly proportional to the injection pressure and the seeds density.

Zaki *et al.* (2008) developed a pneumatic knockout device for rapeseed. The knock out device was tested on a Behkesht (Agrifarm) planter, at various level of seed plate rotational velocity viz., 40, 68, 99 rpm and the air velocity of the knockout device viz., 0, 7-8, and 15-16 m s<sup>-1</sup> respectively. The effects on cell filling and seed damage were measured. The results showed that higher rotational speeds led to decreased cell filling per centages, while increased air velocity effectively reduced mechanical seed damage, such as splitting and scratching.

Bayhan *et al.* (2009) studied the sowing rate and seed distribution efficiency of furrow openers of the pneumatic seed drills, for cereals. The research entailed a critical comparison between the sowing rates listed in the machine's catalogue and the actual results obtained from tests, aimed to assess the accuracy and reliability of the pneumatic precision drills. It was observed that the coefficient of variation in seed distribution from the furrow openers was less than 4 %, shown a high level of precision and uniformity in seed distribution.

Dizaji *et al.* (2010) conducted a study on the optimization of plate-type vacuum seed metering pneumatic precision planters for small seeds. To enhance seed ejection, they developed an air-jet seed knockout device and integrated it with the seed metering device of a vacuum precision planter. The impact of the rotational velocity of the seed plate and the air velocity of the air-jet seed knockout device with respect to the three levels of 40, 68, and 99 rpm for rotational velocity, and 0, 7-8, and 15-16 m s<sup>-1</sup> for air velocity. The findings were significant, showed a decreased in mechanical seed damage with an increased air velocity of the knockout device.

Liu *et al.* (2010) conducted an analysis of the pneumatic seed metering device. The research combined the theoretical modeling with practical experiments to investigate the device performance, for sowing of soyabean. The planter was tested at different rotational speed of seed metering disc and the vacuum pressures in the suction chamber. The results showed that for different rotation speeds the critical threshold beyond which the metering device performed noticeably declined, evidenced by a miss seeding rate

increased to high as 29.63 per cent. At a vacuum of 2.5 kPa w.r.t. an increased rotation speed of the disc adversely affected the standard seeding rate. Rotation speed of the disc of 54 rpm combined with a vacuum pressure at 1.5 kPa showed less miss index and the standard seeding rate as 76.11 % and 80.65 % whereas at a 1.5 kPa vacuum pressure, the device performance was poor.

Losavio (2010) investigated precision seeders aim to increase the operational precision and the overall stability of the machine, for optimizing the seed distribution system. They developed a simple mechanism to change the seeding discs by lifting of a protective shield. They developed the metering mechanism to obtain synchronized movement between the suction chamber and the seed disc. This design enhancement not only reduced the friction between the components but also minimized the air consumption, thereby increasing the planter efficiency.

Zhan *et al.* (2010) conducted experiments to enhance the performance of a vacuum-cylinder seeder for precise sowing of rape seeds. The study employed the CFD software Fluent to calculate the forces acting on seeds during its free flight from the seeder. They utilized a high-speed camera system attached to the laboratory seeder test-rig, captured the motion of the seeds in real time. The result showed that the relative errors for both horizontal displacement and fall time of the seeds were within acceptable limits viz., less than 5.5 and 6.5 %, respectively which confirmed the accuracy of the CFD model. The study showed that both the positive differential pressure ( $\Delta p$ ) applied to the seed and the release angle ( $q$ ) significantly influenced the uniformity of seed distribution. It was concluded that the optimal levels for  $\Delta p$  for precise seeding of rape seeds were in the range of 1-2 kPa, while the optimal release angle ranged from -10 to 0 degrees. Further testing on the vacuum cylinder precision seeder rig demonstrated that the minimum average seed spacing interval error occurred at  $\Delta p = 1.5$  kPa and  $q = -5$  degree. Additionally, the study found out that the error in seed spacing increased linearly with the increased rotational speed of the cylinder.

Dixit *et al.* (2011) conducted comparative studies of a tractor-operated inclined plate planter and a pneumatic planter, for seeding cotton. The results showed that both planters performed satisfactorily for cotton planting. The pneumatic planter achieved a plant-to-plant spacing of 44 cm, closely aligned with the recommended spacing of 45

cm. It had an average of 0.33 missing hills per 10 meters and a 4.35 % incidence of doubles. In contrast, the inclined plate planter recorded a plant-to-plant spacing of 36 cm, an average of 1.33 missing hills per 10 meters, and a 9.64 % rate of doubles. Notably, the number of hills with two or more plants were negligible with the pneumatic planter. Also observed that, the pneumatic planter had a higher capacity of 0.49 hectares per hour compared to 0.35 hectares per hour for the inclined plate planter.

Topakci *et al.* (2011) assessed a modified vacuum seeder for hill drop sowing of sesame in no-till and reduced tillage conditions over two seasons at the Bati Akdeniz Agricultural Research Institute, Turkey. The seeder, equipped with a fluted coulter, double-disc furrow opener, and a modified seed plate, was evaluated on various performance metrics like plants per hill, hill spacing, scattering-distance ratio, sowing depth uniformity, and seed emergence. It was found out that the lower uniformity in hill spacing in no-till conditions adversely affected seed and hill emergence for all sesame varieties.

Rajan and Sirohi (2012) developed a low-cost precision vegetable planter and determined the optimum operational parameters for pneumatic seed metering. The operational parameters such as vacuum pressure, hole size, speed of the seed plate, and forward speed were analyzed under field conditions. Its efficiency was compared with the current practice of manual seeding. The test revealed that pneumatic seed metering unit achieved a singularity index of more than 90 % with less than 3 % misses.

Yasir *et al.* (2012) developed and evaluated a pneumatic precision metering device for wheat seeding. The performance indicators analyzed were the quality of feed index (QFI), multiple index (MULI), miss index (MISI), and seed rate. The study found out that both the rotating speed and negative pressure, as well as their interactions, significantly affected the performance indices. The maximum QFI of 92.98 % was achieved at a rotating speed of 19.0 rpm and a negative pressure of 2.5 kPa, with corresponding MULI and MISI values of 2.01 % and 5.09 %, respectively. The optimal seed rate obtained was 53 kernels per meter length, yielded a QFI of 89.11 %, with MULI and MISI values of 9.00 % and 1.88 % respectively, at the rotating speed of 34 rpm and the negative pressure of 4.5 kPa.

Wei *et al.* (2013) studied the vacuum and airflow influence on the planter performance. The effect of vacuum pressures ranged from 3 to 6 kPa on the planting performance was analysed and found out that the seed metering performance was optimal when the vacuum set between 5 and 6 kPa. Corresponding to these optimal vacuum pressures the required air flow rates were found out between 7.4–8.0 and 8.0–8.8 m<sup>3</sup> s<sup>-1</sup>, respectively.

Jiajia Yang *et al.* (2014) investigated the performance of a pneumatic precision metering device for rapeseed by examining the interplay between positive and negative pressures. They developed fluid models of the chamber to simulate airflow within the device, which employed the k- $\epsilon$  turbulence model to capture pressure and velocity at the nozzles. A three-factor factorial split-split experiment was used for the analysis different negative pressure varied from -1,000 to -4,500 Pa, positive pressure from 50 to 250 Pa, and rotating speeds from 10 to 45 rpm were selected for the studying. The results showed that the most influential factor on these indices was the positive pressure, followed by negative pressure and rotating speed. Also, a concept of a ratio coefficient K was introduced to achieve optimal performance. This coefficient represented the ratio of negative to positive pressures. Mathematical models were fitted to relate this coefficient with positive pressure at different rotating speeds. The rotating speeds between 10 and 30 rpm, the ideal ratio coefficient K was found out within the specific range defined by the fitting equations.

Khambalkar *et al.* (2014) conducted a study to assess the performance of a self-propelled pneumatic planter, for various rainfed crops such as sunflower, sesame, soybean, and cotton. The field efficiency and cost-effectiveness in comparison to traditional planting methods were evaluated. The results showed that the field efficiency varied between 75.86 to 59.5 % for the selected crops. The saving in cost of operation was from 50 to 67 % when compared to traditional manual planting methods. Also, a notable cost of saving in seed cost per hectare was observed, up to Rs. 1350 for cotton and Rs. 1000 for sunflower.

Song *et al.* (2014) designed a novel pneumatic maize precision seed-metering device for enhancing the efficiency, particularly for non-oval seeds like maize. In the field test, a 2BYJMFQC-4 type maize no-tillage precision seeder was used at a constant pressure of 3.0 kPa at various forward speeds, with each test replicated three times. The results

showed a lower miss index of 1.74 % compared to the traditional device having 3.42 per cent.

Wang *et al.* (2014) conducted a study on a pneumatic precision metering device and analyzed the physical and mechanical properties of grains. They also assessed the impact of the nature of holes, pressure, and rotating speed on the sucking effect and the performance of the metering unit. Results showed that both straight and taper holes with  $\phi 1.2$  mm and at taper of  $30^\circ$  subsequently effectively sucked the seed and showed the best results. Optimal performance was achieved at 0.2 kPa and at a negative pressure 1.8 kPa at the rotating speed of 20 rpm. Also maintained a stability variability coefficient of sucking below 5.47 per cent.

Kumar *et al.* (2015) evaluated the performance of a tractor-mounted pneumatic planter, specifically designed for sowing sorghum seeds in dryland conditions. In the laboratory, the planter capability to pick single seeds was tested using a multi-groove metering plate with seed holes of  $\phi 3$  mm and at a vacuum pressure of 2 kPa. The results showed that the average values for plant-to-plant spacing, miss index, and multiple index were 101 mm, 2.07 %, and 3.8 %, respectively. Also, the actual field capacity of the planter was observed  $0.77 \text{ ha h}^{-1}$ , and the field efficiency was found out as 79.7 per cent.

Gao *et al.* (2016) developed a precision seeding control system for maize planters, integrated the GPS technology to enable real-time adjustment speed of seeding which ensured uniform distribution of seeds. The system allowed the users to vary the parameters such as seeding rate, row spacing, and the number of holes in the seed metering device. These inputs were transmitted via a CAN bus to the controller, which calculated the appropriate rotational speed of the sowing axis to match the tractor operating speed. The results showed that at an operating speed of  $5.9 \text{ km h}^{-1}$ , the precision seeding control system achieved a normal spacing rate for the seeds sown and a variable coefficient of 94.1 and 24.6 %, respectively whereas for traditional planter it is 89.1 and 33.1 per cent.

Lijing *et al.* (2016) conducted a case study on the relationship between working parameters and the performance of a pneumatic seeding system, using Cangmai 6004 wheat seeder. The experiments focused on two main factors viz., seeding rate and air



flow rate. The result established regression models on influencing factors w.r.t. the performance indices. From these models, an optimal specific equation to the pneumatic seeding system was derived. It was inferred that a seeding rate of  $250 \text{ kg m}^{-2}$ , the optimal air flow rate obtained was  $7.53 \text{ m}^3 \text{ min}^{-1}$ .

Gupta et al. (2017) introduced an innovative approach to reduce the cost of pneumatic planters, by incorporating a suction unit in the intake pipe of the seed metering device. They developed a bypass system attached to the air intake pipe, utilized the generated pressure for pneumatic functions for the planter. The findings revealed various observations such as increased vacuum pressure, fuel consumption, engine sound, and  $\text{CO}_2$  levels with rising engine rpm, while  $\text{NO}_x$  concentration decreased. The study also observed inconsistent pattern in fuel consumption, sound pressure,  $\text{CO}_2$ , and  $\text{NO}_x$  levels at a different air intake pipe opening, suggested to introduce a bypass system's for pneumatic planters for obtaining increased efficiency system.

Ramesh *et al.* (2017) developed and tested the performance of a pneumatic precision planter for cotton, using computational fluid dynamics (CFD) tools viz., ANSYS and ICEM CFD for optimizing the pneumatic seed metering mechanism. They determined key aerodynamic properties of cotton seeds, including a maximum terminal velocity of  $8.91 \text{ ms}^{-1}$  and a drag coefficient of 0.63. Results showed that suction pressure was influenced by seed density, geometric mean diameter, airflow rate, and the distance between the seed and the cell, with turbulent airflow confirmed by the Reynolds number. Optimal parameters for cotton were found out as a vacuum pressure of 2.72 kPa, rotor speed of  $0.81 \text{ ms}^{-1}$ , and cell diameter of 2.66 mm for the third seed metering model (SMM3), yielded a miss index of 6.76 %, a multiple index of 3.89 %, and a precision index of 10.81 per cent.

Ahmad *et al.* (2018) developed a simple and cost-effective pneumatic metering device for planting medicinal and aromatic seeds, viz. dill and coriander. For dill and coriander crops, the field capacity with the developed machine was 0.20 and 0.29 fad.  $\text{hr}^{-1}$ , respectively, compared to 0.016 and 0.025 fad.  $\text{hr}^{-1}$  for manual planting (1 feddan = 0.420 ha). Field efficiency was about 95 % for both crops with the developed planter.

Alhassan *et al.* (2018) developed a motorized self-propelled multicrop precision planter for maize, cowpea, and soybean. The planter performance was evaluated at the Landmark University Teaching and Research Farm on sandy loam soil, using a 2.2 kW petrol engine as its prime mover. The evaluation involved testing the planter at three different speeds viz. 4.10, 6.14, and 8.25 km hr<sup>-1</sup> respectively to determine the optimal working speed. The results indicated that the speed of operation significantly impacted the performance metrics. The best field performance was achieved at a working speed of 8.25 km hr<sup>-1</sup>, where the planter demonstrated a field efficiency of 81.2 %, a field capacity of 0.1 ha hr<sup>-1</sup>, with minimal seed damage.

Gheorghe *et al.* (2018) designed and optimized a cyclone separator for pneumatic seed drills through computational fluid dynamics (CFD) modelling. The objective was to improve the cyclone performance by enhancing vortex length, thereby reduced the expulsion of dust from seeds into the atmosphere. CFD modelling was used to analyze gas-solid flow in cyclone separators with varying dust outlet geometries. Performance parameters like collection efficiency and pressure drop were obtained numerically. The optimization of the cyclone separator was approached by adjusting the sizing of the inlet and outlet pipes, the gauge of the cyclone, and obtained the optimal air speed using the PTO of the tractor.

Ibrahim *et al.* (2018) designed and evaluated a four-row pneumatic disc planter for rapeseed. The objective was to investigate the efficiency of metering device under various rotating speeds and vacuum pressure conditions. Six rotating speeds ranging from 5 to 30 rpm were tested in combination with varying vacuum pressures to identify the optimal vacuum pressure for effective seed suction at each speed. Results showed the optimal vacuum pressures ranged from 1.1 to 2.0 kPa for the respective speeds. Additionally, a regression model was developed to predict the vacuum pressure required for each rotating speed. The highest seed mass was recorded in a position closest to the center of rotation, while the lowest was in the farthest from the center. It was observed that the multi-row pneumatic disc is effective for sowing seeds with minimal variation in seed quantity between rows and without causing seed damage.

Mandal *et al.* (2018) developed a pneumatic seed metering mechanism for a power tiller operated 3-row precision planter, and studied the need for planting irregular, small, and

expensive seeds commonly grown in medium and marginal farms. The evaluation was carried out using a sticky belt test stand to identify the best design and operating parameters of the modular seed metering device. The seed metering disc, equipped with 8 holes of  $\Phi$  3.5 mm on a pitch circle  $\Phi$  of 116 mm, operated at a peripheral speed of  $0.11 \text{ ms}^{-1}$  and a suction of 6 kPa, was found the best. This configuration led to conclude that more than 67 % of the seeds were distributed within the range of 15–20 cm spacing, indicated a high level of precision in the metering of seeds.

Xiaohui *et al.* (2018) developed a pneumatic centralized seeding system for wheat. The design was optimized using Computational Fluid Dynamics (CFD) in Solidworks. The fold tube was of 16mm corrugated length, a  $90^\circ$  corrugated angle, and a  $120^\circ$  cone angle for the outer cover. Laboratory tests showed low variation coefficients for displacement stability ranged from 1.01-1.19 % and consistency of 3.20 %, an intra-row seeding rate variation of 3.96 %, and damaged seeds of 0.23 per cent. Field experiments results showed total displacement stability variation at 1.06 %, row consistency at 3.34 %, seeding uniformity at 27.35 %, a slightly higher damaged seed per centage of 0.28 %, and a high seeding emergence rate of 89.63 per cent.

Bagherpour, (2019) evaluated the performance of a cylinder-type vacuum precision seeder for sowing of pea seeds in agricultural field. The seeder tested for three parameters viz. vacuum pressure, grease belt speed, and seed hole diameter. The tested vacuum pressures were 40, 60, and 80 mbar; grease belt speeds at 2.5, 5.0, and 7.0  $\text{km h}^{-1}$ , and at seed hole diameters of 3.0, 4.0, and 5.0 mm respectively. The results showed that the seeder performed optimally at a vacuum pressure of 60 mbar, grease belt speed of  $2.5 \text{ km h}^{-1}$ , and at 4.0 mm seed hole diameter. Under these conditions, the seeder achieved a miss index of 10 %, a multiple index of 5.54 %, a quality feed index of 84.46 %, a seed distribution uniformity coefficient of 79.87 %, and an actual mean seed spacing of 11.94 cm. Notably, in the 3-40-7 (hole diameter-vacuum pressure-belt speed) treatment, a higher miss index correlated with greater mean seed spacing, while in the 5-80-2.5 treatment, a higher multiple index resulted in lower mean seed spacing.

Cujbescu *et al.* (2019) developed a mathematical model to estimate the sowing precision of weeding crop planters which included various soil profiles. This model was experimentally validated using the precision planter with SEMO8 vacuum distributor

on two different soil parcels, labeled P1 and P2. The study focused on the impact of soil uniformity and the geometry of the mechanical system used for sowing on seed distribution. The result showed optimal working of the row unit of the planter at speeds between 5.94 and 6.48 km h<sup>-1</sup> on parcel P1 and between 6.12 and 7.56 km h<sup>-1</sup> on parcel P2.

Zaidi *et al.* (2019) evaluated the performance of a pneumatic pea planter. Field evaluations conducted in Gujranwala compared the pneumatic planter performance with manual sowing and broadcasting methods. The planter demonstrated an actual field capacity of 0.45 hectares per hour and a field efficiency of 58.6 % when operated in low-I tractor gear at 1800 engine rpm. The manual seed placement and broadcasting methods incurred costs of Rs. 14,940 and Rs. 5,240 per hectare, respectively, the operating cost of the pneumatic planter was significantly lower at Rs. 3,015. This represented a 395.52 % and 73.8 % cost reduction compared to manual and broadcasted methods.

Maleki *et al.* (2020) designed, developed, and evaluated a pneumatic punch planter specifically for intercropping of sugar beet with sunflower. The tests examined the impact of varying travel speeds of 3.0, 4.0, and 5.0 km h<sup>-1</sup> on several critical planting parameters viz. the depth of seed holes, seed depth, the number of germinated seeds, and overall crop yield. The data analysis was carried out using Duncan multiple range test (DMRT) for comparison. One of the significant findings was that at a travel speed of 3.0 km h<sup>-1</sup>, the planter showed no variations in hole depth. The results demonstrated notable improvements in crop yields, when the pneumatic punch planter was used and also observed that the yield of sugar beet was increased to 9.69 %, and sunflower yields to 12.45 per cent.

Yan *et al.* (2020) developed a gravity-assisted seed filling method to enhance the operating performance of vacuum seed-meters. This aligned the radial components of the seeds gravitational force and the pressure from upper seeds with the direction of the drag force and thereby assisted in seed filling. In the laboratory tests, the optimal operating parameters were found out a velocity of 6.0 km h<sup>-1</sup> and an air pressure of -4.5 kPa. In field tests, the maximum operating velocity recorded was 9.48 km h<sup>-1</sup>, with the optimum field operating velocity of 7.68 km h<sup>-1</sup>. At this optimum velocity, the qualified

index, double index, and missing index were observed as 92.43 %, 0.67 %, and 6.9 %, respectively.

Zhao *et al.* (2020) designed a wheat air suction planter capable of precise single-grain sowing to enhance seeding uniformity and reduce resource wastage. The key parameters affecting seed arrangement performance were gap width, cone surface angle, and negative pressure were observed in the study. At a cone angle of 90°, a gap width of 0.7 mm, and a negative pressure of 4.0 kPa, the planter showed an adsorption rate of 85.89 per cent. Result showed that the necessary negative pressure ranged for successful seed adsorption of 8.0-13.3 kPa and the fan power required should exceed 1.47 kW. Field trials of the wheat seeder with the new suction and metering device resulted an average variation coefficient of sowing uniformity of 31.20 %, which was below the national standard of 45 per cent.

Jing *et al.* (2020) designed an electro-hydraulic downforce control system for planter units to tackle the challenges of uneven germination and soil compaction caused by varying soil conditions in planting. They incorporated Proportional-Integral-Derivative (PID) closed-loop algorithm to adapt planting downforce in response to changing soil conditions. Field experiments were carried out using a four-row corn pneumatic planter, operated at 8 km h<sup>-1</sup> in both tilled (TF) and untilled fields (UTF). The experiments aimed to test seeding depths of 35, 50, and 80 mm under four levels of downforce viz light (18–50 kg), medium (50–90 kg), heavy (90–120 kg), and the conventional type. The findings revealed that the electro-hydraulic control system performed traditional spring adjustments in regulating downforce, thereby enhanced the consistency of seeding depth with improvement of 1.05–2.23 per cent. The qualified index increased by 3.12–34.38 % compared to the spring adjustment by using appropriate downforce inputs.

Karayel *et al.* (2020) found out the efficiency of a precision vacuum planter designed for large seeds, focused on its performance with both pelleted and bare onion seeds (*Allium cepa L.*). Optimal forward speeds were identified as 1.5 m s<sup>-1</sup> for pelleted seeds and 1.0 m s<sup>-1</sup> for bare seeds. Field trials, conducted at optimal speeds, showed that pelleting reduced seed emergence rates from 73.6 to 62.5 per cent. Despite this decrease, the emergence rate of pelleted seeds was deemed acceptable for precision sowing, as it exceeded 60 per cent.

Vasyilkovska *et al.* (2020) optimized pneumatic and mechanical seeding devices used in precision seeding of tilled crops. Precision device constituted of peripheral cells on a seed plate and a passive device for the centrifugal removal of surplus seeds. A critical aspect of the design was the application of suction force to retain the main seed in the cell while allowed for the removal of surplus seeds. The study found out that an increased suction force enlarged the cavity size (angle), which lies between 0.26 and 0.32 rad at seed plate angular velocities of 25 to 30 rad s<sup>-1</sup>. This adjustment ensured the effective removal of surplus seeds, as the movement along the blade exceeded half its diameter.

Wang *et al.* (2020) developed a precision single-row air-suction planter tailored for minituber planting in hilly and mountainous terrains to address the seed damage caused by traditional mechanical miniature potato seeders. This planter consisted of a seeding device, fan, ditching device, and soil and ridging device, enabled simultaneous ditching, sowing, and soil covering respectively. Optimal working parameters were identified through comprehensive testing, which revealed that a negative pressure of 10 kPa at speed of 2.5 km h<sup>-1</sup> achieved a qualified-seeding index above 90 %, miss-seeding index and multiple-seeding index below 5 per cent. Field tests confirmed the planter efficiency, to achieve a qualified-seeding index of 93.28 %, miss-seeding index of 3.25 %, and multiple-seeding index of 3.47 %, indicated its suitability for challenging agricultural landscapes.

Zhang *et al.* (2020) developed and tested a pneumatic drum type seed metering device of variable diameter, designed for varied seed diameters without the replacement of the roller. They analyzed the effect of the negative pressure on inlet pipe and the eyelet shape on airflow velocity in the negative pressure chamber by using ANSYS software. The study showed that the device performed optimally at a negative pressure of 4.0 kPa, at roller speed of 16.93 rpm, and air speed of 11.48 m s<sup>-1</sup>, to achieve a high-quality feed index rate of 92.37 %, with miss-seeding and multiple-seeding rates at 3.74 % and 3.88 %, respectively.

Kryuchin and Gorbachev (2021) studied the impact of a seed flow shaper on the velocity of the seeds in a pneumatic seed planter. The methodology involved the measurement of seed velocity and analyzed the distance between the rods of the shaper influenced the

seed velocity. A key observation was that as the distance between the rods axes increased from 5 to 30 mm, the seed velocity at the diffuser outlet showed a slight increase, within the range of 3.2 to 2.7 m s<sup>-1</sup>. The seed flow shaper was tested on the seed line of the Amazone DMC Primera pneumatic seed planter for sowing sunflower seeds. The results showed a marked improvement in seeding quality. The coefficient of variation in spacing between plants was 61.2 % with the shaper, compared to 78.4 % without it.

Kuş (2021) studied the impact of planter vibration on the quality of single-seed planting. For this purpose, a single-seed planter was outfitted with a vibration meter. He measured the planter vibration under different tillage conditions, specifically conventional and at reduced tillage. The study was methodically designed in a complete factorial design, incorporated three different planter speeds and three different sizes of furrow openers. Result showed that planter vibration lead to increase linearly with the planting speed. Conversely, vibration decreased linearly as the size of the furrow opener was increased. Planting under reduced tillage conditions generally resulted in lower planter vibration compared to conventional tillage. The optimal spatial plant distribution was achieved using a furrow opener size of 180 mm and at a planting speed of 3.96 km h<sup>-1</sup>.

Li *et al.* (2021) developed a wide-strip-till no-till pneumatic maize seeder to address no-till maize seeding in wheat straw residue. Field tests at 8.0 km h<sup>-1</sup> showed the seeder effectiveness, achieved 38.2 % soil disturbance, a 94.4 % straw cleaning rate, and maintained the residue cover on seed plots over 58 per cent. The sowing performance significantly enhanced, with 96.6 % qualified seed spacing index, a 19.1 % uniformity variation coefficient, 95.1 % qualified index of sowing depth, and a 3.2 % variation coefficient of sowing depth, thereby enhanced the efficiency and quality of maize sowing in challenging conditions.

Ahmad *et al.* (2021) evaluated the performance of a bed-type pneumatic maize planter, focused on the impact of different tillage levels and machine travel speeds on sowing uniformity. The study explored three tillage levels (L1, L2, and L3) and four travel speeds S1 (2 km h<sup>-1</sup>), S2 (4 km h<sup>-1</sup>), S3 (6 km h<sup>-1</sup>), and S4 (8 km h<sup>-1</sup>). Result showed that the highest miss-seeding index (22.12 %) was recorded at the combination of L1 and S4, while the maximum multiple index was observed at L1 and S1. At the optimal

tillage level L3, the mean values for missing-index, multi-index, quality-feed, and precision indices were 5.14 %, 5.833 %, 89.03 %, and 17.85 %, respectively.

Emrah (2021) optimized operational parameters of a vacuum single-seed planter for maize sowing under field condition. The research evaluated three tractor forward speeds viz. 4.0, 5.4, and 7.9 km h<sup>-1</sup> and five target seed spacings viz. 102, 147, 195, 247, and 309 mm respectively. Result showed increased in the target seed spacing resulted a 35 % increase in emergence per centage, while an increase in forward speed reduced emergence by 10 per cent. Optimal results were observed at a speed of 4.0 km h<sup>-1</sup>, yielded the lowest indices for miss and multiple, and the highest for precision as 5.1 %, 2.9 %, and 15.3 %, respectively and a quality of feed index of 92 per cent.

Zhang *et al.* (2022) developed an air suction seed metering device for garlic, focused on two critical components: a seed tray and a seed disturbing tooth. The best settings included nine type holes with a diameter of 7.2 mm, a forward speed of 1.0 km h<sup>-1</sup>, and a working negative pressure of 5.5 kPa. Under these conditions, the device achieved a pass seeding rate of 88.54 % and a missed seeding rate of 6.34 %. Field trials confirmed the performance of the device which achieved a pass rate of 87.83 % and a missed rate of 6.85 %, thus meet the requirements for garlic cultivation.

Kuş and Yıldırım (2021) studied the impact of tractor forward speed and shoe furrow openers of varying heights on the performance of a vacuum precision planter. The study was conducted for sunflower and maize seeds in both conventional and reduced tillage systems. Experiments were carried out at the seed drop heights of 12, 18, and 24 cm and tractor forward speeds of 1.1, 1.5, and 2.2 m s<sup>-1</sup>. The target seed spacings were set at 400 mm for sunflower and 206 mm for maize. The study found that optimal plant spacing for both crops was achieved at a forward speed of 1.1 m s<sup>-1</sup> and a seed drop height of 18 cm. However, increased in the forward speed up to 2.2 m s<sup>-1</sup> and the seed drop height to 24 cm significantly affected these values. The precision of plant spacing distribution under different tillage systems, seed drop heights, and forward speeds was found out as below 29 %, which was acceptable for both sunflower and maize seeds.

Li *et al.* (2021) developed a new double-row pneumatic precision metering device, designed specifically for the small size and high sphericity of *Brassica chinensis* seeds.



They optimized the structure and dimensions of the metering plate, and analyzed the forces involved in seed filling, by considered variables like negative pressure (NP), angular velocity (AV) of the metering plate, and the cone angle (CA) of the suction hole. Using single-factor experiments and central composite design (CCD), through ANOVA, the study found optimal conditions, such as CA of 60 degrees, NP of 1.55–1.72 kPa, and AV of 1.1–1.9 rad s<sup>-1</sup>, which significantly enhanced seeding performance. Bench verification under these conditions achieved a qualified index (QI) greater than 94 % and a miss index (MI) below 2.5 per cent.

SK *et al.* (2021) conducted a study to optimize the operational and design parameters of a precision seed drill for planting pigeon pea seeds. Three key parameters were selected for optimization viz. nozzle diameters 2.00, 2.50, 3.00, 3.50, and 4.00 mm, forward speeds as 0.27, 0.55, 0.83, 1.11, and 1.38 m s<sup>-1</sup>, and vacuum pressures as 19.33, 39.32, 43.98, 58.64, and 68.63 kPa respectively. The target seed-to-seed spacing was set at 300 mm. The study identified optimal operational conditions as forward speed of 0.83 m s<sup>-1</sup>, vacuum pressure of 43.98 kPa, and nozzle diameter of 3.50 mm respectively.

Xu *et al.* (2022) conducted a study focused on the air-suction precision seed-metering device, particularly used in high-speed direct seeding of vegetables. They used DEM-CFD coupling method, to analyze the influence of seed behavior on the flow field changes for different hole types. The results showed that the B-type hole exhibited the highest turbulent kinetic energy of 202.65 m<sup>2</sup>·s<sup>-2</sup> and the largest coupling force to the seeds for 0.029 N, making it the best fluid domain structure for the suction hole of the seed-metering plate. The optimal combination of seeding performance parameters for the air-suction seed-metering device was identified as a seed-throwing angle of 13°, the working speed of 14.5 km h<sup>-1</sup>, and negative pressure of 3.1 kPa. Verification experiments with the optimized structure revealed impressive performance indicators such as qualified index of 95.9 %, multiple index of 1.2 %, and missing index of 2.9 per cent.

Li *et al.* (2023) designed a dual-row pneumatic vegetable precision planter, which uniquely combined a pneumatic seeding mechanism with a honeycomb seeding mechanism. Using ADAMS software, the researchers conducted virtual experiments for okra seeds to analyze the impact of varying the number of holes, diameters, and

heights of different types of honeycomb seeding discs on the seeding success rate. The optimal working performance of the combined seeder was achieved at rotating speed of 18 rpm, pneumatic seeding disc hole diameter of 2.4 mm, vacuum pressure of 3.5 kPa, 24 honeycomb seeding disc holes, hole diameter of 13 mm, and a seed height of 60 mm.

Li *et al.* (2023) optimized the pneumatic hill-drop seed metering system for rapeseed, focused on the planter plate layout, diameter, and shape of suction holes. Utilizing Fluent software for flow field simulations, they reported that horn-shaped holes exhibited the highest maximum velocity and average section pressure. The study established optimal operating parameters for the seed metering device viz., a planter plate speed of 30–70 rpm and a negative pressure of 2.5 to 1.5 kPa. The outcomes showed an empty broadcast rate under 3 %, a hole number qualified rate of at least 96 %, and a deviation from theoretical optimization below 5.5 per cent.

Li *et al.* (2023) discussed the critical role of furrowing depth stability in seed germination and growth in precision seeding. It is represented that the global advancements in furrowing depth control technology for planters focused on three main aspects like, profiling adjustment devices, furrowing depth detection methods, and automatic control systems. They identified active and passive profiling adjustment methods and described three methods for detecting furrowing depth, utilizing different sensor technologies. The study also summarized three approaches to regulate furrowing depth systems based on various evaluation methods for depth stability.

Li *et al.* (2023), studied the seeding mechanisms of pneumatic split seeders for cotton by using Ansys Fluent and EDEM software. The study analyzed single and multiple seeding rates as performance metrics which compared simulations with bench test results. The findings indicated optimal performance at 20 to 40 rpm for cavity seeders and 0.5-1.5 kPa positive pressure airflow, achieved a single seeding rate above 83.06 % and a missed seeding rate below 9.23 per cent. These results closely matched bench test outcomes, with a single seeding rate over 80.64 % and missed seeding rate under 9.86 per cent.

Thiet and Thong (2023) reported a significant advancement in the efficiency of pneumatic metering device for maize seeder. The results showed that an inclined seed

disc significantly outperforms the conventional vertical disc in terms of receiving and holding seeds during sowing. The optimal working parameters were identified as a vacuum pressure ranging between 50 to 100 mm, Seed hole diameters of 4 to 5.5 mm, seeding hole velocity of less than  $0.68 \text{ m s}^{-1}$  and the inclination of the seed disc set at an angle between 20 to 35 degrees from the vertical.

Wang *et al.* (2023) studied on pneumatic precision seed metering devices for high-speed corn seeding operations above  $12 \text{ km h}^{-1}$  revealed significant insights into the performance challenges at such speeds. The study highlighted that negative pressure of 3-7 kPa critically influenced the qualified index and leak index of the device. Lower negative pressures were positively correlated with the leak index and negatively with the qualified index. At the lowest negative pressure of 3 kPa, the leak index peaked were high at 32.48 %, 15.61 %, and 66.77 % for different corn seed varieties, but remained below 10 % at above 6 kPa.

#### 2.4 ELECTRONIC SYSTEM INTEGRATION: ADDING INTELLIGENCE TO THE PLANTER

In the era of modern agriculture, precision farming is the major farming technique to enhance productivity and to reduce losses for sustainable agriculture. Electronic systems are very useful for precision planters. These systems have redefined the paradigms of efficiency, accuracy, and adaptability in agricultural machinery. As the global agricultural landscape faces increasing demands for higher yields and sustainable practices, precision planters equipped with sophisticated electronic systems have emerged as a pivotal solution. These electronic systems encompass a wide array of technological advancements, from sensor-based monitoring to automated control mechanisms. They are intricately designed to ensure precise seed placement, optimal seed spacing, and uniform seed depth, which are critical factors in maximizing crop yields and minimizing resource wastage. The use of sensors, such as photoelectric, proximity, and LiDAR sensors, has enabled real-time monitoring of seeding operations, ensuring any deviations from the desired planting parameters which are promptly corrected. Moreover, the integration of microcomputing and wireless data transmission technologies has ushered a new era of data-driven agriculture. This allows for the

collection and analysis of vast amounts of data related to planting operations, facilitating informed decision-making and adaptive responses to varying field conditions.

Inoti and Namikawa (1990) developed an electronic seed sensing system for enhancement of the accuracy of seed delivery in pneumatic precision planter. They developed an electronic detector for detecting a wide variety of seeds with a precision of  $\pm 1$  per cent. Its operation was simple, required no external adjustments for sensitivity, highly user-friendly and efficient in diverse agricultural settings. The detector continuously monitored and recorded parameters such as the coefficient of variation, and the occurrence of misses and doubles/multiples in seeding.

Inoti and Namikawa (1991) developed an electronically-controlled pneumatic precision planter, designed for soybean seeds and grains of similar sizes. It was equipped with solenoid valve, controlled by a sophisticated data acquisition and control unit, coupled with a seed feeder. Result showed its ability to adjust seed dropping intervals between 30 to 210 milliseconds, according to the seed spacing. Laboratory tests used soybean seeds to validate the system efficacy, demonstrating high metering accuracy and show its potential to significantly enhance the accuracy and efficiency of seed planting in agriculture.

Panning *et al.* (2000) studied the seed spacing uniformity in sugar beet planters. They found out the performance of five different planter configurations, utilizing both field and laboratory testing methods. The laboratory method, involved an opto-electronic sensor system, and the field-testing approach offered contrasting insights. The study employed the coefficient of precision as a measure for seed spacing uniformity. The laboratory tests, under controlled conditions, indicated higher seed spacing uniformity compared to the field tests. The research suggested that while laboratory tests can be useful to screen the planter configurations for seed metering uniformity and field tests were indispensable for a comprehensive assessment of planter performance in real-world conditions.

Alchanatis *et al.* (2002) developed a high-resolution optical system to evaluate pneumatic planters. The system, comprised with a line scan camera connected to a frame grabber and a personal computer, enabled real-time image processing. It

calculated the location and spacing of seeds on a virtual belt under the planter and display seed distribution parameters in real time and marked a significant technological advancement in precision agriculture. They compared the optical system accuracy with the traditional grease belt method. The findings showed consistent seed location results between the two methods, validated the optical system accuracy.

Shinde *et al.* (2009) developed an electronic metering mechanism for the Jyoti Multicrop planter, specifically for sowing groundnuts. They integrated electronic components in traditional agricultural machinery to boost efficiency. The developed prototype consisted of a main frame, a fertilizer metering unit, an innovative electronic seed metering system equipped with a distance sensing unit, a microprocessor-controlled check valve activating system, software, and solenoid switches. Result revealed that the field tests of this prototype achieved an average effective field capacity of 0.172 ha h<sup>-1</sup> at an average forward speed of 2.90 km h<sup>-1</sup>, with a field efficiency of 66.05 per cent.

Singh and Mane (2011) developed an electronically controlled metering mechanism for planting okra seeds. The system featured a proximity sensor, pulse generator, BCD counter (IC 4510), timer (IC 4093), relay unit, thumb wheel, DC motor, and a cup-type seed metering unit. The electronic circuit controlled the DC motor, which rotated the metering unit for seed delivery. A lab test was done to evaluate the seed-to-seed spacings at different forward speeds on greased belt. The results showed that the mechanism accurately delivered seeds, closely matched the target spacing with a high feed index, and recorded zero miss and multiple indexes, indicated precise seed placement.

Xia *et al.* (2011) introduced an advanced monitoring system for precision planters tailored to field operations demands. A photoelectric sensor and a MSP430 microcontroller were used to evaluate the seeder-metering device performance, analyzed miss index, multiple index, seeding amount, seeding rate, and plant spacing. A distinctive feature was its sound-light alarm mechanism, using an indicator light to alert about faults in type and location, with data displayed on an LED screen. For real-time data acquisition and analysis, the system used a bluetooth-based wireless transmission, communicated through an FS-BT485A bluetooth module. In laboratory

tests, a stepping motor controlled the seeding rate and ensured uniform drilling and sowing. The system demonstrated high reliability, with the sound-light alarm achieved a 100 % reliability rate and the photoelectric sensor efficiently detected over 95 % of seeds.

Kamgar and Eslami (2012) developed a mechatronic transmission system for row crop planters, primarily addressed the issue of non-uniform seed spacing resulted from the wheel slippage. The mechatronic system was designed to reduce friction in the transmission mechanism, thereby decreased wheel axis torque and improved seed placement precision. This system incorporated advanced components such as an encoder for monitoring the forward velocity, a microprocessor for data processing, and an electromotor for metering system operation. Field evaluations involved varying slippage conditions with rubber tires and steel wheels, different soil preparation methods, and residue management techniques to assess the system adaptability. Results showed that the mechatronic system significantly reduced the multiple index, indicated an improved precision seed placement precision. Particularly, planters equipped with the mechatronic system and rubber tires achieved a higher quality of feed index.

Shi *et al.* in 2017 optimized the parameters of the speed compensation mechanism in an electrically driven maize planter. Utilizing MATLAB, they simulated the impact of various parameters of the speed compensation mechanism on the dibbling trajectory. The study identified that the crank angular velocity, center distance, and assistant crank length significantly influenced the rate of qualified sowing depth and film hole. The optimal parameters were determined as a crank angular velocity of  $89.10 \text{ rad s}^{-1}$ , a center distance of 58.55 mm, and an assistant crank length of 95.1 mm. Under these conditions, the qualified rate of sowing depth and the film hole were found out 94.89 % and 93.61 %, respectively.

Li *et al.* (2015) developed a mechatronic driving system for 2-row pneumatic precision planter and evaluated its field performance. The mechatronic system showed better result than the mechanical system in terms of the quality of feeding index (QFI) and missing-seeding index. Result indicated an average increase of 4.7 % in QFI and a decrease in the missing-seeding index of 3.54 % for mechatronic system in comparison of mechanical system.

Liang *et al.* (2015) conducted a study to resolve the problem of seed spacing variation caused by wheel slip and beating of the chain in conventional pneumatic maize precision seed-metering devices. The study primary aim was to investigate the effect on planting quality by replacing the wheel drive with a motor-driven system. The findings revealed that there was no significant difference in seeding quality between the two types of transmission systems, indicated that the motor-driven system is a feasible alternative for the metering device. The study recommended optimal air pressure values in the range of 1.5-2.5 kPa for the motor-driven system.

He *et al.* (2017) designed an electric-driven control system for the seed meter of a precision planter, aiming to overcome the limitations of poor planting quality and low travel speed in conventional ground wheel and chain-driven planters. The system used a closed-loop Proportional-Integral-Derivative (PID) algorithm to control the rotation speed of the seed plate. The study compared the performance of three PID tuning methods: Ziegler-Nichols step response method (ZNM), Cohen-Coon method (CCM), and Chien-Hrones-Reswick method (CHRM), using MATLAB Simulink simulations. The results showed that the CCM had higher performance with the smallest rise time of 0.018 s, settling time of 0.082 s, and maximum overshoot of 26.1 %. Result showed that in field experiment the average values for the quality of feed index, miss index, and precision index were 98.62 %, 1.29 %, and 14.51 %, respectively at the travel speed of 8.6 km h<sup>-1</sup>. Even at a higher speed of 13.0 km h<sup>-1</sup>, the average QFI maintained a high value of 97.09 per cent.

Koley *et al.* (2017) developed an electronic metering system, with an inclined plate type metering mechanism. The electronic metering unit was designed to synchronize with the forward speed of the planter using a proximity sensor and a microcontroller. The unit was tested in the laboratory setting for groundnut seeds at various forward speeds of 2.5, 3.0, and 3.5 km h<sup>-1</sup>. They identified the optimal operational conditions for the metering unit at a forward speed of 2.5 km h<sup>-1</sup> when a metering plate was operated at a rotational speed of 50 rpm.

Mangus *et al.* (2017) evaluated the accuracy of electric seed metering systems used in high-speed planting of row crops. The experiment simulated planting conditions at two different seeding rates and used a high-speed imaging system developed in LabVIEW.

This system recorded real-time seed meter singulation at 300 frames per second, combining machine states with seed tube sensor data and vision-based seed measurements. The findings revealed an average singulation accuracy of 98.45 %, when planting at speeds ranging from 2.4 km h<sup>-1</sup> to 16.1 km h<sup>-1</sup>. Due to rapid acceleration, deceleration and abrupt changes like headland turns, errors nearly get doubled. Planting above 1,250 seeds per minute led to increased singulation errors. The vision-based measurements were found to be very close to the readings of commercial seed tube sensors, with  $0.8 \pm 0.2$  % difference.

Shi *et al.* (2017) developed an advanced electric driving corn hill-drop planter tailored for plot corn farming in northwest regions. This planter, equipped with differential motor drives, an electromagnetic clutch, and a motor crankshaft sprocket system. It achieved precise seed dispensation and vertical movement using a non-uniform rotation mechanism and a sowing device assembly linked to a slider and spring damper. It also featured a forward speed compensation mechanism for near-zero speed compensation, a depth-limiting mechanism, and a rear-height adjusting mechanism to cater to film mulching and ridge tillage. Result showed good performance on field testing with a hole rate of 1.1 %, qualified rate of seeds per cavity of 93.2 %, and accuracy in sowing depth under the film was 90.1 per cent.

Abdolazare and Mehdizadeh (2018) conducted a study to improve the assessment of seed spacing uniformity for pneumatic planters, bridging the gap between laboratory and field conditions. They employed a high-speed camera system to analyze the trajectory of falling seeds, focused on maize and castor seeds under different parameters such as two speed ranges of 3 to 4.5 km h<sup>-1</sup> and 6 to 8.5 km h<sup>-1</sup> and four vacuum pressures of 30, 40, 50, 60 kPa. The study found out the best feed quality index for castor seeds was 98.31 % at 3.0 to 4.5 km h<sup>-1</sup> speed at 40 kPa vacuum pressure, while maize seeds peaked at an 80 % feed quality index under similar conditions. They derived equations for seed trajectories for each treatment and a general equation,  $y = 3.523e-0.077x$  with coefficient of determination ( $R^2$ ) of 0.902.

Abdolazare and Mehdizadeh (2018) studied the performance of pneumatic planter under field conditions. Optimal conditions were identified for seeds such as maize, castor, sorghum, and sugar beet performed the best at lower speed and 4.0 kPa pressure;



watermelon at higher speed and 4.5 kPa cucumber at lower speed and 4.5 kPa. Additionally, a genetic programming (GP) algorithm was used to develop regression models, correlating operational parameters and seed physical properties with the planter performance. The GP model, incorporating all seed properties and operational factors, showed a high accuracy ( $R^2 = 0.938$ ), with root mean squared error of 3.01, mean absolute error of 3.362087, and a highly significant P-value of  $2.9851e-17$ . This model explained the traditional regression models in demonstrating the relationship between operational parameters, seed properties, and seed spacing uniformity.

Borja *et al.* (2018) addressed the challenge of missed seeding during planting operations. Their approach involved retrofitting a conventional seed meter with advanced components such as a camera for monitoring the seed plate and a microprocessor for image analysis, and a stepper motor to control the seed meter drive system with precision. This integration of technology aimed to enhance the seed meter performance by enabling it to detect and compensate for unfilled holes on the seed plate and thereby reducing the incidence of missed seeding. Result showed that newly developed control system was capable to operate effectively within a forward speed range of 2.0 to 6.0 km h<sup>-1</sup>. The study revealed the efficiency decreased when the speed was more than 6.0 km h<sup>-1</sup> which was due to limitations in production of torque from the mechatronic drive and hence the latency capture of images by the camera.

Cay *et al.* (2018) conducted a research on the precision planter to achieve an uniform seed spacing. They identified that the issues like spinning and slipping of the ground wheel, vibration, seizing, and jamming in the chain-sprocket systems in single seed corn planters especially at high operating speeds. Accordingly, they developed an electro-mechanic drive system (EMDS) for the seed metering units. The study involved laboratory testing of the EMDS and compared its performance with the classic drive system (CDS) at three different operating speeds of 5.0, 7.5, 10 km h<sup>-1</sup> and ten different seed spacings from 6.0 to 29.3 cm. Results showed that for EMDS, quality of feed index ranged from 2.91–95.36 %, multiple index from 0–1.73 %, miss index from 4.45–97.09 %, and precision index from 8.79–22.14 per cent. The CDS performance indices like quality of feed index, multiple index, miss index and precision index were varied from 2.09–98.55 %, 0–0.36 %, 1.09–97.91 %, and 5.79–20.92 % respectively.

Cay *et al.* (2018) addressed the limitations of conventional seed metering units in single seed corn planters, particularly drive wheel slippage, by developing an electro-mechanic drive system (EMDS) and comparing it with the classic driving system (CDS). Their study demonstrated EMDS superiority through various performance indices. Plant spacing uniformity and distribution were rated as “good” with EMDS, compared to “moderate” with CDS, and experimental plant spacing values were closer to theoretical values with EMDS. Notably, the EMDS reduced negative slippage in the planter drive wheel to 1.33 %, compared to 6.79 % with CDS, and offered about 22 % fuel savings in field operations. The study suggested that the EMDS as a viable alternative to CDS for enhancing planting quality and operational efficiency in single seed corn planters, though further optimization in seed metering unit designs was recommended.

Fu *et al.* (2018) developed a GNSS/IMU-based control system using a hydraulic motor instead of the ground wheel to address an inconsistent seed spacing in maize no-tillage seeding, caused by land wheel skidding. This system tested on a 2BQX-6 maize no-tillage drill, allowed for real-time seeding speed adjustments which enhanced seeding and fertilizer application quality. When the seed seeding spacing was reduced by 40 %, the quality of feed index for the hydraulic and land wheel-driven planters were 90.01 and 63.23 % respectively.

El-Sheikha *et al.* (2019) modified a planter with an electronic unit by featuring a dual feeding system with a primary cell/disc device and a secondary cone hole device. This design ensured automatic compensation for missed seeds by the secondary feeder which employed three sensors in conjunction with an electronic circuit. The circuit, contained a PIC 16f877 microcontroller, included an LM016LCD display and a pot-hg resistor, powered by a 3V battery, and fixed in a protective box. Two infrared sensors were placed at the seed exit points of the cylinder and cone seed boxes, and a third IR sensor (guide-gear sensor) was installed in front of the guide gear. The overall efficiency of the feeding system was increased approximately 1.2 times at a travel speed of 1.42 ms<sup>-1</sup> and at a reduction ratio of 0.49, which showed the effectiveness of the electronic unit for improving planting accuracy.

Jin *et al.* (2019) developed a novel electric seeder optimized for small-size vegetable seeds of 2-10 mm, integrated power drive and optical fiber detection technologies for enhanced efficiency and precision. Field tests with crops like coriander, pakchoi, and radish demonstrated the seeder high accuracy, showed a precision of 95 per cent, when used such electric seeders.

Strasser *et al.* (2019) investigated the performance of electric drive seed metering system, particularly in its accuracy and response time in lab-simulated planting scenarios. The study aimed to assess these systems under various planting speeds varied from 7.2 to 16.1 km h<sup>-1</sup> on straight paths, 6.0 to 14.5 km h<sup>-1</sup> on curves and conditions like acceleration/deceleration rates of 0.4 and 0.6 m s<sup>-2</sup>, compared with the actual and target speeds of the seed meter. Using eight high-frequency encoders and a custom Data Acquisition system, the study found improved metering accuracy with increased ground speed. However, during speed transitions, a response lag of 3 to 4 seconds resulted in rpm errors ranging from -3.7 % to 3.6 % at the lower seeding rate and from -3.8 % to 3.2 % at the higher rate. In curvilinear planting, steady-state rpm errors were between -0.5 % and 0.8 %, caused seeding rate errors of -223 to 370 seeds per ha. In transient states, rotational speed errors increased to -7.2 % to 7.9 %, lead to more significant seeding rate errors of -5,886 to 7,187 seeds per ha.

Soyoye (2020) developed an electrically powered maize planter. It consisted of a light-reflecting optoelectronic field counter that was capable of detecting objects falling at a distance of 0.7 mm or more in the planter delivery tube. The planter, particularly efficient with a forward speed of 1.38 m s<sup>-1</sup> and a seed delivery tube diameter of 24 mm. The per centage damaged seed, spacing efficiency, sensor efficiency and functional efficiency were found out as 14 %, 97 %, 96 % and 86 per cent respectively in the laboratory test. The overall sowing efficiency of the planter at field was found out as 78 per cent.

Coelho *et al.* (2020) developed a single row manual planter equipped with a horizontal perforated disc distributor. A direct-current electric motor was used to drive the seed metering device. Controller operation was managed by a BeagleBone Black single-board computer. Python language used to write the program and PyQt5 to feature a graphical user interface. The system effectiveness was demonstrated in field trials with

maize seeds. These trials utilized a 28-hole disc and a prescription seeding map that defined four distinct management zones. They evaluated the number of plants that were germinated, to confirm the variations in the motor speed which in turn resulted the required changes in planting density. Importantly, the planting density in each management zone aligned with the predetermined seeding map, validated precision and effectiveness of the system.

Wang *et al.* (2020) developed an 'integrated seeding and compensated potato planter based on a single way clutch to decrease the miss-seeding in spoon-type potato seed-metering device. The system included a seeding-monitoring setup based on infrared radiation and an open-loop compensation control plan. Result showed a significant reduction in miss-seeding rates in the field test, with seed-metering chain speeds varied from 0.2 to 0.8 m s<sup>-1</sup>. The combined missing and wrong detection possibility were kept below 1.0 %, and the miss-seeding rate dropped from 4.0 to 1.0 % at the highest speed of 0.8 m s<sup>-1</sup>.

Borja *et al.* (2021) developed a pneumatic seed meter for mechanical corn planting by integrating a machine vision system with a mechatronic drive to reduce missed seeding incidents. Tested in a stationary lab rig at 2, 4, and 6 km h<sup>-1</sup>, to minimize missed seeding. The machine vision system demonstrated high accuracy of 0.2564 % error rate in detecting filled and unfilled seed plate holes across 780 images. At 2 km h<sup>-1</sup> and 4 km h<sup>-1</sup> of speed it was observed a missed seeding and indicated the performance was very poor.

Pradhan *et al.* (2021) developed a LiDAR-navigated electronic seed metering system for check row planting. This system comprised of a LiDAR-based distance measurement unit, an electronic seed metering mechanism, and wireless communication. Laboratory tests conducted with different level of cell sizes varied from 8.80 to 12.83 mm and linear cell speeds varied from 89.15 to 133.72 mm s<sup>-1</sup>. They found out that highest miss index of 20 % was obtained at a linear cell speed of 133 mm s<sup>-1</sup> and cell size of 8.80 mm and lowest multiple index of 7 % was obtained at a linear cell speed of 89.15 mm s<sup>-1</sup> and cell size of 12.83 mm. The best optimal setting was obtained at the cell size of 11.90 mm and linear speed at 99.46 mm s<sup>-1</sup>. A Check Row Quality

Index (ICRQ) was devised to assess the planter performance. At forward speeds of 2, 3, and 5 km h<sup>-1</sup>, the standard deviation of ICRQ was highest at 5 km h<sup>-1</sup>.

Xia *et al.* (2021) developed and evaluated an optoelectronic measurement system for a pneumatic roller-type seeder, specifically designed for sowing vegetable plug-trays. They assess the performance of the newly developed measurement system across various sowing speeds and for ten different types of vegetable seeds. The system achieved an average missed-seeding consistency ratio of 99.81 %, indicating a high level of reliability in detecting any missed seeding events. Seeds with a sphericity greater than 85 % achieved an average consistency ratio for single seeding and multiple seeding over 99 per cent.

Shah *et al.* (2022) developed a variable rate multi-crop pneumatic seed metering unit. This innovative unit replaced the traditional ground wheel and chain-gear disc mechanism with a drive-by-wire system with motors and sensors for variable rate planting. Laboratory tests using maize and soybean seeds at various rates and speeds focused on accuracy and seed counts. The unit showed marked improvements over traditional systems, with an average miss-count of 5.4 seeds, an average multiple-count of 2.5 seeds, and a coefficient of variation in spacing (precision) of 0.34 inches, at varied travel speeds from 2 km h<sup>-1</sup> to 4 km h<sup>-1</sup>.

Fangyan *et al.* (2022) designed a new pneumatic carrot planter to enhance the precision and efficiency of carrot planting in greenhouses. It consisted of an electrically driven carrot precision seeder system, which used a rotary encoder for speed measurement and a PLC for real-time sowing rate adjustment, ensuring synchronization between seed sowing and the seeder forward speed. Additionally, a bijective matrix fiber optic sensor monitoring system was developed for small grain seeds, displaying leaky seeds and sowing area with a counting relative error of not more than 4.6 per cent. Field experiments revealed that the planter had 10-hour battery endurance, a plant spacing qualified rate exceeding 93.7 %, reseeding rate below 2.4 %, and leaky seeding rate under 3.9 %, which met the standard field condition.

Moreno *et al.* (2023) studied the impact of sensor installation position on the pneumatic meter at varied operating speeds for the monitoring of maize sowing. They used a static

simulation bench to conduct the experiments. A completely randomized design were adopted with two main factors viz., sensor installation position (upper, middle, and lower portion of the conductive tube and conveyor belt) and at the simulated speeds of 3.0, 5.0, 7.0, 9.0, and 11.0 km h<sup>-1</sup>. The study concluded that the sensor placement at the final portion of the conductive tube produced more accurate results.

Tang *et al.* (2023) studied the seed drop tube structural parameters for air-blowing precision seed-metering device to enhance maize seeding quality. Utilizing computational fluid dynamics (CFD), the study determined optimal airflow velocity in a seed drop tube with specific dimensions of 24 mm inlet diameter and 30 mm throat height and further examined maize seed movement dynamics through CFD-DEM coupled simulation. This simulation, corroborated by high-speed camera and bench tests, indicated that maize seeds had collisions within the tube, resulted a consistent and rapid average fall time of  $0.12 \pm 0.008$  seconds. The research also demonstrated that under certain conditions like 4.5 kPa working pressure and 41 rpm speed, the seed drop tube significantly improved seeding quality, reduced coefficient of variation by 3.66 % and increased the qualified index by 1.06 per cent. At the speed of 32 rpm, achieved the lowest coefficient variation of 9.58 % and the qualified index of 96.56 per cent.

## 2.5 NO-TILL PLANTING: CULTIVATING SUSTAINABILITY

No-till farming, a cornerstone of sustainable agriculture, represents a paradigm shift in crop cultivation practices. It preserves soil structure, reducing erosion, and enhancing soil health. The adoption of no-till practices requires specialized machinery and techniques, tailored to sow seeds and apply fertilizers without disturbing the soil. This section of the literature review delves into the advancements in agricultural engineering that have made no-till farming not only feasible but also efficient and productive. It explores the development of innovative planting equipment, such as no-till planters and drills, which are designed to operate effectively in the undisturbed soil. These machines must navigate residue from previous crops, penetrate the soil with minimal disturbance, and ensure accurate seed placement and depth. It highlights how modern no-till equipment incorporates advanced features like electronic control systems, precision seed metering, and GPS-guided navigation to enhance planting accuracy and efficiency. These features are crucial for achieving uniform seed

distribution, optimal planting depth, and effective fertilizer placement, leading to an improved crop yields and soil health. Additionally, this section underscores the environmental benefits of no-till farming, such as reduced soil erosion, improved water retention, and enhanced carbon sequestration. It also addresses the economic aspects, noting how no-till practices can reduce fuel and labor costs and thereby making the farming more economically sustainable.

Kaspar and Erbach (1998) studied the effects of different planter attachments on stand establishment, emergence rate, and yield in no-till corn and soybean farming. Examined three attachments, like an offset-bubble coultter, staggered-discs row cleaner, and powered horizontal-disc row cleaner in various crop rotation sequences. The study found out that while continuous corn rotations affected subsurface residue and emerged populations in certain years, the row cleaner attachments generally reduced residue levels and improved stand establishment and emergence rates, particularly for corn in 1990 and soybean in 1991. Despite these benefits, there was no significant impact on grain yield, suggested that row cleaner attachments enhanced stand establishment in no-till farming, potentially lead to more consistent and productive yields of corn and soybean.

Chen *et al.* (2004) investigated the impact of drill configurations on the efficiency of no-till seeding. Their research involved a two-year field trial on clay loam soils, where they planted wheat, corn, and soybeans using a no-till drill with a double disc opener, gauge wheel, press wheel, and an optional fertilizer attachment. The study revealed that removing the press wheel had negative effect in normal and dry seeding conditions. It reduced the speed of emergence and plant population.

Erenstein and Laxmi (2008) presented an analysis of zero-tillage (ZT) impacts in the rice-wheat systems of India's Indo-Gangetic Plains (IGP). Their study synthesize experiences with ZT in this region, highlighted the appropriateness for rice-wheat systems by facilitating earlier wheat planting, aiding in the control of the weed (*Phalaris minor*), reducing production costs, and conserving water. The study showed that substantial farm-level benefits of ZT wheat after rice, saved approximately Rs 2,250 per hectare.

Sarauskis *et al.* (2009) conducted a study on the economic and energy efficiency of sustainable tillage and cereal sowing technologies and compared with traditional methods. The study revealed that sustainable practices significantly reduce labor time by 20 to 49 % and are less invasive to soil processes, contrasted sharply with the soil degradation and environmental issues caused by conventional methods. Fuel consumption for direct sowing was about 6.25 liters per hectare, which was 2 to 5 times lower than the fuel requirements for conventional techniques.

Singh *et al.* (2010) examined the impact of zero-tillage wheat cultivation in the rice-wheat cropping systems of central Uttar Pradesh in the Indo-Gangetic Plain (IGP). Over two years, data from six on-farm demonstrations revealed that zero-tillage wheat not only increased grain yields but also reduced cultivation costs per hectare compared to conventional methods. Furthermore, zero tillage effectively lowered weed density especially *Phalaris minor*, and enhanced water conservation. The research attributed the rapid adoption and success of zero-tillage wheat sowing in central Uttar Pradesh to field demonstrations and farmer training programs, indicated a transformative shift in tillage practices which was crucial for sustaining the rice-wheat system's productivity in the IGP.

Grover and Sharma (2011) studied the significant impact of zero-tillage technology in rice-wheat systems. This method, involved minimal soil disturbance and recommended for its benefits like water conservation, fuel saving, timely sowing, and reduced labor. Remarkably, the area under zero-tillage wheat cultivation escalated from just 750 hectares in 2000-01 to over 200,000 hectares by 2008-09. The economic analysis revealed that zero tillage not only yield higher grain production but also lowered production costs compared to conventional methods.

Karayel and Šarauskis (2011) studied the impact of downforce on disc furrow opener performance in maize cultivation. They conducted two soil types viz., clay-loam and loamy, delved into how varied the downforces of 680, 880, 1150, and 1400 N influenced the parameters such as seed spacing and sowing depth uniformity, along with emergence metrics. The study revealed that a direct correlation between increased downforce and enhanced opener performance, highlighted an optimal downforce threshold above 880 N for precise no-till sowing in these soil conditions.



Liu *et al.* (2016) developed a no-till precision planter for corn. The newly designed corn no-tillage precision seeder consisted of a notched disc opener for deep fertilization, an involute tooth disc grass divider for efficient grass and straw separation, and a multifunctional sowing unit for ditching, seeding, soil covering, and pressing in one pass. Field experiments showed that when operated at  $9 \text{ km h}^{-1}$ , the seeder achieved 92 % seed depth qualified index, 9.6 % coefficient of variation in seed spacing, 2.5 % leakage index, and 4.5 % reseeding index, which indicted its efficiency and adaptability in challenging agricultural conditions.

Yu *et al.* (2019) developed a pneumatic conveying seeder that integrated several agricultural processes like stubble elimination, fertilization, sowing, soil covering, and suppression. A central feature of this seeder was its centralized airflow seeding/fertilizer device that used a shared air channel for simultaneous seed and fertilizer transportation, ensured synchronized seeding and application of fertilizer and enhanced process efficiency and uniformity. Field tests showed that the qualified rates of sowing depth, fertilization depth, and spacing were 93.0, 93.6, and 85.4, per cent respectively, with coefficients of variations as 4.7, 2.8, and 5.3 per cent.

Shi *et al.* (2021) optimized structural parameters of a no-tillage planter with straw-smashing and strip-mulching features, designed for fully stubbled paddy fields. The two structural components viz., diversion device and the strip-rotary tillage device were examined to find out the out-enlarge angle ( $\eta$ ) and slide-push angle ( $\gamma$ ) of the diversion device affect the coefficient of variation ( $\zeta_1$ ) of cover-straw width, and the influence of the rotary tillage-blade number (N) and its configuration on the broken rate ( $\zeta_2$ ) of strip soil. The study established that both  $\eta$  and  $\gamma$  significantly impact  $\zeta_1$ , with  $\eta$  having a more pronounced effect, while N was found to be a crucial factor in determining  $\zeta_2$ , again with  $\gamma$  playing a significant role. The ideal structural parameter combination was identified as a  $45^\circ$  out-enlarge angle ( $\eta$ ), a  $40^\circ$  slide-push angle ( $\gamma$ ), and a 4-blade rotary tillage setup (N). Field tests of this optimized no-tillage planter configuration showed mean values of 10.47 % for  $\zeta_1$  and 90.95 % for  $\zeta_2$ , demonstrated the effectiveness of the planter in terms of operational quality standards in paddy fields.

Cao *et al.* (2023) developed a pneumatic pressure control device (PPCD), designed with an air spring at its core to maintain stable press wheel pressure (PWP) to address

inconsistent seed furrow compaction and seeding depth. Using the gas-structure coupling finite element simulation method (FESM), the study evaluated the PPCD performance, tested the key factors like piston radius, piston angle, and cord angle of the air spring with vertical stiffness as the primary test index. The optimal parameters were found out as the piston radius of 27.2 mm, a piston angle of 11.7°, and a cord angle of 30.0 degree. Bench tests confirmed the simulation accuracy, with vertical stiffness and internal air pressure simulation errors of 7.1 % and 3.0 %, respectively.

## CHAPTER - III

### MATERIALS AND METHODS

In this chapter, the methodology adopted in the design, development and testing of tractor operated pneumatic no-till pulse planter with an electronic control system as influenced by the seed properties, soil, machine and operational parameters are detailed. The optimum design values are essential requirement for development and evaluation of the planter. Studies were therefore, conducted to determine optimum design values leading to the development of a prototype unit.

The development of the machine was undertaken at the research workshop of the Department of FMPE, KCAEFT, Tavanur. Before the prototype development, a laboratory model was meticulously developed and subjected to rigorous testing under various controlled variables. This chapter delves into the selection of independent variables for the testing and optimization process, aiming to maximize the machine output. The field evaluation of the machine performance was conducted at Instructional Farm KCAEFT, Tavanur. A comprehensive analysis was carried out to determine the optimal conditions for the operation of machine. The major parameters of seeds and soil influencing the design and development of a pneumatic no-till pulse planter with an electronic control system are elaborated below. The development of the planter, its field performance evaluation and cost economics are summarized.

#### 3.1 SEED PROPERTIES AND QUALITY ASSESSMENT

The physical, and engineering properties of two selected types of pulses, black gram (*Vigna mungo*) and horse gram (*Macrotyloma uniflorum*), were studied. The study encompasses a range of physical properties viz., size, aspect ratio, sphericity, roundness, and thousand seed weight; bulk density, true density, and porosity; and engineering properties viz., angle of repose, coefficient of static friction, terminal velocity and drag coefficient were analyzed. Each of these properties will be determined using standardized testing procedures, which in turn helped for a comprehensive understanding of the seeds characteristics to optimize the planter performance and efficacy in sowing operations.

### **3.1.1 Physical properties**

Two varieties of seeds namely VBN-6 of black gram and KS-2 of horse gram were selected for the study. The seeds underwent a thorough manual cleaning process to remove any foreign matter, as well as broken or immature seeds which ensured the purity and consistency of the samples.

#### ***3.1.1.1 Moisture content***

The initial moisture content of these seeds was determined through a standardized oven drying method. This involved heating the seeds at a controlled temperature of  $105 \pm 2^\circ\text{C}$  for a duration of five hours, in accordance with the guidelines set forth by AOAC (2002). This procedure was critical in establishing a baseline for the moisture content of the seeds, which is a pivotal factor in assessing their properties. Each property was tested in triplicate to ensure reliability and statistical robustness. The moisture content of the seed samples, expressed as a percentage on a dry weight basis, was calculated using the formula:

$$M = \frac{W_1 - W_2}{W_2} \times 100$$

Where, 'M' represents the moisture content, 'W<sub>1</sub>' is the initial weight of the seeds sample, and 'W<sub>2</sub>' is the weight of the sample after oven-drying.

#### ***3.1.1.2 Size***

The axial dimensions of the seeds were measured to ascertain its length (L), width (W), and thickness (T). Using a digital Vernier calipers having a precision of 0.01mm.

A representative sample of 100 seeds from black gram and horse gram were selected for the analysis. Each seed within these samples was measured individually to ensure accuracy. The data collected from these measurements were then used to calculate the mean values for the length, width, and thickness for each seed variety.

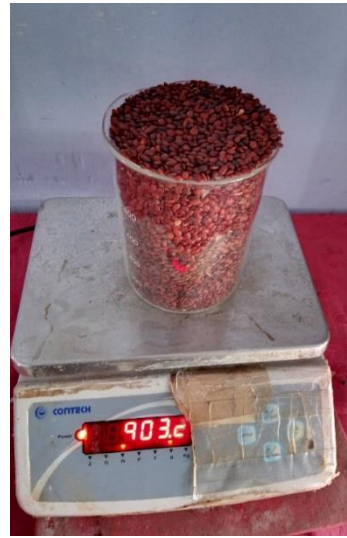


**Plate 3.1 Measurement of black gram (VBN-6) and horse gram (KS-2) seeds**

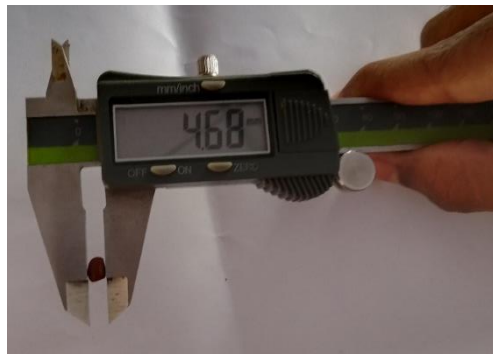


**Plate 3.2 Measurement of linear dimension of seeds**



**Plate 3.3 Measurement of coefficient of friction**

### **3.1.1.3 Arithmetic mean diameter**

The arithmetic mean diameter ( $D_a$ ) of the seeds was calculated using the formula proposed by Kiani Deh Kiani et al. (2008) and Mohsenin (1986):

$$D_a = \frac{L + W + T}{3}$$

Where, ' $D_a$ ' represents the arithmetic average diameter of the seeds, with 'L', the major diameter, 'W', the intermediate diameter, and 'T', the minor diameter.

### **3.1.1.4 Geometric mean diameter**

The geometric mean diameter ( $D$ ) was determined using the formula given by Pradhan *et al.* (2013):

$$D = (L \times W \times T)^{\frac{1}{3}}$$

### **3.1.1.5 Aspect Ratio**

The aspect ratio, is the ratio of the width (W) to the length (L) of the seeds, given by Mohsenin, 1970.

$$R = \frac{W}{L} \times 100$$

This ratio is indicative of the seed shape and is important in understanding how seeds will interact with planting machinery.

### **3.1.1.6 Sphericity**

Sphericity, ( $\phi$ ) is a measure of the degree of roundness of a seed. It is determined by comparing the surface area of a sphere, having the same volume as the seed, to the actual surface area of the seed:

$$\phi = \frac{\text{Surface Area of Sphere}}{\text{Surface Area of Seed}} \quad (\text{Mohsenin, 1970})$$

This calculation quantifies the roundness of the seeds.

### **3.1.1.7 Roundness**

It is a measure of the edges sharpness on solid materials as described by Maduako & Hamman (2005) and Manoharan (2018), was evaluated using the equation,

$$R = \frac{Ap}{Ac}$$

Where 'Ap' is the largest projected area of the seed in its natural rest position, and 'Ac' is the area of the smallest circumscribing circle.

### **3.1.1.8 One thousand seed weight**

The weight of one thousand seeds, an important factor influencing the suction pressure required for seed pickup in planting machinery, measured using an electronic balance. A sample of one thousand seeds was randomly selected and weighed, and this process was replicated five times to ensure accuracy (Vaishnavi *et al.*, 2018).

## **3.1.2 Gravimetric properties**

The gravimetric properties of black gram and horse gram seeds, are the basis for understanding the behavior in storage and planting systems. These properties include bulk density, true density, and porosity.

### **3.1.2.1 Bulk density**

Bulk density is the mass of the seeds per unit volume. To determine the bulk density of seeds, a 10×10×10 cm box was uniformly filled with seeds. The total weight of the seeds was measured using an electronic scale with a precision of 0.01 g. This procedure was repeated 10 times, with each replication using a different sample of seeds to ensure representativeness. Bulk density ( $\rho_b$ ) was subsequently calculated as the average weight of the seeds divided by the volume of the box, employing the formula,

$$\rho_b = \frac{M}{V}$$

Where, 'M' is the mass of the seeds in grams, and 'V' is the volume of the box.

### **3.1.2.2 True density**

True density ( $\rho_t$ ) refers to the mass of the seeds per unit volume, excluding the spaces between them. The toluene displacement method, recommended by Deshpande et al. (1993), was used.

Seeds were immersed in toluene, a substance with low surface tension that does not get absorbed by the seeds. The volume of the displaced toluene, which represents the volume of the seeds, was meticulously measured.

The true density ( $\rho_t$ ) can be calculated using the formula,

$$\rho_t = \frac{W_s}{V_s}$$

Where, ' $W_s$ ' is the weight of the seeds, and ' $V_s$ ' is the true volume of the seeds in cubic meters.

### **3.1.2.3 Porosity**

Porosity ( $\rho$ ), a measure of the void spaces in a mass of seeds, was calculated using the relationship outlined by Mohsenin in 1970.

Porosity was determined by the formula,

$$\rho = \frac{(\rho_T - \rho_B)}{\rho_T}$$

Where, ' $\rho_T$ ' is the true density and ' $\rho_B$ ' is the bulk density.

## **3.1.3 Engineering properties**

The engineering properties viz., angle of repose, coefficient of friction, terminal velocity and drag coefficient were turned out to understand the handling and storage characteristics, which are essential for the efficient operation of pneumatic planters.

### **3.1.3.1 Angle of repose**

The angle of repose refers to the steepest angle at which a pile of granular material remains stable without sliding or collapsing. It determined by factors like the shape, size, and friction properties of the particle involved. To determine the angle of repose



of the seeds, a uniform experimental approach was used. Seeds were permitted to flow from a horizontally positioned rectangular box onto a circular disc until to form a stable heap. The methodology for measuring the heap parameters adhered closely to the procedures outlined by Munde (1999). The height (H) and base diameter (D) of the heap were measured to provide essential data for subsequent analysis. The angle of repose ( $\theta$ ) was calculated using the formula:

$$\theta = \tan^{-1} \frac{2H}{D}$$

This formula helped to determine the natural angle at which the seeds settled, providing insights into its flow behavior and stackability.

### ***3.1.3.2 Coefficient of friction***

The coefficient of friction is a measure of the amount of resistance between two objects as they move against each other. It quantifies the frictional force between the surfaces of the objects and is typically represented by the symbol ' $\mu$ '. A higher coefficient of friction indicates greater resistance to motion, while a lower coefficient indicates less resistance. The coefficient of friction of the seeds against various surfaces was determined using a method described by Bahnasawy (2007) and (Balasubramanian, 2001).

A sample of 250 g seeds was taken in a box, which was then positioned on various surfaces such as plywood, aluminum, galvanized iron, mild steel and stainless steel. Employing a wire-pulley system, the box was systematically pulled across each surface, and the force necessary to initiate movement was recorded. To determine the static coefficient of friction ( $\mu$ ), the frictional force was divided by the normal force. Ten trials per variety were carried out and ' $\mu$ ' was found out by using the formula.

$$\mu = \frac{F}{W}$$

Where, 'F' is the weight needed to slide the box, kg and 'W' is the weight of the seeds, kg.

### **3.1.3.3 Terminal velocity**

Terminal velocity refers to the constant maximum velocity reached by an object falling through a fluid (such as air or water) when the gravitational force pulling it downward is balanced by the opposing drag force exerted by the fluid. At terminal velocity, the net force acting on the object becomes zero, resulting in a constant velocity.

The terminal velocity of seeds was determined using an experimental setup as suggested by cetin *et al.* (2010), which comprised a vertical transparent glass tube tightly sealed between two flanges. At the bottom flange, an air flow control valve was fixed, connected to a blower for generating air flow during operation. Above the valve, a mesh weir was positioned to hold the seeds during testing. A seed was placed on the mesh, and the blower was activated, gradually increasing its speed until maximum velocity was attained. The air flow control valve was then slowly adjusted until the seeds began to float in the strong air stream. In each trial, a small sample of 10 g seeds was evenly distributed over the bottom screen. The upward air flow from beneath the weir mesh suspended the seeds in the air stream for a duration of 30 seconds. Most of the suspended seeds were carried away and collected in a designated interceptor. Any heavier seeds that fell during suspension were collected in a pan positioned beneath the vertical transparent column. The air velocity was directly measured using an anemometer once the seeds were suspended.

### **3.1.3.4 Drag coefficient**

The drag coefficient is a dimensionless quantity that quantifies the resistance an object encounters as it moves through a fluid, such as air or water. The drag coefficient depends on various factors including the shape and surface characteristics of the object, as well as the properties of the fluid. A lower drag coefficient indicates less resistance to motion through the fluid, while a higher drag coefficient indicates greater resistance. This is an important factor to analyse the aerodynamic properties of seeds. The drag coefficient was derived from various parameters including the weight of the seed, the mass density of the seed, the projected area, the terminal velocity of the seeds, and the mass density of air under standard temperature and pressure conditions. It is calculated by using an equation given by Bilanski *et al.* (1962) as

$$C_d = \frac{2W(\rho_P - \rho_a)}{V_t^2 A_p \rho_P \rho_a}$$

Where,  $C_d$  is drag coefficient;  $W$  is weight of seed (kg);  $\rho_p$  is mass density of particle ( $\text{kg s}^{-2} \text{m}^{-4}$ );  $\rho_a$  is mass density of air ( $\text{kg s}^{-2} \text{m}^{-4}$ );  $V_t$  is terminal velocity ( $\text{m s}^{-1}$ );  $A_p$  is projected area ( $\text{m}^2$ ).

### **3.1.4 Seed quality assessment**

#### **3.1.4.1 Seed viability**

The Tetrazolium (TZ) test was conducted at the laboratory of KVK, Malappuram to evaluate the viability and vigor of seeds. This test was an alternative to the germination test, offering a reliable indication of a seed potential to emerge under optimal conditions. The procedure was adopted as per the AOSA recommendations (Miller, 2005).

Tetrazolium test was conducted as follows:

Initially, the seeds were soaked overnight to soften the seed coat. Each seed was then carefully cut longitudinally to expose the embryo. A 1.0 % solution of 2,3,5-triphenyl tetrazolium chloride was prepared by dissolving one gram of the salt in distilled or tap water to make a 100 ml solution. The seeds were then immersed in this solution and placed in a water bath at 40°C for one hour. This duration was found optimal for achieving sufficient staining of the seeds. After staining, the solution was drained off, and the seeds were examined for stained and unstained embryos. Seed viability was calculated as the per centage of stained embryos relative to the total number of embryos, using the formula,

$$\text{Seed viability, percentage} = \frac{\text{Number of stained embryos}}{\text{Total number of embryos}} \times 100$$

Seeds with a viability per centage above 94 % are considered germinable and suitable for sowing.

#### **3.1.4.2 Germination test**

The germination count of seeds, particularly a batch of 100, was effectively conducted using the paper towel method, a simplicity and reliable method. This method involved several systematic steps.

Initially, relevant details about the seed sample were noted down at the middle of a paper towel. The towel was then uniformly moistened with distilled water. The moist towel was laid out on a clean, flat surface. On the side opposite to the information was written, 50 seeds are carefully placed over half of the towel. The arrangement was typically in 5 rows, with each row containing 10 seeds. A 3 cm margin was maintained from the lower and right edges of the towel. The other half of the towel was then used to cover the seeds. The right and lower portions of the towel were folded over, ensuring both ends were properly closed. The prepared towel, with the seeds inside, was rolled from one end and then wrapped in wax paper. Rubber bands were used at both ends to keep the roll secure. The rolled towel was placed vertically in a seed germinator, ensuring that the open end faces upwards.

This technique was found useful for assessing the germination potential of a variety of seeds under controlled conditions

### 3.2 SELECTION OF A PROPER SEED METERING SYSTEM

The selection of a proper seed metering system is crucial for effective seed planting, as no common system suits all planters. This decision often requires a balanced effect of various factors and sometimes used multiple metering systems for different crops, especially for diversified farming systems.

The foremost requirement is to understand the specific requirements of the crop being planted. The requirements such as the desired population density, germination rates, and field emergence levels are to be identified. Additionally, the acceptable range of row spacing, uniformity of plant spacing, and the physical properties of the seeds such as seed size, shape, and fragility are also having significant role in determining the most suitable metering system. The selected metering system shall handle the seeds gently and efficiently to ensure optimal planting results. The advantages like simplicity, cost-effectiveness and ease of adjustments or cleaning are also to be taken into account while selecting a proper seed metering system.

**Table 3.1 PoP, recommendations of KAU for planting of black gram and horse gram**

SN	Parameters	Black gram	Horse gram
1	Row to row spacing, cm	30	40
2	Plant to plant spacing, cm	15	10
3	Depth of placement, cm	4 - 5	4 - 5
4	Seed rate, kg ha <sup>-1</sup>	12	14
5	Seedbed configuration	Furrow	Furrow

The review of literature indicated that vacuum disc type metering mechanism for precision planting become more prevalent now a days especially when dealing with small and fragile seeds like black gram and horse gram. Based on the PoP, KAU recommendations as outlined in Table 3.1 it is evident that these crops require proper planting to achieve optimal yield. The black gram and horse gram seeds showed variation in size and shape. In this context, the vacuum disc type metering mechanism offering several advantages tailored to the specific needs of these seeds. Certain seed metering systems, like plate types, work the best when seeds are all the same size and shape. On the other hand, systems like vacuum disc types can handle a range of seed sizes and shapes without affecting performance (Heyns, 1989; Zulin *et al.*, 1991; Yazgi and Degirmencioglu, 2007; Liu *et al.*, 2022). By operating on the principle of vacuum suction, this system enables precise seed singulation, uniform spacing, and minimal seed damage, thereby ensuring optimal seed placement and maximizing crop yield potential (Pareek *et al.*, 2023). Additionally, its adaptability, efficiency, and ease of calibration further enhance its suitability for handling small and delicate seeds like black gram and horse gram.

### 3.3 STUDY OF THE PNEUMATIC VACUUM PLANTER

Precision planting is important to maximizing crop yields and optimizing resource use. The pneumatic vacuum planter ensures accurate seed placement. It includes a hopper to hold the seeds, a vacuum-based metering mechanism (including a seed plate, vacuum chamber, and aspirator blower) to pick up single seeds, and a seed tube to guide the seed into a furrow created by the furrow opener. Supporting components include the frame, ground wheels (which drive the metering unit), a power source (usually a tractor), and compression wheel. Additionally, the planter may feature markers for straight rows, depth control mechanisms, and hoppers for fertilizer or micro-granule application. It operates by means of cardan shaft attached to the power take off of a tractor with a three-point universal joint. In meter mechanism it has a vertically oriented rotating disc with holes around its circumference, a split housing, and an aspirator blower that generates a vacuum. Unlike the plate type metering mechanism, the seeds fall or pass through holes, the disc rotation combined with vacuum causes to pick up seeds through each hole, simplifying the singulation process. During operation, seeds attached to the holes are exposed to an adjustable wiper, ensuring one seed in one hole while others are wiped out. Proper adjustment of the wiper ensures optimal singulation, with the remaining seed carried to the base of the meter.

Several critical factors contribute to the optimal performance of this system. The size of the holes in the disc must be carefully controlled to prevent the smallest seeds from passing through or getting lodged. Maintaining the correct pressure differential is essential to hold the seeds to the disc while allowing for effective singulation. Proper adjustment of the wiper/cut-off is crucial for preventing multiple seeds or misses. Additionally, controlling the disc speed is important, as excessive speed can decrease metering performance by reducing exposure time and increasing the force needed to maintain seed adhesion. This metering system offers several advantages and adjustment options. It provides seed size flexibility, as seeds do not need to precisely match the hole size, offering versatility with different seed sizes and shapes. Seed grading is not mandatory. Furthermore, adjustments can be made to the metering rate by changing the disc speed relative to ground speed and selecting discs with varying numbers of holes.

This technology facilitates precise seed metering, crucial for achieving optimal plant spacing and uniformity.



**Plate 3.4 Vacuum seed metering mechanism**

By considering factors like seed type, planting patterns, seeding rate, and plate material, the system can be optimized for the best possible performance. Seed discs are designed with different hole sizes to accommodate a diverse range of seed types. This is essential for the system versatility, allowing it to efficiently handle different seeds without compromising on accuracy. The shape and size of the holes in the seed plate is made according to the physical properties of the seeds. This approach follows the guidelines established by RNAM in 1991, ensuring a tailored fit for each seed type. The spacing between seeds for specific crops can be varied. This is achieved by either altering the size of the ground drive wheel or changing the transmission ratio or by modifying the number of cells on the metering plate. Such flexibility, as noted by Varshney *et al.* in 2005, allows for customized planting to meet diverse crop requirements. Adjusting the spacing between the metering holes on the seed plate is crucial for achieving the desired seeding rate. Denser hole arrangements are necessary for higher seeding rates, ensuring a consistent and accurate distribution of seeds. The

material of the seed plate is an important consideration. It should be durable, able to withstand wear and tear, and be compatible with the type of seeds being used. Common materials include aluminium, and stainless steel, each offering unique benefits in terms of durability and seed compatibility.

### **3.3.1 Dynamic force analysis**

To ensure accurate seed placement, seeds were managed through a system by synchronization with the rotation of seed plate. Every single seed picked up and transported by seed cell positioned on the plate. Using negative pressure, the seed cell firmly gripped the seed against the plate surface. As the plate rotated, the seed was conveyed to a designated position where the suction was terminated. Subsequently, the seed was released and allowed to descend onto the soil surface under the influence of gravity.

The trajectory of seed movement has three stages from its initial entry into the seed lot to its release into the seed tube. These stages encompass the fulfillment phase (involving the flow into the seed lot) are pick-up phase, transporting phase, and ejecting or releasing phase. It is pertinent to note that the discernible influence of negative pressure and rotational speed manifests prominently during both the pick-up and transporting stages.

#### ***3.3.1.1 Analysis of Force on seed during pick up***

At seed pickup stage in vacuum metering mechanism, various forces acting on a single seed are shown in Fig. 3.1. Majorly five forces are acting on the seeds viz., friction force ( $F_F$ ) caused by seed plate, normal force from seed plate ( $F_N$ ), force of the negative pressure ( $F_Q$ ) caused by sucking air out from chamber by aspirator blower and centrifugal force ( $F_C$ ) possess by seed due to rotary motion and gravity force ( $G$ ) due to seed weight. As for the analogy given by Satti *et al.* (2013) in working of rotary type pneumatic device, the various forces act in equilibrium.



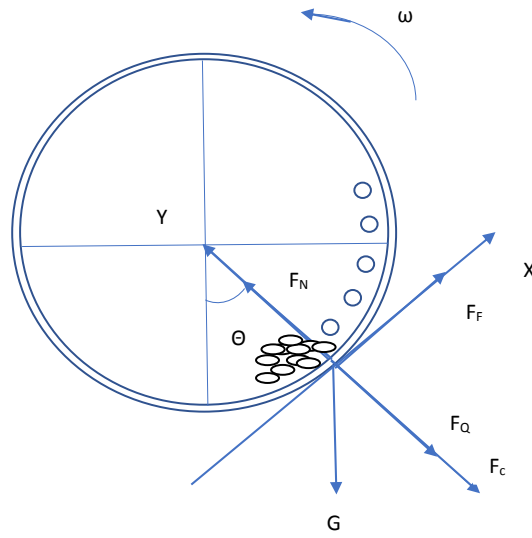


**Fig. 3.1 Forces acting on seeds during pick-up stage**

The summation of all the forces acting on the seed in X and Y direction are given below

$$\sum F_X = F_F - G \sin \theta = 0$$

$$\sum F_Y = F_N - G \cos \theta - F_Q - F_c = 0$$

The relationship between friction forces  $F_F$  and supporting normal force  $F_N$  can be given as

$$F_F = F_N \tan \alpha_f$$

Where,  $\alpha_f$  is the friction angle between the seed and seed plate.

Substituting  $F_F$  from equation

$$\sum F_X = F_N \tan \alpha_f - G \sin \theta = 0$$

$$\sum F_Y = F_N - G \cos \theta - F_Q - F_c = 0$$

From above equation a relationship was derived

$$F_N = \frac{G \sin \theta}{\tan \alpha_f}$$

Substituting  $F_N$

$$F_Q = G \frac{\sin \theta}{\tan \alpha_f} - G \cos \theta - F_c$$

The force of the negative pressure  $F_Q$  either to be greater than or equal to the forces to pick up seeds so,

$$F_Q \geq G \frac{\sin \theta}{\tan \alpha_f} - G \cos \theta - F_c$$

$$F_Q = G \frac{\cos \alpha_f \sin \theta}{\sin \alpha_f} - G \cos \theta - F_c$$

Thus,

$$F_Q = G \frac{\sin(\theta - \alpha_f)}{\sin \alpha_f} - F_c$$

Theoretical force required for seed pickup is given by

$$F_Q = C_d S \frac{\rho V_0^2}{2}$$

Where,  $C_d$  is drag coefficient;  $S$  is projected area ( $m^2$ );  $\rho$  is air density ( $kg\ m^{-3}$ );  $V_0$  is air velocity ( $m\ s^{-1}$ ).

Air velocity required to pick and held the seed against the seed cell can be calculated from the following equation

$$V_0 = \frac{Q}{2\pi R^2}$$

$$S = \frac{\pi d_s^2}{4}$$

$$G = \frac{\pi \rho_s g d_s^3}{32}$$

After substituting all the values

$$\frac{C_d \rho Q^2}{\pi^2 \rho_s d R^4 g} \geq \frac{\sin(\theta - \alpha_f)}{\sin \alpha_f} - F_c$$

Where,  $\alpha_f$  is friction angle between seed and seed rotor.

### 3.3.1.2 Analysis of force on seed during transport

The summation of all the forces acting on the seed in X and Y direction are as given below as shown in Fig. 3.2.

Subjected to the condition,  $0 < \beta \leq 90^\circ$

$$\begin{aligned}\sum F_X &= F_F - G \sin \beta = 0 \\ \sum F_Y &= F_N - G \cos \beta - F_Q - F_c = 0 \\ F_F &= F_N \tan \alpha_g \\ F_c &= m\omega^2 R_c\end{aligned}$$

Where,  $F_c$  is the centrifugal force. Thus, equation becomes

$$F_N = G \frac{\sin \beta}{\tan \alpha_f}$$

Substituting  $F_N$

$$\begin{aligned}G \frac{\sin \beta}{\tan \alpha_f} - G \cos \beta - F_c &= F_Q \\ \text{put } F_c &= m\omega^2 R_c \\ F_Q &\geq -m\omega^2 R_c + G \left( \frac{\sin \beta}{\tan \alpha_f} - \cos \beta \right)\end{aligned}$$

Or

$$F_Q = -m\omega^2 R_c + G \left( \frac{\sin \beta \cos \alpha_g - \cos \beta \sin \alpha_g}{\sin \alpha_f} \right)$$

Put  $\beta = 90^\circ$

$$F_Q = G \frac{\cos \alpha_f}{\sin \alpha_f} - m\omega^2 R_c = m \left( \frac{G}{\tan \alpha_f} - \omega^2 R_c \right)$$

The force of the negative pressure can also be given by the following equation

$$F_Q = PS = P \frac{\pi d_s^2}{4} \geq m \left( \frac{G}{\tan \alpha_f} - \omega^2 R_c \right)$$

Where,  $\tan \alpha_f$  is the friction index for the friction force  $F_F$ .

This indicates that, as the seed picked up and while in transport with the seed plate, it was influenced by many factors such as cell diameter ( $d$ ), mass of the kernel ( $m$ ), the rotational speed of rotor ( $\omega$ ), the radius of the seed plate ( $R_c$ ), the negative pressure ( $P$ ) and the friction index  $\tan\alpha_f$ .

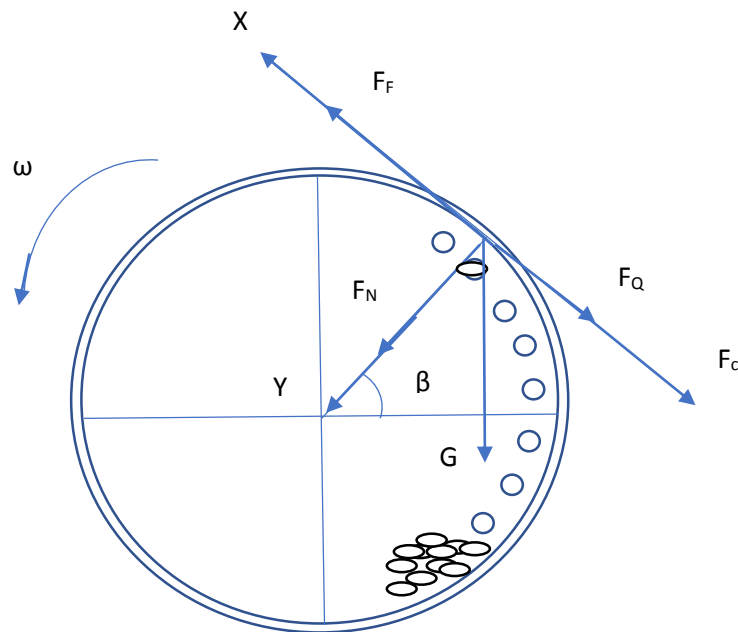


**Fig. 3.2 Forces acting on seeds during transport stage**

### 3.3.1.3 Analysis of force on seed during release

At this stage, the force of gravity ( $G$ ) and centrifugal force influence more than the force of negative pressure. Negative pressure sudden cut off and plate expose to the atmosphere. Due to decreased negative air pressure and self-weight of seed the force of gravity helps in releasing seed from seed cell and drops in to seed outlet spout.

The theoretical analysis of the forces acting on seeds under dynamic conditions assists in identifying key parameters that impact the functionality of the seed metering mechanism. This analysis highlights the significance of vacuum pressure, plate hole size, and angular velocity of the plate as crucial factors and can be selected for lab model testing at different levels.

### 3.4 MODIFICATION OF THE PLANTER

The existing pneumatic planter relies on a mechanical system, including a frame, aspirator blower, metering mechanism, hopper, furrow opener, covering device, ground wheel, and compression wheel. Mechanical power transmission systems, utilizing components such as chains, sprockets, shafts, gearboxes, bearings, and bevel gears. These mechanical systems present several disadvantages such as more weight, susceptibility to wear and tear, and power losses due to friction.

To address these limitations and enhance planter performance, the following key modifications were implemented:

- i. **Electronically controlled metering mechanism:** The mechanical power transmission system for the metering mechanism was replaced with an electronic control system. This system leverages a stepper motor for precise seed plate rotation, along with a sensor for distance measurement of planter and a microcontroller to manage the overall process.
- ii. **Seed-specific hopper design:** Hoppers were redesigned to accommodate the specific requirements of black gram and horse gram seeds, ensuring optimal seed flow and delivery.
- iii. **Furrow opener evaluation:** To assess performance under varying soil conditions, different furrow openers were tested in both tilled and no-till field.

In conventional pneumatic planters, the metering mechanism is powered by the ground wheels and transmits power through a mechanical system. The modified design seeks to improve the planter efficiency and precision by transitioning to an electronic drive system. In the modified planter, the metering mechanism operates electronically through a stepper motor for each metering mechanism, ensuring precise rotation of the plate. Another advantage electronic control seed meter mechanism is its suitability for intercropping or mixed cropping methods. In this setup, the seed-to-seed distance for each metering mechanism can be controlled independently, offering greater flexibility and precision in planting various crops simultaneously.

### 3.4.1 Integration of electronic control system in pneumatic metering system

Pneumatic metering systems, recognized for its accurate seed placement and spacing, are increasingly integrated with electronic control systems. These systems enhance the precision of vacuum pressure, seed singulation, and delivery, ensuring optimal planting efficiency.

Major components of electronic control system

- i. **Sensors:** Essential for gathering critical data like ground wheel travel distance, and vacuum pressure. Sensors include rotary encoder, pressure sensor, and proximity sensor.
- ii. **Data Acquisition System:** This system processes the data from sensors, transforming it into actionable information for the control unit.
- iii. **Control Unit:** Acting as the system brain, the control unit receives and interprets sensor data to make real-time decisions for managing the seed delivery mechanisms. Microcontrollers or embedded systems are typically employed for this purpose.
- iv. **Actuators:** Responding to the control unit commands, actuators adjust the vacuum seed metering mechanism. It includes stepper motors.

Integrating electronic control systems in vacuum seed metering offers numerous benefits, such as enhanced seed singulation for consistent seed pickup and reduced incidences of double seeding or misses.

Several factors contribute to the effectiveness and reliability of the pneumatic seed metering system with electronic control system. Firstly, the quality of sensors plays a crucial role in providing accurate and reliable information to the control unit. These sensors must be capable of delivering precise data to ensure optimal system performance. Secondly, the control algorithm must be optimized to regulate vacuum pressure, seed singulation, and delivery based on sensor inputs. An adept algorithm is essential for ensuring precise control over the seeding process. Thirdly, the performance of actuators is paramount. Actuators must be compatible with the control unit and respond swiftly and accurately to control signals to facilitate seamless operation of the system. Additionally, the system should exhibit environmental resilience, capable of

withstanding challenges such as dust, moisture, and vibrations. Robust construction and design are necessary to ensure the system operates reliably in diverse environmental conditions. Lastly, the system should feature a user-friendly interface and comprehensive operator training. An intuitive interface simplifies system operation, while thorough training ensures effective utilization of the system capabilities. Together, these factors contribute to the overall effectiveness and efficiency of the pneumatic seed metering system with electronic control unit.

### **3.4.1.1 Selection of motor**

The selection of the motor for the seed metering is crucial to ensure precise and consistent seed delivery. A stepper motor was chosen for the pneumatic seed metering mechanism due to its ability to provide precise control over speed and position. Stepper motors can rotate in precise increments, allowing for accurate control of seed spacing and placement. They are also more cost-effective compared to other options, such as servo motors.

#### **a. Calculation of rotational speed and torque for the motor**

Rotational Speed of ( $n_p$ ) can be calculated as:

$$n_p = \frac{60 \times 10^3 \times V_m}{3.6 \times S \times Z}$$

Where,

$V_m$  = Tractor forward speed (1-8 km h<sup>-1</sup>)

S = Seeding distance

Z = Number of plate holes (26)

After solving the equation, the calculated motor speed range is between 55 rpm and 140 rpm.

#### **b. Torque calculation:**

$$M_a = J \times \alpha$$

The torque ( $M_a$ ) for the seeding system is calculated using the formula  $M_a = J \times \alpha$ , where  $M_a$  represents the torque in Newton-meters (N-m). In this context,  $J$  is the total rotational inertia of the seeding system, which is  $1.668 \times 10^{-2} \text{ kg m}^2$ , calculated by using solid work. The maximum angular acceleration ( $\alpha$ ) is then used to determine the required motor torque. Based on these parameters, the calculated motor torque required was 1.852 N-m.

**c. Calculation of total torque generated by motor to rotate seed plate**

To calculate the total torque generated by the stepper motor to rotate the seed plate, we consider the effect of a bevel gear fitted inside the metering mechanism. This gear increases the torque and changes the direction of motion, helping to rotate the vertical plate.



**Plate 3.5 Bevel gear in metering mechanism**

Given:

Teeth on small gear = 10

Teeth on large gear = 25

Gear ratio = 2.5 (calculated as 25/10)



Torque input by stepper motor = 2.3 N-m

Torque output = torque  $\times$  gear ratio

$$= 2.3 \times 2.5$$

$$= 5.75 \text{ N-m (58.65 kilogram-cm)}$$

### **3.4.2 Electronic components of the system**

The system comprises of a stepper motor, micro-step drive, microcontrollers, encoder and sensors. The details of the above items are briefly explained below.

#### ***3.4.2.1 Stepper motor***

Stepper motors are brushless, synchronous electric motors that convert digital pulses into precise, incremental shaft rotations. This allows for accurate positioning and speed control without the need for feedback sensors. As a two-phase stepper motor, integrates seamlessly into various applications demanding precise motion control.



**Plate 3.6 Stepper motor**

**Table 3.2 Technical specifications of the stepper motor**

<b>Parameters</b>	<b>Details</b>
Model Number	57CM23-3A
Motor Type	Hybrid Stepper Motor
Phase	2
Frame Size	NEMA 23
Holding Torque	2.3 N·m (326 oz-in)
Phase Current	3 A
Step Angle	1.8 degrees
Shaft Diameter	8 mm (0.315 inch)
Motor Length	76 mm (2.99 inches)
Voltage	<100 V

The features of the stepper motor include high torque coupled with low noise and vibration levels, precision engineering for high accuracy, and efficiency marked by low heat generation. The benefits of integrating this system are manifold, including enhanced precision and accuracy in applications, improved efficiency and productivity, and reduced maintenance costs, all contributing to an extended motor life.

#### ***3.4.2.2 Micro-step Drive***

A micro-step drive is an electronic controller for stepper motors that divides each full step into smaller increments. It designed with advanced DSP-based control algorithms, is having capable of driving 2-phase and 4-phase hybrid stepper motors. This fully digital drive is versatile and suitable for various demanding applications.

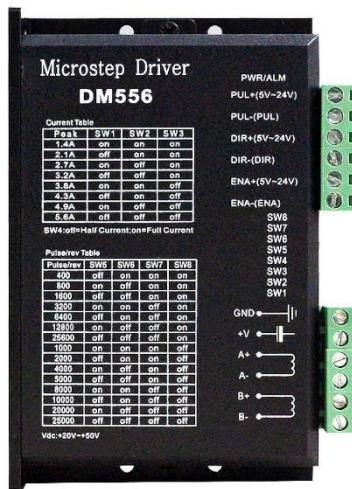


**Plate 3.7 Micro-step driver DM556**

**Table 3.3 Technical specifications of the micro-step drive**

Parameters	Details
Input Voltage	20-50 VDC
Output Current	0-5.6 A
Micro-stepping Resolution	Up to 25000 steps/rev
Pulse Input Frequency	Up to 200 KHz
Protection	Overvoltage, overcurrent, short-circuit
Dimensions	110 mm x 86 mm x 60 mm
Weight	0.7 kg
Other Features	Automatic idle-current reduction, TTL compatible and optically

This system delivers high performance and accuracy, ensuring smooth and quiet operation with minimal vibration.

### 3.4.2.3 PCB with Microcontrollers

Printed Circuit Boards (PCBs) are fundamental components in modern electronics, serving as the backbone for electrical connectivity in devices ranging from smartphones to automobiles. Composed of an insulating substrate with conductive copper tracks, pads, and vias, PCBs enable electrical connections without wires. A standard PCB comprises the following elements:

- Substrate: The base material, often FR-4, FR-2, or CEM-1, providing structural support.
- Copper Tracks: Conductive pathways for electrical connections between components.
- Pads: Points where components are soldered to the board.
- Vias: Holes that link different layers of copper tracks.
- Solder Mask: A protective layer, typically green, guarding against corrosion.
- Silkscreen: Labels for component identification.

### Microcontroller

Components are soldered onto the pads, forming robust electrical connections. Integration of Arduino Nano microcontrollers. This PCB is uniquely equipped with three Arduino Nano microcontrollers, each serving distinct functions:

- Arduino Nano 1: The primary controller, managing overall PCB functions and coordinating other microcontrollers.
- Arduino Nano 2: Dedicated to sensor data management, interfacing with different sensors.
- Arduino Nano 3: Controls actuators such as motors, LEDs, and servos.

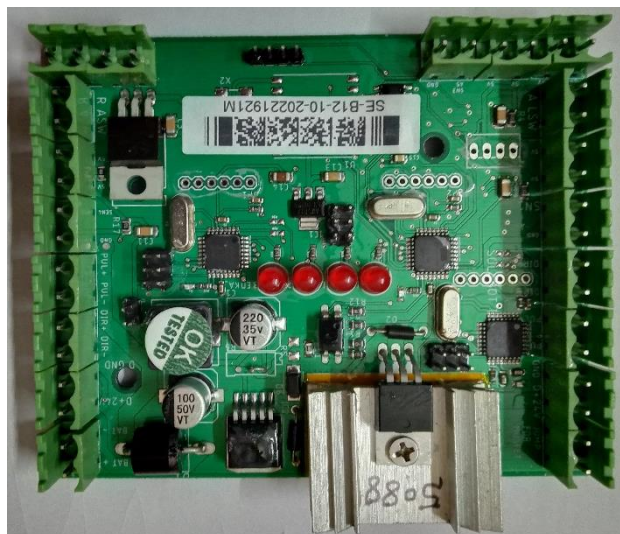


**Plate 3.8 PCB control board**

Additional components on the PCB are as follows:

- i. **Voltage Regulators:** These components play a crucial role in maintaining a stable power supply for microcontrollers and other sensitive electronic components on the PCB. By converting varying input voltages into a consistent output level, voltage regulators protect the system from fluctuations and ensure reliable performance.
- ii. **MOSFETs:** As power switching devices, MOSFETs control the actuators on the PCB. Their ability to handle high currents and voltages makes them ideal for driving motors, valves, or other electromechanical components that require precise control from the circuit board.
- iii. **Resistors, Capacitors, Crystals, and Headers:** Resistors act as current limiters, protecting components from excessive electrical flow. Capacitors smooth out power fluctuations and filter noise, promoting stability. Crystals provide an accurate clock signal essential for the timing and synchronization of the microcontrollers. Headers offer connection points for external devices, enhancing the PCB's functionality and adaptability.

The PCB incorporates several user-friendly features for simplified operation and troubleshooting. These include 6-pin connectors for convenient power supply and microcontroller programming, reset buttons allowing easy microcontroller restarts, and LED indicators that offer instant visual feedback on the PCB and microcontroller status. In summary, PCBs form the foundation of electronics, providing the wiring for components. This particular PCB uses three Arduino Nano microcontrollers for control, sensing, and actuation. Additional components and user-friendly features enhance its functionality and ease of use.

### 3.4.2.4 Rotary encoder

A rotary encoder is an electromechanical sensor that converts the angular position or rotation of a shaft into digital or analog signals. A 2500 PPR incremental optical rotary encoder is a high-resolution sensor that generates 2500 pulses per revolution (PPR) and three-channel output (A, B, and Z) for accurate angle and direction detection. The use of incremental encoding provides reliable relative position information. Its optical design ensures non-contact sensing, which is essential for wear-free and dependable operation. The compact size of the device makes it ideal for applications where space is limited. Additionally, it boasts IP54 protection, making it resistant to dust and water, thus suitable for use in harsh environmental conditions.



**Plate 3.9 Rotary encoder (2500 PPR)**

**Table 3.4 Technical specifications of the rotary encoder**

Parameters	Details
Company & Model no.	The Orange 2500 PPR ABZ 3-Phase Incremental
Power Supply	DC 5V $\pm$ 5 %
Current Consumption	$\leq$ 30 mA
Output Signal	A, B, Z (TTL level)
Pulse Width	$\geq$ 500 ns
Operating Temperature	-20 °C to + 85 °C
Shaft Diameter	6 mm
Shaft Length	20 mm
Output Cable Length	2 m

### 3.4.2.5 Proximity sensor

A proximity sensor is designed to identify the presence of objects in its vicinity without requiring any physical contact. It operates by emitting an electromagnetic field or a beam of electromagnetic radiation, such as infrared, ultrasonic, capacitive and monitors for alterations in this field or the returning signal. These changes in the signal are then interpreted as the detection of an object. Among the various types of proximity sensors, inductive proximity sensors are particularly notable. These sensors function by generating an electromagnetic field and detecting any modifications in this field caused by the proximity of a conductive object.



**Plate 3.10 Proximity sensor**

**Table 3.5 Technical specifications of the proximity sensor**

Parameters	Details
Model	Autonics PR 12-4DN
Sensor Type	Inductive proximity sensor
Sensing Distance	4 mm
Target Material	Ferrous metals
Output Type	PNP Normally Open (NO)
Supply Voltage	22-24 V DC
Current Consumption	Max 200 mA
Response Time	500 $\mu$ s
Repeatability	$\pm$ 10 %

Protection Rating	IP67
Connector Type	M12 3-pin connector

---

### 3.4.2.6 Vacuum pressure sensor

It is an electronic device used to measure pressures below atmospheric pressure across a range of applications, such as pneumatic systems, vacuum pumps, and process control systems. It has high accuracy and stability.



**Plate 3.11 Vacuum pressure sensor**

**Table 3.6 Technical specifications of the vacuum pressure sensor**

Parameters	Details
Manufacturer	Flyrobo
Sensor Type	Piezoresistive
Pressure Range	-100 kPa to 0 kPa (absolute pressure)
Accuracy	±1 % of full scale (F.S.)
Sensitivity	100 mV/kPa
Operating Temperature Range	-20°C to +80°C
Supply Voltage	5V DC
Output Signal	0.5V to 4.5V DC (ratiometric)
Response Time	≤10 ms
Connection Type	G1/4" threaded fitting



### 3.4.2.7 ESP32

The ESP32, renowned for its affordability and low power consumption, is a highly capable System on a Chip (SoC) microcontroller. It seamlessly integrates Wi-Fi and Bluetooth functionalities, making it a popular choice for a myriad of applications ranging from Internet of Things (IoT) devices and wearables to home automation systems and industrial controls.

The ESP32 with its powerful dual-core Tensilica LX6 microprocessor, capable of speeds up to 240 MHz, making it suitable for complex applications. It offers robust wireless connectivity, featuring built-in Wi-Fi (IEEE 802.11 b/g/n) and Bluetooth (v4.2 BR/EDR and BLE), enabling seamless communication with other devices and networks. Designed for energy efficiency, its ultra-low power consumption mode, with deep sleep states consuming as little as 5  $\mu$ A, is ideal for battery-operated and sensitive applications. The ESP32 also boasts a wide range of peripherals, including GPIOs, ADCs, DACs, capacitive touch sensors, UARTs, SPIs, and I2Cs, enhancing its versatility in electronic interfaces. Additionally, it supports multiple programming languages like C, C++, and MicroPython, offering flexible and accessible development options for various developers.



**Plate 3.12 ESP32**

**Table 3.7 Technical specifications of the ESP32**

Parameters	Details
Processor	Dual-core Tensilica LX6 microprocessor
Clock Speed	Up to 240 MHz
SRAM	520 KB
ROM	448 KB
Flash Memory	Up to 4 MB
Wi-Fi	IEEE 802.11 b/g/n
Bluetooth	Bluetooth v4.2 BR/EDR and BLE
Operating Voltage	3.3 V
Operating Temperature Range	-40 °C to + 85 °C
Package Type	QFN48 (4 x 4 mm)

**3.4.2.8 Battery and charger**

LiFePO4 batteries were used in this study. They are used in the applications where reliability and safety are paramount, such as in electric vehicles, medical devices, and backup power systems. Benefits of these batteries include a long lifespan, high safety level, impressive low-temperature performance, low self-discharge rate, high energy density, and recyclability.



**Plate 3.13 Lithium iron phosphate battery**

**Table 3.8 Technical specifications of the battery**

<b>Parameters</b>	<b>Details</b>
Nominal voltage	25.6 V
Capacity	12 Ah
Power	307.2 Wh
Cycle life	5000 cycles
Operating temperature	-20°C to 60°C
Dimensions	26 × 7 × 6 cm
Weight	400 g

To charge the battery a charger of 24 V, 3 A used specifically needed for charging Lithium Iron Phosphate battery designed to safely and efficiently charge. The charger is equipped with automatic voltage and current adjustment, coupled with overcharge and short circuit protection. It also includes LED indicators to display charging status. Compact and lightweight in design, this charger is both easy to transport and store.

### **Power Consumption**

To determine the power consumption of the electronic system, particularly focusing on the stepper motors, the following calculations were performed:

i. **Maximum power consumption for one stepper motor:**

The maximum power consumption for a single stepper motor was found as 40 Wh.

ii. **Power consumption for four stepper motors:**

For four stepper motors, the total power consumption is:

$$4 \times 40 \text{ Wh} = 160 \text{ Wh}$$

iii. **Maximum Battery Power:**

The battery used is a 25.6 V, 12 Ah Lithium Iron Phosphate battery.

The total energy capacity of the battery is calculated using the formula:

$$\text{Power} = V \times I$$

Substituting the given values:

$$25.6 \text{ V} \times 12 \text{ Ah} = 307.2 \text{ Wh}$$

iv. **Working time for stepper motors after one full charge:**

The working time for the stepper motors, given the battery total capacity and the motors power consumption, is calculated as follows:

$$\frac{\text{Battery capacity}}{\text{Total power consumption}} = \frac{307.2 \text{ Wh}}{160 \text{ Wh}} = 1.92 \text{ hours}$$

For simplicity, this is approximated to 2 hours.

Thus, after a full charge, the battery can power the four stepper motors for approximately 2 hours.



**Plate 3.14 Charger**

**Table 3.9 Technical specifications of the charger**

Parameters	Details
Brand	DigiTech
Model	E-bike Charger
Power	307.2 Wh
Output Voltage	24 V
Output Current	3 A
Cut-off Voltage	29.2 V

All electronic components, such as the PCB and step drive, are housed in a weatherproof enclosure made of ABS plastic, measuring 380 x 190 x 130 mm. This enclosure is both dust-tight and watertight, boasting an IP 66/67 rating. Additionally, its IK 07 rating signifies its resilience to impacts up to 5 joules, equivalent to a 1.7 kg object dropped from 300 mm. ABS plastic, chosen for its strength, lightweight nature, and resistance to corrosion and chemicals, is also cost-effective, making it an ideal material for such durable enclosures. These international protection ratings confirm the enclosure robustness against environmental factors and mechanical impacts, ensuring the safety and durability of the contained electronics at the agriculture field.

### 3.5 WORKING OF THE ELECTRONIC SYSTEM

The electronic system for the vacuum seed metering mechanism in a pneumatic planter integrating several components. These include a stepper motor, rotary encoder, proximity sensor, a printed circuit board (PCB) equipped with an Arduino Nano microcontroller, a vacuum pressure sensor, a micro-step drive for the stepper motor, a battery, and a protective box. The primary objective of this system is the precise rotation of the metering plate, which is crucial for accurate seed placement.

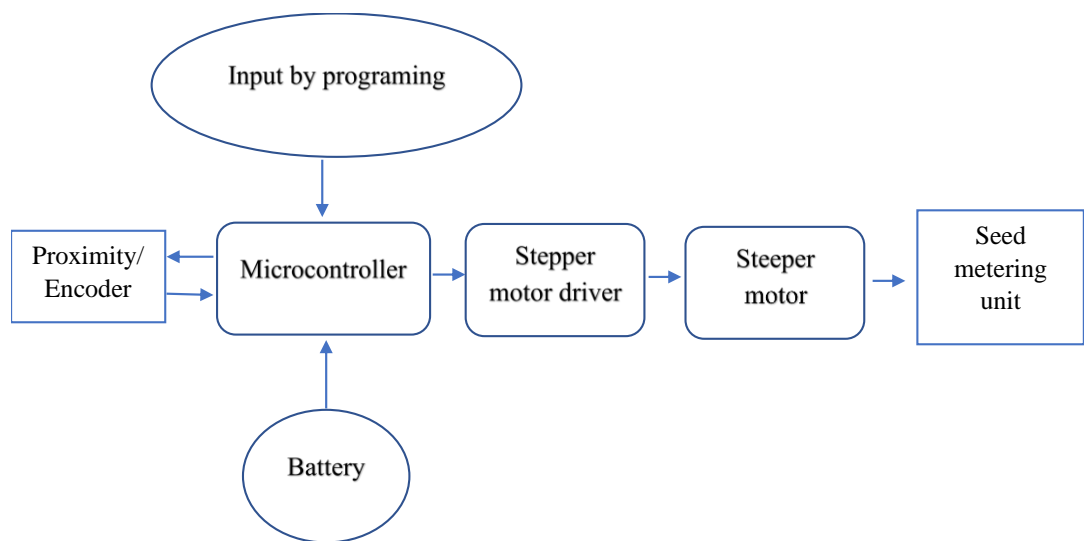


**Fig. 3.3. Power flow diagram of the electronic control circuit**

The metering plate has 26 holes, and the system task is to ensure rotation appropriately to align with these holes for seed dispensing. The precise distance traveled by the planter is crucial and is monitored using two types of sensors, namely a proximity sensor and a rotary encoder.

- i. **Proximity sensor functionality:** This sensor plays a pivotal role in detecting spokes attached to the planter wheel. As the wheel rotates, the sensor senses the spokes and relays this information to the PCB.
- ii. **Rotary encoder application:** The rotary encoder provides detailed feedback on the position and speed of the wheel, enhancing the precision of the seed dispensing process.

The PCB, embedded with an Arduino Nano microcontroller, receives signals from both sensors. It processes these inputs according to pre-flashed programming, dictating

the subsequent actions of the stepper motor. The microcontroller serves as the central processing unit, interpreting sensor data and coordinating the system responses.

Instructions from the PCB are conveyed to the microstep drive, which then precisely controls the stepper motor. The stepper motor, directly affixed to the shaft, rotates the metering plate with exact increments. This ensures that the seed-to-seed distance is consistently maintained throughout the operation, vital for uniform seed spacing.

The entire assembly is powered by connecting a battery to the system. The operational commencement is contingent upon the vacuum sensor detecting a predetermined vacuum level within the metering mechanism. This ensures that the system only activates when optimal conditions for seed metering are met.

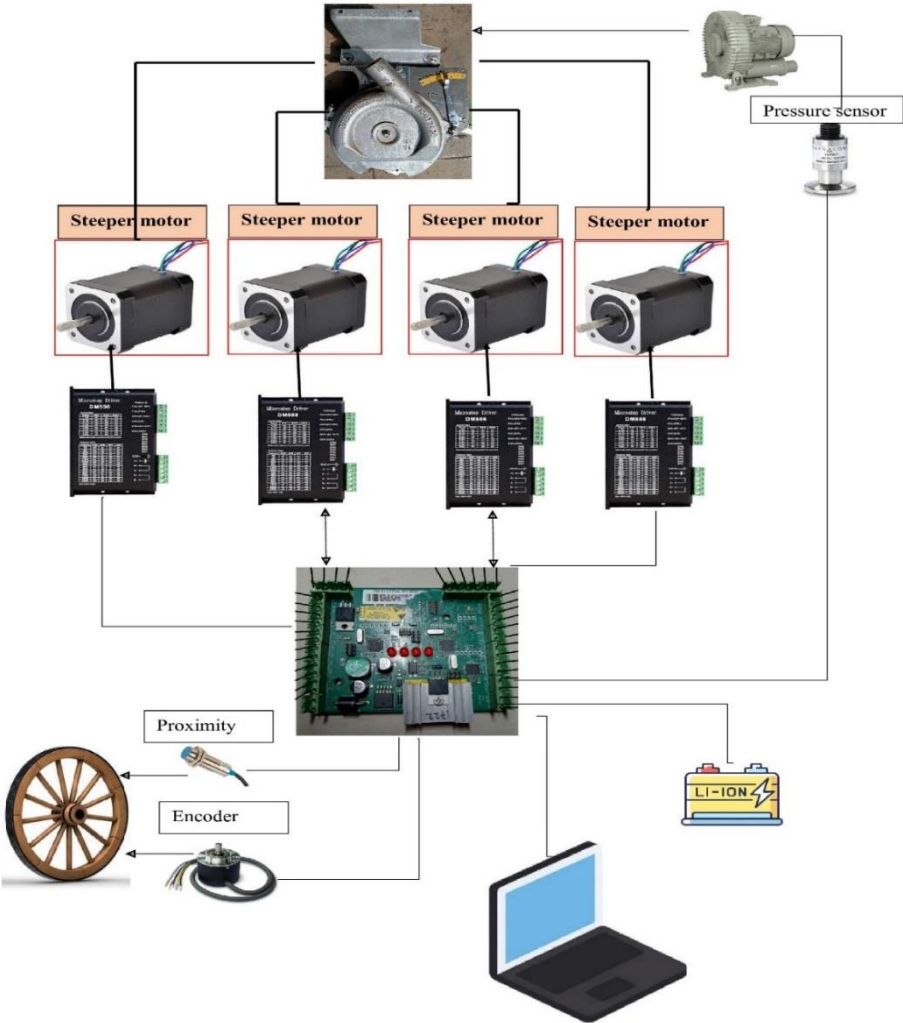


**Fig. 3.4 Block diagram of the electronic unit**

In laboratory settings, both the proximity and rotary encoder sensors are tested individually to ascertain their effectiveness and precision in this specific application. This comparative analysis is critical to determining the most suitable sensor for achieving high accuracy in seed distribution within the pneumatic planter system.

Optimization strategies include

- i. Sensor calibration: Calibrating the sensors regularly ensures accurate distance measurements and consistent seed spacing.
- ii. Software optimization: Refining the Arduino Nano programming can optimize system performance and improve seed metering precision.
- iii. Hardware: Using higher-resolution encoders or powerful micro-step drives, enhanced system accuracy and reliability.
- iv. Environmental considerations: Protecting the system from dust, moisture, and extreme temperatures extend its lifespan and maintain optimal performance.

The development of this electronic system for a pneumatic planter represents a sophisticated integration of various components, each contributing to the overall efficiency and precision of the seed planting process. The system design not only focuses on accurate seed placement but also incorporates mechanisms for ensuring reliability and consistency in diverse planting environments.

### 3.6 LABORATORY SETUP

The experimental set up under laboratory testing was to analysis the performance of the electronically controlled vacuum seed metering mechanism for the selected seed of black gram (VBN-6) and horse gram (KS-2)

Testing and optimization of the electronically driven seed metering unit for the planter was carried out using a specialized sticky belt system. This experimental setup included a durable nylon conveyor belt with dimensions of 6000 mm in length, 400 mm in width, and a thickness of 2 mm, designed to function as an endless sandwich-type conveyor. The core structure of the setup was a made with a rectangular frame of  $3.0 \times 0.85$  m size using  $40 \times 40 \times 3$  mm galvanized iron (GI) square pipe. This frame was positioned at a height of 0.9 m above the ground level, to ensure optimal ergonomic benefits for observers, allowing easy monitoring and recording the observations. The frame was strengthened by  $50 \times 50 \times 5$  mm MS angles, affixed on all four sides. To facilitate smooth rotation of the belt, a pair of rollers, of  $\text{Ø } 80$  mm, was fixed. These rollers were supported at both ends of the rectangular section by self-aligning bearings, to ensure efficient and consistent movement. The rollers were mounted on shafts  $\text{Ø } 20$  mm.

A 1.0 hp AC motor, was used as the prime mover for the setup. It was linked through a chain and sprocket system. To regulate the belt linear speed with precision, the AC motor was equipped with a variable frequency drive. This allowed for fine-tuning of the belt speed as per the requirements of the metering process. Also, it enabled precise regulation of electric motor speed and torque. By adjusting the frequency and voltage of the electrical supply to the motor, the VFD offer seamless control over rotational speed, allowing motors to operate at varying speeds, from slow to maximum rated speed.

A side channel vacuum pressure blower of compact design and lightweight was fitted to produce sufficient vacuum inside the seed meter mechanism.





**Plate 3.15 Side channel vacuum pressure blower**

**Table 3.10 Technical specifications of the Vacuum blower**

<b>Parameters</b>	<b>Details</b>
Model	PTBSC-100
Power supply	Single-phase 220 V or three-phase 380 V
Motor power	1 HP
Maximum pressure	250 mbar
Maximum vacuum	180 mbar
Flow rate	120 to 180 m <sup>3</sup> h <sup>-1</sup>
Noise level	Less than 65 dB
Weight	15.5 kg
Dimensions (L x W x H)	400 mm x 260 mm x 250 mm

### **3.6.1 Experimental setup**

The seed metering mechanism was mounted onto a sticky belt using a robustly constructed frame made of rectangular MS pipes. The metering mechanism was affixed at the center of the frame using an M.S. rectangular section with three adjustable holes positioned at varying heights to allow for a telescopic adjustment of the vertical distance between the mechanism and the sticky belt. A vacuum system was connected to the

seed metering mechanism. This setup is an assembly of galvanized iron (GI) pipes, plastic pipes, steel collars, and GI nipples to create a vacuum within the metering mechanism. A vacuum pressure gauge and a vacuum sensor were fitted to monitor the vacuum pressure, and a vacuum relief valve was fitted to regulate the pressure as and when required. A stepper motor was installed and coupled with the shaft of the metering mechanism. Additionally, spokes were attached to the roller of the sticky belt, with a proximity sensor positioned in front of it, to maintain a gap of less than 4 mm. A rotary encoder was also installed on the roller shaft. These sensors, along with the motor, were interconnected with an electronic system comprised of a microcontroller and a step drive, all powered by a lithium iron phosphate battery.

**Table 3.11 Details of the experiments**

Sl. No.	Parameters	Levels	Responses	
1.	Seeds	i.	Black gram	Seed spacing, (cm)
		ii.	Horse gram	Miss index, ( %)
2.	Sensors	i.	Proximity	Multiple index, ( %)
		ii.	Rotary encoder	Quality of feed index ( %)
3.	Plate hole size in diameter (mm)	i.	2.1	Precision of spacing
		ii.	2.5	
4.	Vacuum pressure (kPa)	i.	3.0	
		ii.	4.0	
		iii.	5.0	
5.	Planter operating speed (km h <sup>-1</sup> )	i.	1.0	
		ii.	2.0	
		iii.	3.0	

\* Planter operating speed is the grease belt speed or forward speed for planter

Treatments =  $2 \times 2 \times 2 \times 3 \times 3 = 72$

Replications = 3

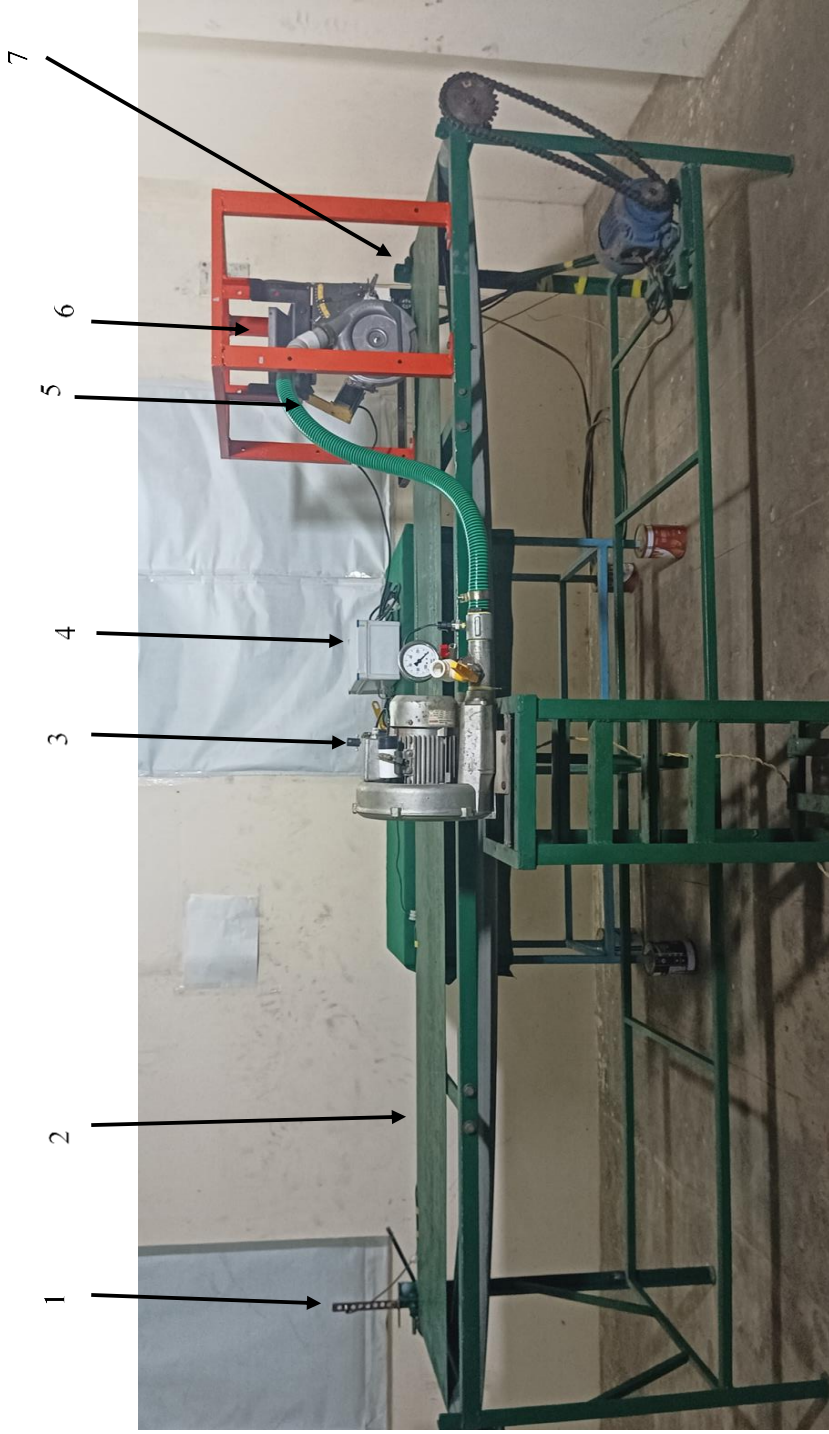
Total no. of experiments:  $72 \times 3 = 216$

In order to assess the impact of different variable levels on the evaluation parameters, a statistical approach was employed. Experimental data underwent analysis

using a factorial completely randomized design. Statistical software Design Expert 13, was utilized for the data analysis.

### **3.6.2 Testing**

Initially, a metering plate was installed within the vacuum metering mechanism. The hopper was filled with clean seeds. The vacuum system was then activated, and the pressure was adjusted to the desired level using a pressure vacuum relief valve. The battery was connected to the electronic system, ensuring all components function correctly. Spokes were attached to the roller shaft. The distance of the proximity sensor from the spokes was checked. The sticky belt motor, linked to a Variable Frequency Drive (VFD), was switched on. The VFD was calibrated to achieve the required linear speed on the sticky belt and verified with a tachometer. After calibration, the entire system was ready for testing. The grease-coated belt allowed one full rotation, after that both the belt and metering mechanism were halted. The distance between seeds (spacing of seed placement) on the belt was measured. The performance of the metering mechanism was analyzed by finding the missing index, multiple index, and quality of feed index. Each test was replicated three times to eliminate experimental errors. The same process was repeated thrice for all treatment combinations to investigate the individual and interactive effects of the independent parameters on the performance indices. The above process was for proximity sensor. For a rotary encoder, instead of a proximity sensor, used a rotary encoder attached directly to the shaft to measure the speed and distance of the belt.



1. Proximity sensor
2. Sticky belt
3. Vacuum pressure blower
4. Electronic control system
5. Stepper motor
6. Seed metering mechanism
7. Rotary encoder

**Plate 3.16 Experimental setup for testing of seed metering mechanism  
with electronic control system**

### **3.6.3 Performance evaluation of the metering mechanism with electronic control system under laboratory condition**

The performance parameters of the metering mechanism, viz., mean seed spacing, miss index, multiple index, quality of feed index, and precision of spacing, were found out using standard equations as explained below. The calculations were derived from the spacing between seeds, referencing studies by Singh et al. (2005) and Kachman and Smith (1995).

#### **3.6.3.1 Mean seed spacing**

The mean seed spacing ( $D$ ), representing the mean distance between consecutive seeds in a row, was determined using the equation

$$D = \frac{\sum S_a}{N}$$

Where, ' $S_a$ ' is the actual spacing between two seeds, and ' $N$ ' is the total count of observations.

#### **3.6.3.2 Miss index**

The miss index ( $I_{miss}$ ) is defined as the per centage of spacing exceeding 1.5 times the recommended spacing (Singh *et al.*, 2005; Madhu Kumar, 2017). It was calculated by using the equation,

$$I_{miss} = \frac{n_1}{N}$$

Where, ' $n_1$ ' denotes the number of spacing greater than 1.5 times the recommended spacing, and ' $N$ ' is the total number of spacing measured.

#### **3.6.3.3 Multiple index**

The multiple index ( $I_{multi}$ ) is defined as the per centage of spacing that are less than or equal to half of the recommended spacing (Singh *et al.*, 2005; Madhu Kumar, 2017) and calculated by using the equation

$$I_{multi} = \frac{n_2}{N}$$

Where, ' $n_2$ ' represents the count of spacing that are less than or equal to half of the recommended spacing.

#### **3.6.3.4 Quality of feed index**

The quality of feed index ( $I_{QFI}$ ) reflects the per centage of seed spacing falling between 0.5 and 1.5 times the theoretical seed spacing (Kachman and Smith, 1995), and calculated by the equation,

$$I_{QFI} = 100 - (I_{\text{miss}} + I_{\text{multi}})$$

Where,

$I_{QFI}$  = per centage of quality of feed index.

### **3.6.3.5 Precision in spacing**

Precision in spacing ( $I_p$ ) measures the coefficient of variation (CV) which, accounts for variations caused by both multiples and misses (Kachman and Smith, 1995). More specifically, CV is calculated by dividing the standard deviation of seed spacing by the mean spacing between seeds. It is represented as a decimal value, where lower value indicates more precise seed spacing. This precision metric can fluctuate based on factors such as crop type, seed discs, planting conditions, and varying ground speeds. To ensure optimal planter performance, it has to assess regularly the ground population and spacing. Precision in spacing is calculated as:

$$I_p = \frac{S_d}{s}$$

Where, ' $S_d$ ' is the standard deviation of spacing that are more than half but not more than 1.5 times the recommended spacing.

Interpreting CV values helps in assessing planting quality, a CV of 0 % implies perfect uniformity in spacing, 0-20 % is considered excellent, 20-30 % very good, 30-35 % good, 35-40 % acceptable, and 40-50 % poor. Additionally, seed germination rates directly influence CV values. For instance, with a 1 % non-germination rate, achieving a CV of 10 % is challenging, and a 5 % non-germination rate typically results in a CV exceeding 20 % (Bozdogan., 2019).

### **3.6.3.6 Visible Seed Damage**

The per centage of visible seed damage, was evaluated by the physical inspection conducted on the seeds discharged outlets of the metering mechanism. This process involved identifying and counting seeds that exhibited noticeable damage when observed with the naked eye. The calculation for determining the visible seed damage per centage is as follows:

$$\text{seed damage (\%)} = \frac{\text{total no. of seed damaged}}{\text{total no. of seed delivered}} \times 100$$

### 3.7 DESIGN OF THE MAJOR COMPONENTS OF THE PROTOTYPE

The design of major components such as furrow openers, seed hopper, seed plate and ground wheel are discussed here

#### 3.7.1 Design of inverted T-type furrow opener

The inverted T-furrow opener is used to direct sowing of seeds under un-ploughed soil conditions. The furrow opener makes a narrow slit, does not cause too much disturbance and promotes plant emergence under no tillage conditions.

The developed no till pneumatic planter utilizes an inverted T-type furrow opener is shown in Fig. 3.5 to make narrow slit without much soil disturbance. The working face and lower portion of the blade is coated with hard surfacing electrode to provide enough hardness in order to prevent the edges from excessive wearing. This increases the useful life of the furrow opener blade. After welding it was grinded to obtain V-shape sharp working edge. Both sides of the blade were also hard surface to provide strength. A 45 mm wide bottom plate and 5 mm thick, 60 mm long stiffener is provided at the back of the furrow opener to avoid buckling of the blade. The depth of cut can be adjusted by adjusting the holes provided in the shank and rake angle of the furrow opener.

The inverted-T furrow openers were fitted on with a universal-type single bolt clamp, able to be adjusted to achieve the desired depth of seeding. The rake angle of the furrow opener is 55 degree with hollow shank type. The length of furrow opener is 32.5 cm with shank.

The details of inverted-T type furrow opener, dimensions are listed below.

#### The draft load on the inverted T-type furrow opener

Now, the depth of seed planting in the bottom of furrow,

$$w = 6 \text{ cm}$$

$$w_1 = 2.5 \text{ cm}$$

$$d = 10 \text{ cm}$$

$$k = 0.41 \text{ kg cm}^{-2} \quad (\text{Kepner } et \text{ al.}, 1987)$$

where,  $w$  = Width of furrow opener;  $w_1$  = Width of strip;  $d$  = depth of the furrow;

k = unit draft

After, putting the values in equation

$$D_f = 0.41 \times \left[ \frac{(6+2.5)}{2} \right] \times 10$$

$$D_f = 17.43 \text{ kgf}$$

Factor of safety for mild steel tyres is 2. Therefore, design draft of furrow opener would be

$$= D_f \times \text{factor of safety}$$

$$= 17.43 \times 2$$

$$= 34.85 \text{ kgf}$$

Since the developed planter has four furrow openers, therefore, the total draft for all the four-furrow openers would be determined as:

$$\text{Total draft} = 34.85 \times 4$$

$$= 139.4 \text{ kgf (1.37 kN)}$$

The designed draft of the planter would be 1.37 kN

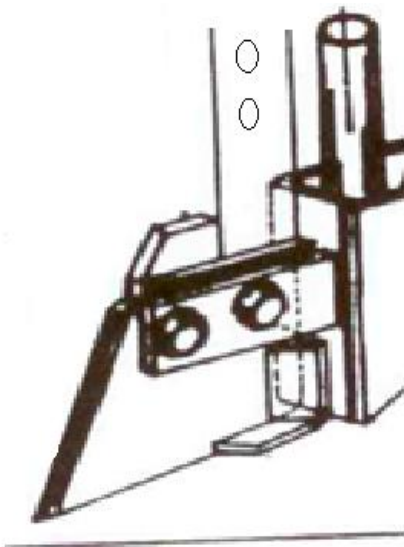


**Fig. 3.5 Inverted t-type furrow opener**



### **Design of shank of the inverted T-type furrow opener**

Now, consider the furrow opener cantilever tine as a cantilever beam of 650 mm size fixed to the frame at one end (Krutz *et al.*, 1984).

Then, the maximum bending moment in the tine is given by,

$$\begin{aligned} M &= \text{Design draft (kg)} \times \text{Beam span (cm)} \\ &= 34.85 \times 65 \\ &= 2,265.25 \text{ kg-cm} \end{aligned}$$

### **Inverted T-type furrow opener shank**

An inverted T-type furrow opener was fitted at one end of the shank and the section modulus of the shank was computed using classical flexure formula as given below.

$$f_b = \frac{M_b Y}{I}$$

Where,  $f_b$  = bending stress,  $\text{kgf cm}^{-2}$ ;  $M_b$  = bending moment,  $\text{kgf-cm}$ ;  $Y$  = distance from the neutral axis to centre line,  $\text{cm}$ ;  $I$  = moment of inertia for rectangular cross-section about the neutral axis,  $\text{cm}^4$

From the above equation section modulus was given below

$$z = \frac{I}{Y} = \frac{M_b}{f_b} = \frac{db^2}{6}$$

$$M_b = D_d L$$

Where  $D_d$  = design draft ( $\text{kgf}$ ) which is kept 3 to 5 times of actual draft for safety point of view. A factor of safety of 5 has been considered for this design

$L$  = length of shank

Actual draft =  $k_o A$

Where,  $k_o$  = soil resistance,  $\text{kgf cm}^{-2}$ ;  $A$  = cross- section area of furrow,  $\text{cm}^2$

Therefore,  $M_b = 5 k_o A L$

Here the length of shank ( $L$ ) = 30 cm

Area of cross-section of furrow =  $4.0 \text{ cm}^2$

fb for mild steel rectangular cross-section =  $1000 \text{ kgf cm}^{-2}$

It is assumed that  $b:d = 1:4$  or  $d = 4b$

$$b^3 = 0.98$$

$$b = 0.99 \text{ cm say } 10 \text{ mm}$$

Therefore,  $d = 40 \text{ mm}$

Standard MS flat of size  $40 \times 10 \text{ mm}$  size was used for fabricating the shank of furrow opener and the standard MS flat is  $600 \times 50 \times 15 \text{ mm}$  was selected for the furrow opener.

### 3.7.2 Design of shoe type furrow opener

The details of shoe type furrow opener, its tyne and various dimensions are listed below.

#### The draft load on shoe type furrow opener

Now, the depth of seed planting in the bottom of furrow,

$$w = 15 \text{ cm}$$

$$w_1 = 15 \text{ cm}$$

$$d = 5 \text{ cm}$$

$$k = 0.41 \text{ kg cm}^{-2} \quad (\text{Kepner } et \text{ al.}, 1987)$$

Therefore, putting the values in equation (3.13), we get

$$D_f = 0.41 \times \left[ \frac{(15+15)}{2} \right] \times 10$$

$$D_f = 61.5 \text{ kgf}$$

Then, we can take factor of safety of 2 for mild steel tynes. Therefore, design draft of furrow opener would be

$$= D_f \times \text{factor of safety}$$

$$= 61.5 \times 2$$

$$= 123 \text{ kgf} = 1.2 \text{ kN}$$

Since the developed planter has four furrow openers, therefore, the total draft for all the four-furrow openers would be determined as:

$$\begin{aligned} \text{Total draft} &= 123 \times 4 \\ &= 492 \text{ kgf (4.8 kN)} \end{aligned}$$

The designed draft of the planter would be 4.8 kN

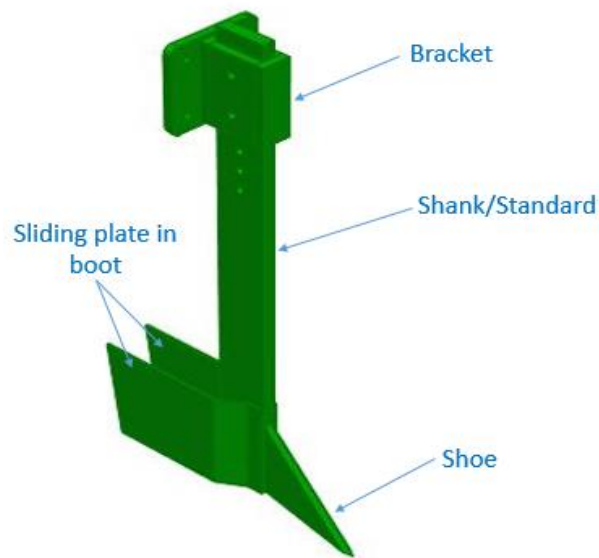


**Fig. 3.6 Shoe type furrow opener**

#### **Design of shoe type furrow opener shank**

Now, consider the furrow opener cantilever tine as a cantilever beam of 650 mm size fixed to the frame at one end (Krutz *et al.*, 1984).

Then, the maximum bending moment in the tine is given by,  $M = \text{Design draft (kg)} \times \text{Beam span (cm)}$

$$\begin{aligned} &= 123 \times 65 \\ &= 7995 \text{ kg-cm} \end{aligned}$$

Now, the section modulus of the tyne 'Z' is calculated as

$\sigma_b$  is the bending stress in tine,  $\text{kg cm}^{-2}$ . We can take bending stress in mild steel flat as  $1000 \text{ kg cm}^{-2}$  (Sengar, 2002).

Then, for rectangular sections,

$$Z = \frac{t \times b^2}{6}$$

The ratio between the thickness to width (t: b) can be taken from 1: 3 to 1: 4, (Sharma and Mukesh, 2008)

So,  $t : b = 1 : 3$   
 $b = 3 \times t$

Therefore,

$$Z = \frac{t \times (4t)^2}{6} = \frac{16t^3}{6}$$

Also,  $Z = \frac{M}{\sigma_b}$

$$Z = \frac{7995}{1000} = 7.995 \text{ cm}$$

So,  $7.995 = \frac{16t^3}{6}$

$$t = 1.44 \text{ cm} = 14.4 \text{ mm}$$

$$b = 3 \times 14.4 = 43.2 \text{ mm}$$

Therefore,

$$\text{Cross section of the tyne standard} = 14.4 \times 43.5 \text{ mm}$$

Standard MS flat of size 45 × 15 mm size were used for fabricating the shank of furrow opener and the standard MS flat is 600×50×15 mm was selected for the shoe type furrow opener.

### ***3.7.2.1 Drawbar horse power requirement***

Drawbar horsepower required to pull the planter can be determined as under:

$$\text{DBHP (kW)} = \text{Draft (kN)} \times \text{Speed (m s}^{-1}\text{)}$$

Assuming the maximum speed of operation of planter as 5.0 km h<sup>-1</sup> (1.38 m s<sup>-1</sup>)

$$\begin{aligned} \text{DBHP (kW)} &= 4.8 \text{ kN} \times 1.38 \text{ m s}^{-1} \\ &= 6.62 \text{ kW} \end{aligned}$$

In general, the power available at the drawbar of the tractor is about 60 % of its

engine power (BHP)

Therefore, the total power required to operate the four-row prototype planter would be:

$$\text{BHP} = \text{DBHP}/0.6 = 6.62/0.6 = 11.04 \text{ kw} = 14.8 \text{ hp}$$

Hence, a 20 hp and above engine would be able to pull the four-row planter using shoe- type furrow opener.

### 3.7.3 Design of seed hopper

The seed hopper was designed as illustrated below

$$\begin{aligned} \text{Working width of planter} &= \text{Number of rows} \times \text{Row spacing} \\ &= 4 \times 40 = 160 \text{ cm} \end{aligned}$$

Now, the maximum seed rate of pulses = 40 kg ha<sup>-1</sup> as per the KAU, Package and Practices, (2016)

Let us assume, speed of the planter is 2 km h<sup>-1</sup> and field efficiency assumed to be 70 %

$$\begin{aligned} \text{Actual field capacity of planter} &= \\ &= \frac{\text{Speed (km}\cdot\text{h}^{-1}) \times \text{Working width of planter (m)} \times \text{Field efficiency}}{10} \\ &= \frac{2 \times 1.6 \times 0.7}{10} \\ &= 0.224 \text{ ha h}^{-1} \end{aligned}$$

Let us design a seed box for such a capacity, assuming that it requires refilling of seed after 2 hours.

Therefore,

Weight of seed to be used in 2 hours = Seed rate (kg ha<sup>-1</sup>) × Area covered per hr × time (hr)

$$\begin{aligned} &= 40 \times 0.224 \times 2 \\ &= 17.92 \text{ kg} \end{aligned}$$

We have four units, so four separate hoppers developed for the machine. For feasibility and used of different seeds, we designed the hopper that it could handle 7 kg

of black gram seeds.

$$\text{Volume of seed box} = \frac{\text{Weight of seed (Kg)}}{\text{Bulk density (kg m}^{-3}\text{)}}$$

$$\text{Bulk density of black gram seeds} = 810 \text{ kg m}^{-3} \quad (\text{RNAM, 1991})$$

$$\text{Therefore, Volume of seed box} = \frac{7}{810} = 0.0086 \text{ m}^3$$

$$\text{Volume of seed box (Vs)} = 8642 \text{ cm}^3$$

The shape of box proposed is shown in Fig. 3.7 The volume is computed by selecting the box as shown in 1, 2 and 3 and areas of sections are computed and is multiple width of box.

$$\text{Volume of seed box} = \text{Area} \times \text{height of seed box}$$

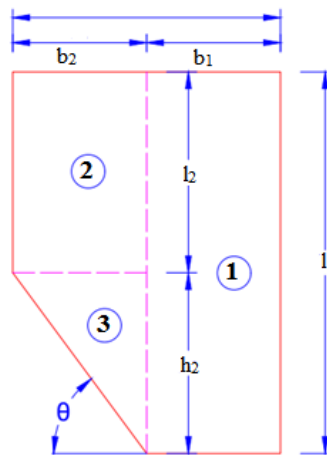


**Fig. 3.7 Cross sectional view of seed box**

i. Volume of section 1

$$\begin{aligned} V &= \text{Length } (l_1) \times \text{width } (b_1) \times \text{height } (h) \\ &= 30 \times 15 \times 14 \\ &= 6300 \text{ cm}^3 \end{aligned}$$

ii. Volume of section 2

$$V = \text{Length } (l_2) \times \text{width } (b_2) \times \text{height } (h)$$

$$= 15 \times 10 \times 14$$

$$= 2100 \text{ cm}^3$$

iii. Volume of section 3

$$V = \frac{1}{2} \times \text{base} \times \text{height} \times \text{width}$$

$$= \frac{1}{2} \times a_1 \times b_2 \times w$$

$$= \frac{1}{2} \times 10 \times 10 \times 14$$

$$= 700 \text{ cm}^3$$

So, Total volume computed under (i), (ii) and (iii) are

$$= 6300 + 2100 + 700$$

$$= 9100 \text{ cm}^3$$

Each mild steel seed hopper has a capacity of 7 kg and a volume of 0.0091 m<sup>3</sup>. The hoppers are constructed with a 45° angle to optimize seed flow. A total of 4 seed hoppers are required for the planter design.

### **3.7.3.1 Thickness of the hopper sheet**

The thickness of the hopper sheet was designed in such a manner that the hopper walls should be able to withstand the lateral pressure developed by the loaded Pulses seeds. The hopper is made up of MS sheet. The relation for maximum lateral bending moment developed on the walls of the hopper was determined from Rankine's formula as under:

$$M_b = \frac{\rho h^2 b^2 \cos \theta}{8}$$

Where,

$M_b$  = Maximum lateral bending moment, N-m;  $\rho$  = bulk density of the seeds, kg m<sup>-3</sup>;  $h$  = total height of the hopper, m;  $b$  = total breadth of hopper, m;  $\theta$  = angle of repose of black gram (25°)

From above equation, considering the maximum angle of repose of black gram as 25°, the maximum lateral bending moment on the walls of the hopper can be calculated as,

$$M_b = \frac{810 \times (0.3)^2 \times (0.25)^2 \cos 25}{8}$$

$$M_b = 0.516 \text{ kg m or } 5.16 \text{ N m}$$

Stress developed on the walls of the hopper due to bending can be calculated from the following relation:

$$\sigma_{b \max} = \frac{M_b Y}{I}$$

Where,

$\sigma_{b \max}$  = maximum bending stress, N m<sup>-2</sup> (250 N m<sup>-2</sup> for mild steel)

$M_b$  = Maximum lateral bending moment on the walls of hopper, N-m

$Y$  = distance of sheet from the neutral axis, m

$I$  = moment of inertia of the sheet, m<sup>4</sup>

$$\text{allowable stress} = \frac{250 \times 10^6}{\text{factor of safety}}$$

Take factor of safety as 2

$$\text{allowable stress} = \frac{250 \times 10^6}{2} = 125 \times 10^6 \text{ N mm}^2$$

So,

$$125 \times 10^6 = \frac{5.16 \times \frac{t}{2}}{0.25 \times \frac{t^3}{12}}$$

After solving,

$$t = 0.996 \text{ mm or } 1 \text{ mm}$$

The thickness of the mild steel sheet required to withstand lateral pressure due to loading of black gram was found as 1.0 mm. However, for safety and as per the availability of material from the market, a mild steel sheet of thickness of 2 mm was used for fabrication of hopper.

### 3.7.4 Design of seed plate

Design of seed metering plate for black gram and horse gram seeds in a vacuum seeding system

- i. Shape of openings on the seed plate was recommended as a circular hole by Barut and Özmerzi (2004).



## 2. Angle of openings on the seed plate

To prevent multiple seed pick-up, the seed openings on the metering plate should have a conical shape with a 120° angle. This design allows a single seed to fully close the opening, preventing additional seeds from entering (Singh *et al.*, 2005).

## 3. Diameter of openings on the seed plate

In order to determine the diameter of opening on the seed (metering) plate ( $d_o$ ) for pulse seeds, the study considered the opening diameter based on less than 50 % size of the geometric mean diameter ( $D_g$ ) that means “ $d_o \leq 50\%$  of  $D_g$ ” (Singh *et al.* (2005).

In the present research, the diameter of openings on the seed plate ( $d_o$ ) was also based on the less than 50 % size of the geometric mean diameter of the black gram and horse gram seeds as shown. The maximum geometric mean diameter of black gram seeds was 3.69 mm and for horse gram 4.00 mm.

### For black gram,

$$d_o \leq 0.50 \times D_g$$

$$d_o \leq 0.50 \times 3.69 \text{ mm, then } d_o \leq 1.845$$

Based on Sial and Persson (1984), Afify *et al.* (2009)

The value for  $2\beta=90^\circ$  or  $120^\circ$  or  $150^\circ$ ;

$$D_g \cos\beta \leq d_o < D_g \dots\dots\dots (ii)$$

$$\text{When } 3.69 \cos 45^\circ \leq d_o < 3.69, \text{ then } 2.61 \leq d_o < 4.13;$$

$$\text{When } 3.69 \cos 60^\circ \leq d_o < 3.69, \text{ then } 1.845 \leq d_o < 3.69;$$

$$\text{When } 3.69 \cos 75^\circ \leq d_o < 3.69, \text{ then } 0.96 \leq d_o < 3.69;$$

Therefore, in this study, the opening diameter of the seed plate (metering plate) must be considered between 0.96 to 3.69 for black gram seeds.

### For horse gram,

$$d_o \leq 0.50 \times D_g \text{ and } d_o \leq 0.50 \times 4.00 \text{ mm, then } d_o \leq 2$$

Based on Sial and Persson (1984), Afify *et al.* (2009)

And for  $2\beta=90^\circ$  or  $120^\circ$  or  $150^\circ$ ;

$$D_g \cos\beta \leq d_o < D_g$$

$$\text{When } 4.00 \cos 45^\circ \leq d_o < 4.00, \text{ then } 2.83 \leq d_o < 4.00;$$

$$\text{When } 4.00 \cos 60^\circ \leq d_o < 4.00, \text{ then } 2 \leq d_o < 4.00;$$

When  $4.00 \cos 75^\circ \leq d_o < 4.00$ , then  $1.04 \leq d_o < 4.00$ ;

Therefore, in this study, the opening diameter of the seed plate (metering plate) must be considered between 1.04 to 4 mm for horse gram seeds.

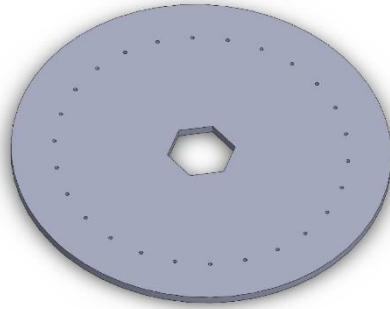


**Fig. 3.8 Seed plate**

#### 4. Number of openings on the seed plate

Circumference of ground wheel ( $C_w$ )

$$C_w = \pi \times D_w$$

Where,  $D_w$  is the diameter of the wheel

$$C_w = \pi \times 63.5 = 199.4 \text{ cm} \approx 200 \text{ cm}$$

If seed spacing within row ( $X_s$ ) for black gram and horse gram seeds is 15 cm, the number of openings or cells on the seed plate with assuming  $N_r = 0.5$ , can be

$$n = \frac{C_w}{X_s \times N_r}$$

Then,

$$n = \frac{200}{15 \times 0.5}$$

$$N = 26.67 \approx 26$$

#### 5. Pitch circle diameter

It can be given in terms of a circumference of pitch circle seed plate as follows:

$$D_p = \frac{C_p}{\pi} = \frac{(N \times (D_o + C_o))}{\pi}$$

Where  $C_o$  = distance between two holes

$$D_p = \frac{(26 \times (12 + 4))}{3.14}$$

$$D_p = 132 \text{ mm}$$

## 6. Outside diameter of the seed plate

For determining the outside diameter of the seed plate,

$D_s$

$$D_s = D_p + D_o + 2C_e$$

$C_e$  = distance between hole and outer diameter

$$\text{Then, } D_s = 132 + 12 + (2 \times 20) = 184 \text{ mm}$$

### 3.7.5 Design of steel ground wheel

The ground wheel was mounted on the mainframe with a freely suspended beam. The bush bearing was provided to support the counter shaft and the beam is fixed to the main frame with U-clamp. The ground wheel was pulled by the tractor during forward motion. The required traction was obtained by the lugs provided on the circumference of the ground wheel.

The ground wheel made of Fe-410 made of 5 mm thick steel sheet of diameter 500 mm was selected and weight of ground wheel equivalent to 65.19 N (Khurmi and Gupta, 2003).

#### 3.7.5.1 Design of lugs

The lugs are provided on the circumference of the ground wheel to obtain proper traction. The lugs are welded to the outer face of the ground wheel. Lugs provided in the ground wheel are subjected to force due to weight of ground wheel and acceleration force ( $F_{s1}$ ) acting on the lugs.

The soil acceleration force is calculated using the under given equation as used by Srivastava et al. (2003).

$$F_{s1} = \rho b \times d \times V_0^2 \left( \frac{\sin \theta}{\sin \theta + \epsilon} \right)$$

The size of lugs are selected as 50 ISF6 of length 75 mm, made of Fe-410 (Khurmi and Gupta, 2003).

The projection of lug is considered from the tip of circumference of ground wheel as 35 mm, depth of lug penetration in the soil as 35 mm and the width of lug as 50 mm for the design of lugs on ground wheel. Lugs were welded perpendicular to ground wheel. The bulk density of the soil was measured as 1350 kg m<sup>-3</sup>. It is assumed that the angle of internal friction as 32°, maximum forward speed as 9.6 km h<sup>-1</sup> (Kepner *et al.*, 1987).

Angle of forward failure was taken as 27°

Soil acceleration force acting on each lug is given by

$$F_{s1} = 1350 \times 0.05 \times 0.035 \times (2.67)^2 \left( \frac{\sin 90}{\sin 90 + 29} \right)$$

$$F_{s1} = 19.26$$

Considering three lugs are in contact with the soil. Total soil acceleration force is given by

$$B_0 = 3 \times F_{s1}$$

Where,

$B_0$  = total soil acceleration force on ground wheel, N

$F_{s1}$  = total soil acceleration force on each lug, N

$$B_0 = 19.26 \times 3$$

$$= 57.78 \text{ N}$$

The total soil acceleration force is acting at the center of projected length of lug and hence the maximum bending moment will be acting at this point. The maximum bending moment is given by equation.

$$M = B_0 L$$

Where,

$M$  = maximum bending moment, N-mm

$B_0$  = total soil acceleration force on ground wheel, N

$L$  = distance between point of action of soil resistance and top edge of ground wheel, mm.

$$M = 57.78 \times 17.5$$

$$= 1011.15$$

The bending stress induced in the material of the lug is calculated as

$$f_b = \frac{M}{Z} \quad \text{Khurmi and Gupta, 2003}$$

Where,

M = maximum bending moment on lug, N mm

$f_b$  = stress induced in the material of lug, N mm<sup>-2</sup>

Z = section modulus, ground wheel lugs, mm<sup>3</sup>

Section modulus for rectangular section is given by Varshney et al. (2005).

$$Z = \frac{1}{6} b t^2$$

Where,

Z = section modulus, mm<sup>3</sup>

t = thickness of lug, mm

b = width of lug, mm

$$Z = \frac{1}{6} \times 50 \times 6^2$$

$$Z = 300$$

Substituting the values of Z from above equation the bending stress produced in the material  $f_b$  is obtained from equation as given below

$$f_b = \frac{1011.15}{300}$$

$$f_b = 3.37$$

The selected lug is made of St-42 –S having ultimate bending stress of 420 mm<sup>2</sup>, the factor of safety is taken as 6, Allowable bending stress in the material is 70 N mm<sup>-2</sup> (Khurmi and Gupta, 2003).

Bending stress produced (3.36 N mm<sup>-2</sup>) is less than allowable bending stress (70 N mm<sup>-2</sup>).

3.36 N mm<sup>-2</sup> is less than 70 N mm<sup>-2</sup>

Hence the design is safe

Considering the spacing between lugs as 130 mm and number of lugs ground wheel is obtained as

$$N = \frac{\pi D_g}{S_1}$$

Where,

$D_g$  = diameter of ground wheel, mm

S = spacing between lug, mm

N = number of lugs

$$N = \frac{3.14 \times 500}{130}$$

$$N = 12$$

12 lugs on ground wheel have been provided

### 3.7.5.2 Design of ground wheel shaft

The shaft of ground wheel is fitted with ground wheel at one end and another end with sprocket. The power transmitted by the ground wheel shaft is given by

$$P = B_0 \times V_g$$

Where,

P = power transmitted, W

B<sub>0</sub> = total soil acceleration force, N

V<sub>g</sub> = speed of ground wheel shaft m s<sup>-1</sup>

Let the maximum speed of ground wheel shaft is 1.38 m s<sup>-1</sup> (5 km h<sup>-1</sup>)

Substituting value of B<sub>0</sub> and V<sub>g</sub> for power transmitted by the ground wheel shaft is obtained as

$$P = 57.78 \times 1.38$$

$$P = 79.74 \text{ W}$$

The ground wheel shaft is subjected to combined torsion and bending the torque transmitted by the shaft is given by the Equation.

$$T = \frac{P \times 60}{2\pi N}$$

Where,

T = torque transmitted by the ground wheel shaft, Nm

P = power transmitted by the ground wheel, W

N = speed of ground wheel shaft, rpm

$$T = \frac{79.74 \times 60}{2\pi \times 52.73} = 14448.27 \text{ N-mm}$$

The ground wheel shaft is subjected to bending moment because of the force due to weight of ground wheel acting perpendicular to the axis of the shaft. Soil acceleration force acting on the lug parallel to the axis of the shaft.

The bending moment due to axial force acting parallel to the shaft on the lug of the ground wheel is calculated by.

$$M_1 = B_0 L$$

Where,

$M_1$  = maximum bending moment, N-mm

$B_0$  = total soil acceleration force, N

$L$  = center distance between shaft and lug, mm

$$\begin{aligned} M_1 &= 57.78 \times 287.5 \\ &= 16622.75 \text{ N mm} \end{aligned}$$

The bending moment of the force due to weight of ground wheel is given by the equation

$$M_2 = F_g \times L_1$$

Where,

$F_g$  = force due to ground wheel weight, N

$L_1$  = distance of ground wheel from center of the bearing, mm

$$\begin{aligned} M_2 &= 65.19 \times 250 \\ M_2 &= 16297.5 \text{ N mm} \end{aligned}$$

Resultant bending moment on the ground wheel shaft is given by the equation (Khurmi and Gupta, 2003).

$$M_g = \sqrt{M_1^2 + M_2^2}$$

Where,

$M_g$  = resultant bending moment, N-mm

$M_1$  = bending moment acting parallel to shaft, N-mm

$M_2$  = bending moment acting perpendicular to shaft, N-mm

$$\begin{aligned} M_g &= \sqrt{(16622.75)^2 + (16297.5)^2} \\ M_g &= 23279.27 \text{ N-mm} \end{aligned}$$

The ground wheel shaft is subjected to twisting moment (T) and resultant bending moment (M), therefore equivalent twisting moment is calculated by the equation.

$$T e_g = \sqrt{T^2 + M_g^2}$$

Where,

$T_e$  = Equivalent twisting moment, N-mm

$T$  = Twisting moment N-mm

$M_g$  = Resultant bending moment, N-mm

$$T_e = \sqrt{(14448.27)^2 + (23279.27)^2}$$

$$T_e = 27391.06 \text{ N mm}$$

The ground wheel shaft is subjected to combined bending and torsion. The shaft is supported by bush bearing of length 900 mm, one end of the shaft is fitted with ground wheel and another end fitted with sprocket to transmit the power to feed shaft of seed metering unit through main shaft. The selected shaft is made of having ultimate tensile stress of  $450 \text{ N mm}^{-2}$  and the factor of safety is taken as 5. Allowable shear stress in the shaft material is  $50 \text{ N mm}^{-2}$  (Khurmi and Gupta, 2003). Diameter of the shaft obtained by equation.

$$d^3 = \frac{16 \times T_e}{\pi \times \tau}$$

Where,

$T_e$  = equivalent Torque, N mm

$\tau$  = allowable shear stress,  $\text{N mm}^{-2}$

$d$  = diameter of the shaft, mm

$$d^3 = \frac{16 \times 27391.06}{\pi \times 50}$$

$$d^3 = 2789.73$$

$$d = 14.92$$

Diameter of ground wheel shaft as of 14 mm.



## 3.8 DEVELOPMENT OF PNEUMATIC PLANTER

### 3.8.1 Frame

The main frame was designed to provide support for the seed metering units and furrow openers, which were attached using a four-bar parallelogram mechanism. The frame also included provisions for the aspirator blower. The hitch system was integrated with the frame, while the aspirator blower was mounted behind the hitch system. The overall dimension of the pneumatic planter with electronic control system was  $2.8 \times 1.4 \times 1.2$  m and the main frame was rectangular in shape with  $2.6 \times 0.1 \times 0.15$  m in size. It is fabricated with  $50 \times 50 \times 8$  mm of ST42S conform to IS: 808-1964 (Bajaj, 1993). The four-bar parallelogram mechanism was fitted on the frame with 'U' clamp. The main tool bar frame was perfectly aligned to obtain line of pull centrally to facilitate the various planter components mounting and to reduce side draft while in operation. Two supporting foot mounted at each end to provide support to the machine at standing position.

### 3.8.2 Aspirator blower

The design of the aspirator blower involves converting mechanical energy into kinetic energy, utilizing an impeller to accelerate air flow. This process, akin to that of a centrifugal pump, involves creating a partial vacuum within a confined housing (volute), inducing air intake. By carefully considering parameters such as inlet vane angles, volute dimensions, and impeller speed, an efficient blower system was selected. Power is transferred to the blower through a cardan shaft connected to the power take-off (PTO) of a tractor. A cardan shaft is a rotating mechanical component that transmits torque between parts that are misaligned or change distance. It features universal joints (U-joints) to accommodate the misalignment and is typically made from high-strength steel.



**Plate 3.17 Aspirator blower**

This mechanism ensures efficient transmission of rotational power from the tractor P.T.O. to the blower, enabling the operation of pneumatic seeding systems. The calculated theoretical flow rate and power input to the blower demonstrate its effectiveness in generating airflow and facilitating pneumatic seeding operations.

### **3.8.3 Four-bar parallelogram linkage**

In parallelogram mechanism, each furrow opener is linked to an individual frame unit, which is then connected to the mainframe or toolbar of the machine via a parallelogram linkage. This design enables vertical movement of the opener frame unit, ensuring independence from fluctuations in the mainframe height. Additionally, it allows for autonomous movement relative to other opener frames attached to the same toolbar or mainframe. Control over the height of the frame unit, and consequently the depth of the furrow opener, is facilitated by a gauge or press wheel affixed to the frame. The depth adjustment can be achieved by either moving the gauge wheel(s) or raising/lowering the opener relative to the frame. The stability of seeding depth in the four-bar parallelogram mechanism is influenced primarily by parameters such as sub-crank length, main crank angular velocity, and center distance (Li *et al.*, 2023).



**Plate 3.18 Four-bar parallelogram mechanism**

The implementation of a four-bar parallelogram mechanism within the profiling adjustment device ensures smooth transfer of tractor pulling force to the furrowing device, maintaining consistent furrowing depth across varying terrain conditions. This mechanism, including elements like the depth-limiting wheel. The arrangement of the depth-limiting wheel determines the profiling adjustment device type, which can be categorized into front profiling, rear profiling, and synchronized profiling. In the existing planter, rear profiling is utilized, positioning the profiling wheel at the rear end of the planter. This placement not only reduces the unit width and weight but also enhances maneuverability and passability, with the depth-limiting wheel doubling as a compacting device. The incorporation of a downforce adjustment passive mechanism utilizing mechanical springs enhancing the precision and reliability of furrow depth control. Plate 3.18 depicts a view of four bar parallelogram mechanism mounted on the frame. The seed box, seed metering system (vacuum disc type), runner-type opener, and rear gauge/press wheel are all affixed to a frame suspended from the toolbar through a parallelogram linkage. This setup ensures that the depth of the furrow opener remains independent of the toolbar.

#### **3.8.4 Seed meter mechanism**

Vacuum disc seed meters comprises a seed box, split housing, a vertically rotating disc featuring a row of holes around its circumference, and an aspirator blower. The disc thickness is inconsequential in the singulation process, and seeds are held by suction to the hole. The disc rotates between two halves of the housing, exposed to

negative pressure (vacuum) on one side and seeds on the other. As the disc rotates, each hole passes through the seed lot, picking up seeds due to pressure difference, held in place by suction.

A wiper adjusts to cover more or less of the hole diameter, ensuring singulation—wherein all seeds except one are wiped from each hole and fall back under gravity to the seed lot. The remaining single seeds are carried towards the base of the meter, where the pressure difference is removed, allowing them to fall into the seed delivery system. Metering performance relies on factors such as hole size matching the smallest seed in the lot, optimal pressure differential, correct wiper/cutoff position for singulation, and disc speed within the required range for seed pickup and adhesion. Vacuum level adjustment ensures sufficient pressure difference for seed retention but allows singulation by the wiper. The seed metering rate adjusts by varying the disc speed relative to ground speed and selecting discs with different numbers of holes. Grading seeds to match hole size isn't mandatory. Plate 3.4 illustrates a vacuum disc metering unit.

### **3.8.5 Hopper**

Four seed hoppers units were developed from mild steel with a thickness of 2 mm, meeting specifications. Each hopper unit measures 140 mm in length, 250 mm in width, and 300 mm in height. Its bottom surface is inclined at a 45° angle to facilitate seamless seed flow towards the outlet. Engineered to accommodate up to 7 kg of black gram seeds, these hoppers ensure optimal seed distribution while in operation.



**Plate 3.19 Seed hopper**



### 3.8.6 Electronic system

The electronic system of the vacuum pneumatic planter is designed to efficiently operate the metering mechanism, ensuring precise seed placement. The system primary function is to measure the distance traveled by the planter and control the seed plate accordingly. To achieve this, both a proximity sensor and a rotary encoder were initially considered for measuring the distance traveled by the planter. These sensors were mounted on the wheel to capture accurate data. After thorough evaluation, the best-performing sensor was selected for the final prototype.

Once the sensor detects the distance traveled, it sends the data to the Printed Circuit Board (PCB). The PCB is equipped with three Arduino microcontrollers, which manage and control the entire process. These microcontrollers operate on both 24V and 5V power supplies, ensuring efficient functioning of the system.

To drive the seed plate accurately, the PCB is connected to four stepper drivers and stepper motors for four seed metering unit in the planter. These stepper motors precisely control the movement of the seed plate based on the input from the sensors. This precision is crucial for achieving the target seed-to-seed spacing, ensuring uniformity and consistency in planting.

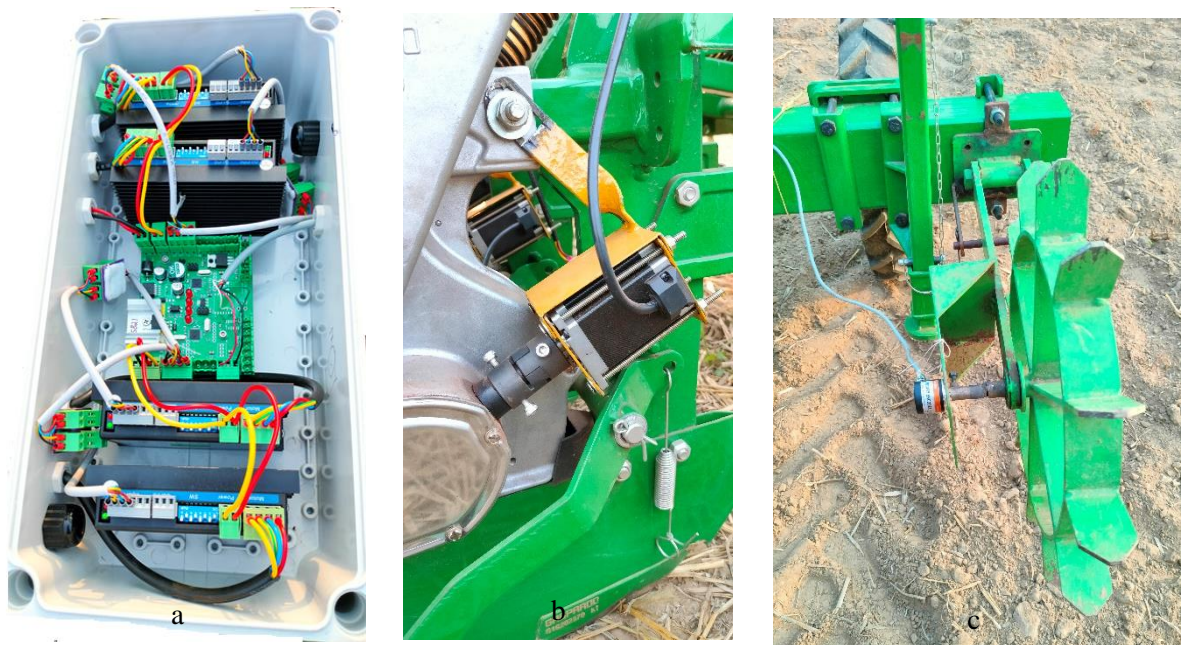


**Plate 3.20 a) Electronic system in box b) Stepper motor fixed with metering mechanism c) Rotary encoder fixed at ground wheel**

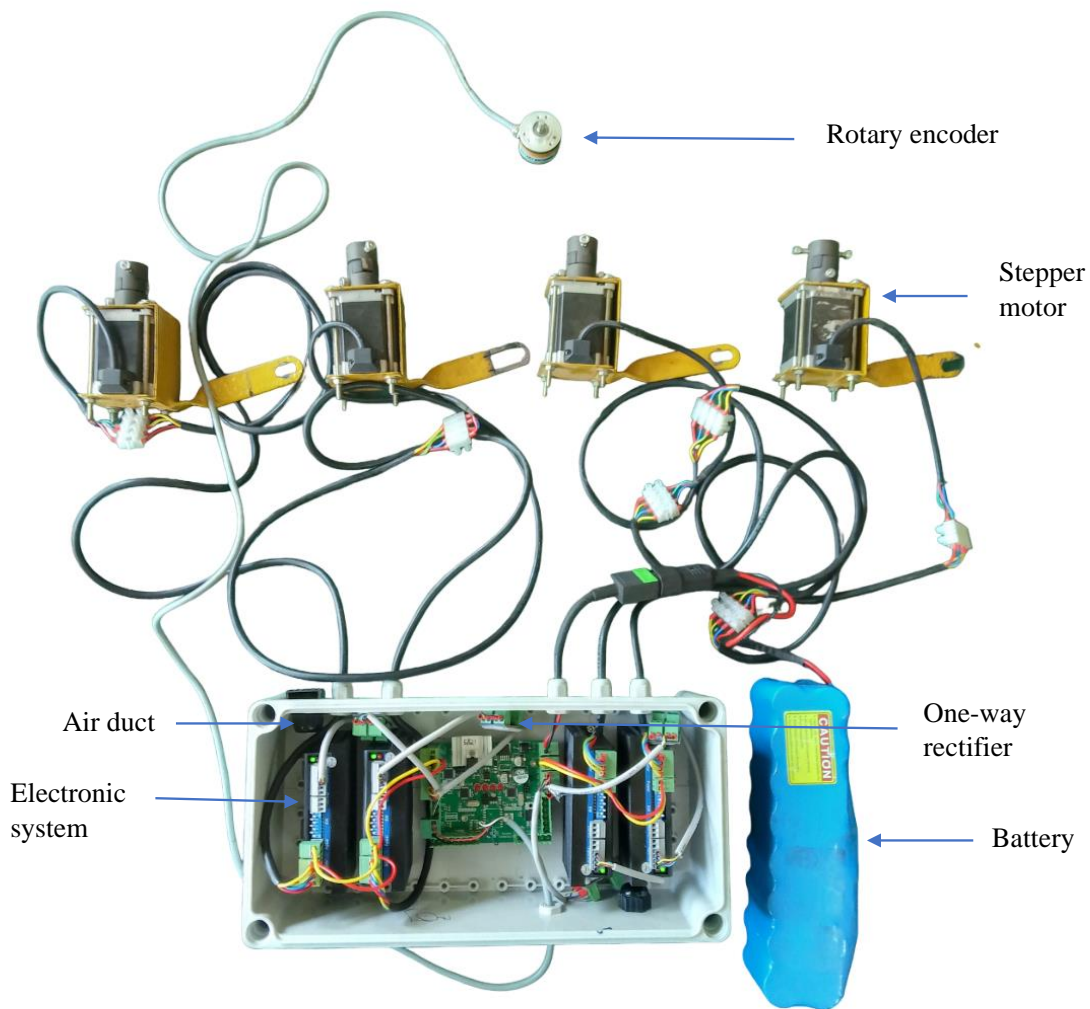


**Plate 3.21 Complete electronic system**

The entire electronic system is powered by a 25.6V, 12Ah Lithium Iron Phosphate (LiFePO<sub>4</sub>) battery as shown in plate 3.21. This robust battery provides a reliable power source for the system and is charged using an appropriate charger to maintain its efficiency and longevity.

All the electronic components are housed in an ABS plastic enclosure, which is designed to be weatherproof, dust-tight, and watertight as shown in plate 3.20 (a). This enclosure has a protection rating of IP66/67, ensuring high resistance against dust and

water ingress, and an impact protection rating of IK07. A one-way rectifier, also known as a diode, used in electronic control systems that allows current to flow in only one direction. By preventing backflow of current, it protects sensitive components like microcontrollers and PCBs from potential damage caused by short circuits or reverse polarity. Heat generated by the electronic components was managed by two ducts that were provided on enclosure to facilitate heat dissipation from it to maintain optimal operating temperature.

### **3.8.7 Furrow openers**

Furrow openers are essential components of precision planting systems, responsible for creating seed furrows in the soil. When planting through crop residues, it is crucial for furrow openers and covering devices to avoid incorporating residue into the seed furrow. The goal of furrow opener design is to improve soil conditions for emergence without excessive disturbance to the seedbed. Factors like opener design, soil type, and operational speed influence seed placement accuracy. Negatively raked furrow openers, like runner and double disc types, are useful in high-strength soil conditions but may struggle to maintain optimal furrow depth. Over compaction can occur if additional weight is added to achieve penetration, impacting both the furrow sidewalls and base. In this study three furrow opener was used viz., inverted t-type, shoe type and stub runner type.

#### ***3.8.7.1 Inverted type furrow opener***

The furrow opener assembly consists of four inverted-T type tines securely clamped onto the rear beam of the frame using clamps and bolts. Each tine comprises a leg, furrow/slit opener, shin, deflector plates, and side cover plates. The legs are constructed from MS flats measuring  $450 \times 50 \times 20$  mm, providing sturdy support for the assembly. To prevent soil from entering the furrow during seed placement, two side plates are welded to the lower end of the leg. Additionally, a MS flat measuring  $75 \times 50 \times 5$  mm is welded to the bottom of the front face of the tine, with one end trapezoidal in shape, extending up to 35 mm length, and having a tip width of 0.08 m. This configuration aids in cutting and sharing the soil efficiently, enhancing the furrow opening process. Moreover, the side of the furrow opener is machined with a  $45^\circ$  cone angle, further improving cutting and sharing capabilities.

### ***3.8.7.2 Shoe type furrow opener***

A shoe-type furrow opener was fabricated and fitted into the parallelogram mechanism of the planter, comprising a shank, shoe, and adjustment frame. The shank, fabricated from 50 x 15 mm thickness mild steel flat, measured 600 mm in length and was positioned vertically. The shoe, cut from a 10 mm thickness mild steel sheet into a right-angle triangle shape with sides measuring 120 mm, 100 mm, and 160 mm, was affixed to the bottom edge of the shank. One edge of the shoe was welded slightly downwards to facilitate soil penetration, serving as a sharp share for the furrow opener.

To secure the furrow opener to the frame, mild steel flats measuring 250 x 250 x 2 mm were welded to the shank. Additionally, two pieces of 5 mm thick mild steel flat, each 150 mm in length and 60 mm in height, were extended behind the shoe at the outer edge of the sides, forming two wings. These wings acted as a boot section to prevent soil from sliding into the furrow. The shank featured 10 mm holes at 25 mm intervals, while corresponding holes were made in the bracket. This allowed for height adjustment of the shank, enabling control over the depth of the furrow and seed placement. Through the brackets, the depth of the furrow and seed placement could be precisely regulated.

### ***3.8.7.3 Stub runner type furrow opener***

The stub runner type furrow opener is a crucial component of the planting system, designed to create furrows or slits in the soil for seed placement as shown in plate 3.22. This type of furrow opener typically consists of a sturdy frame onto which the furrow opener units are attached. Each unit comprises a stub runner, which is the main component responsible for cutting through the soil. The stub runner is typically constructed from durable materials such as steel or iron to withstand the rigors of agricultural operations. Attached to the stub runner are additional components such as deflector plates, side cover plates, and possibly a shin for added stability and performance. These components work together to ensure proper soil management and seed placement during planting.





**Plate 3.22 Stub type runner and seed covering device**

The design of the stub runner is optimized for efficient soil penetration and minimal soil disturbance. It often features a streamlined shape with a sharp leading edge to facilitate smooth cutting through the soil. Additionally, the runner may be angled or shaped to provide optimal soil engagement and furrow formation. During operation, the stub runner is guided along the soil surface by the planting equipment, creating clean, uniform furrows or slits of the desired depth and width.

### **3.8.8 Seed covering device**

Seed covering devices are tailored to facilitate soil flow back into the furrow after seed placement, ensuring proper covering and firming. Operational requirements include adaptability to various field conditions, uniform soil cover depth, prevention of seed displacement, and compatibility with row spacings. The need for a covering device depends on factors like soil type, furrow opener design, residue amount, and operational speed.

Some planters, like drill seeders, rely solely on soil flow around the opener for seed covering. Successful implementation requires a well-prepared seedbed and a narrow furrow opener operating at an appropriate speed. In this study, opposed paddle covering devices were utilized, featuring elongated blades positioned horizontally with curved trailing ends to facilitate soil movement and seed covering.

### 3.8.9 Wheels

Wheels are essential components of precision planters, providing stability, traction, and maneuverability in field operations. They play a critical role in ensuring smooth movement across various terrains while supporting the weight of the planter and its components. Additionally, wheels contribute to seed placement accuracy by maintaining consistent ground contact and minimizing soil compaction, ultimately optimizing crop emergence and yield.

#### 3.8.9.1 *Pneumatic drive wheel*

The pneumatic drive wheel as shown in plate 3.23 (a), serves as a key component in providing traction and propulsion for the planter. Utilizing pneumatic technology, this wheel is typically equipped with a tire inflated with air, offering resilience and grip to navigate various terrains efficiently. Its design ensures optimal traction, minimizing slippage during operation, and facilitating precise seed placement. The pneumatic drive wheel contributes to the overall stability and maneuverability of the planter, enhancing its performance in diverse field conditions.

#### 3.8.9.2 *Compression wheel*

The compression wheel plays a crucial role in ensuring proper seed-to-soil contact after seed placement. Positioned behind the furrow opener, this wheel exerts downward pressure on the soil, compacting it around the seeds to promote germination and establishment. Plate 3.23 (b) showed compression wheel and it designed to apply consistent pressure, preventing air pockets and promoting uniform seed depth. By enhancing soil-seed contact, the compression wheel contributes to improved seedling emergence and overall crop yield.



**Plate 3.23 a) Pneumatic drive wheel, b) Compression wheel**

### 3.8.9.3 Steel ground wheel

The mild steel ground wheel provides support and stability to the planter, serving as a foundation for smooth and controlled movement across the field. Fabricated from durable mild steel, this wheel withstands the rigors of field operations while maintaining structural integrity. Its design ensures optimal weight distribution and ground contact, minimizing soil compaction and maximizing traction. The ground wheel's robust construction and reliability make it an integral component in the efficient operation of the planter, facilitating precise seed placement and uniform crop emergence.

A 50 mm wide mild steel flat was rolled to form a circle with a diameter of 500 mm, creating the ground wheel for the seeding machine. At the center of the ground wheel, a 50 mm length bush with inner and outer diameters of 25 mm and 50 mm, respectively, was fabricated to accommodate the drive shaft, as depicted in the Fig. 3.8. To prevent slippage during operation, 12 mild steel flat lugs (75 x 50 x 5 mm) were welded equidistantly around the circumference of the ground wheel. The attachment of the ground wheel to the mainframe was facilitated by a lifting and lowering arm link, crafted from a 50 mm square tube with a length of 400 mm. Circular bushes were welded at both ends of the arm link to house the drive shaft of the ground wheel. Bearings were utilized to fit the driven shaft onto the mainframe, enabling the installation of an encoder for speed synchronization between the ground wheel and the seed metering shaft.

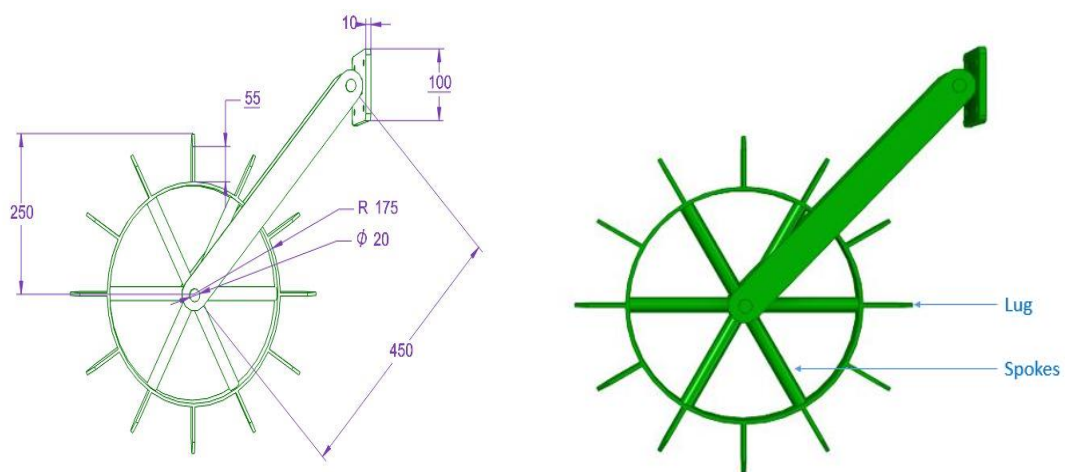


**Fig. 3.9 Steel ground wheel**

The rotary shaft encoder provides pulse counts (with one revolution of the ground wheel equivalent to 2500 pulse counts) to the Microcontroller. The Microcontroller is programmed based on the desired crop spacing and the distance covered by the ground wheel per revolution. It then transmits output signals to the stepper motor to regulate the speed of the metering mechanism effectively.

### 3.9 FIELD TESTING

Field experiments for assessing the developed pneumatic no-till planter integrated with an electronic system were undertaken at the Instructional Farm of KCAEFT, Tavanur. Prior to initiating the tests, the field was prepared and key soil characteristics were examined. This section delves into the impact of certain soil properties on the effectiveness of no-till pneumatic planters equipped with electronic controls. Key soil characteristics such as moisture content, bulk density, and soil resistance, which influence the planter field performance, were the focus of this study. Soil samples from varied field locations were gathered and analyzed to ascertain these characteristics. These tests were carried out in Soil and Water Laboratory at KCAEFT, Tavanur.

#### **Soil Parameters Evaluated:**

1. Soil type
2. Moisture content
3. Bulk density
4. Cone Index

#### **3.9.1 Soil properties**

Black gram and Horse gram were cultivated at KCAEFT, Tavanur Instructional Farm in Kerala for this study. Soil samples were collected from various parts of the farm for analysis. Around five samples from different field areas were obtained for this purpose. Post-analysis, the soil was classified as sandy loam based on the USDA soil classification system, as noted by Madhu Kumar, (2017).

##### **3.9.1.1 Moisture content**

Moisture content (MC) is defined as the proportion of water weight to the dry solids weight. The MC was calculated using the formula:

$$MC (\%) = \frac{W_1 - W_2}{W_1} \times 100$$

Where,

$W_1$  = Initial weight of the sample soil, g

$W_2$  = Dry weight of the sample soil, g

Moisture content, expressed as a per centage, was determined using the oven-dry method. Soil samples from various locations and depths (0 - 7 cm) were collected and dried in a controlled environment at 105°C for 24 hours. An electronic balance with a precision of 0.01g was used to measure the weight before and after drying. Soil moisture is critical for seed germination and growth, thus maintaining optimal moisture levels at sowing is vital to reduce germination losses.

### **3.9.1.2 Bulk density**

Bulk density, indicating soil compactness, was measured using the core cutter method. The bulk density 'ρ' of the soil sample was calculated using:

$$\text{Bulk density } (\rho) = \frac{M}{V}$$

Where,

$\rho$  = Bulk density, g cm<sup>-3</sup>

M = Mass of the soil, g

V = Volume of the soil, cm<sup>3</sup>

The volume of the cylindrical core cutter was determined by measuring its internal diameter and height. The cutter's empty weight was recorded, and then it was used to extract a soil sample from the experimental field. After careful trimming and weighing the filled cutter, the bulk density was calculated.

### **3.9.1.3 Cone index**

Soil resistance was measured using a soil cone penetrometer. This tool was used to determine the penetration resistance of the soil at constant rates. The cone index reflects soil resistance, calculated as the force per square centimeter needed for a standard-sized cone to penetrate the soil to various depths. Measurements were taken for depths of 5 cm. The penetrometer force reading, corresponding to the depth of cone insertion, was recorded. This process was repeated across different study locations to obtain a comprehensive understanding of the soil resistance as shown in plate 3.24.

$$\text{Resistance} = \frac{PF}{BA}$$

$$\begin{aligned}\text{Surface area of cone} &= \pi r^2 = \pi/4 \times D^2 \\ &= \pi/4 \times 3^2 = 7.068 \times 10^{-4} \text{ m}^2\end{aligned}$$

Where,

PF = Penetration force, N

BA = Surface area of cone,  $\text{cm}^2$

$$\text{PF} = \text{PR} \times 0.0098$$

PR = Mean dial gauge reading, N

D = Diameter of cone, 3 cm



**Plate 3.24 Measurement of cone index of soil using proving ring cone penetrometer**





**Plate 3.25 Developed tractor operated pneumatic no-till pulse planter with electronic control system**



**Plate 3.26 Working of pneumatic planter with electronic control system**

### 3.9.2 Field evaluation

The pneumatic no-till planter with an electronic control system underwent field testing to assess its performance. These tests were carried out at the Instructional Farm of Kelappaji College of Agricultural Engineering and Food Technology, Tavanur. The field evaluation was done on tilled and no tilled field for the both pulses seeds. Mostly the optimized variable, which was obtained from the laboratory experiment were used in the field performance. A total area of 80 cents were used for the field testing. The total plot was divided in two equal parts for black gram and horse gram each.

**Table 3.12 Plan of experiment for field evaluation**

Parameters	Levels	Responses
Location of encoder	Steel wheel with spokes	Seed spacing (cm)
	Pneumatic ground wheel	Miss index (%)
Furrow opener	Inverted T	Multiple index (%)
	Shoe type	Quality feed index (%)
	Stub runner	Precision index (%)
Seeds	Black gram	Germination (%)
	Horse gram	

Treatments =  $2 \times 3 \times 2 = 12$ ; Replications = 3

Total no. of experiments =  $12 \times 3 = 36$

In order to assess the impact of different variable levels on the evaluation parameters, a statistical approach was employed. Experimental data underwent analysis using a factorial completely randomized design. Statistical software Design Expert 13, was utilized for data analysis. The plot was tilled and a fine seedbed was prepared using a rotavator, operated twice on the test plots. One plot keeps untilled after the harvesting of paddy crop. A 55 hp tractor was employed for these field tests.

The final evaluation was carried out using steel wheel with spokes and different furrow openers were used and focused on several parameters, as detailed below.

#### i. Seed Spacing Assessment

In the field trials, the distance between individual seeds (in centimeters) over a meter length was precisely measured using a steel scale, as per RNAM standards (1991)



as shown in plate 3.26. This measurement was taken at five randomly selected locations within the field.

ii. **Row Spacing Measurement**

The distance between adjacent rows (in centimeters) was measured using a steel tape. This measurement was similarly done at five random locations in the field, following the methodology outlined by Madhu Kumar, (2017).



**Plate 3.27 Measurement of seed to seed and plant to plant spacing**

iii. **Operation Width Determination**

The total operational width of the machine (in centimeters) was measured with a steel scale during the field trials. This width was recorded at five different, randomly selected spots in the field.

iv. **Depth of Seed Placement**

To measure the depth at which seeds were planted, the soil covering the seeds was carefully removed, and the depth was measured from the furrow surface to the seed.

v. **Wheel Slippage Calculation**

The slippage of the tractor wheels was evaluated by marking the rear tyre lugs over a 50-meter distance, according to the RNAM Test Code (1983). The per centage of wheel slippage was then calculated.

vi. **Draft Measurement**

The draft force exerted by the planter was determined using the rolling method as per the RNAM Test Code (1983). A load cell dynamometer was attached to the front of the test tractor, with the planter mounted, and pulled by an auxiliary tractor. The force exerted was recorded by the load cell dynamometer over a 50-meter distance, and multiple readings were taken. A no-load test was also conducted for comparison.



**Plate 3.28 Draft measurement**

**vii. Fuel Consumption Rate**

Fuel consumption was measured using the top-fill method. The tractor fuel tank was filled before and after the test, and the amount of fuel needed to refill the tank was recorded. This measurement was taken with the tank on level ground, ensuring no air gaps remained. Fuel consumption was then calculated and expressed in liters per hour ( $l\ h^{-1}$ ).

**viii. Theoretical field capacity**

The theoretical field capacity was determined by factoring in the operational width and the speed at which the tractor operated. This capacity, denoted in hectares per hour ( $ha\ h^{-1}$ ), was calculated utilizing the formula outlined by Kepner et al. (1987).

$$\textit{Theoretical field capacity} = \frac{\text{Width of operation (m)} \times \text{Travel speed (km hr}^{-1}\text{)}}{10} \times 100$$

**ix. Effective field capacity**

During field tests, time losses incurred for various events such as refilling seeds and fertilizer in the planter, as well as turning losses, were documented. However, when computing the effective field capacity, both the time spent on actual productive work and the time lost due to other activities such as turning and refilling of seed and fertilizer were taken into account, as per the methodology outlined by Kepner et al. (1987).

$$c = \frac{A}{T_p \times T_n}$$

Where,

C = Effective field capacity,  $ha\ h^{-1}$

A = Area covered, ha

T<sub>p</sub> = Productive time, hr

T<sub>n</sub> = Non-productive time, hr

$$(T_n = T_{\text{refill}} + T_{\text{turning}})$$

In order to track the operational time of the planter, an electronic system incorporated using an ESP32 microcontroller. This enabled operators to conveniently monitor operations via a mobile application. It records operational time data, transmitting it in real-time to the Blynk mobile application, offering operators remote monitoring capabilities. The Blynk app provides an intuitive interface displaying operational time metrics, aiding in better management and maintenance practices. The circuit involves connecting the ESP32 to the electronic system sensors or switches and utilizing its WiFi module for communication with the Blynk app, facilitating seamless data transmission

#### x. Field efficiency

Field efficiency (E<sub>f</sub>) is calculated as a per centage, derived from the ratio of effective field capacity to theoretical field capacity, multiplied by 100, according to the formula outlined by Kepner et al. (1987).

$$\text{Field efficiency} = \frac{\text{Effective field capacity}}{\text{Theoretical field capacity}} \times 100$$
$$E_f \frac{W_e \times V_e \times T_p}{w_t \times V_t \times (T_p + T_n)} \times 100$$

Where,

W<sub>e</sub> = Effective working width, m

W<sub>t</sub> = Theoretical working width, m

V<sub>e</sub> = Effective operating speed, m s<sup>-1</sup>

V<sub>t</sub> = Theoretical operating speed, m s<sup>-1</sup>

T<sub>p</sub> = Productive time, s

T<sub>n</sub> = Non-productive time, s

#### xi. Plant population

Plant population refers to the number of plants per unit area of land.

$$\text{Plant population} = \frac{\text{Number of plants}}{\text{unit area, } m^2} \text{ Plants } m^{-2}$$



**Plate 3.29 Measurement of plant population**

### 3.10 COMPARISON BETWEEN MECHANICAL AND DEVELOPED PNEUMATIC PLANTER

The comparative evaluation of a mechanical pneumatic planter and the developed pneumatic planter with an electronic control system was conducted to assess their performance in planting black gram and horse gram seeds. A commercially available mechanical pneumatic planter was selected for comparison with the newly developed planter, which was equipped with an electronic seed metering system and control mechanisms.

Both planters were operated under the same test conditions, with a vacuum pressure of 4 Kpa and a forward speed of 2 km h<sup>-1</sup>. The planters performance was assessed based on seed spacing, miss index, multiple index, and quality of feed index using standard data collection and analysis techniques.

### 3.11 COST ECONOMICS

The decision to adopt a machine hinges primarily on factors such as machine cost, efficiency, unit operating cost, and payback period. Economic analysis plays a crucial role in determining whether an individual farmer should purchase a planter or opt for custom hiring.

The total cost of a pneumatic planter with an electronic control system was assessed. This cost encompasses fabrication costs and operational costs, which include both fixed and variable costs. The operation costs, including the break-even point and

payback period, were calculated in accordance with BIS standard IS: 9164-1979. Detailed procedures and calculations are provided in the Appendix.

### **Break Even Point (BEP)**

The break-even point occurs when there is no profit or loss. It is calculated by dividing the annual fixed cost by the difference between the custom rate per hour and the operating cost per hour. The break-even point was calculated as:

$$BEP = \frac{AFC}{CC - OC}$$

Where,

- BEP = Break-even point, h yr<sup>-1</sup>
- AFC = Annual fixed cost for the machine, Rs. yr<sup>-1</sup>
- CF = Custom fee, Rs. h<sup>-1</sup>
- C = Operating cost, Rs. h<sup>-1</sup>
- CC = (cost of operation h<sup>-1</sup> + 25 per cent overhead charges) + (25 per cent profit over new cost)

### **Pay Back Period (PBP)**

The payback period is the number of years required for an investment to recover its initial cost through the annual cash revenues it generates, assuming the net cash revenues remain constant each year. The payback period is calculated as follows:

$$PBP = \frac{IC}{ANP}$$

Where,

- PBP = Payback period, yr
- IC = Initial cost of the machine, Rs
- ANP = Average net annual profit, Rs yr<sup>-1</sup>
- ANP = (CF - C) x AU
- AU = Annual use, h yr<sup>-1</sup>

## CHAPTER - IV

### RESULT AND DISCUSSION

In this chapter, the factors affecting the performance of an electronically controlled pneumatic planter, focusing on both seed and machine parameters were analyzed. The chapter presents laboratory experimental results for seed metering mechanism, emphasizing the optimized settings. Additionally, it covers the calibration, testing, and performance evaluation of the pneumatic planter (prototype) for planting black gram and horse gram seeds at field. Extensive experimental trials were conducted to identify the optimal settings for vacuum pressure, plate hole size, forward speed, and the most suitable input sensors. The collected data were statistically analyzed, and the results are detailed in the following sections. An economic analysis of the developed machine is also provided, highlighting its cost-effectiveness and financial viability.

#### 4.1 PROPERTIES OF SEEDS

The comprehensive analysis of the properties of seeds were determined. This study focused on two types of pulses viz., black gram (*Vigna mungo*) and horse gram (*Macrotyloma uniflorum*). The investigation encompasses a detailed examination of their physical, gravimetric, and engineering properties, each of which is important for the planter design and functionality.

##### 4.1.1 Physical Properties

The physical properties of seeds such as size, shape, and weight, are fundamental in determining the suitability of the planting mechanism.

In this investigation, the moisture content for both black gram (VBN-6) and horse gram (KS-2) was found and established at 11 per cent on a dry weight basis, with a standard deviation of  $\pm 0.50$  per cent. This moisture level serves as a baseline for evaluating the seeds physical, gravimetric, and engineering properties. At this specific moisture content, assessments were conducted to determine essential seed attributes for optimizing the tractor operated pneumatic no-till pulse planter with electronic control system.

#### ***4.1.1.1 Size***

The size analysis of black gram seeds revealed a range of dimensions that are critical to consider for the hole diameter provided in the seed plate. The length of the seeds varied from a minimum of 2.32 mm to a maximum of 3.88 mm, with an average length of 3.12 mm. The width measurements showed a minimum of 1.99 mm, a maximum of 3.65 mm, and a mean value of 2.90 mm. In terms of thickness, the seeds had a minimum of 1.56 mm, a maximum of 2.07 mm, and an average of 1.85 mm. The variance and standard deviation values suggest a moderate dispersion in the size of the seeds, with standard deviations of 0.484 mm, 0.532 mm, and 0.148 mm for length, width, and thickness, respectively.

Horse gram seeds, on the other hand, exhibited larger dimensional attributes in comparison to black gram. The seed length ranged from 6.02 mm to 6.27 mm, with a mean of 6.14 mm. The width ranged from 4.10 mm to 4.35 mm, with a mean of 4.23 mm. The thickness measurements were between 2.16 mm and 2.45 mm, with an average thickness of 2.31 mm. The variance in size dimensions was notably smaller for horse gram seeds, indicated a higher uniformity in size compared to black gram seeds. The standard deviations for length, width, and thickness were found to be 0.074 mm, 0.077 mm, and 0.089 mm, respectively.

The contrast in size between the two seed varieties necessitated distinct handling characteristics within the planter mechanism. The larger horse gram seeds may require greater suction force and a large plate hole size than the smaller black gram seeds. These differences underlined the importance of adjustable and versatile mechanisms in the planter design to accommodate varying seed sizes for optimal planting performance.

#### ***4.1.1.2 Arithmetic Mean Diameter***

The arithmetic mean diameter provides insight into the average size of the seeds based on their three principal dimensions. Black gram seeds exhibited a range in arithmetic mean diameter from 1.95 mm to 3.20 mm, with an average value of 2.62 mm, indicating a moderate uniformity in size. Arithmetic mean diameter for horse gram seeds was found between 4.09 mm and 4.36 mm, with a mean of 4.22 mm, which suggest a greater consistency in seed size compared to black gram.

#### ***4.1.1.3 Geometric Mean Diameter***

The geometric mean diameter is a measure that is more sensitive to the seed shape and is used in the calculation of other shape descriptors. The geometric mean diameter of black gram ranged from 1.92 mm to 3.05 mm, with an average of 2.53 mm. In the case of horse gram, the geometric mean diameter ranged from 3.71 mm to 4.00 mm, with an average of 3.86 mm.

#### ***4.1.1.4 Aspect Ratio***

The aspect ratio is indicative of the seed shape and is crucial for the interaction of seeds with the planter mechanisms. Black gram seeds had an aspect ratio ranging from 85.69 to 99.68 per cent, with a mean of 92.62 per cent. Horse gram seeds demonstrated an aspect ratio between 67.96 and 69.50 per cent, averaging 68.88 per cent, which reflects a more elongated shape relative to black gram.

#### ***4.1.1.5 Sphericity***

Sphericity relates to the roundness of the seed and affects how it rolls and is metered through planting equipment. Sphericity measurements varied from 78.34 to 85.12 per cent, with an average of 83.61 per cent for black gram. The sphericity for horse gram was consistent with black gram, ranging from 61.43 to 67.86 per cent, with an average of 63.68 per cent.

#### ***4.1.1.6 Roundness***

Roundness provides an understanding of how angular or rounded the seed is, which can impact the flow ability and orientation when sown. The roundness of black gram seeds varied from 0.45 to 0.57, with an average value of 0.53. Horse gram seeds showed a roundness between 0.33 and 0.42, with a mean of 0.38.

#### ***4.1.1.7 One thousand seed weight***

The one thousand seed weight of black gram was 44.2 g, while for horse gram it was 38.4 g.



### **4.1.2 Gravimetric Properties**

Gravimetric properties, such as bulk density, true density, and porosity, are crucial for understanding the seeds behavior in bulk and their interaction with storage and handling systems.

#### **4.1.2.1 Bulk Density**

The bulk density for black gram seeds ranged from 800.00 to 814.00 kg m<sup>-3</sup>, with a mean value of 806.93 kg m<sup>-3</sup>. The standard deviation was 4.29 kg m<sup>-3</sup>, indicating relatively consistent packing characteristics among the seeds. Horse gram seeds displayed a bulk density between 916.00 kg m<sup>-3</sup> and 935.00 kg m<sup>-3</sup>, averaging 925.80 kg m<sup>-3</sup>. The standard deviation of 6.21 kg m<sup>-3</sup> suggested a slightly greater variability in bulk density compared to black gram.

#### **4.1.2.2 True Density**

The true density of black gram seeds was found to vary from 1428.00 to 1440.00 kg m<sup>-3</sup>, with an average of 1433.50 kg m<sup>-3</sup>. The standard deviation was 3.41 kg m<sup>-3</sup>, reflecting a moderate homogeneity in the seed material. While for horse gram seeds, the true density ranged from 1380.00 to 1396.00 kg m<sup>-3</sup>, with a mean of 1387.93 kg m<sup>-3</sup>. A standard deviation of 4.02 kg m<sup>-3</sup> was observed, which demonstrated a consistent density throughout the seed samples.

#### **4.1.2.3 Porosity**

Porosity is the measure of the void spaces within a mass of seeds and affects the airflow through the seeds during pneumatic planting. The porosity of black gram seeds ranged from 43.08 to 44.17 per cent, with a mean porosity of 43.71 per cent. The low standard deviation of 0.283 per cent indicates a uniform distribution of void spaces within the seeds. Horse gram seeds exhibited a porosity between 33.62 and 33.02 per cent, with an average value of 33.297 per cent. The standard deviation of 0.395 per cent suggests a slightly higher variability in the distribution of void spaces compared to black gram.

The gravimetric properties of the seeds impact the design of the seed hopper and airflow system in the pneumatic planter. Horse gram higher bulk density and lower

porosity require adjusted airflow for effective seed handling, while black gram lower bulk density and higher porosity have different aerodynamic needs for optimal planting.

### **4.1.3 Engineering Properties**

The engineering properties, such as the angle of repose, coefficients of static friction against various materials, terminal velocity and drag coefficient provide a better understanding for mechanical behavior of the seeds. These properties are essential for designing the components of the planter that come into contact with the seeds, ensuring minimal damage and maximum efficiency during the planting process.

#### ***4.1.3.1 Angle of Repose***

The angle of repose is a measure of the stability of a granular pile and reflects the flow characteristics of the seeds. The angle of repose for black gram seeds was observed to range from 25.01° to 25.31°, averaging at 25.18°. This narrow range suggests a consistent flow behavior, which is advantageous for uniform planting. Horse gram seeds exhibited a slightly wider range, from 23.41° to 25.06°, with a mean angle of 24.45°. The lower average angle of repose indicated better flow ability compared to black gram, which can be beneficial in the design of the seed metering system.

#### ***4.1.3.2 Coefficient of Friction***

The coefficient of friction is crucial for understanding the interaction between seeds and the surfaces they contact within the planter. For black gram, the coefficient of friction ( $\mu$ ) varied across different materials used for constructing surfaces, with wood ranging from 0.49 to 0.53 and averaging at 0.52. Galvanized iron exhibited values between 0.45 and 0.51, with a mean of 0.47. Aluminium surfaces showed a range of 0.35 to 0.41, with a mean value of 0.38. Mild steel surfaces ranged from 0.32 to 0.37, with an average of 0.35. Stainless steel surfaces demonstrated coefficients ranging from 0.27 to 0.32, with a mean value of 0.29. On the other hand, for horse gram, the coefficient of friction varied differently across materials. Wood surfaces ranged from 0.58 to 0.63, averaging at 0.61. Galvanized iron exhibited values between 0.39 and 0.45, with a mean of 0.42. Aluminium surfaces showed a wider range from 0.51 to 0.62, with a mean of 0.58. Mild steel surfaces ranged from 0.38 to 0.49, with an average of 0.45. Stainless steel surfaces demonstrated coefficients ranging from 0.26 to 0.35, with a

mean value of 0.31. The higher coefficients of friction for Horse gram on materials like wood and aluminum suggest a greater resistance to movement.

#### ***4.1.3.3 Terminal Velocity***

Terminal velocity indicates the speed at which the seeds settle in air and is related to their aerodynamic properties. The terminal velocity of black gram seeds was found to be between 8.13 m s<sup>-1</sup> and 8.26 m s<sup>-1</sup>, with an average velocity of 8.21 m s<sup>-1</sup>. Horse gram seeds had terminal velocities ranging from 8.6 m s<sup>-1</sup> to 8.79 m s<sup>-1</sup>, with a mean of 8.68 m s<sup>-1</sup>. The higher terminal velocities for horse gram suggested that it experienced less drag than black gram seeds.

#### ***4.1.3.4 Drag coefficient***

The drag coefficient values for black gram ranged from 0.63 (minimum) to 0.68 (maximum), with a mean value of 0.64. In comparison, for horse gram, the drag coefficient varied between 0.54 (minimum) and 0.59 (maximum), with a mean value of 0.55. The slight variations in terminal velocity and drag coefficient observed among the seed varieties may be attributed to differences in individual seed mass and projected area.

#### **4.1.4 Seed quality assessment**

In evaluating the seed quality of black gram and horse gram, the tetrazolium test showed good viability with 95 per cent and 94 per cent viable seeds, respectively. The germination test using the paper towel method with black gram showed a germination rate of 96 per cent and horse gram 92 per cent.

## 4.2 PNEUMATIC SEED METERING SYSTEM

The selection of the vacuum disc type precision seed metering system was made based on its recognized efficiency and adaptability to modern agricultural practices. This metering mechanism, chosen for integration into present research study for developing tractor operated pneumatic no-till pulse planter with electronic control system, offers precise seed placement critical for optimizing crop yields. Its operation relies on a vertically oriented rotating disc with holes around its circumference, facilitated by an aspirator blower creating a vacuum. Seeds are singulated and accurately metered, ensuring optimal plant spacing and uniformity.

## 4.3 DYNAMIC ANALYSIS OF PICKUP, TRANSPORT AND SEED DISCHARGE STAGES

In this present investigation, the forces acting on seeds at various stages of seed metering mechanism were studied and presented in the section 3.3.1. In this design, the pick-up process starts at the bottom of the seed rotor (under the seed lot), and the seed which are ready for picking up will be always close to the seed cell influenced by the movement and weight of the other seeds. Therefore, the magnitude of  $R$  (distance between seed and cell surface) shall be very small. When the air flow rate ( $Q$ ) increased and the distance between seed and cell ( $R$ ) decreased, the efficiency of sucking will increase. When the friction angle between seeds and seed rotor surface increased, the seeds will be easily picked by seed cell. Enlarging the cell diameter and increasing the negative pressure and friction index shall improve the efficiency of picking up seeds, any variation in these factors, however will lead to high values of multiple seed pickups. Keeping acceleration due gravity ( $g$ ), the radius of the seed plate ( $R_c$ ) and friction index ( $\tan\alpha_f$ ) are constants, the force of the negative pressure will increase when the rotating speed decreases.

From equation in section 3.3.1.1, it can be deduced that, the force required to pick up the seed was affected by seed parameters, seed density, drag coefficient and seed diameter ( $\rho_s, C_d, d_s$ ), radius between seed and cell ( $R$ ), friction angle between seeds and seed rotor surface ( $\alpha_g$ ) and air characteristics air density and air flow rate ( $\rho, Q$ ).

The seed sucking force is influenced by both seed density and geometric mean diameter, *i.e.*, the sucking force is directly proportional with seed density and geometric mean diameter. The sucking force is also directly proportional with square of air flow rate ( $Q_2$ ) and inversely proportional with the distance between seed and cell ( $R$ ).

Analytically it is proved that, the force of vacuum pressure created in the chamber should be greater than the weight of seed, then only the intended process of pickup and transport of seed will takes place. During the transportation stage, the force of seed weight, gravity, vacuum pressure and centrifugal forces should balance, unless the seed will drop before it reaches to discharge point. When seed cell exposes to atmospheric pressure, vacuum pressure will be suppressed at this zone and force of gravity and centrifugal force has more influence, so the seed will drop in to seed delivery spout. Hence, cell diameter, negative air pressure and forward speed were considered for the optimization for black gram and horse gram seeds.

#### 4.4 MODIFICATION OF THE PLANTER

The mechanical pneumatic planter with vacuum metering mechanism was modified to electronic driven pneumatic planter. The transition from a mechanical metering mechanism to an electronically controlled metering system, utilizing a stepper motor regulated by a microcontroller. This modification ensured precise rotation of the seed plate, resulting in a substantial reduction of double seeding and misses, thereby optimizing planting density and uniformity.

The customized hopper designs for black gram and horse gram seeds facilitated an uninterrupted and consistent seed flow, addressed the issues related to seed bridging and blockage. The performance of different furrow openers was rigorously evaluated under varied soil conditions, including both tilled and no-till environments. The electronically controlled metering system demonstrated superior adaptability, maintained consistent seed depth and spacing across diverse soil textures and conditions.

Integration of advanced sensors, including rotary encoders, proximity sensors, and vacuum pressure sensors, enabled real-time monitoring and adjustments of the

metering mechanism. These sensors provided precise data on seed singulation and vacuum pressure, which were processed by the microcontroller to ensure optimal performance. The use of actuators, such as stepper motors, allowed for precise control over seed delivery, further enhancing the accuracy of the planting process.

The robustness of the electronic control system was ensured through the use of high-quality components, such as the Arduino Nano microcontrollers, which managed various functions including sensor data processing and actuator control. The system resilience to environmental challenges, such as dust, moisture, and vibrations, was bolstered by housing the electronic components in a weatherproof ABS plastic enclosure with IP 66/67 and IK 07 ratings.

Overall, these modifications have resulted in a pneumatic planter that offered enhanced precision, efficiency, and versatility, making it well-suited for modern agricultural practices. The integration of electronic control systems has not only improved the accuracy of seed placement but also provided the flexibility to accommodate different cropping systems, such as intercropping and mixed cropping, thereby supporting diverse agricultural needs.

**Table 4.1 Specification of the developed tractor operated pneumatic planter with electronic controlled system**

<b>Sl. No.</b>	<b>Components</b>	<b>Specifications</b>
<b>1.</b>	<b>Overall dimensions</b> Length × Width × Height (mm)	2800 × 1400 × 1200
<b>2.</b>	<b>Main frame</b> Length × Width × Height (mm)	2800 × 100 × 150
<b>3.</b>	<b>Aspirator blower</b>	
	a. Radius, mm	275
	b. Vacuum pressure, k Pa	0 – 10
	c. Inlet, mm	Rectangular (300 × 60)
	d. Outlet opening, No.	12
	e. Large pulley dia, mm	300
	f. Small pulley dia, mm	100
<b>4.</b>	<b>Metering mechanism</b>	Vacuum type
<b>5.</b>	<b>No. of seed metering unit</b>	4
<b>6.</b>	<b>Seed plate</b>	
	a. Diameter, mm	184
	b. Shape	Conical
	c. No. of holes	26
	d. Hole diameter, mm	2.1
<b>7.</b>	<b>Seed hopper</b>	
	a. Shape	Trapezoidal with Top and bottom side cuboidal
	b. Size (Length × Width × Height), mm	300 × 250 × 140
	c. Thickness, mm	2
	d. Volume, cm <sup>3</sup>	9100
<b>8.</b>	<b>Furrow openers</b>	Stub runner, Inverted-T type, Shoe type
<b>9.</b>	<b>Four bar linkage, mm</b>	330 × 500 × 450 × 330
	<b>Spring length, mm</b>	220

<b>10. Mild steel wheel, (Radius, mm)</b>	175
<b>11. Pneumatic ground wheel</b>	
a. Radius, mm	350
b. Width, mm	140
<b>12. Compression wheels</b>	
a. Radius, mm	160
b. Width, mm	160
<b>13. Soil covering device</b>	Opposed paddle
<b>14. Height of resting foot, mm</b>	500
<b>15. PTO</b>	6 splines
<b>16. Profiling for height adjustment</b>	Rear profiling
<b>17. Electronic system</b>	Stepper motor, Driver, proximity, rotary encoder, PCB, rectifier diode, heat duct.
<b>18. Battery</b>	LiFePO4 (Lithium Iron Phosphate)
Dimension, mm	250 × 70 × 80
<b>19. Weight of the complete electronic system</b>	4 kg
<b>20. Weight of the planter</b>	320 kg

---



## 4.5 WORKING OF THE ELECTRONIC SYSTEM

The electronic system integrated into the vacuum seed metering mechanism of the pneumatic planter is a sophisticated assembly designed to ensure precise seed placement. It comprises several critical components, including a stepper motor, rotary encoder, proximity sensor, Arduino Nano microcontroller on a PCB, vacuum pressure sensor, micro-step drive, battery, and protective enclosure. The primary objective was to rotate the metering plate precisely, which featured 26 holes for seed dispensing. This rotation was facilitated by the stepper motor, controlled by the microcontroller based on inputs from the proximity sensor and rotary encoder. The proximity sensor detected wheel spokes, provide basic positional data, while the rotary encoder offered detailed feedback on position and speed, with high precision. Activation relies on the vacuum sensor detected optimal conditions within the metering mechanism. Calibration, software optimization, hardware upgrades, and environmental protection strategies were employed for system optimization.

## 4.6 PERFORMANCE EVALUATION OF SEED METERING MECHANISMS UNDER LAB CONDITIONS

Laboratory tests were conducted to evaluate seed spacing uniformity, miss index, multiple index, quality of feed index, and precision of spacing, as detailed in section 3.6.3. Results from these analyses are presented in subsequent sections. The design and operational parameters of the pneumatic seed metering mechanism were optimized using statistical techniques based on experimental data. A quadratic polynomial model and numerical optimization were employed to determine the optimal vacuum pressure, forward speed, plate hole size, and sensors for assessing seed metering performance. The impact of these parameters on the pneumatic seed metering system for black gram and horse gram is discussed below.

### **4.6.1 Effect of independent variables on the performance of the developed pneumatic seed metering mechanism for black gram**

The effect of design and operational (Independent variables) parameters were evaluated based on the measures of theoretical seed spacing. According to ISO (1984) defined measures of seed metering mechanism includes miss index, multiple index,

quality of feed index and precision of spacing were set as dependent variables for the optimization. Numerical optimization technique is used to select the best suitable design model and optimum treatment combination.

#### 4.6.1.1 Effect of sensor, vacuum, hole size and forward speed on mean seed spacing for black gram

The analysis revealed that seed spacing is significantly influenced by sensors, forward speed, and its interaction as given in the Table 4.2. The model was highly significant, explaining 80.49 per cent of the variance with an adjusted R<sup>2</sup> of 0.79 and a predicted R<sup>2</sup> of 0.78, indicated good model reliability. Despite the significant lack of fit (p-value = 0.0191), the adequate precision value of 24.189 indicated a strong signal-to-noise ratio, revealed that the model can be effectively navigated the design space.

**Table 4.2** Analysis of variance for seed spacing of black gram in the laboratory testing

Source	Sum of Squares	df	Mean Square	F-value	p-value	
<b>Model</b>	38.90	5	7.78	84.17	< 0.0001	significant
A-Sensors	9.42	1	9.42	101.95	< 0.0001	
D-Forward Speed	25.49	2	12.74	137.89	< 0.0001	
AD	3.99	2	1.99	21.57	< 0.0001	
<b>Residual</b>	9.43	102	0.0924			
Lack of Fit	4.08	30	0.1360	1.83	0.0191	significant
Pure Error	5.35	72	0.0743			
<b>Cor Total</b>	48.33	107				
<b>Std. Dev.</b>	0.304					R <sup>2</sup> 0.804
<b>Mean</b>	15.46					Adjusted R <sup>2</sup> 0.795
<b>C.V. %</b>	1.97					Predicted R <sup>2</sup> 0.781
						Adeq Precision 24.189

The main effect of independent parameters on seed spacing is illustrated in Fig. 4.1. The spacing for black gram ranged from 14.5 to 16 cm. The target spacing for seeds is 15 cm and it is observed that the sensor and the forward speed different levels have significant effect on seed spacing. The seed spacing observed at encoder sensor is near to 15 cm while in proximity it is very near to 16 cm. Similarly, at forward speed of 1.0 km h<sup>-1</sup>, seed spacing is near to 15 cm and at 2.0 km h<sup>-1</sup> it is near to 16 cm. These findings

are consistent with previous studies by Karayel et al. (2020) and Kumar et al. (2015), which observed similar trends.

In the Fig. 4.2, shows the interaction plot of all the independent parameter for seed spacing. The abscissa represents independent parameters such as sensor type, hole size, and vacuum pressure, which all relate to the spacing characteristics. The ordinate indicates the mean seed spacing. This interaction graph is a half-matrix graph, where the top section displays the interaction effects between sensor and hole size. The non-parallel lines in this section suggest a significant interaction effect between the sensor and hole size. If the lines are parallel, it would indicate no interaction effect. Fig.4.2 specifically highlights that the interaction between sensor and forward speed is more significant, compared to other interactions, which are not significant for seed spacing.

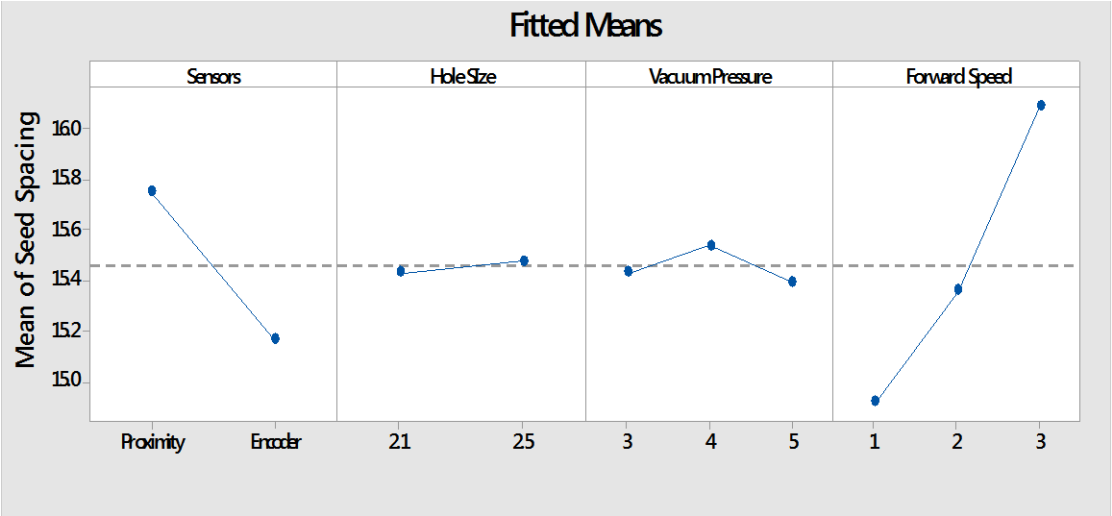


**Fig. 4.1 Effect on seed spacing of black gram**

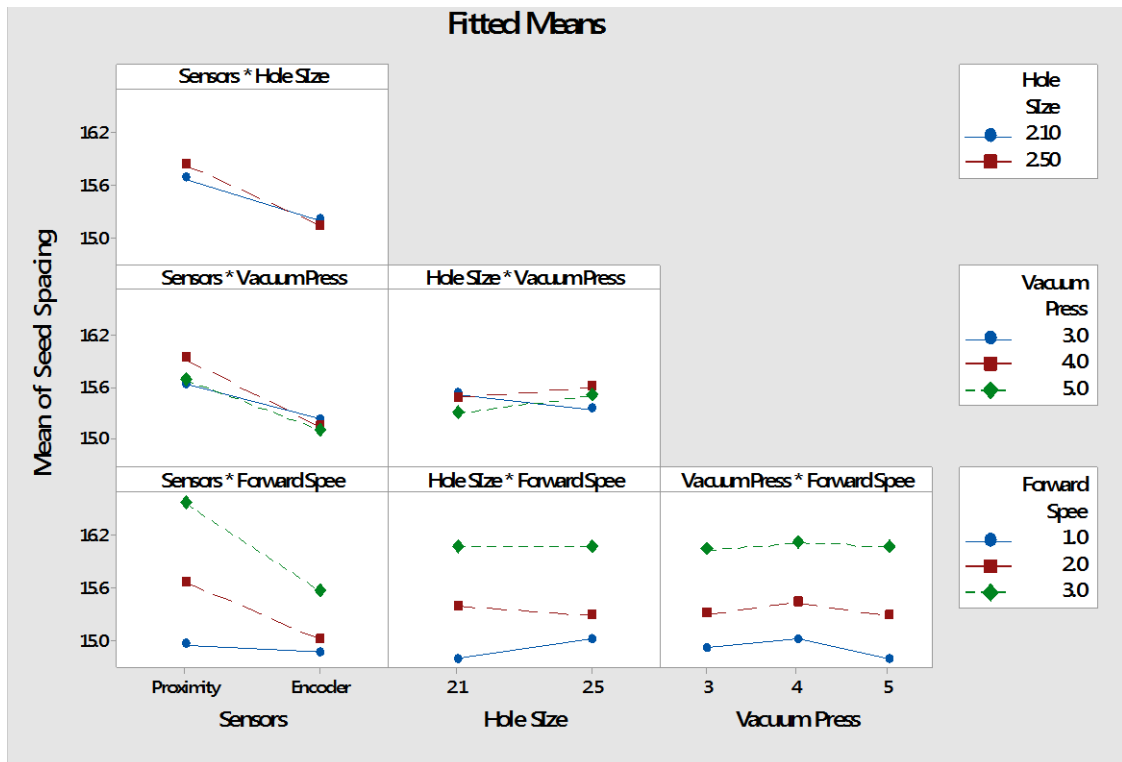


**Fig. 4.2 Interaction effect on seed spacing of black gram**

#### **4.6.1.2 Effect of sensor, vacuum, hole size and forward speed on miss index for black gram**

The analysis of variance (Table 4.3) shows that the model is statistically significant ( $p\text{-value} < 0.0001$ ), indicated that there is a relationship between the factors and the miss index. Sensors (A), hole size (b), forward speed (d), and the interactions between sensors and forward speed (ad) and hole size and vacuum pressure (cd) all have significant effects on the miss index. Vacuum pressure (C) on the other hand, does not have a significant effect. The model explains a high percentage of 98.91 variance in miss index and there is good model fit ( $p\text{-value for lack of fit} = 0.64$ ).

**Table 4.3 Analysis of variance for miss index of black gram in the laboratory testing**

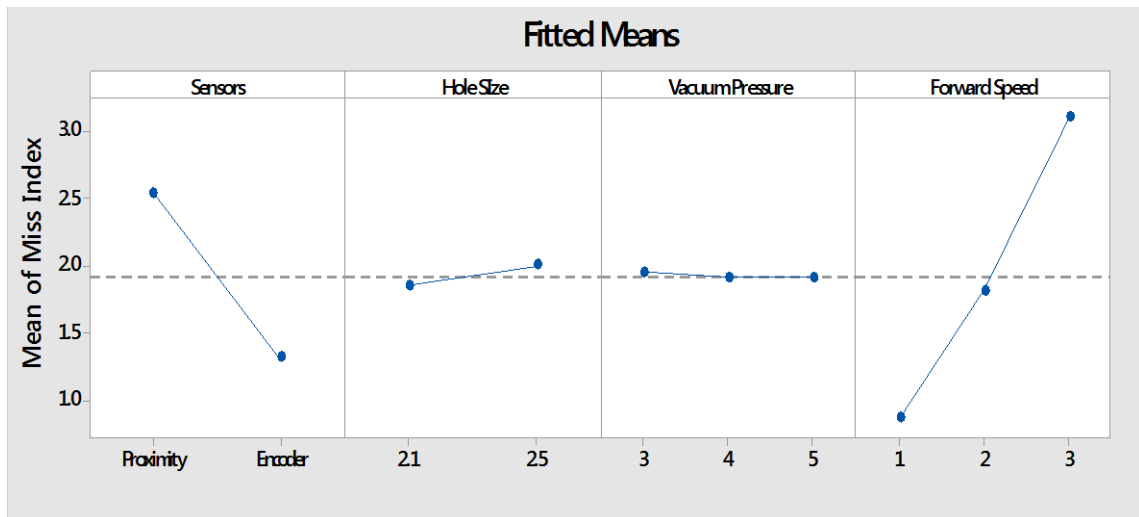
Source	Sum of Squares	df	Mean Square	F-value	p-value	
<b>Model</b>	141.62	12	11.80	720.49	< 0.0001	significant
A-Sensors	41.07	1	41.07	2507.31	< 0.0001	
B-Hole Size	0.5633	1	0.5633	34.39	< 0.0001	
C-Vacuum Pressure	0.0369	2	0.0184	1.12	0.3290	
D-Forward Speed	92.07	2	46.04	2810.53	< 0.0001	
AD	7.54	2	3.77	230.28	< 0.0001	
CD	0.3337	4	0.0834	5.09	0.0009	
<b>Residual</b>	1.56	95	0.0164			
Lack of Fit	0.3361	23	0.0146	0.8624	0.6444	not significant
Pure Error	1.22	72	0.0169			
<b>Cor Total</b>	143.18	107				
<b>Std. Dev.</b>	0.128				R <sup>2</sup>	0.989
<b>Mean</b>	1.92				Adjusted R <sup>2</sup>	0.987
<b>C.V. %</b>	6.65				Predicted R <sup>2</sup>	0.986
					Adeq Precision	86.829

Fig. 4.3 depicts the influence of various independent parameters on the miss index. It is evident that as forward speed increases, the miss index per centage increases from 1.0 to 3.0 per cent. Observations of the hole size and vacuum pressure reveal that the mean miss index does not significantly change across different levels. This stability is attributed to the relatively uniform size of black gram seeds, which exhibit minimal size variation. However, smaller hole sizes result in a lower miss index compared to larger holes, as larger holes sometimes allow two or more seeds to adhere to a single hole in the vertical plate. The adjustable singulation wiper, designed to remove extra seeds, occasionally causes both seeds to fall, contributing to a higher miss index at 3 kPa compared to 4 and 5 kPa.

The data also indicate that the miss index is lower with the rotary encoder sensor compared to the proximity sensor. This difference is due to the encoder sensor's higher precision and faster communication between sensors. Fig. 4.4, indicated an interaction between different independent parameters and the miss index also shows a significant effect on that the interaction between the sensor and the encoder. Other interaction lines

are parallel, indicating their insignificance. This implies that at lower forward speeds, cells have more time to pick seeds even at lower air pressures, resulting in a minimal miss index at lower forward speeds.

The fitted quadratic polynomial model was found to be significant at the 1.0 per cent level, highlighting the influence of all selected variables on the miss index. These findings are as per the result reported by Kumar et al. (2015). The optimal levels of peripheral speed, hole diameter, and vacuum pressure for precision seeders here indicated similar trends. Wang et al. (2023) also reported comparable results for different seed varieties in pneumatic planters, noting that miss index values decreased with increased pressure but increased with higher speeds



**Fig. 4.3 Effect on miss index of black gram**

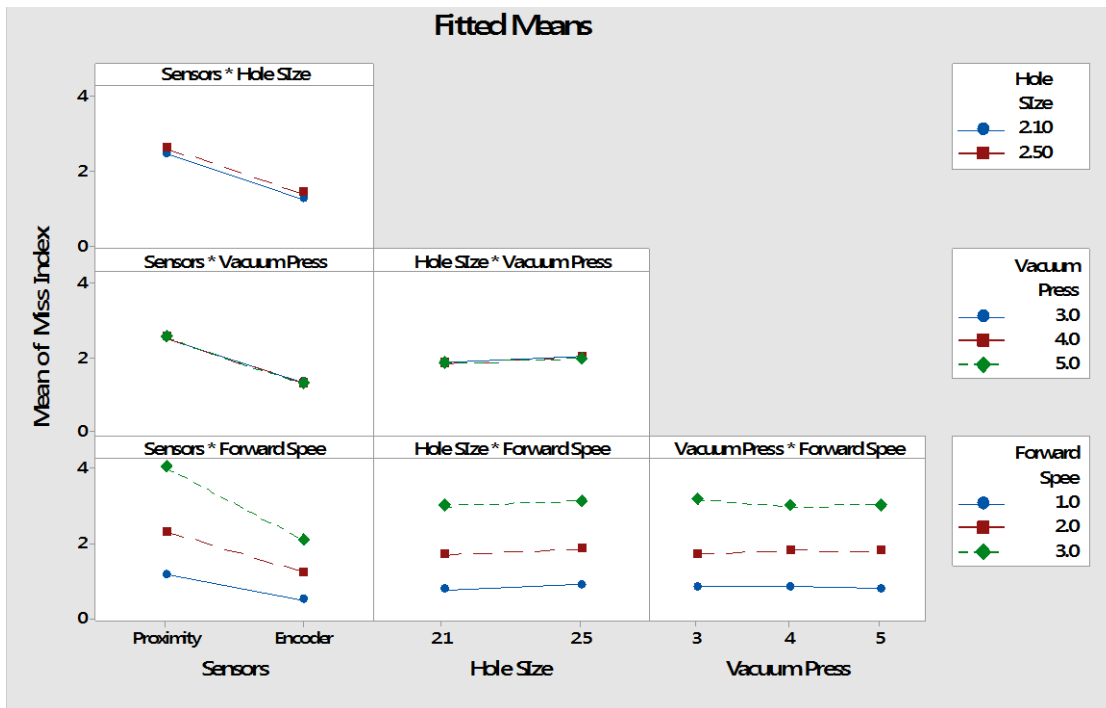


**Fig. 4.4 Interaction effect on miss index of black gram**

#### 4.6.1.3 Effect of sensor, vacuum, hole size and forward speed on multiple index for black gram

The multiple index analysis identified significant influences due to hole size, vacuum pressure, forward speed, and their interactions. The model explained 95.90 per cent of the variance with an adjusted  $R^2$  of 0.95 and a predicted  $R^2$  of 0.95, indicating strong model performance. The adequate precision value of 54.35 indicates a strong signal, confirming the model ability to navigate the design space effectively.

**Table 4.4 Analysis of variance for multiple index of black gram in the laboratory testing**

Source	Sum of Squares	df	Mean Square	F-value	p-value	
<b>Model</b>	44.84	9	4.98	254.51	< 0.0001	significant
B-Hole Size	22.96	1	22.96	1173.11	< 0.0001	
C-Vacuum Pressure	3.00	2	1.50	76.69	< 0.0001	
D-Forward Speed	18.52	2	9.26	473.10	< 0.0001	
CD	0.3511	4	0.0878	4.48	0.0023	
<b>Residual</b>	1.92	98	0.0196			
Lack of Fit	0.7850	26	0.0302	1.92	0.0161	significant
Pure Error	1.13	72	0.0157			
<b>Cor Total</b>	46.76	107				
<b>Std. Dev.</b>	0.139					R <sup>2</sup> 0.959
<b>Mean</b>	3.53					Adjusted R <sup>2</sup> 0.955
<b>C.V. %</b>	3.97					Predicted R <sup>2</sup> 0.950
						Adeq Precision 54.350

Fig. 4.5 illustrates the influence of various independent parameters on the multiple index for black gram seeds. The main effect plot indicates that hole size, vacuum pressure, and forward speed significantly affect the multiple index. Fig. 4.6 further demonstrates that the interaction between vacuum pressure and forward speed is significant for the multiple index. This significance may be due to the uneven shape of black gram seeds, combined with different hole sizes and vacuum pressures, affects the adherence of seeds to the holes. At high vacuum pressure, more than one seed can be adhered and hence, lead to a higher multiple index.

The decrease in the multiple index with increasing belt linear speed is attributed to the reduced time available for seed picking and potential internal friction among the seeds, which may cause misses. The study found an average multiple index of 3.38 per cent. It was observed that the multiple index increases with larger hole sizes on the plate, providing more space to hold seeds. Additionally, increasing the hole diameter and vacuum pressure also raises the multiple index, as larger plate hole diameters enhance vacuum pressure, increasing the likelihood of picking multiple seeds. These findings



align with Gautam et al. (2023), who reported similar trends in variation regarding the multiple index. Singh et al. (2005) noted that the multiple index value was minimum at an operating pressure of 1.0 kPa and at higher forward speeds.

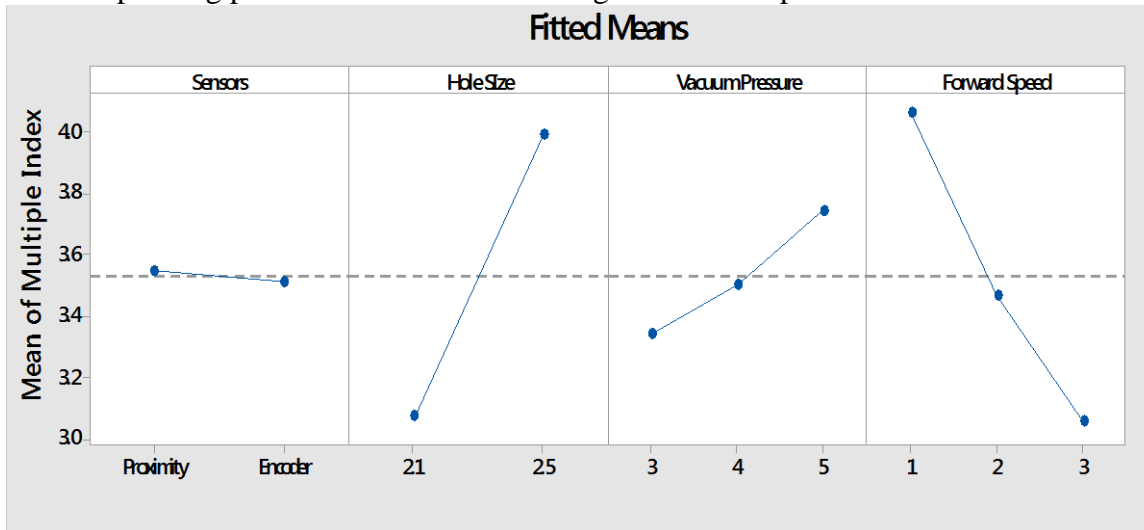


Fig. 4.5 Effect on multiple index of black gram

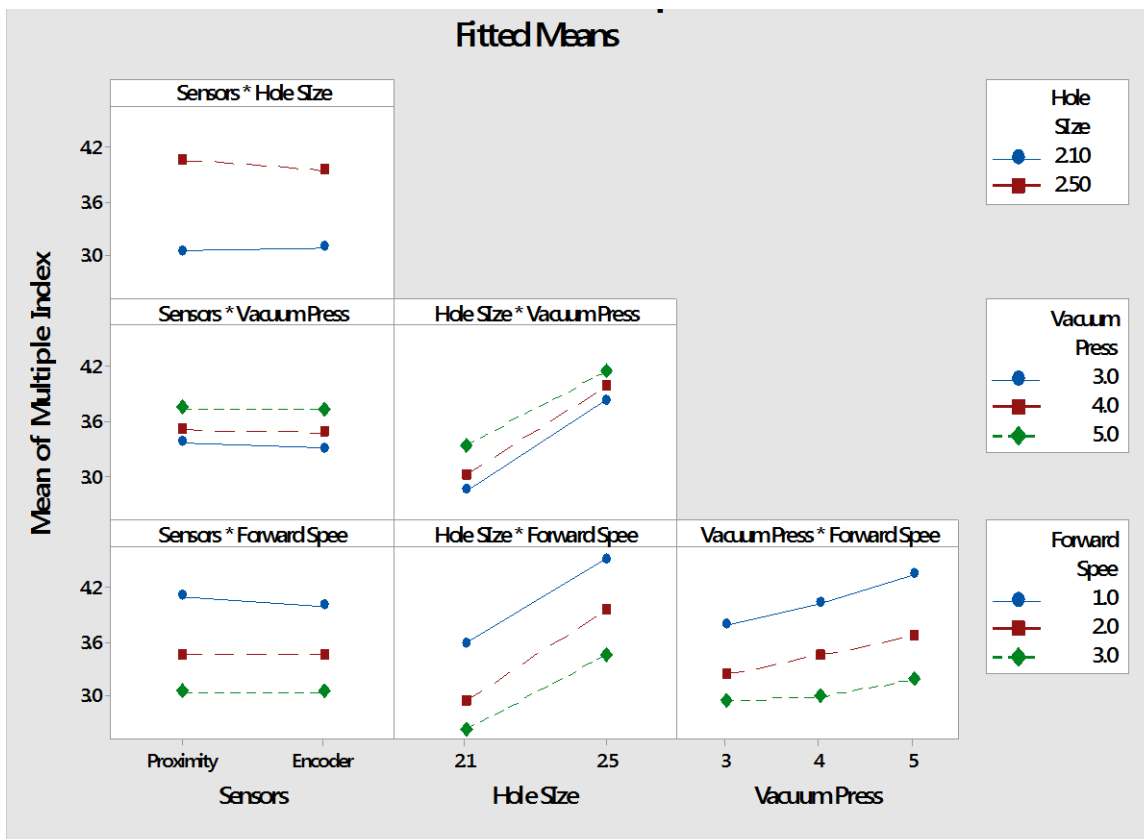


Fig. 4.6 Interaction effect on multiple index of black gram

#### 4.6.1.4 Effect of sensor, vacuum, hole size and forward speed on quality of feed index for black gram

The analysis for quality of feed index revealed significant effects w.r.t. sensors, hole size, vacuum pressure, forward speed, and their interactions. The model was highly significant, explaining 97.19 per cent of the variance with an adjusted R<sup>2</sup> of 0.96 and a predicted R<sup>2</sup> of 0.96. The lack of fit was not significant (p-value = 0.18), indicating a good model fit. An adequate precision value of 74.97 confirms a strong signal-to-noise ratio, suggesting the robustness of the model in navigating the design space.

**Table 4.5 Analysis of variance for quality of feed index of black gram in the laboratory testing**

Source	Sum of Squares	df	Mean Square	F-value	p-value	
<b>Model</b>	114.15	12	9.51	273.65	< 0.0001	significant
A-Sensors	43.57	1	43.57	1253.55	< 0.0001	
B-Hole Size	30.72	1	30.72	883.77	< 0.0001	
C-Vacuum Pressure	2.46	2	1.23	35.40	< 0.0001	
D-Forward Speed	29.62	2	14.81	426.03	< 0.0001	
AD	6.75	2	3.38	97.13	< 0.0001	
CD	1.02	4	0.2555	7.35	< 0.0001	
<b>Residual</b>	3.30	95	0.0348			
Lack of Fit	0.9822	23	0.0427	1.33	0.1829	not significant
Pure Error	2.32	72	0.0322			
<b>Cor Total</b>	117.45	107				
<b>Std. Dev.</b>	0.186				R <sup>2</sup>	0.971
<b>Mean</b>	94.55				Adjusted R <sup>2</sup>	0.968
<b>C.V. %</b>	0.197				Predicted R <sup>2</sup>	0.963
					Adeq Precision	62.053

Fig. 4.7 shows that the Quality of Feeding Index (QFI) of the seeds was significantly affected by all the independent factors. For instance, the QFI was generally higher when using the encoder sensor compared to the proximity sensor, suggesting that the encoder sensor may be more accurate and provide precise input even at higher speed. Additionally, the QFI was generally higher for a hole size of 2.1 mm than for a hole size

of 2.5 mm, indicating that the smaller hole size may be better for feeding black gram seeds, which can vary in size and shape. In Fig. 4.8 it is shown that the interaction sensor and forward speed as well as between vacuum pressure and forward speed was significant. Throughout the experiments, encoder sensors consistently provided higher QFI values than proximity sensors. This increased precision is likely due to the encoders ability to offer real-time feedback on seed placement accuracy, reducing the likelihood of misses or multiple seed drops. At higher speed the QFI decreases at higher speed as well as it decreases with the increasing pressure. This may be due to the increase of missing and multiples seed with increasing forward speed and pressure respectively.

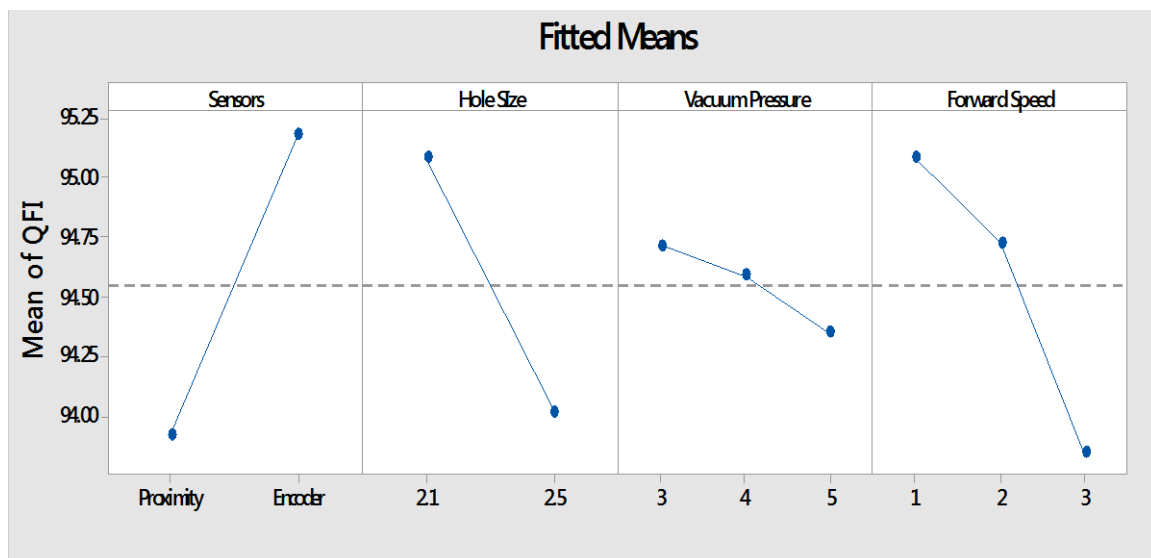


**Fig. 4.7 Effect on quality feed index of black gram**

Using encoder sensors, a vacuum pressure of 3.0 kPa, and a forward speed of 1.0 km h<sup>-1</sup>, the QFI was 96.6 per cent for the 2.1 mm hole size compared to 95.3 per cent for the 2.5 mm hole size. An intermediate vacuum pressure of 4.0 kPa provided the best QFI values. Lower forward speeds typically resulted in higher QFI values, as higher speeds may not allow sufficient time for precise placement, reducing the QFI. Generally low vacuum pressure may not hold the seeds properly, leading to missed placements, while high pressure can cause seeds to be placed very close together, affecting uniformity. These results align with those reported by Kuş and Yıldırım (2021) and Karayel et al. (2020), who observed similar trends.

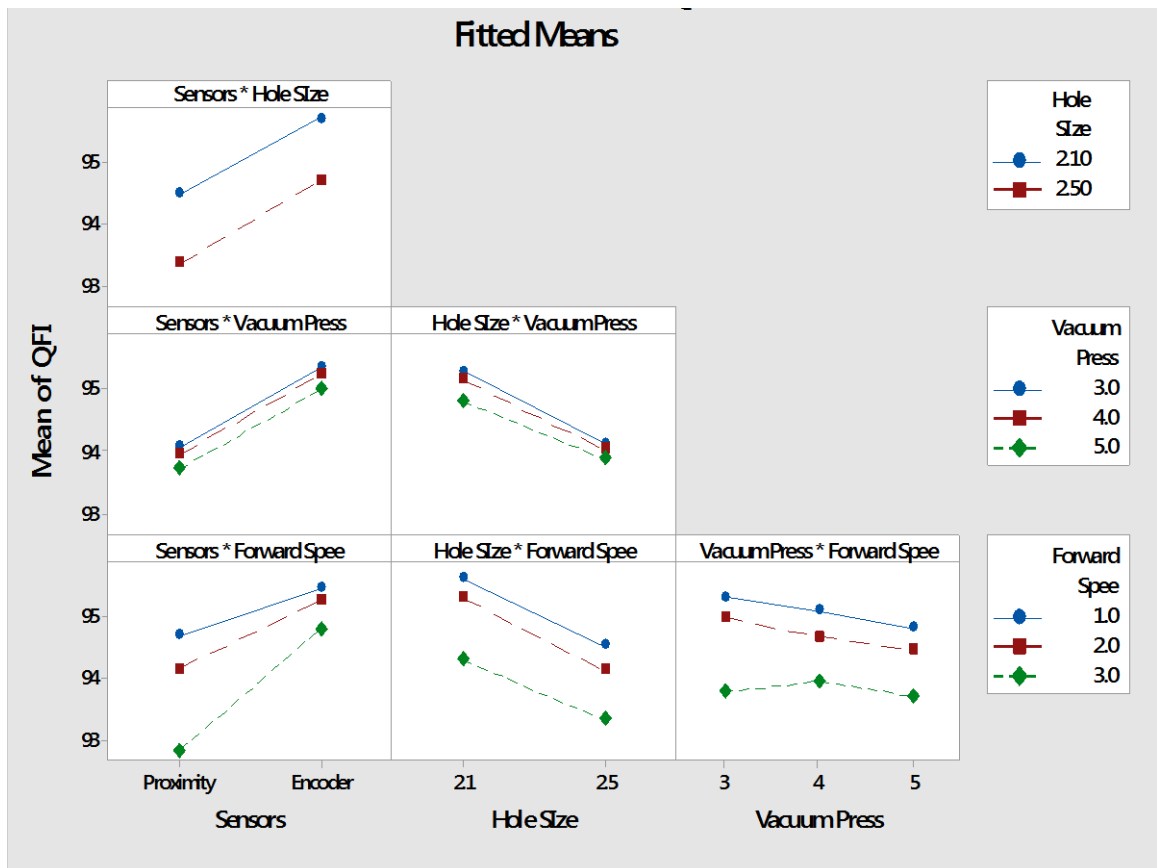


**Fig. 4.8 Interaction plot for quality feed index of black gram**

#### ***4.6.1.5 Effect of sensor, vacuum, hole size and forward speed on precision of spacing for black gram***

Precision analysis indicated significant influences w.r.t. sensors, hole size, vacuum pressure, forward speed, and their interactions. The model explained 93.43 per cent of the variance with an adjusted  $R^2$  of 0.92 and a predicted  $R^2$  of 0.91. The lack of fit was not significant ( $p$ -value = 0.089), suggesting a good model fit. The adequate precision value of 49.50 confirms a strong signal-to-noise ratio, ensuring the reliability of the model.

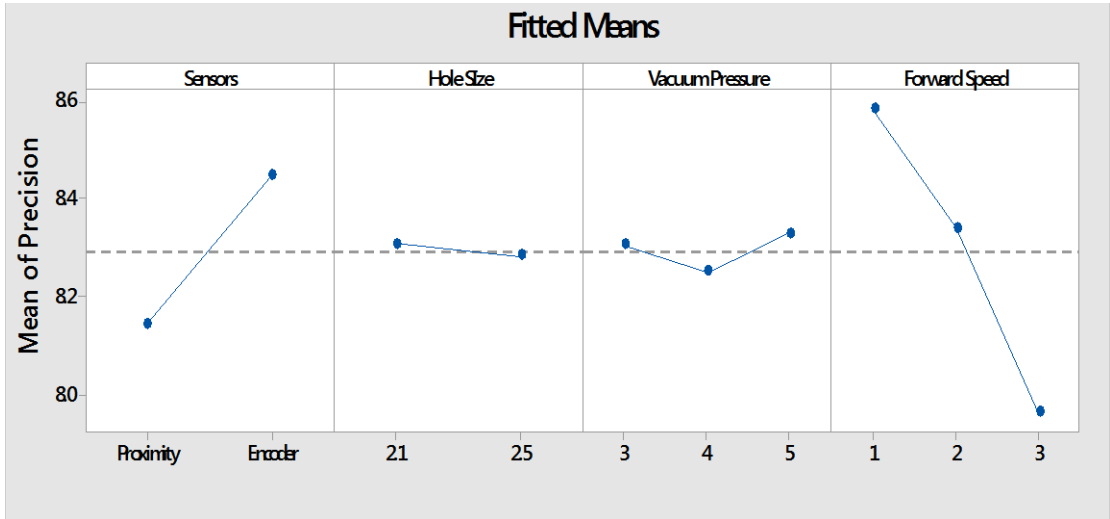
**Table 4.6 Analysis of variance for precision of spacing of black gram in the laboratory testing**

Source	Sum of Squares	df	Mean Square	F-value	p-value	
<b>Model</b>	10.55	5	2.11	75.99	< 0.0001	significant
A-Sensors	2.47	1	2.47	89.15	< 0.0001	
D-Forward Speed	7.08	2	3.54	127.45	< 0.0001	
AD	0.9963	2	0.4981	17.94	< 0.0001	
<b>Residual</b>	2.83	102	0.0278			
Lack of Fit	1.22	30	0.0407	1.82	0.0206	significant
Pure Error	1.61	72	0.0224			
<b>Cor Total</b>	13.38	107				
<b>Std. Dev.</b>	0.166					R <sup>2</sup> 0.788
<b>Mean</b>	8.30					Adjusted R <sup>2</sup> 0.778
<b>C.V. %</b>	2.01					Predicted R <sup>2</sup> 0.762
						Adeq Precision 22.875

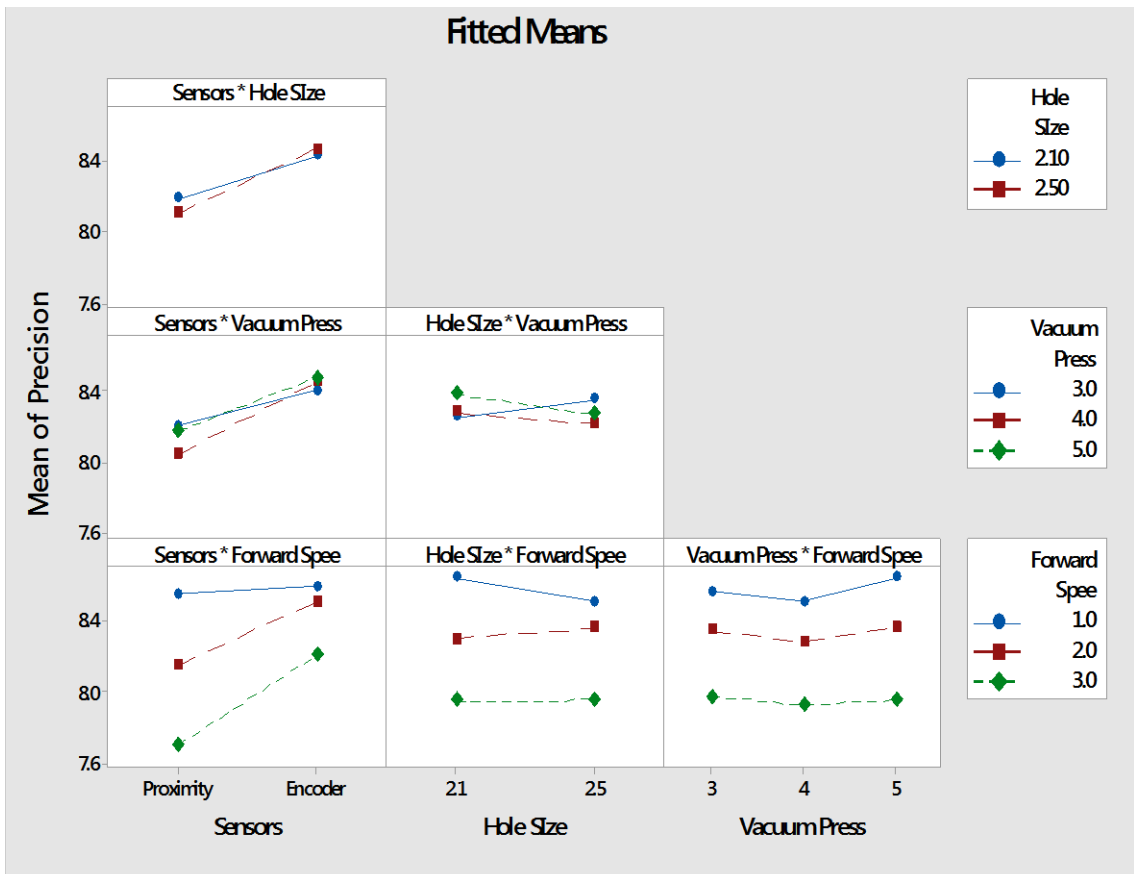
The study found that the average precision in seed spacing was 8.27 per cent. As forward speed increased, precision decreased, but it decrease as vacuum pressure increased from 4.0 kPa to 5.0 kPa. The best value of precision of spacing were observed at the vacuum pressure of 4.0 kPa. Precision measures the variability in seed spacing, accounting for both multiple seeds and misses. Lower precision values indicate better performance of the metering device and its operating parameters.

Fig. 4.9 indicates that both the sensor type and forward speed significantly affect precision at the 1.0 per cent level, and their interaction is also significant. Fig. 4.10 shows the interaction plot between various independent parameters for the precision of seed spacing for black gram. These findings are consistent with those of Karayel et al. (2020) and Gautam et al. (2023).

The precision index across the tested models varied between 7.0 and 9.0 per cent, significantly lower than the theoretical upper limit of 50 per cent. According to Katchman and Smith (1995), a practical upper limit for precision is 29 %, which suggests that all spacings are uniformly spread within the target range. Values consistently greater than 29% seriously be viewed with suspicion.



**Fig. 4.9** Effect on precision of spacing of black gram



**Fig. 4.10** Interaction effect on precision of spacing of black gram

The numerical optimization for evaluation of the lab model was performed by setting the goal for all parameters as given in Table 4.7 to obtain optimum solution.

**Table 4.7 Multi response numerical optimization constraints**

Parameters	Goal
<b>1. Independent</b>	
a. Vacuum Pressure, (k Pa)	is in range (3.0, 4.0 & 5.0)
b. Sensor	is in range (Proximity & encoder)
c. Hole size (mm)	is in range (2.1 & 2.5)
d. Forward speed, (km h <sup>-1</sup> )	is in range (1.0, 2.0 & 3.0)
<b>2. Dependent</b>	
a. Seed spacing (cm)	Exact
b. Miss Index (per cent)	Minimum
c. Multiple Index (per cent)	Minimum
d. Quality feed index	Maximum
e. Precision Index (per cent)	Minimum

. The desirability for evaluation of the lab model of pneumatic planter with electronic control system was found as shown in the Fig. 4.11 the desirability of optimum parameters of unit was 0.80 for black gram seeds.

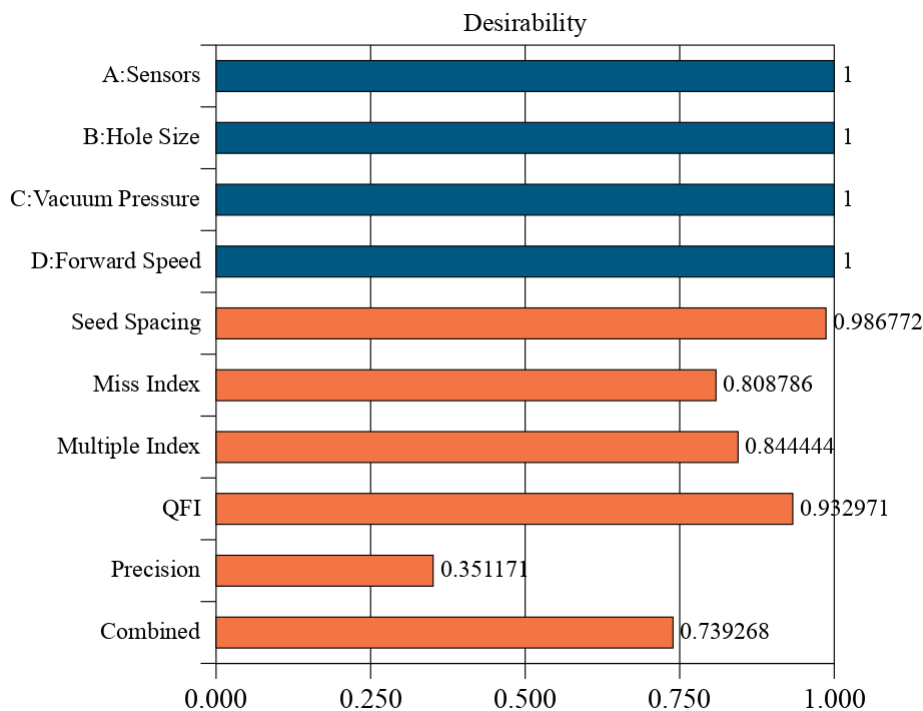


**Fig. 4.11 Desirability index for lab model of vacuum metering mechanism with electronic control system for black gram**

The presented graphs depict the optimized results from a laboratory experiment investigating the influence of various parameters on a pneumatic planter metering mechanism designed for black gram seeds. The experiment employed an electronic control system to manage the metering process.

Four key parameters were manipulated viz., sensor type (proximity vs. rotary encoder), plate hole size (2.1 and 2.5 mm), vacuum pressure (3.0, 4.0, and 5.0 kPa), and planter operating speed (1.0, 2.0, and 3.0 km h<sup>-1</sup>). The experiment evaluated the impact of these parameters on five key responses viz., seed spacing (cm), miss index (%), multiple index (%), quality of feed index (%), and precision of spacing (%).

From Fig. 4.12, it can be concluded that rotary encoder with hole size of 2.1 mm at 4.0 kPa at speed of 1.0 km h<sup>-1</sup> is the best treatment combination for the vacuum seed metering mechanism with electronic control system to obtained best result in term of seed spacing, miss and multiple index.

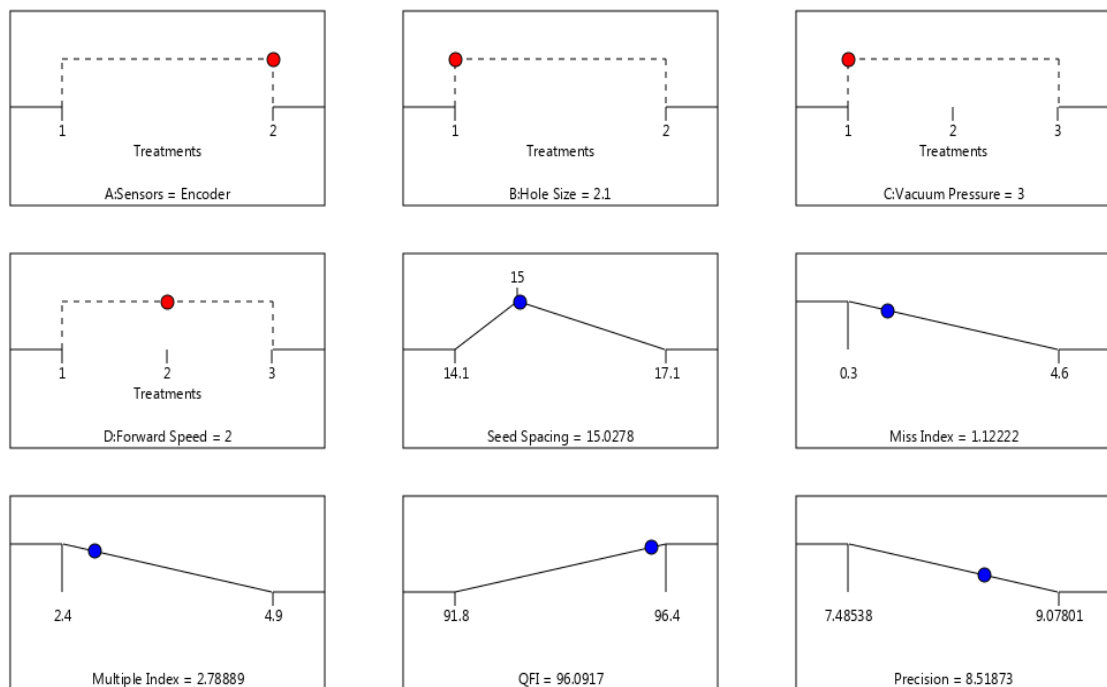


**Fig. 4.12 Optimum value for sensor, hole size, vacuum pressure and forward speed on performance parameters for black gram**



## 4.6.2 Effect of independent variables on the performance of the developed pneumatic seed metering mechanism for horse gram

### 4.6.2.1 Effect of sensor, vacuum, hole size and forward speed on mean seed spacing for horse gram

The ANOVA for seed spacing of horse gram seeds reveals that the model is highly significant (F-value = 226.82,  $p < 0.0001$ ), is shown in Table 4.8. It is indicating that the independent variables significantly affect seed spacing. The sensors (A) and forward speed (D) individually, as well as their interaction (AD), are all significant factors influencing seed spacing, as evidenced by their p-values ( $< 0.0001$ ). The high  $R^2$  value of 0.91 suggests that 91.75 per cent of the variation in seed spacing can be explained by the model. The low lack of fit F-value (0.57) and high Adequate Precision (45.24) indicate that the model fits well and has a strong signal-to-noise ratio. Therefore, optimizing these factors can lead to improved seed spacing uniformity, which is crucial for achieving optimal plant population and yield.

**Table 4.8** Analysis of variance for seed spacing of horse gram in the laboratory testing

Source	Sum of Squares	df	Mean Square	F-value	p-value	
<b>Model</b>	147.81	5	29.56	226.82	$< 0.0001$	significant
A- Sensors	6.36	1	6.36	48.77	$< 0.0001$	
D- Forward Speed	94.66	2	47.33	363.17	$< 0.0001$	
AD	46.79	2	23.40	179.51	$< 0.0001$	
<b>Residual</b>	13.29	102	0.1303			
Lack of Fit	2.58	30	0.0860	0.5780	0.9515	not significant
Pure Error	10.71	72	0.1488			
<b>Cor Total</b>	161.10	107				
<b>Std. Dev.</b>	0.361				$R^2$	0.917
<b>Mean</b>	10.43				Adjusted $R^2$	0.913
<b>C.V. %</b>	3.46				Predicted $R^2$	0.907
					Adeq Precision	45.246

The seed spacing parameter is crucial for ensuring uniformity in plant growth and maximizing yield. The results indicate that seed spacing is influenced by sensor type, hole size, vacuum pressure, and forward speed. For instance, when using proximity sensors with a hole size of 2.1 mm, a vacuum pressure of 3 kPa, and a forward speed of 1 km h<sup>-1</sup>, the seed spacing was recorded at 9.2 cm. However, increasing the forward speed to 3 km h<sup>-1</sup> resulted in increased seed spacing of 12.9 cm. The target spacing for black gram was 10 cm. Encoder sensors generally provided more consistent seed spacing, with values ranging from 9.8 cm to 11.1 cm under similar conditions. This consistency is likely due to the precise feedback mechanism of encoder sensors, which ensures accurate seed placement.

Fig. 4.13 demonstrates that increased forward speed leads to increased seed spacing. Both sensor type and forward speed were significant at the 1 % level. An interaction plot between different independent parameters is shown in Fig. 4.14, indicating that the interaction between sensor type and forward speed is significant at the 1 % level. In this Fig., parallel lines indicate non-significant interactions, while non-parallel lines indicate significant interactions. These findings are consistent with those of Lijing et al. (2016) and Kuş and Yıldırım (2021).

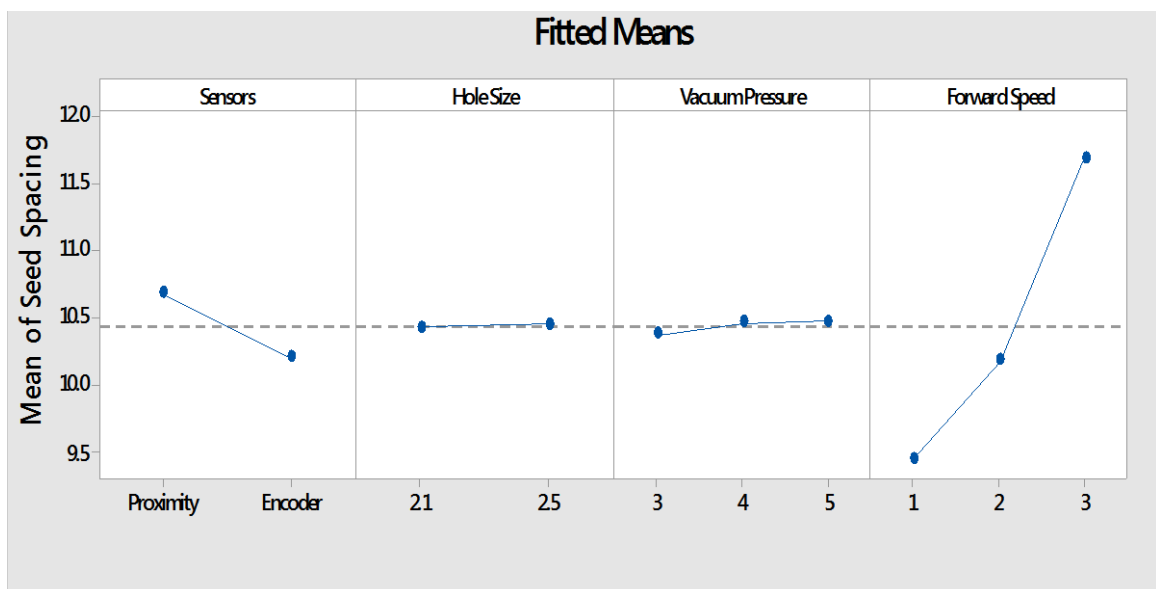


**Fig. 4.13 Effect on seed spacing of horse gram**

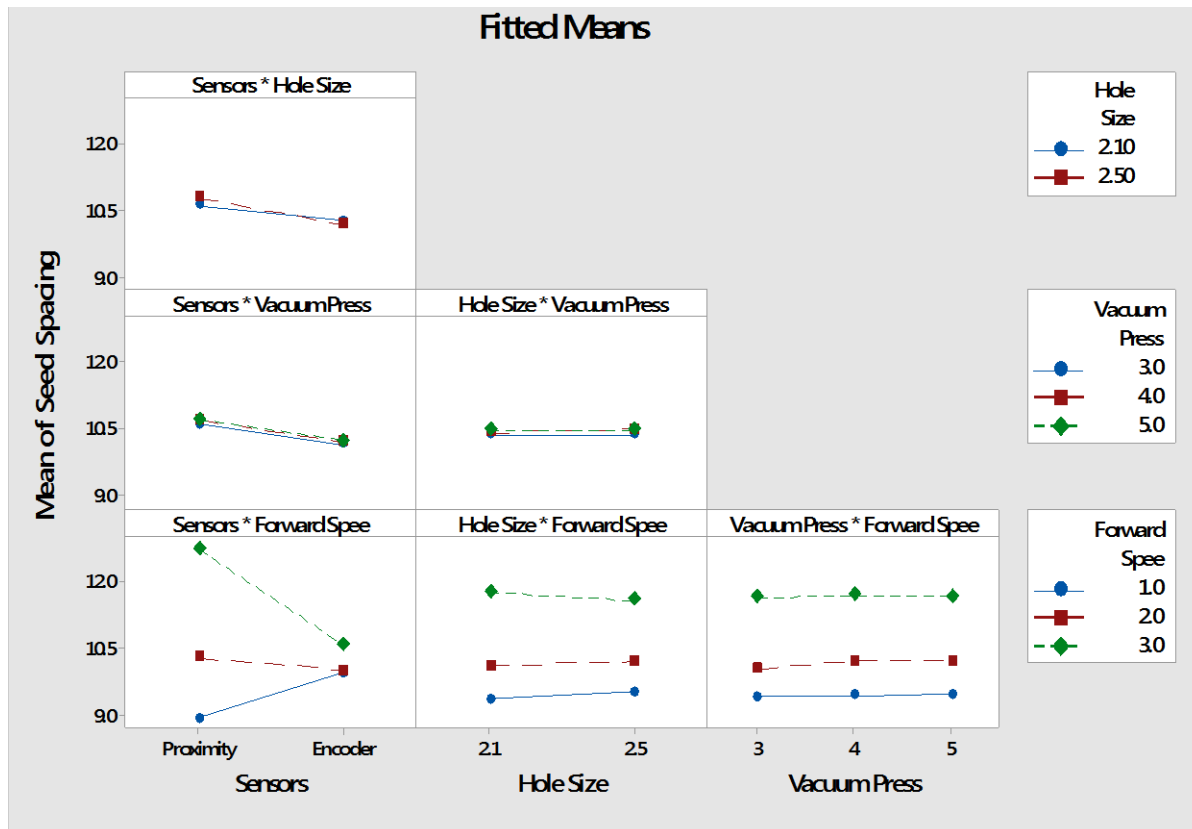


**Fig. 4.14 Interaction effect on seed spacing of horse gram**

**4.6.2.2 Effect of sensor, vacuum, hole size and forward speed on miss index for horse gram**

The ANOVA for the miss index of horse gram seeds shows that the model is extremely significant (F-value = 1180.76,  $p < 0.0001$ ) is given in Table 4.9. The significant factors include sensors (A), hole size (B), forward speed (D), and their interactions (AB, AD), with all p-values being  $< 0.0001$ . The model  $R^2$  value of 0.98 indicates that 98.80 per cent of the variability in the miss index is accounted for by these factors. Despite the relatively low lack of fit probability (8.11%), which suggests some concern, the high Adequate Precision (107.51) confirms the model reliability in navigating the design space. Minimizing the miss index is essential for ensuring better seed placement and higher germination rates.

**Table 4.9 Analysis of variance for miss index of horse gram in the laboratory testing**

Source	Sum of Squares	df	Mean Square	F-value	p-value	
<b>Model</b>	154.16	7	22.02	1180.76	< 0.0001	significant
A-Sensors	48.13	1	48.13	2580.62	< 0.0001	
B-Hole Size	2.28	1	2.28	122.36	< 0.0001	
D-Forward Speed	95.64	2	47.82	2563.88	< 0.0001	
AB	0.7008	1	0.7008	37.57	< 0.0001	
AD	7.41	2	3.70	198.51	< 0.0001	
<b>Residual</b>	1.87	100	0.0187			
Lack of Fit	0.6919	28	0.0247	1.52	0.0811	not significant
Pure Error	1.17	72	0.0163			
<b>Cor Total</b>	156.03	107				
<b>Std. Dev.</b>	0.136				R <sup>2</sup>	0.988
<b>Mean</b>	2.05				Adjusted R <sup>2</sup>	0.987
<b>C.V. %</b>	6.67				Predicted R <sup>2</sup>	0.986
					Adeq Precision	107.513

The miss index measures the frequency of missing seeds during planting, which can lead to gaps in the field and reduced crop yields. The results indicate that lower miss indices were achieved using encoder sensors compared to proximity sensors. For example, with a hole size of 2.1 mm and vacuum pressure of 3 kPa, the miss index for encoder sensors was as low as 0.5 per cent at a forward speed of 1 km h<sup>-1</sup>, while proximity sensors recorded a miss index of 1.2 per cent under the same conditions. This suggests that encoder sensors are more effective in minimizing seed misses, likely due to their higher precision and better control over the seed metering process.

Fig. 4.15 presents the main effect plot for the miss index with various independent parameters. The sensor type, hole size, and forward speed were all significant factors. As the hole size of the metering plate increased, the miss index also increased. This is because seeds can sometimes get jammed in larger holes, leading to a higher multiple index and a reduced miss index. At higher forward speeds, the miss index was higher due to insufficient time for seed pickup and increased friction between seeds and between the seeds and the metering plate. These findings are consistent with those observed by Karayel et al. (2020) and Kumar et al. (2015).

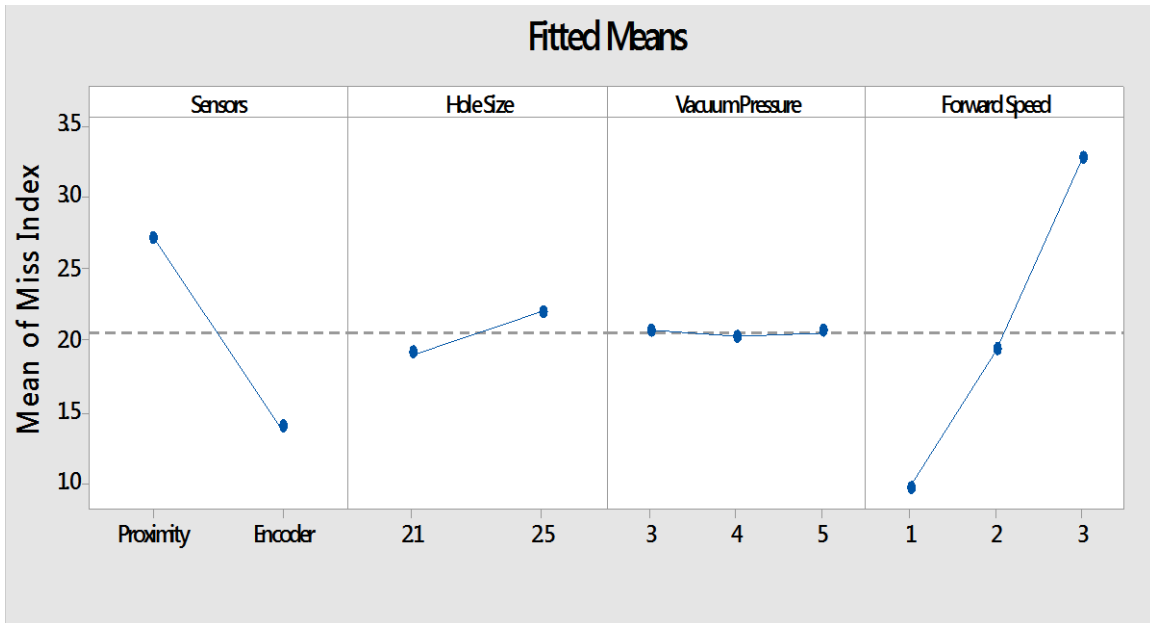


Fig. 4.15 Effect on miss index of horse gram

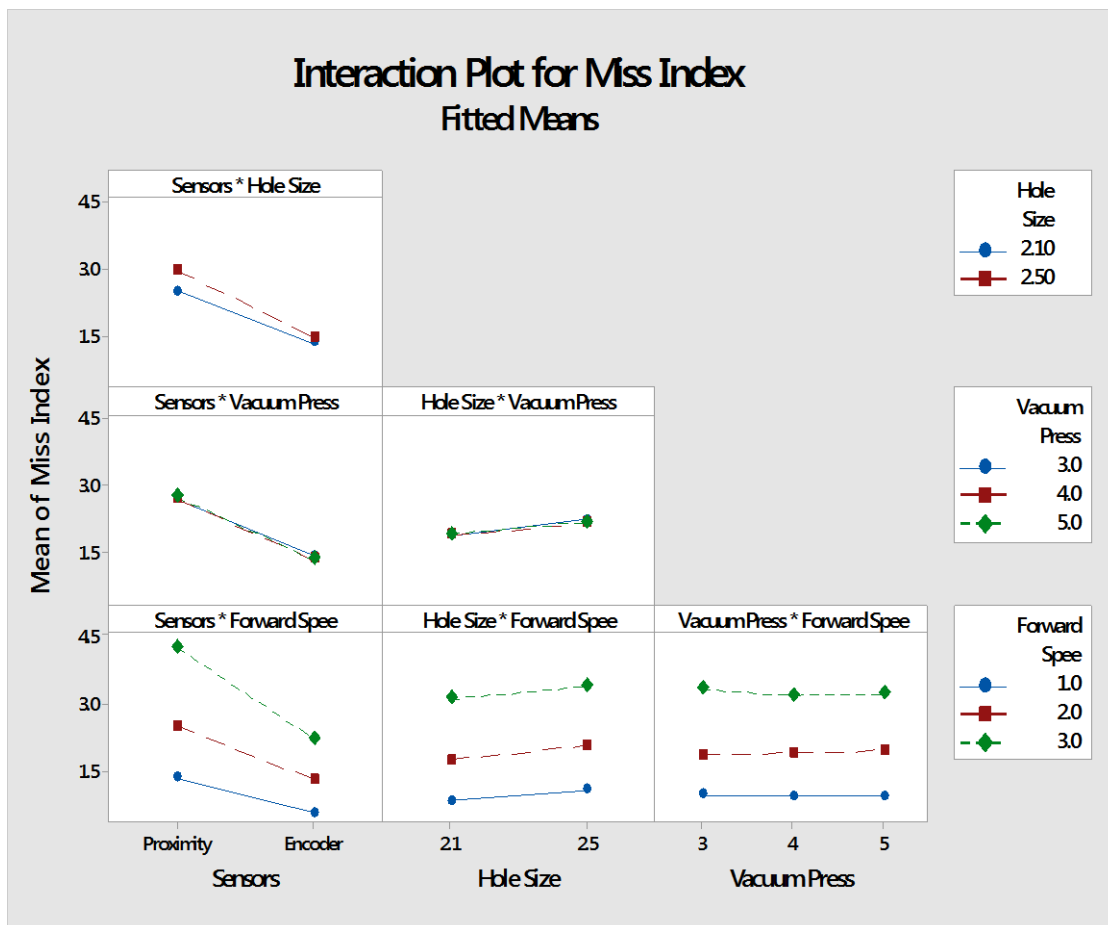


Fig. 4.16 Interaction effect on miss index of horse gram

#### 4.6.1.3 Effect of sensor, vacuum, hole size and forward speed on multiple index for horse gram

The ANOVA table for the multiple index of horse gram seeds indicates a highly significant model (F-value = 306.56,  $p < 0.0001$ ). Significant factors include hole size (B), vacuum pressure (C), and forward speed (D), each with  $p$ -values  $< 0.0001$ . The model explains 93.76 per cent of the variance in the multiple index ( $R^2 = 0.93$ ). However, the significant lack of fit (F-value = 2.77,  $p = 0.0002$ ) indicates some discrepancies between the model and observed data. The high Adequate Precision (58.11) suggests a strong model signal. Reducing the multiple index is important for preventing overcrowding and ensuring optimal spacing for each plant.

**Table 4.10** Analysis of variance for multiple index of horse gram in the laboratory testing

Source	Sum of Squares	df	Mean Square	F-value	p-value	
<b>Model</b>	50.46	5	10.09	306.56	< 0.0001	significant
B-Hole Size	28.01	1	28.01	850.84	< 0.0001	
C-Vacuum Pressure	3.60	2	1.80	54.72	< 0.0001	
D-Forward Speed	18.85	2	9.42	286.26	< 0.0001	
<b>Residual</b>	3.36	102	0.0329			
Lack of Fit	1.80	30	0.0599	2.77	0.0002	significant
Pure Error	1.56	72	0.0217			
<b>Cor Total</b>	53.82	107				
<b>Std. Dev.</b>	0.181				$R^2$	0.937
<b>Mean</b>	3.71				Adjusted $R^2$	0.934
<b>C.V. %</b>	4.88				Predicted $R^2$	0.930
					Adeq Precision	58.112

The multiple index represents the occurrence of multiple seeds being planted in the same spot, leading to competition for resources among seedlings. The results from lab testing showed that the multiple index is higher for proximity sensors compared to encoder sensors, as illustrated in Fig. 4.17, which plots the main effects of independent parameters on the multiple index. For instance, at a hole size of 2.5 mm and vacuum pressure of 5 kPa, the multiple index for proximity sensors was 5.2 per cent at a forward speed of 1 km h<sup>-1</sup>, whereas for encoder sensors, it was 4.5 per cent under the same

conditions. The smaller hole size (2.1 mm) generally resulted in lower multiple indices, indicating better control over seed drop, especially when paired with encoder sensors. In Fig. 4.18 interaction plot of independent parameter for horse gram is shown. Most of the lines are parallel in the plot, represents no interaction between the factors.

As hole size increases, the multiple index also increases due to the larger area pulling more seeds. Similarly, as vacuum pressure increases from 3 kPa to 5 kPa, the multiple index for black gram increases from 3.4 to 4.0 per cent. As forward speed increases, the multiple index decreases. This might be due to the faster speed reducing the time available for seeds to adhere to the seed plate, and the singulation mechanism more effectively removing extra seeds at higher plate speeds. Fig. 4.17 supports the observation, showing a decrease in the multiple index with increased forward speed. Similar trends were reported by Singh et al. (2005), Arzu and Adnan (2007), Kamgar et al. (2012), and Yasir et al. (2012) for pneumatic precision seeders.

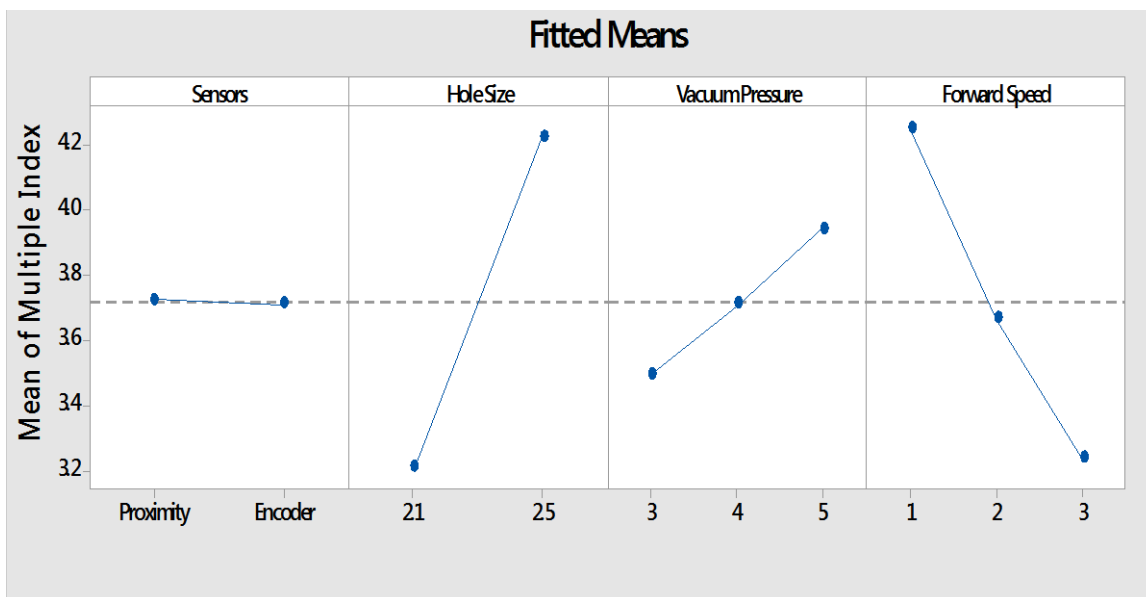


**Fig. 4.17 Effect on multiple index of horse gram**

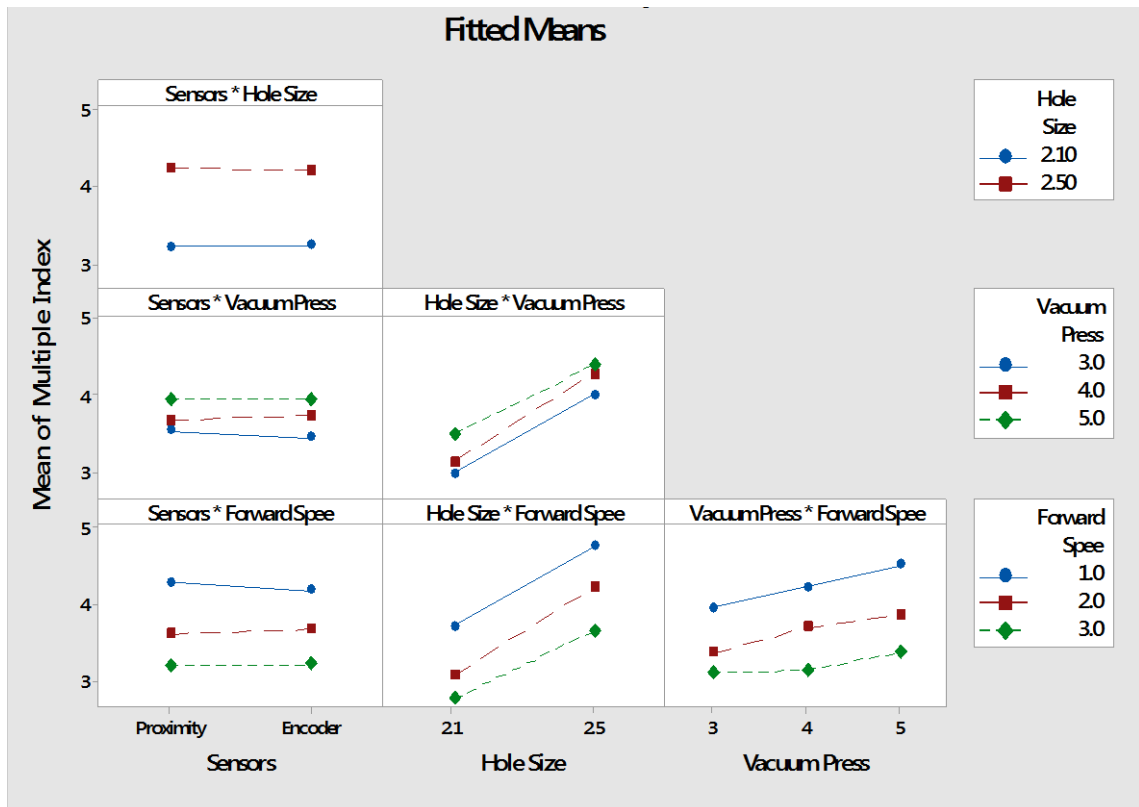


Fig. 4.18 Interaction effect on multiple index of horse gram

#### 4.6.1.4 Effect of sensor, vacuum, hole size and forward speed on quality of feed index for horse gram

The ANOVA Table 4.11 for the Quality of Feed Index (QFI) of horse gram seeds shows that the model is significant (F-value = 246.80,  $p < 0.0001$ ). Significant factors affecting QFI include sensors (A), hole size (B), vacuum pressure (C), forward speed (D), and their interactions (AB, AD, CD), all with p-values  $< 0.0001$ . The  $R^2$  value of 0.97 indicates that 97.15 per cent of the variation in QFI is explained by the model. The significant lack of fit (F-value = 2.57,  $p = 0.0014$ ) suggests some model misfit, but the very high Adequate Precision (59.67) confirms the model effectiveness in navigating the design space. Optimizing these factors will improve the precision and uniformity of seed placement, enhancing overall planting quality.



**Table 4.11 Analysis of variance for quality of feed index of horse gram in the laboratory testing**

Source	Sum of Squares	df	Mean Square	F-value	p-value	
<b>Model</b>	138.05	13	10.62	246.80	< 0.0001	significant
A-Sensors	48.94	1	48.94	1137.35	< 0.0001	
B-Hole Size	46.28	1	46.28	1075.63	< 0.0001	
C-Vacuum Pressure	3.43	2	1.72	39.90	< 0.0001	
D-Forward Speed	30.99	2	15.49	360.07	< 0.0001	
AB	0.9075	1	0.9075	21.09	< 0.0001	
AD	6.58	2	3.29	76.50	< 0.0001	
CD	0.9193	4	0.2298	5.34	0.0006	
<b>Residual</b>	4.04	94	0.0430			
Lack of Fit	1.78	22	0.0808	2.57	0.0014	significant
Pure Error	2.27	72	0.0315			
<b>Cor Total</b>	142.09	107				
<b>Std. Dev.</b>	0.207					R <sup>2</sup> 0.971
<b>Mean</b>	94.24					Adjusted R <sup>2</sup> 0.967
<b>C.V. %</b>	0.220					Predicted R <sup>2</sup> 0.962
						Adeq Precision 59.671

The Quality of Feeding Index (QFI) is a composite measure that reflects the accuracy and consistency of seed placement, indicating the overall performance of the seed metering mechanism. The results demonstrate that encoder sensors consistently achieved higher QFI values than proximity sensors. For example, with a hole size of 2.1 mm, vacuum pressure of 3 kPa, and forward speed of 1 km h<sup>-1</sup>, the QFI for encoder sensors was 96.2 per cent, compared to 95.4 per cent for proximity sensors.

Fig. 4.19 shows that all the parameters significantly impacted QFI. The higher QFI values with encoder sensors suggest that they provide a more reliable and efficient seed metering process, essential for achieving uniform crop stands and optimizing yield. As the hole size increase from 2.1 to 2.5 mm the QFI decreased.

The interaction plot for QFI, shown in Fig. 4.20, indicates that the interactions between sensor type and hole size, sensor type and forward speed, and vacuum pressure and forward speed were significant at the 1% level. The average value of QFI for horse gram was 93.51 per cent. These findings align with those reported by Karayel et al.

(2020), Kuş and Yıldırım (2021), and Gautam et al. (2023), who observed similar trends.

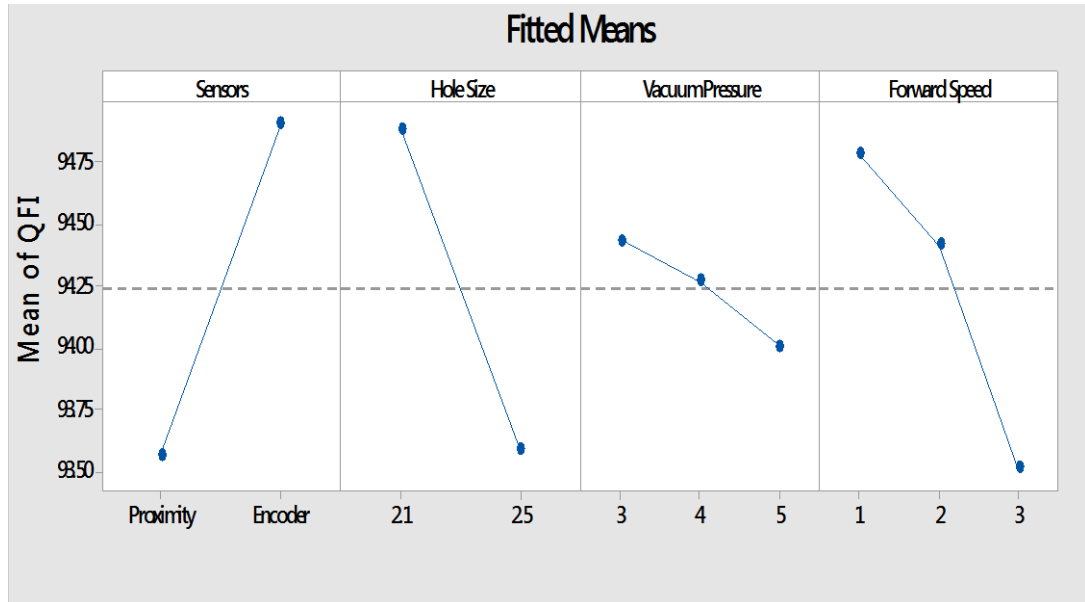


**Fig. 4.19** Effect on quality of feed index of horse gram

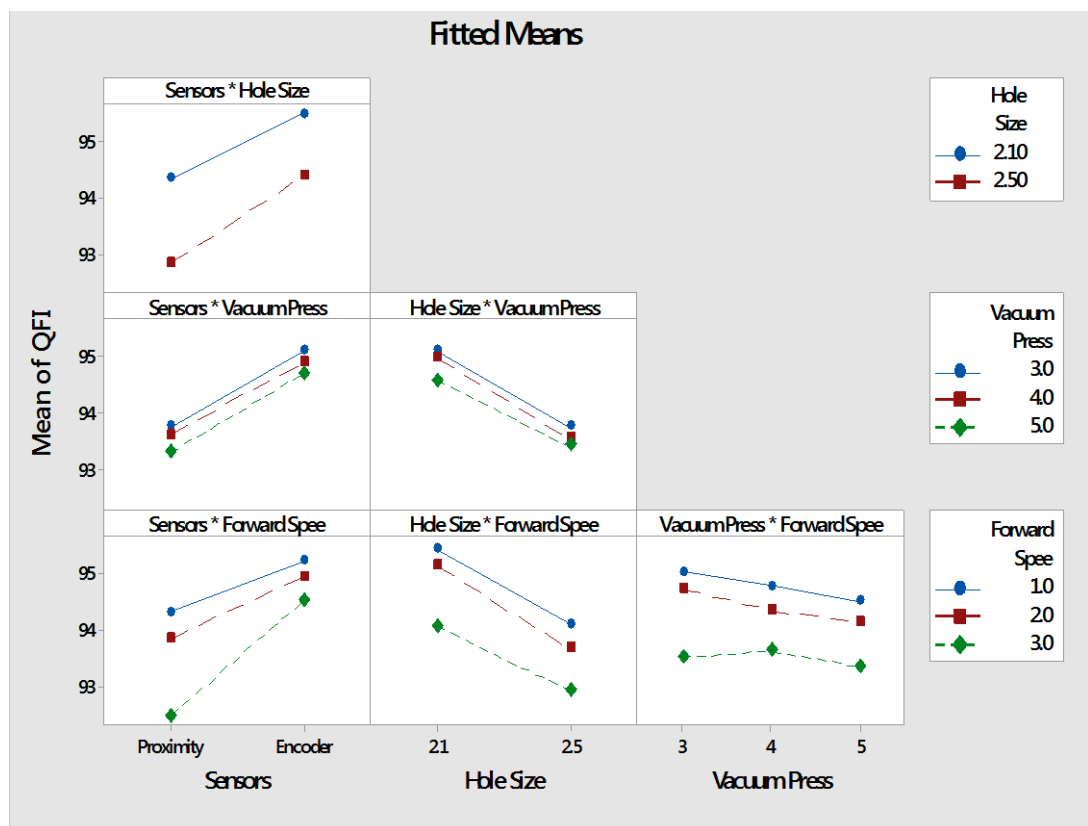


**Fig. 4.20** Interaction effect on quality of feed index of horse gram

#### 4.6.1.5 Effect of sensor, vacuum, hole size and forward speed on precision of spacing for horse gram

The ANOVA table for the precision of spacing in horse gram seeds reveals a highly significant model (F-value = 224.96,  $p < 0.0001$ ). The significant factors include sensors (A), forward speed (D), and their interaction (AD), each with  $p$ -values  $< 0.0001$  as shown in Table 4.12. The model  $R^2$  value of 0.91 indicates that 91.69 per cent of the variability in spacing precision is explained by these factors. The non-significant lack of fit (F-value = 0.75,  $p = 0.80$ ) and the high Adequate Precision (46.11) suggest that the model fits well and is reliable. Achieving high precision in seed spacing is critical for uniform crop establishment and maximizing yield.

**Table 4.12** Analysis of variance for Precision of spacing of horse gram in the laboratory testing

Source	Sum of Squares	df	Mean Square	F-value	p-value	
<b>Model</b>	242.57	5	48.51	224.96	$< 0.0001$	significant
A-Sensors	3.37	1	3.37	15.61	0.0001	
D-Forward Speed	162.16	2	81.08	375.96	$< 0.0001$	
AD	77.04	2	38.52	178.63	$< 0.0001$	
<b>Residual</b>	22.00	102	0.2157			
Lack of Fit	5.25	30	0.1748	0.7515	0.8060	not significant
Pure Error	16.75	72	0.2327			
<b>Cor Total</b>	264.57	107				
<b>Std. Dev.</b>	0.464				$R^2$	0.916
<b>Mean</b>	14.56				Adjusted $R^2$	0.912
<b>C.V. %</b>	3.19				Predicted $R^2$	0.906
					Adeq Precision	46.119

Precision of spacing is a critical parameter for ensuring uniform plant distribution and optimal use of field space. The results indicate that lower forward speeds generally result in higher precision of spacing. For example, with proximity sensors, a hole size of 2.1 mm, and vacuum pressure of 3 kPa, the precision of spacing was 16.30 per cent at a forward speed of 1 km h<sup>-1</sup>, but decreased to 11.63 per cent at a forward speed of 3 km h<sup>-1</sup>. Encoder sensors provided more consistent precision of spacing, with values ranging from 13.51 to 15.31 per cent under similar conditions.

Fig. 4.21 shows the main effect plot of independent parameters on the precision of spacing for black gram, highlighting that forward speed is highly significant. As forward speed increases, the mean precision decreases, likely due to suboptimal conditions for minimizing both miss and multiple indices. Encoder sensors consistently showed higher precision in spacing, reflecting their variability in the spacing. Fig. 4.22 displays the interaction plot between different independent parameters for the precision of spacing, further emphasizing the significant interactions between forward speed and sensor. These results align with the findings of Karayel (2009), Singh et al. (2005), and Gautam et al. (2023).

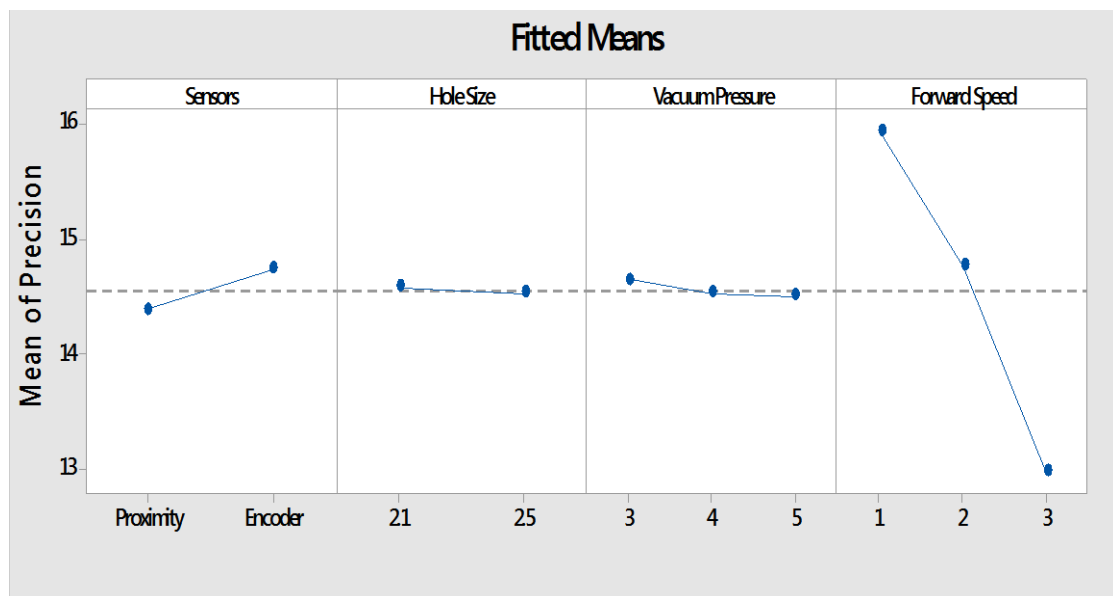


**Fig. 4.21 Effect on precision of spacing of horse gram**

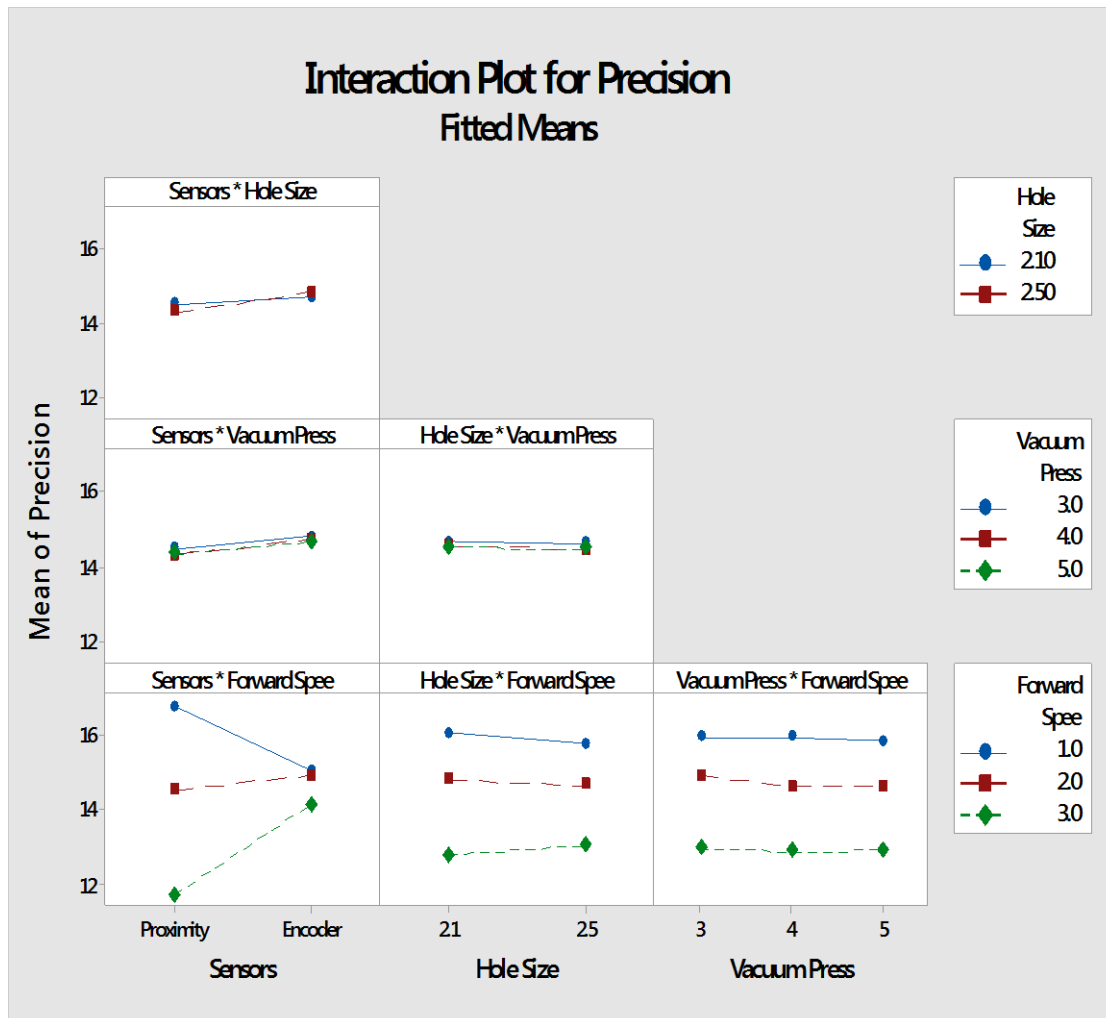


**Fig. 4.22 Interaction effect on precision of spacing of horse gram**

The numerical optimization for evaluation of the lab model was performed by setting the goal for all parameters same as given in table 4.7 to obtain optimum solution. The desirability for evaluation of the lab model of pneumatic planter with electronic control system for horse gram was found and shown in the Fig. 4.23. The desirability of optimum parameters of unit was 0.77 for horse gram.

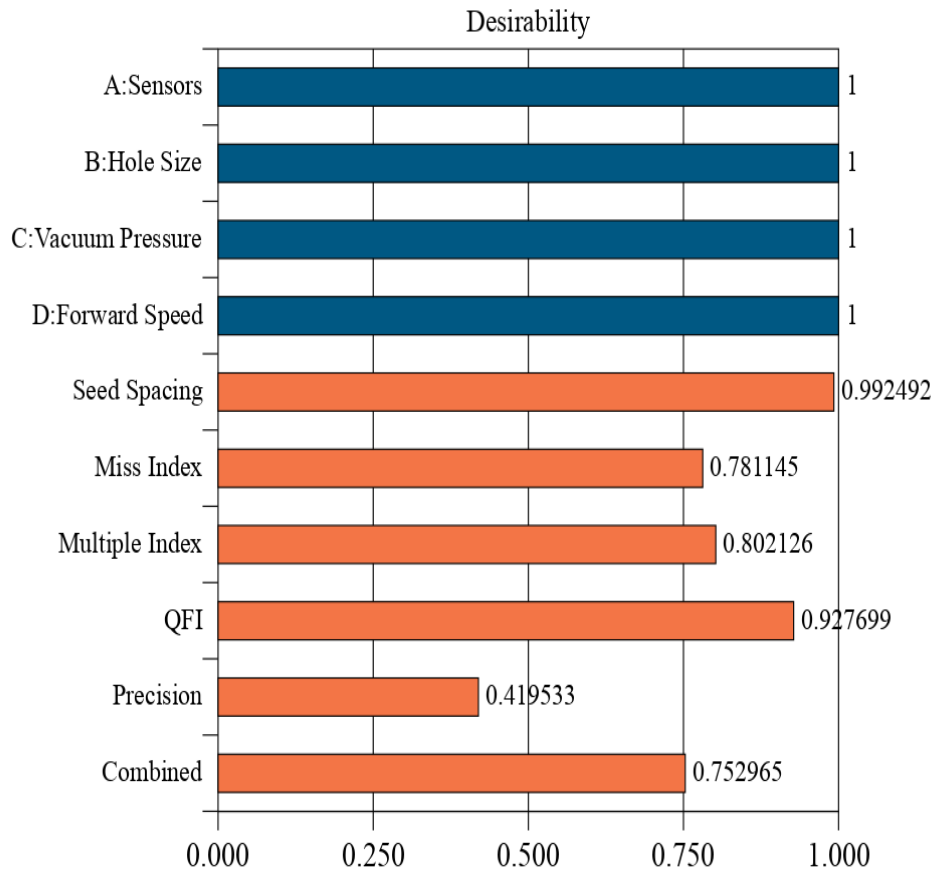


**Fig. 4.23 Desirability index for lab model of vacuum metering mechanism with electronic control system for horse gram**

The Fig. 4.24 depict the optimized results from a laboratory experiment investigating the influence of various parameters on a pneumatic planter metering mechanism designed for horse gram seeds. The experiment employed an electronic control system to manage the metering process.

Four key parameters were manipulated: sensor type (proximity vs. rotary encoder), plate hole size (2.1 and 2.5), vacuum pressure (3.0, 4.0, and 5.0 kPa), and planter operating speed (1.0, 2.0, and 3.0 km h<sup>-1</sup>). The experiment evaluated the impact of these parameters on five key responses: seed spacing (cm), miss index (%), multiple index (%), quality of feed index (%), and precision of spacing.

By analysing, it can be said that rotary encoder with hole size of 2.1 mm at 4.0 kPa at speed of 1.0 km h<sup>-1</sup> is the best treatment combination for the metering mechanism for horse gram to obtained best result in term of seed spacing, miss and multiple index.

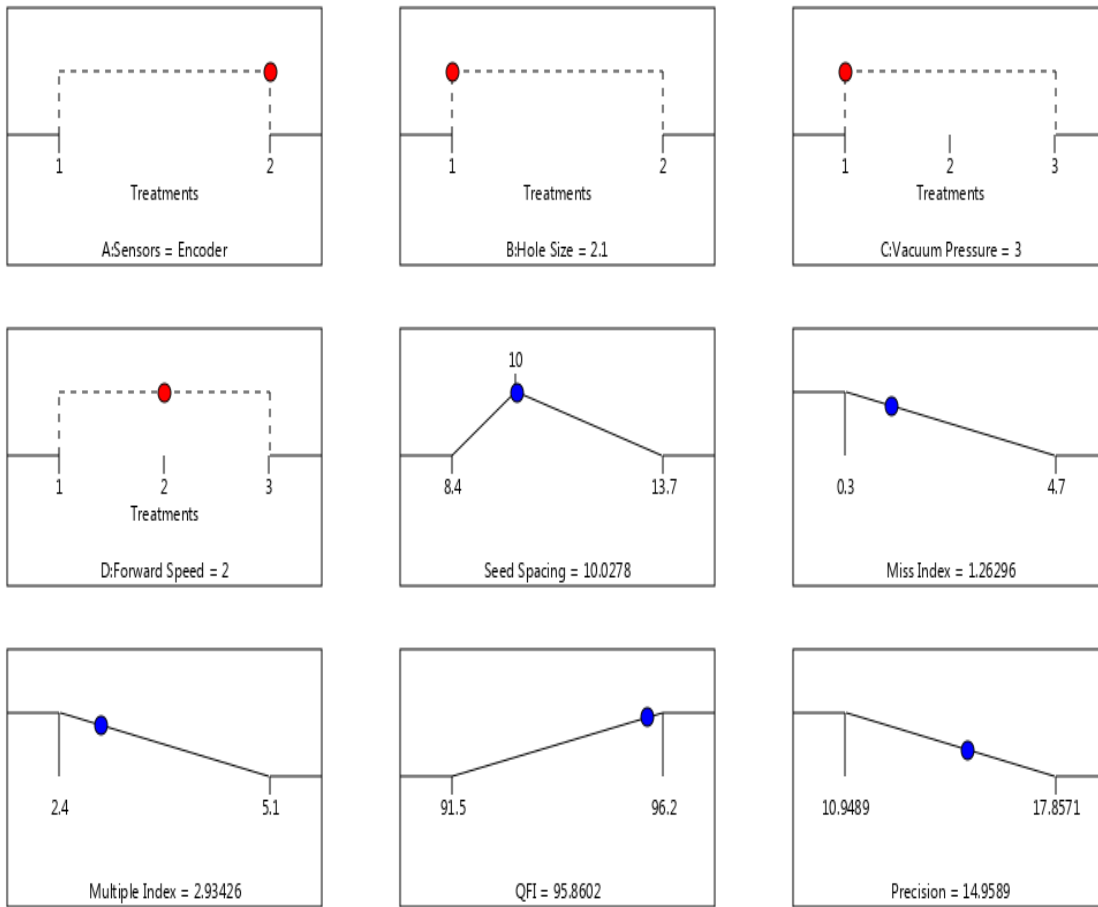


**Fig. 4.24 Optimum value for sensor, hole size, vacuum pressure and forward speed on performance parameters for horse gram**

#### 4.7 DESIGN OF THE MAJOR COMPONENTS OF THE PROTOTYPE

The design of the major components of the pneumatic planter prototype done in section 3.7 includes the design of furrow openers, seed hopper, seed plate, and ground wheel. The furrow openers are designed to create precise furrows for seed placement. Two type of furrow openers were designed Shoe type and Inverted T-type to suit different soil conditions. Standard MS flats were used for fabricating furrow openers: 35 x 8 mm for the shank, 600 x 50 x 15 mm for the inverted-type furrow opener, and 45 x 15 mm for the shank of the shoe-type furrow opener, with 600 x 50 x 15 mm for the shoe-type furrow opener of the precision planter.

The seed hopper ensures a steady supply of seeds to the metering mechanism, designed to minimize seed damage and blockage. Seed hopper for black and horse gram seeds were designed. Mild steel seed hopper, angled optimally at 45° for efficient seed flow, has a capacity of 7 kg and a volume of 0.0091 m<sup>3</sup>. Although 1.0 mm thickness is sufficient to withstand lateral pressure from loading black gram, a 2.0 mm thick mild steel sheet was used for fabrication due to market availability and safety considerations.

The seed plate is crucial for accurately metering seeds, with customized plates for different seed types to ensure uniform distribution. The seed plate design for black gram and horse gram seeds features circular openings with a 120° conical angle to prevent multiple seed pick-up. Recommended opening diameters of holes in the seed plate range from 0.96 mm to 3.69 mm for black gram and 1.04 mm to 4.00 mm for horse gram. Approximately 26 openings are arranged based on seed spacing, with a pitch circle diameter of 132 mm and an outside diameter of 184 mm for optimal seed metering in the vacuum seeding system.

The ground wheel maintains consistent planter speed and depth, synchronizing the seed metering mechanism with the planter movement. The ground wheel, made of 5 mm thick Fe-410 MS sheet with a diameter of 500 mm and weighing 65.19 N, is mounted on the mainframe using a freely suspended beam fixed with a U-clamp. It is pulled by the tractor for forward motion, utilizing traction from 12 lugs on its circumference. The ground wheel shaft, chosen with a diameter of 14 mm, is supported by bush bearings on the counter shaft.



#### 4.8 DEVELOPMENT OF PNEUMATIC PLANTER

The pneumatic planter features a robust main frame ( $2.6 \times 0.10 \times 0.15$  m) and four bar parallelogram linkage designed to support seed metering units, furrow openers, and an aspirator blower, which is powered by a cardan shaft connected to the tractor PTO. The four-bar parallelogram linkage ensures consistent furrow depth, enhancing seed placement accuracy. The vacuum disc seed meter utilizes suction to pick up and dispense seeds, while the planter includes four 2 mm thick mild steel seed hoppers. Various furrow openers and wheels, including pneumatic wheel and compression wheels, facilitate efficient soil penetration and seed covering, optimizing the planting process.

#### 4.9 FIELD EVALUATION OF PNEUMATIC PLANTER WITH ELECTRONIC CONTROL SYSTEM

The tractor operated pneumatic planter using electronic control system was tested in the field to assess the operational parameter for sowing of black and horse gram seeds precisely. The parameters selected for testing the planter in the field were location of encoder and furrow openers. Two location and three furrow openers were chosen for the field testing

##### **4.9.1 Effect of independent variables on the performance of the developed pneumatic planter with electronic control system for black gram**

###### ***4.9.1.1 Seed spacing***

The ANOVA for seed spacing of black gram is given in Table 4.13. The result indicated a highly significant model (F-value = 633.90,  $p < 0.0001$ ), which depicts that the independent variables significantly affect seed spacing. The factors such as location of encoder (A) and furrow opener (B), as well as their interaction (AB), were significant ( $p < 0.0001$  for A,  $p = 0.0004$  for B, and  $p = 0.0053$  for AB). The high  $R^2$  value of 0.99 indicates that the model explains 99.62 % of the variability in seed spacing. The adjusted  $R^2$  of 0.99 and predicted  $R^2$  of 0.99 suggest that the model is reliable and can predict new data accurately. The adequate precision ratio of 52.82 indicates a strong signal-to-noise ratio, confirming the model robustness in navigating the design space.

**Table 4.13 Analysis of variance for seed spacing of black gram in the field testing**

Source	Sum of Squares	df	Mean Square	F-value	p-value	
<b>Model</b>	14.09	5	2.82	633.90	< 0.0001	significant
A-Location of Encoder	13.87	1	13.87	3120.50	< 0.0001	
B-Furrow Opener	0.1433	2	0.0717	16.12	0.0004	
AB	0.0744	2	0.0372	8.38	0.0053	
<b>Pure Error</b>	0.0533	12	0.0044			
<b>Cor Total</b>	14.14	17				
<b>Std. Dev.</b>	0.066					R <sup>2</sup> 0.996
<b>Mean</b>	13.90					Adjusted R <sup>2</sup> 0.994
<b>C.V. %</b>	0.479					Predicted R <sup>2</sup> 0.991
						Adeq Precision 52.827

The experiment aimed to determine the optimal seed spacing for black gram using different furrow opener types and encoder locations. The parameters tested included three furrow opener types namely inverted T, stub runner, and shoe. Two locations for the rotary encoder were selected namely one on the pneumatic wheel and the other on the steel wheel with spokes. Accurate distance measurement is crucial for achieving precise seed spacing in planters, and the rotary encoder provides the distance travelled by the planter. Results indicated that the steel wheel, which experienced less slip, consistently provided seed spacings closer to the target across all furrow opener types. Specifically, with the use of shoe type furrow opener, the spacing of approximately 14.8 cm, the inverted T-type around 14.87 cm, and the stub runner type around 14.7 cm. In contrast, the pneumatic wheel, which may be subject to higher slip, resulted in wider variability and generally lower seed spacings. The seed spacing with encoder on steel wheel with shoe type furrow opener averaged around 12.83 cm, inverted t-type around 13.17 cm, and the stub runner type around 13.07 cm.

Fig. 4.25 shows the resulting seed spacing data. The abscissa indicates the type of furrow opener, the ordinate indicates the seed spacing (cm), and the applicate indicates the encoder locations. The red bars represent the shoe type, the green bars indicate the inverted T-type, and the blue bars denote the stub runner type furrow opener.

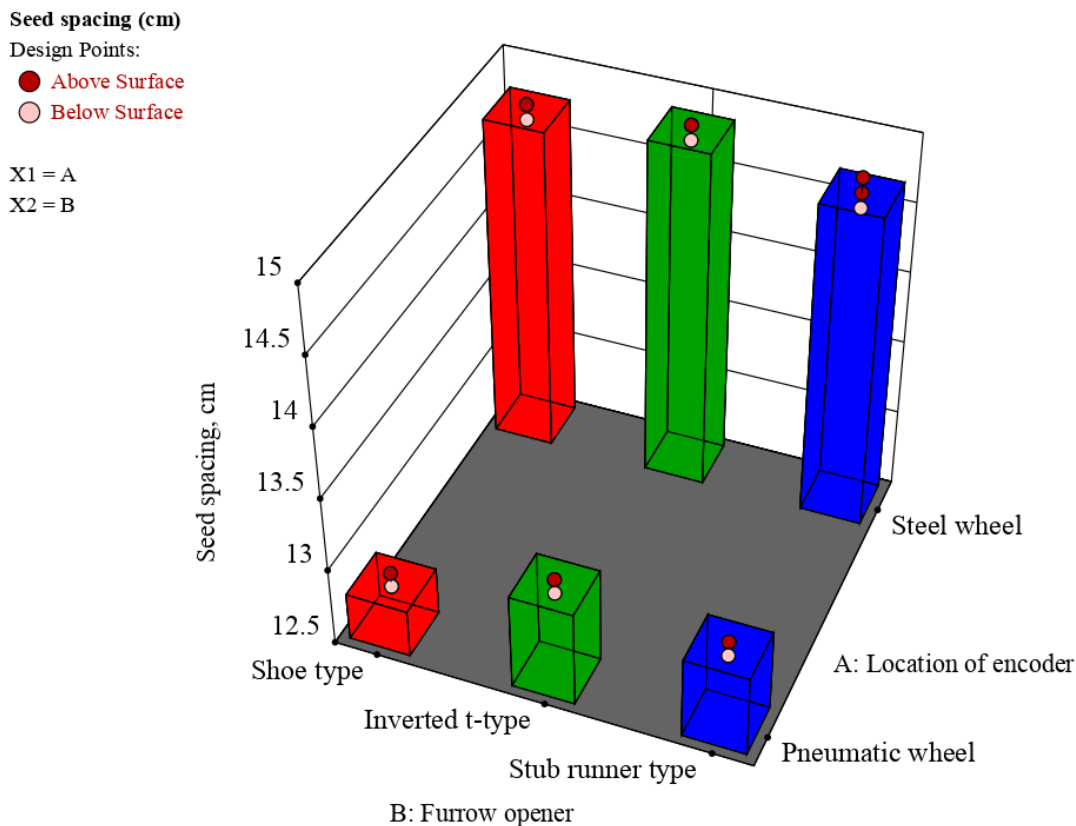


**Fig. 4.25 Effect of furrow opener and location of encoder on seed spacing for black gram**

A comparison of seed spacing revealed notable trends and differences. The inverted T-type furrow opener showed a marked variation in seed spacing depending on the encoder location, with larger spacing observed when the encoder is fitted to the steel wheel. Fig. 4.25 depicts that all furrow openers have similar variations, with the shoe type and inverted T-type furrow openers being closer to the target spacing of 15 cm for black gram. The location of the encoder had a significant effect, with the encoder fitted to the steel wheel resulted closer to the target spacing. This may be due to the reduced slip in the steel wheel compared to the pneumatic wheel. These findings are consistent with those reported by Hoque et al. (2021) and Chen et al. (2004).

#### 4.9.1.2 Miss index

The analysis of variance for miss index of black gram is shown in Table 4.14. For the miss index, the model was not significant ( $p > 0.05$ ), and the lack of fit was not significant. This suggests that the chosen factors do not significantly impact the miss index, and the variation observed can be attributed to random error.

**Table 4.14 Analysis of variance for miss index of black gram in the field testing**

Source	Sum of Squares	df	Mean Square	F-value	p-value	
<b>Model</b>	0.0000	0				
<b>Residual</b>	0.0444	17	0.0026			
Lack of Fit	0.0111	5	0.0022	0.8000	0.5705	not significant
Pure Error	0.0333	12	0.0028			
<b>Cor Total</b>	0.0444	17				
<b>Std. Dev.</b>	0.051				<b>R<sup>2</sup></b>	0.000
<b>Mean</b>	1.24				<b>Adjusted R<sup>2</sup></b>	0.000
<b>C.V. %</b>	4.11				<b>Predicted R<sup>2</sup></b>	-0.121
					<b>Adeq Precision</b>	NA <sup>(1)</sup>

<sup>(1)</sup> Case(s) with leverage of 1.0000: Pred R<sup>2</sup> and PRESS statistic not defined.

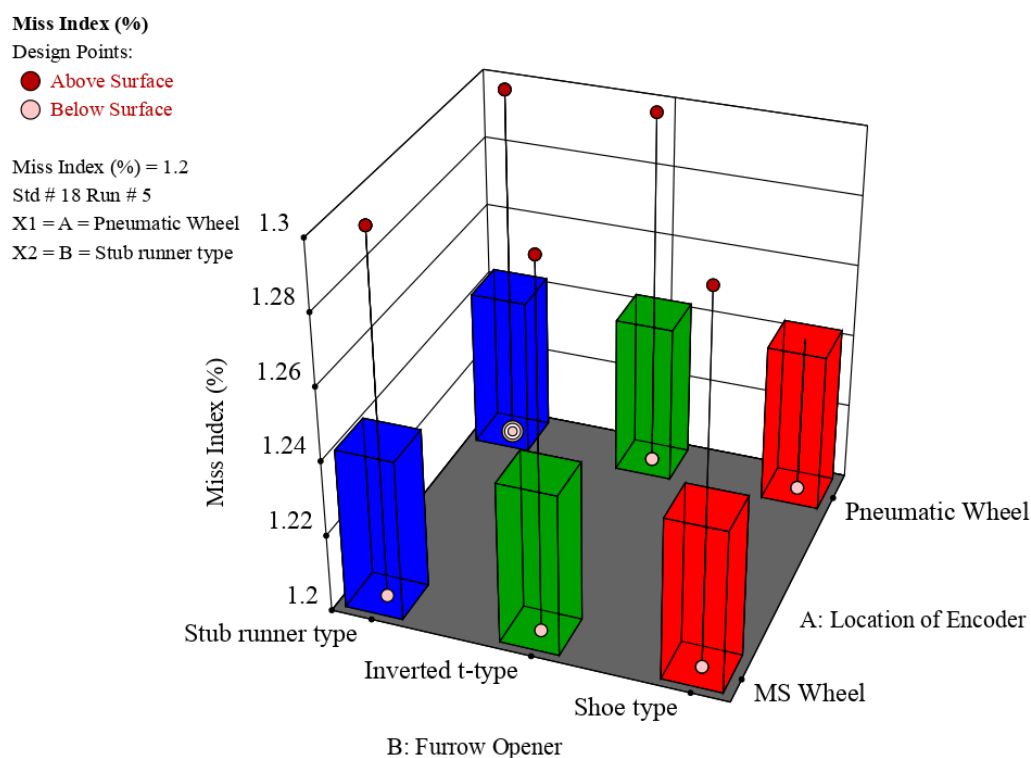


**Fig. 4.26 Effect of furrow opener and location of encoder on miss index for black gram**

The miss index is a critical parameter indicating the frequency of missed seeds, which can adversely affect crop yield. Results showed that both encoder locations and furrow opener types yielded relatively low miss indices, with values ranging from 1.2

to 1.3 per cent. The shoe type furrow opener consistently recorded a miss index of 1.2 per cent regardless of the encoder location, suggesting a high level of reliability in seed placement. The inverted T-type and stub runner type furrow openers exhibited slightly more variability but remained within the 1.2 to 1.3 per cent range. The steel wheel location did not show a significant difference compared to the pneumatic wheel in terms of miss index, indicated that both encoder locations are having similar effects on minimizing seed misses. This might be because of uniform forward speed and rotor speed by stepper, which controlled precisely with decreased missing per centage.

#### 4.9.1.3 Multiple index

The ANOVA for the multiple index showed a highly significant model ( $p < 0.0001$ ), with both location of encoder and furrow opener having significant main effects and a significant interaction between location of encoder and furrow opener. High R-squared values was 0.99 with Adjusted R<sup>2</sup> and Predicted R<sup>2</sup> were 0.99 and 0.98 respectively. An Adeq Precision value of 50.00 indicate a strong model fit and reliability for prediction.

**Table 4.15 Analysis of variance for multiple index of black gram in the field testing**

	Sum of Squares	df	Mean Square	F-value	p-value	
<b>Model</b>	8.53	5	1.71	511.77	< 0.0001	significant
A-Location of Encoder	8.13	1	8.13	2440.17	< 0.0001	
B-Furrow Opener	0.2011	2	0.1006	30.17	< 0.0001	
AB	0.1944	2	0.0972	29.17	< 0.0001	
<b>Pure Error</b>	0.0400	12	0.0033			
<b>Cor Total</b>	8.57	17				
<b>Std. Dev.</b>	0.057				R <sup>2</sup>	0.995
<b>Mean</b>	3.31				Adjusted R <sup>2</sup>	0.993
<b>C.V. %</b>	1.75				Predicted R <sup>2</sup>	0.989
					Adeq Precision	50.00

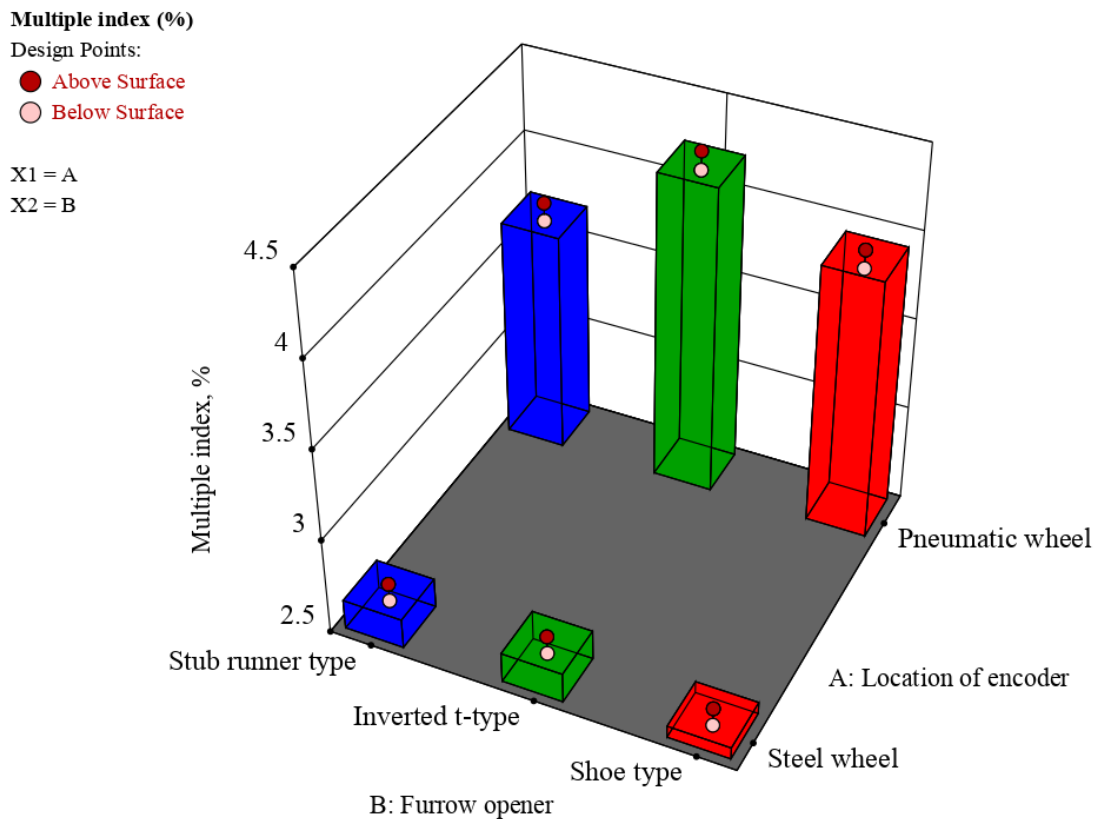


**Fig. 4.27 Effect of furrow opener and location of encoder on multiple index for black gram**

The experiment aimed to evaluate the effect of different furrow opener types and encoder locations on the multiple index for black gram seeding. Fig. 4.27 presents the multiple index for black gram across various furrow opener types and encoder locations.

The results indicated that the encoder location significantly affects the multiple index. When the encoder was placed on the steel wheel, the multiple index ranged from 2.5 to 2.7 per cent, indicated relatively consistent and low rates of multiple seed drops. In contrast, the multiple index increased substantially when the encoder was placed on the pneumatic wheel, it was from 3.7 to 4.3 per cent, due to more slip compared to the pneumatic wheel on the pulverise soil. Among the furrow openers, the inverted T-type recorded the highest multiple index when the encoder was on the pneumatic wheel, raised up to 4.3 per cent. This may be due to the obstruction created by the rice stalk residue on the field. The shoe type and stub runner type also showed higher multiple

indices with the pneumatic wheel encoder location, but remained within a slightly lower range compared to the inverted T-type. These findings suggested that the steel wheel encoder location provided better control over seed drop, resulted in lower multiple indices and thereby reduced the likelihood of seedling competition.

The higher multiple index with the pneumatic wheel encoder is likely due to the greater slip associated with the pneumatic wheel compared to the steel wheel. Both the location of the encoder and the type of furrow opener, as well as its interaction, are at the 1.0 per cent level of significance. These findings are consistent with the results reported by Fu et al. (2018) and Zaidi et al. (2019).

#### 4.9.1.4 Quality of feed index

The ANOVA for quality of feed index showed a significant model (F-value = 296.58,  $p < 0.0001$ ), with the location of the encoder (A), furrow opener (B), and their interaction (AB) being significant contributors ( $p < 0.0001$  for A,  $p = 0.0002$  for B, and  $p = 0.0005$  for AB). The model  $R^2$  value of 0.99 indicates that 99.20 per cent of the variability in the quality of feed index is explained. The adjusted  $R^2$  of 0.98 and predicted  $R^2$  of 0.98 suggest a reliable and accurate model. The adequate precision ratio of 38.730 further indicates a robust signal-to-noise ratio, affirming the model utility in the design space.

**Table 4.16 Analysis of variance for quality feed index of black gram in the field testing**

Source	Sum of Squares	df	Mean Square	F-value	p-value	
<b>Model</b>	8.24	5	1.65	296.58	< 0.0001	Significant
A-Location of Encoder	7.87	1	7.87	1416.10	< 0.0001	
B-Furrow Opener	0.2033	2	0.1017	18.30	0.0002	
AB	0.1678	2	0.0839	15.10	0.0005	
<b>Pure Error</b>	0.0667	12	0.0056			
<b>Cor Total</b>	8.31	17				
<b>Std. Dev.</b>	0.074					$R^2$ 0.992
<b>Mean</b>	95.45					Adjusted $R^2$ 0.988
<b>C.V. %</b>	0.078					Predicted $R^2$ 0.981
						Adeq Precision 38.729

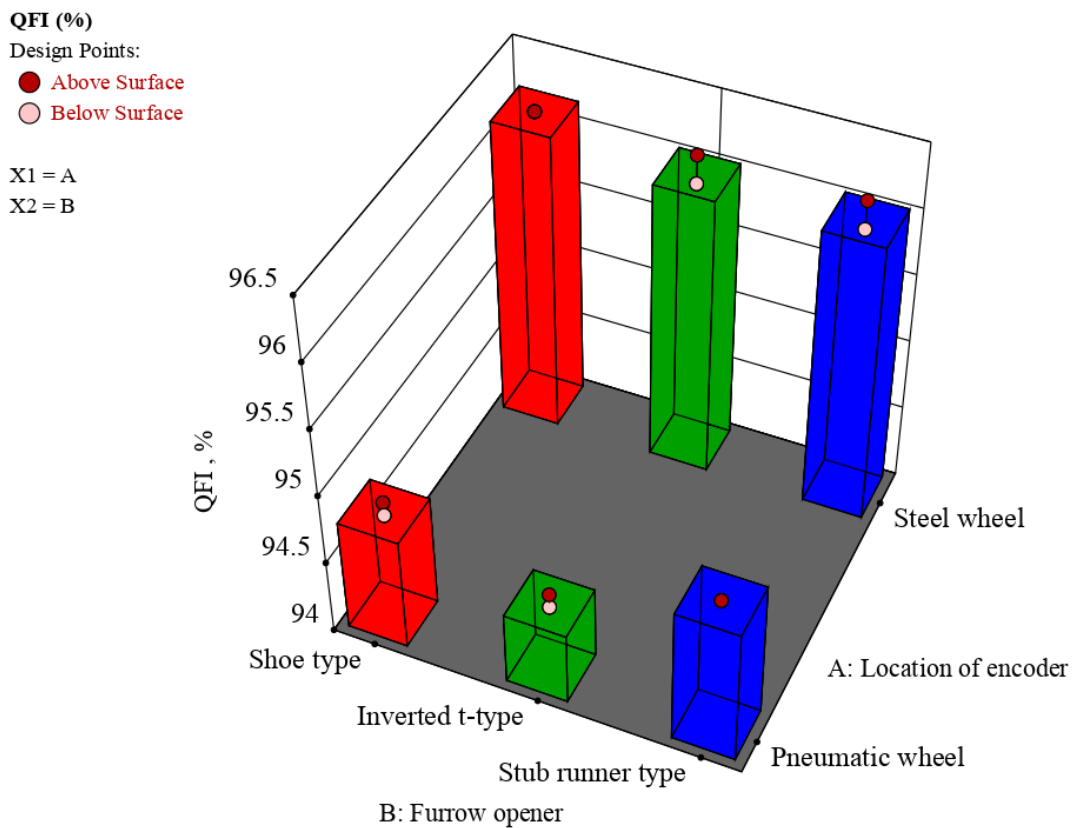


**Fig. 4.28 Effect of furrow opener and location of encoder on QFI for black gram**

The results clearly showed that the encoder location had a significant impact on QFI. When the encoder was placed on the steel wheel, the QFI values were consistently higher, ranged from 96 to 96.2 per cent, indicated superior seed metering performance. Conversely, the QFI values were lower with the encoder placed on the pneumatic wheel, ranging from 94.5 to 95 per cent. Among the furrow openers, the shoe type consistently achieved a QFI of 96.2 per cent with the steel wheel encoder, outperforming other types. The inverted t-type and stub runner type also performed well with the steel wheel encoder, maintained a QFI close to 96.2 per cent. However, their performance dropped slightly when the encoder was placed on the pneumatic wheel. These findings suggested that the steel wheel encoder location ensured more precise and consistent seed placement, thereby enhanced the overall performance of the seed metering mechanism.



#### 4.9.1.5 Precision index

The ANOVA for precision index indicated a highly significant model (F-value = 653.42,  $p < 0.0001$ ). The location of the encoder (A), furrow opener (B), and its interaction (AB) were significant factors ( $p < 0.0001$  for A,  $p = 0.0002$  for B, and  $p = 0.0018$  for AB). The model high  $R^2$  of 0.99 demonstrated that it accounts for 99.63 per cent of the variance in the precision index. The adjusted  $R^2$  of 0.99 and predicted  $R^2$  of 0.99 indicated a strong model fit and predictive capability. The adequate precision ratio of 53.97 underscored a strong signal-to-noise ratio, confirmed the model adequacy for design space navigation.

**Table 4.17 Analysis of variance for Precision Index of black gram in the field testing**

Source	Sum of Squares	df	Mean Square	F-value	p-value	
<b>Model</b>	3.18	5	0.6357	653.42	< 0.0001	significant
A-Location of Encoder	3.12	1	3.12	3206.80	< 0.0001	
B-Furrow Opener	0.0369	2	0.0185	18.98	0.0002	
AB	0.0217	2	0.0109	11.17	0.0018	
<b>Pure Error</b>	0.0117	12	0.0010			
<b>Cor Total</b>	3.19	17				
<b>Std. Dev.</b>	0.031					$R^2$ 0.996
<b>Mean</b>	6.59					Adjusted $R^2$ 0.994
<b>C.V. %</b>	0.473					Predicted $R^2$ 0.991
						Adeq Precision 53.975

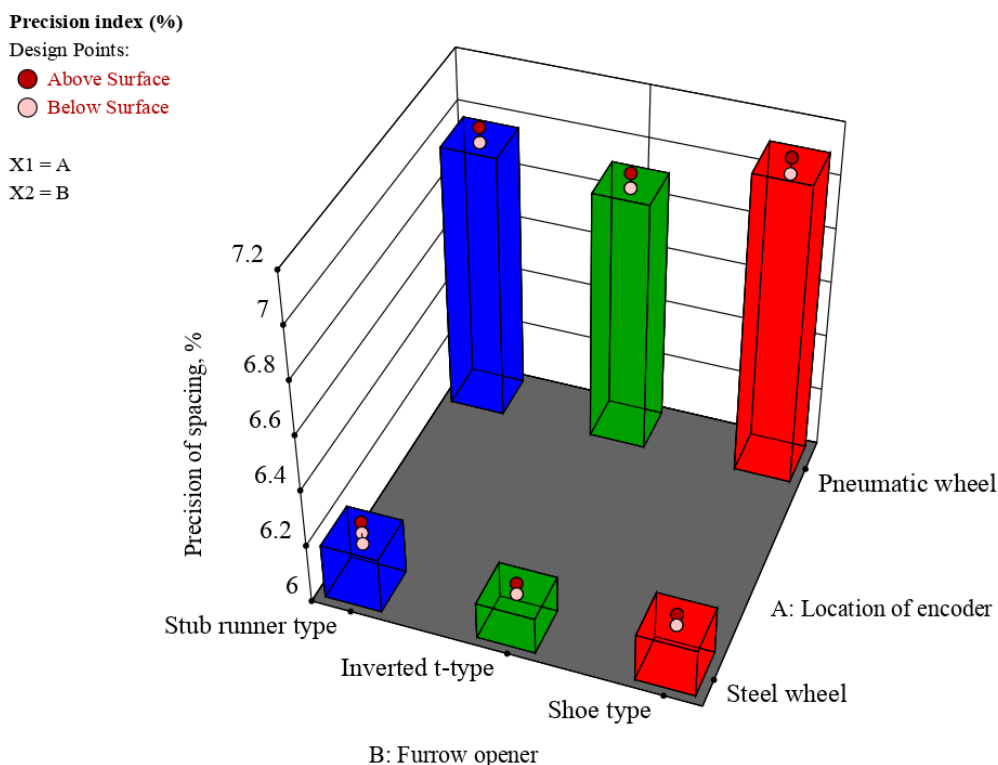


**Fig. 4.29 Effect of furrow opener and location of encoder on precision index for black gram**

The results indicated that the location of the encoder significantly affected the precision of spacing. With the encoder on the steel wheel, the precision values ranged from 6.12 to 6.24 per cent, showed relatively low variability and thus higher precision. In contrast, when the encoder was placed on the pneumatic wheel, the precision values were higher, ranged from 6.90 to 7.12 per cent, indicated increased variability and lower precision.

Among the furrow opener types, the inverted T-type and stub runner type furrow openers showed similar precision values when the encoder was on the MS wheel, maintained a precision close to 6.12%. The Shoe type furrow opener also performed well with precision values around 6.16%. However, with the encoder on the pneumatic wheel, the precision of spacing increased for all furrow openers, with the shoe type showing the highest variability at approximately 7.12%. Lower the value of precision, the better is the type of metering mechanism.

These findings suggested that using the steel wheel for the encoder location results had better precision of spacing, enhanced seed placement accuracy and overall planting performance.

#### 4.9.1.6 Germination

**Table 4.18 Analysis of variance for germination of black gram in the field testing**

Source	Sum of Squares	df	Mean Square	F-value	p-value	
<b>Model</b>	320.11	2	160.06	232.34	< 0.0001	significant
B-Furrow	320.11	2	160.06	232.34	< 0.0001	
Opener						
<b>Residual</b>	10.33	15	0.6889			
Lack of Fit	5.00	3	1.67	3.75	0.0413	significant
Pure Error	5.33	12	0.4444			
<b>Cor Total</b>	330.44	17				
<b>Std. Dev.</b>	0.830					R <sup>2</sup> 0.968
<b>Mean</b>	91.44					Adjusted R <sup>2</sup> 0.964
<b>C.V. %</b>	0.907					Predicted R <sup>2</sup> 0.955
						Adeq Precision 30.004

For germination, the model was highly significant ( $p < 0.0001$ ), with the furrow opener (B) having a significant main effect. The lack of fit was significant, suggested that there is unexplained variation that might be due to other factors not included in the model. High R-squared values, adjusted R<sup>2</sup>, and predicted R<sup>2</sup> was 0.96, 0.96, and 0.95 respectively and an Adeq precision value of 30.00 indicate a strong model fit and reliability for prediction.

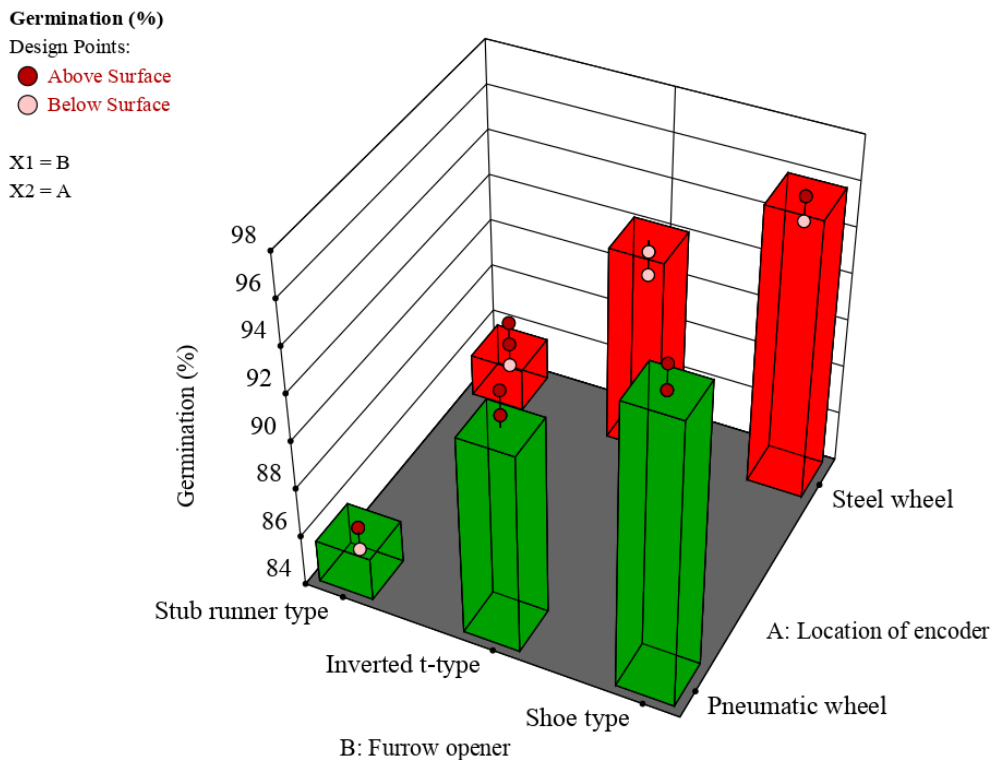


**Fig. 4.30 Effect of furrow opener and location of encoder on germination index for black gram**

The results indicated that the location of the encoder significantly influenced germination rates. With the encoder on the steel wheel, the germination per centages ranged from 85 to 96 per cent. The shoe type furrow opener achieved the highest germination rates at 95-96 per cent, suggested optimal seed placement and favorable conditions for seedling emergence. The inverted T-type furrow opener showed slightly lower germination rates, between 91 and 92 per cent, while the Stub Runner type had the lowest germination rates, ranged from 85 to 87 per cent.

Conversely, when the encoder was placed on the pneumatic wheel, the germination per centages varied slightly, with values ranged from 85 to 97 per cent. The shoe type furrow opener performed well, with germination rates of 96 to 97 per cent. The inverted T-type showed improved performance compared to its steel wheel counterpart, achieved germination rates of 93 to 94 per cent. The stub Runner type, however, showed similar results with the steel wheel, with germination per centages between 85 and 86 per cent.

These findings suggested that the choice of furrow opener and encoder location was significantly affected the germination rates of black gram seeds. The Shoe type furrow opener, particularly when paired with the pneumatic wheel encoder, consistently resulted in higher germination rates, indicated better seed placement and more favorable conditions for germination.

**Table 4.19 Multi response numerical optimization constraints**

<b>Parameter</b>	<b>Goal</b>
<b>Independent</b>	
a. Location of Encoder	is in range (on pneumatic wheel & ground wheel)
b. Furrow Opener	is in range (Inverted t-type, shoe type, stub runner)
<b>Dependent</b>	
a. Seed Spacing	Target
b. Miss Index	minimum
c. Multiple Index	minimum
d. QFI	maximum
e. Precision Index	minimum
f. Germination	maximum

The numerical optimization for the furrow opener and location of the encoder was performed by setting the goal of all parameters as given in the Table 4.19. The desirability index (Fig. 4.30) of the field testing of pneumatic planter with electronic control system for black gram for different type of furrow opener and location of the encoder was found out as 0.870.

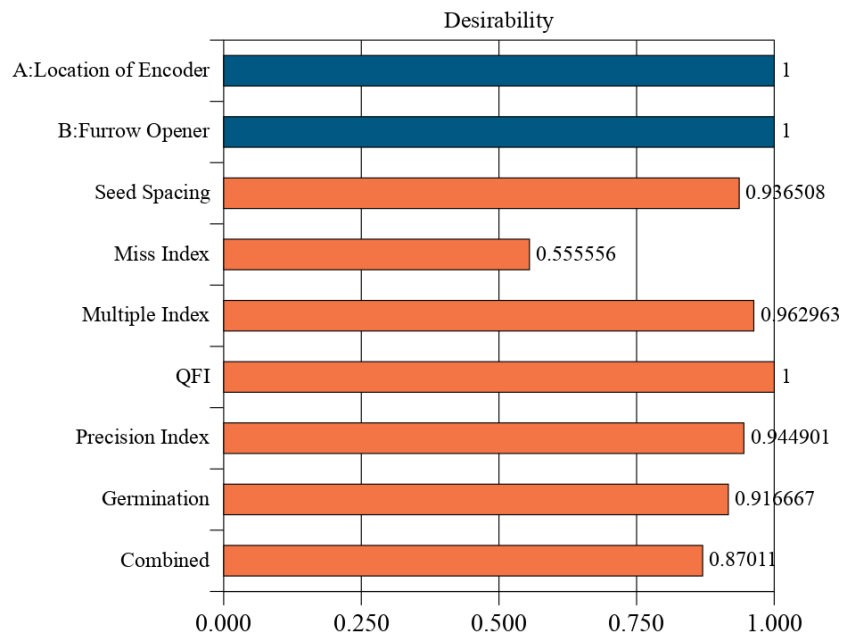


**Fig. 4.31 Desirability index for field testing of pneumatic planter with electronic control system for black gram**

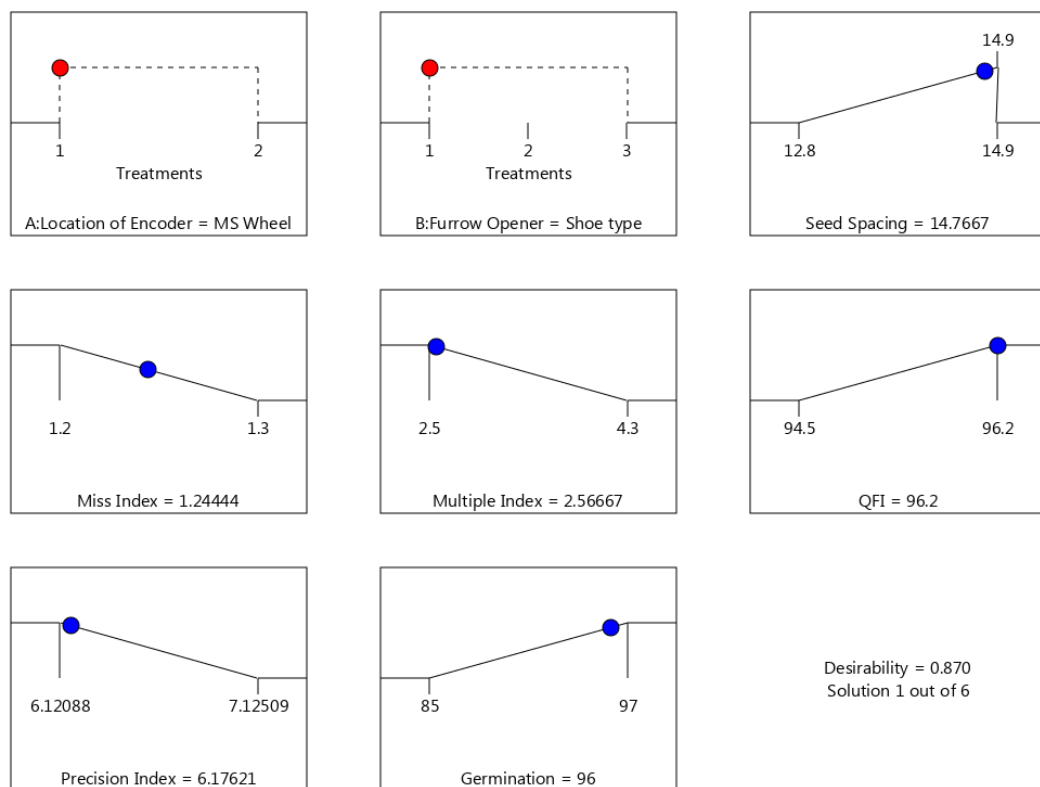


**Fig. 4.32 Optimum level of independent parameter on performance parameters for black gram**

The results analysis of various treatment combinations involving furrow opener types and encoder locations aimed to optimize several performance indicators viz., seed spacing, miss index, multiple index, quality of furrow (QFI), precision index, and germination per centage for black gram planting. The desirability index, reflecting both maximum and minimum performance were considered across treatments, yielded an optimized value of 0.870. This optimal performance was achieved with the encoder located at the MS wheel and utilizing a furrow opener shoe type.

The corresponding optimal values of the dependent parameters were determined as follows: seed spacing of 14.76 cm, miss index of 1.24 per cent, multiple index of 2.56 per cent, QFI of 96.2 per cent, precision index of 6.17 per cent, and germination per centage of 96 per cent, as depicted in Fig. 4.31. These findings underscored the recommended configuration of independent parameters for achieving peak performance of the pneumatic planter specifically tailored to black gram seeds.

## 4.9.2 Effect of independent variables on field performance of developed pneumatic planter with electronic control system for horse gram

### 4.9.2.1 Seed spacing

The Analysis of variance (ANOVA) for seed spacing shows a significant model ( $p < 0.0001$ ), indicating that the location of the encoder significantly impacts the seed spacing. The adjusted  $R^2$  of 0.96 suggests that the model explains a large proportion of the variability in seed spacing. The lack of fit is not significant, implying that the model adequately captures the relationship between the predictor and the response variable. The adequacy precision value of 33.00 indicates a strong signal-to-noise ratio, suggesting that the model is reliable for predicting seed spacing.

**Table 4.20 Analysis of variance for seed spacing of horse gram in the field testing**

Source	Sum of Squares	df	Mean Square	F-value	p-value	
<b>Model</b>	5.44	1	5.44	544.50	< 0.0001	significant
A-Location of Encoder	5.45	1	5.45	544.50	< 0.0001	
<b>Residual</b>	0.1600	16	0.0100			
Lack of Fit	0.0533	4	0.0133	1.50	0.2634	not significant
Pure Error	0.1067	12	0.0089			
<b>Cor Total</b>	5.60	17				
<b>Std. Dev.</b>	0.100				$R^2$	0.971
<b>Mean</b>	9.12				Adjusted $R^2$	0.969
<b>C.V. %</b>	1.10				Predicted $R^2$	0.963
					Adeq Precision	33.000



**Seed Spacing (cm)**

Design Points:

- Above Surface
- Below Surface

X1 = A

X2 = B

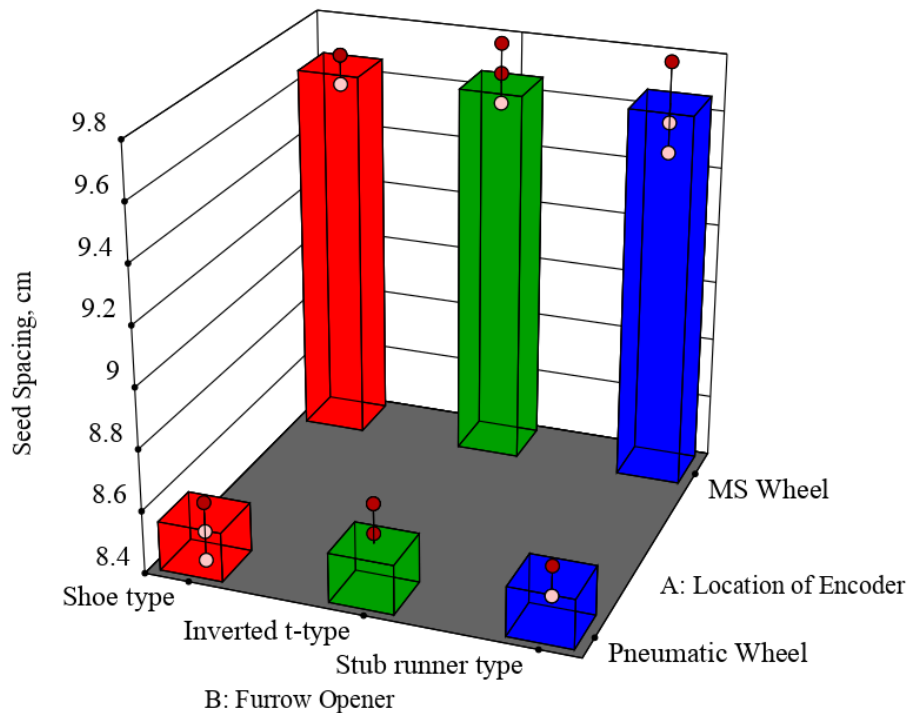


**Fig. 4.33 Effect of furrow opener and location of encoder on seed spacing for horse gram**

The Fig. 4.33 shows the seed spacing measurements for horse gram using different furrow opener types and encoder locations. Achieving accurate seed spacing is crucial for optimizing plant distribution and ensuring efficient use of field space. The target spacing for horse gram in this study was 10 cm.

The results indicate that the location of the encoder significantly affects the seed spacing. When the encoder is placed on the steel wheel, the seed spacing values range from 9.5 to 9.8 cm. The shoe type furrow opener consistently achieved a spacing of 9.6 to 9.7 cm, which is close to the target spacing of 10 cm. The inverted T-type furrow opener showed similar results with a spacing of 9.6 to 9.8 cm. The stub Runner type had a slightly wider range of spacing, from 9.5 cm to 9.8 cm, close to the target.

With the encoder located on the pneumatic wheel, the seed spacing values are slightly lower, ranging from 8.4 cm to 8.7 cm. The shoe type furrow opener showed spacing values from 8.4 cm to 8.6 cm, which is below the target spacing. The inverted

T-type had a spacing of 8.6 cm to 8.7 cm, also falling short of the target. The stub runner type demonstrated consistent spacing of 8.5 cm to 8.6 cm.

These findings suggest that the steel wheel encoder location is more effective in achieving seed spacing closer to the target of 10 cm for horse gram. The shoe type and inverted t-type furrow openers, when used with the steel wheel encoder, provided the most accurate seed spacing. In contrast, the pneumatic wheel encoder resulted in seed spacing consistently below the target, indicating low precision and less variability with the steel wheel.

#### 4.9.2.2 Miss index

The ANOVA for the miss index produced a significant model (F-value = 7.91, p-value = 0.0017). The 'Location of Encoder' (F-value = 16.00, p-value = 0.0018) and the interaction term 'AB' (F-value = 10.33, p-value = 0.0025) were significant factors. The residual error was 0.06, with a mean square of 0.005. The model R<sup>2</sup> was 0.76, with an adjusted R<sup>2</sup> of 0.67 and a predicted R<sup>2</sup> of 0.47, indicating moderate explanatory power. The adeq precision was 7.34, suggesting a satisfactory signal-to-noise ratio.

**Table 4.21 Analysis of variance for miss index of horse gram in the field testing**

Source	Sum of Squares	df	Mean Square	F-value	p-value	
<b>Model</b>	0.1978	5	0.0396	7.91	0.0017	significant
A-Location of Encoder	0.0800	1	0.0800	16.00	0.0018	
B-Furrow Opener	0.0144	2	0.0072	1.44	0.2741	
AB	0.1033	2	0.0517	10.33	0.0025	
<b>Pure Error</b>	0.0600	12	0.0050			
<b>Cor Total</b>	0.2578	17				
<b>Std. Dev.</b>	0.070				R <sup>2</sup>	0.767
<b>Mean</b>	1.49				Adjusted R <sup>2</sup>	0.670
<b>C.V. %</b>	4.75				Predicted R <sup>2</sup>	0.476
					Adeq Precision	7.348

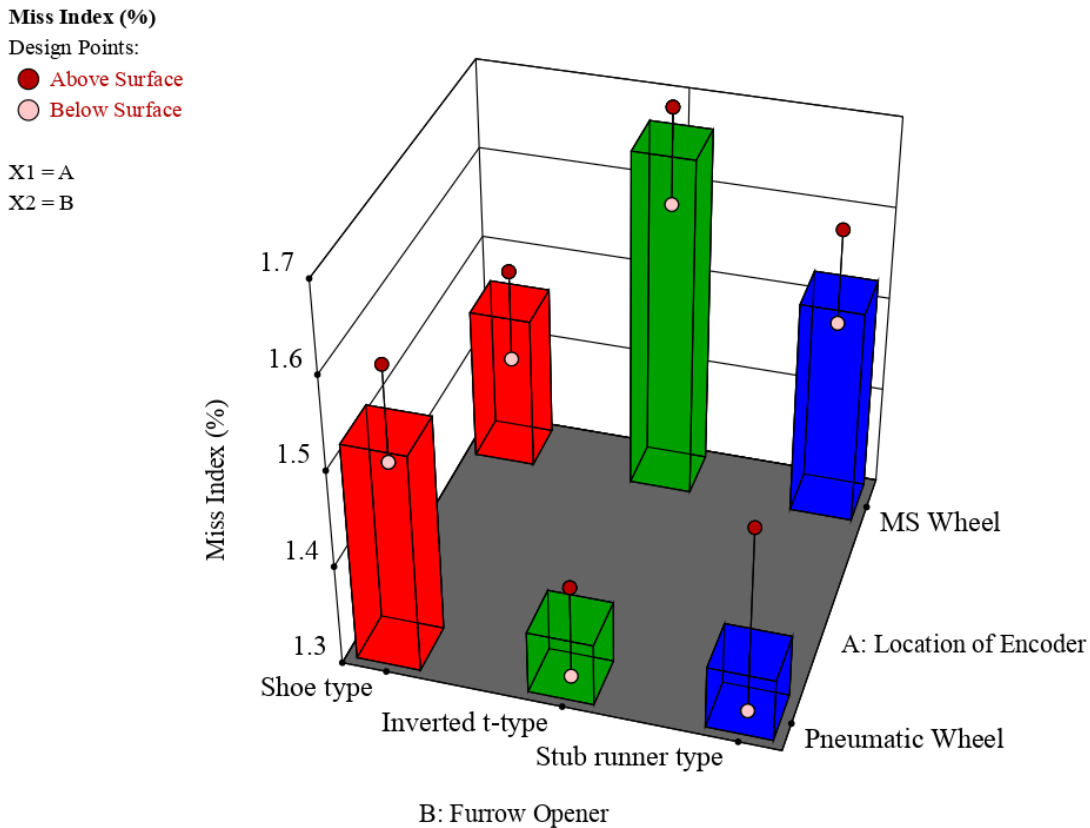


**Fig. 4.34 Effect of furrow opener and location of encoder on miss index for horse gram**

The Fig. 4.34 outlines the miss index (per cent) for horse gram seeding using different furrow opener types and encoder locations. The miss index is a crucial parameter indicating the frequency of missing seeds during planting, which can lead to gaps in the field and subsequently reduced crop yields.

The data reveal that the location of the encoder has a noticeable impact on the miss index. When the encoder is placed on the steel wheel, the miss index ranges from 1.4 to 1.7 per cent. The shoe type furrow opener generally shows a lower miss index, ranging from 1.4 to 1.5 per cent, indicating better performance in minimizing missed seeds. The inverted T-type furrow opener has a slightly higher miss index, ranging from 1.6 to 1.7 per cent. The stub runner type has a consistent miss index of around 1.5 to 1.6 per cent.

With the encoder located on the pneumatic wheel, the miss index, ranging from 1.3 to 1.6 per cent. The shoe type furrow opener exhibits a miss index of 1.5 to 1.6 per

cent. The inverted T-type furrow opener shows improved results with a miss index of 1.3 to 1.4 per cent. The stub runner type also shows similar performance with a miss index of 1.3 to 1.5 per cent.

These results suggest that the encoder location on the pneumatic wheel generally results in a lower miss index, indicating a more reliable performance in terms of seed placement accuracy. Among the furrow openers, the shoe type and inverted t-type show relatively better performance in minimizing the miss index when paired with the pneumatic wheel encoder.

#### 4.9.2.3 Multiple index

The ANOVA for multiple index shows a significant model ( $p < 0.0017$ ), indicating that the location of the encoder and the interaction between the location of the encoder and furrow opener significantly impact the multiple index. The adjusted  $R^2$  of 0.67 suggests that the model explains a moderate proportion of the variability in the multiple index. The lack of fit is significant ( $p = 0.0176$ ), suggesting that the model may not fully capture the relationship between the predictors and the response variable. The adequacy precision value of 7.34 indicates a moderate signal-to-noise ratio, implying that the model provides reasonable reliability in predicting the multiple index.

**Table 4.22 Analysis of variance for multiple index of horse gram in the field testing**

Source	Sum of Squares	df	Mean Square	F-value	p-value	
<b>Model</b>	5.69	3	1.90	156.09	< 0.0001	significant
A-Location of Encoder	5.44	1	5.44	448.41	< 0.0001	
B-Furrow Opener	0.2411	2	0.1206	9.93	0.0021	
<b>Residual</b>	0.1700	14	0.0121			
Lack of Fit	0.0833	2	0.0417	5.77	0.0176	significant
Pure Error	0.0867	12	0.0072			
<b>Cor Total</b>	5.86	17				
<b>Std. Dev.</b>	0.110					R <sup>2</sup> 0.971
<b>Mean</b>	3.57					Adjusted R <sup>2</sup> 0.964
<b>C.V. %</b>	3.08					Predicted R <sup>2</sup> 0.952
						Adeq Precision 26.630

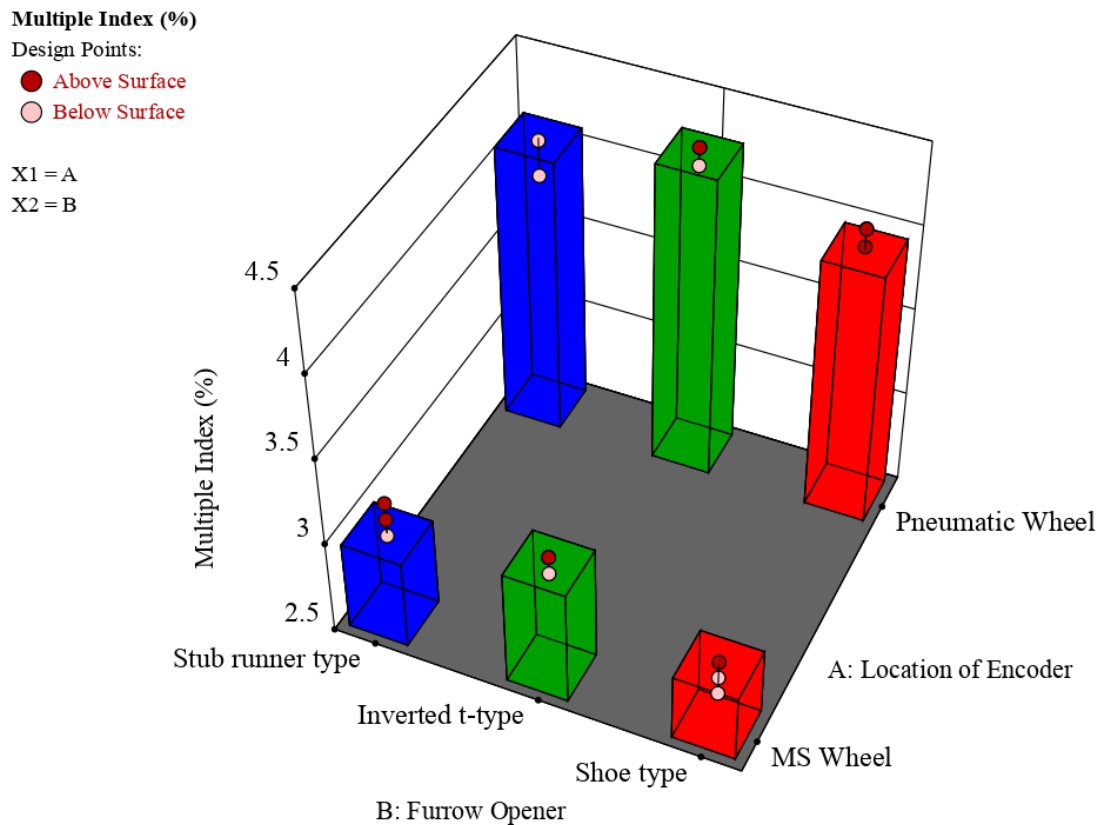


**Fig. 4.35 Effect of furrow opener and location of encoder on multiple index for horse gram**

The data shows a clear distinction between the performance of the steel wheel and the pneumatic wheel in terms of the multiple index. When the encoder is placed on the steel wheel, the multiple index ranges from 2.7 to 3.2 per cent. The Shoe type furrow opener generally exhibits a lower multiple index, ranging from 2.7 to 2.9 per cent, indicating better control over seed drop. The inverted T-type furrow opener has a slightly higher multiple index, ranging from 3.1 to 3.2 per cent. The stub runner type shows a multiple index of around 3.0 to 3.2 per cent.

With the encoder located on the pneumatic wheel, the multiple index is higher, ranging from 3.9 to 4.3 per cent. The shoe type furrow opener shows a multiple index of 4.0 to 4.1 per cent. The inverted T-type furrow opener exhibits the higher multiple index, ranging from 4.2 to 4.3 per cent. The stub runner type shows a multiple index of 3.9 to 4.1 per cent.

These results indicate that the steel wheel generally results in a lower multiple index, suggesting it provides better performance in terms of minimizing the planting of multiple seeds in the same spot. Among the furrow openers, the Shoe type exhibits relatively better control over seed drop when paired with the steel wheel encoder. The inverted T-type and stub Runner types show higher multiple indices, particularly when paired with the pneumatic wheel encoder, highlighting the importance of encoder location in optimizing seed placement accuracy.

#### 4.9.2.4 Quality of feed index

The ANOVA for quality of feed index reveals a significant model ( $p < 0.0001$ ), suggesting that the location of the encoder and the furrow opener significantly impact the quality feed index. The adjusted  $R^2$  of 0.95 indicates that the model explains a large proportion of the variability in the quality feed index. The lack of fit is significant ( $p = 0.0176$ ), suggesting that the model may not fully capture the relationship between the predictors and the response variable. The adequacy precision value of 26.63 suggests a strong signal-to-noise ratio, implying that the model provides reasonable reliability in predicting the quality of feed index.

**Table 4.23 Analysis of variance for quality feed index of horse gram in the field testing**

Source	Sum of Squares	df	Mean Square	F-value	p-value	
<b>Model</b>	4.80	5	0.9592	69.06	< 0.0001	significant
A-Location of Encoder	4.21	1	4.21	302.76	< 0.0001	
B-Furrow Opener	0.2878	2	0.1439	10.36	0.0024	
AB	0.3033	2	0.1517	10.92	0.0020	
<b>Pure Error</b>	0.1667	12	0.0139			
<b>Cor Total</b>	4.96	17				
<b>Std. Dev.</b>	0.117					R <sup>2</sup> 0.966
<b>Mean</b>	94.94					Adjusted R <sup>2</sup> 0.952
<b>C.V. %</b>	0.124					Predicted R <sup>2</sup> 0.924
						Adeq Precision 20.085

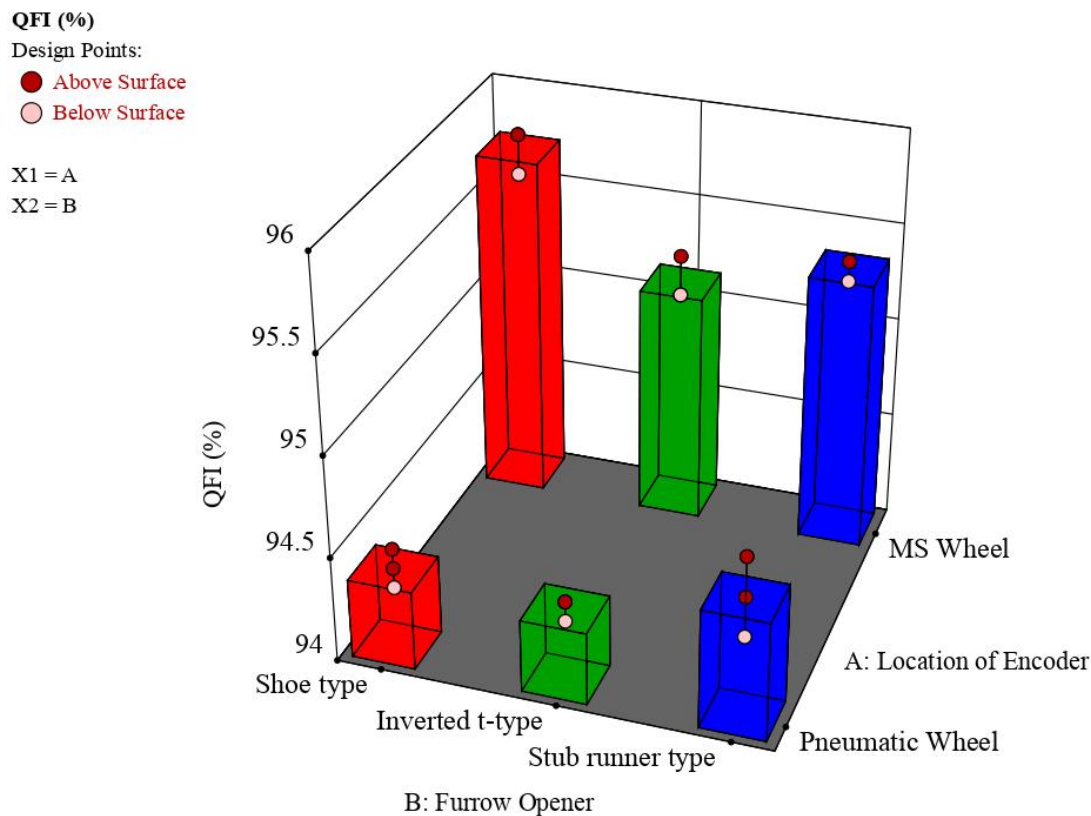


**Fig. 4.36 Effect of furrow opener and location of encoder on QFI for horse gram**

The Fig. 4.36 indicates a difference in QFI between the steel wheel and the pneumatic wheel. When the encoder is placed on the steel wheel, the QFI ranges from 95.1 to 95.8 per cent. The shoe type furrow opener generally exhibits the highest QFI values, ranging from 95.6 to 95.8 per cent, suggesting superior performance in seed placement accuracy. The inverted T-type furrow opener shows slightly lower QFI values, ranging from 95.1 to 95.3 per cent. The stub Runner type exhibits QFI values around 95.3 to 95.4 per cent.

With the encoder located on the pneumatic wheel, the QFI is slightly lower, ranging from 94.3 to 94.8 per cent. The shoe type furrow opener shows QFI values ranging from 94.3 to 94.5 per cent. The inverted T-type furrow opener exhibits QFI values of 94.3 to 94.4 per cent, while the stub Runner type shows QFI values from 94.4 to 94.8 per cent.

These results suggest that the steel wheel provides a higher QFI, indicating better performance in terms of seed placement accuracy and consistency. Among the

furrow openers, the shoe type demonstrates the highest QFI values when paired with the steel wheel encoder. The inverted T-type and stub runner types show lower QFI values, particularly when paired with the pneumatic wheel encoder. This highlights the importance of encoder location in optimizing the overall performance of the seed metering mechanism.

#### 4.9.2.5 Precision index

The ANOVA for the precision index yielded a significant model (F-value = 528.04, p-value < 0.0001), with 'Location of Encoder' as a significant term (F-value = 528.04, p-value < 0.0001). The residual error was minimal, with a sum of squares of 0.079 and a mean square of 0.005. The lack of fit was not significant (F-value = 1.92, p-value = 0.1711), indicating good model fit. The model had a high R<sup>2</sup> value of 0.97, with an adjusted R<sup>2</sup> of 0.96 and a predicted R<sup>2</sup> of 0.96. Adeq Precision was 32.49, indicating an excellent signal-to-noise ratio.

**Table 4.24 Analysis of variance for precision index of horse gram in the field testing**

Source	Sum of Squares	df	Mean Square	F-value	p-value	
<b>Model</b>	2.62	1	2.62	528.04	< 0.0001	significant
A-Location of Encoder	2.62	1	2.62	528.04	< 0.0001	
<b>Residual</b>	0.0794	16	0.0050			
Lack of Fit	0.0310	4	0.0078	1.92	0.1711	not significant
Pure Error	0.0484	12	0.0040			
<b>Cor Total</b>	2.70	17				
<b>Std. Dev.</b>	0.070				R <sup>2</sup>	0.970
<b>Mean</b>	6.32				Adjusted R <sup>2</sup>	0.968
<b>C.V. %</b>	1.11				Predicted R <sup>2</sup>	0.962
					Adeq Precision	32.497



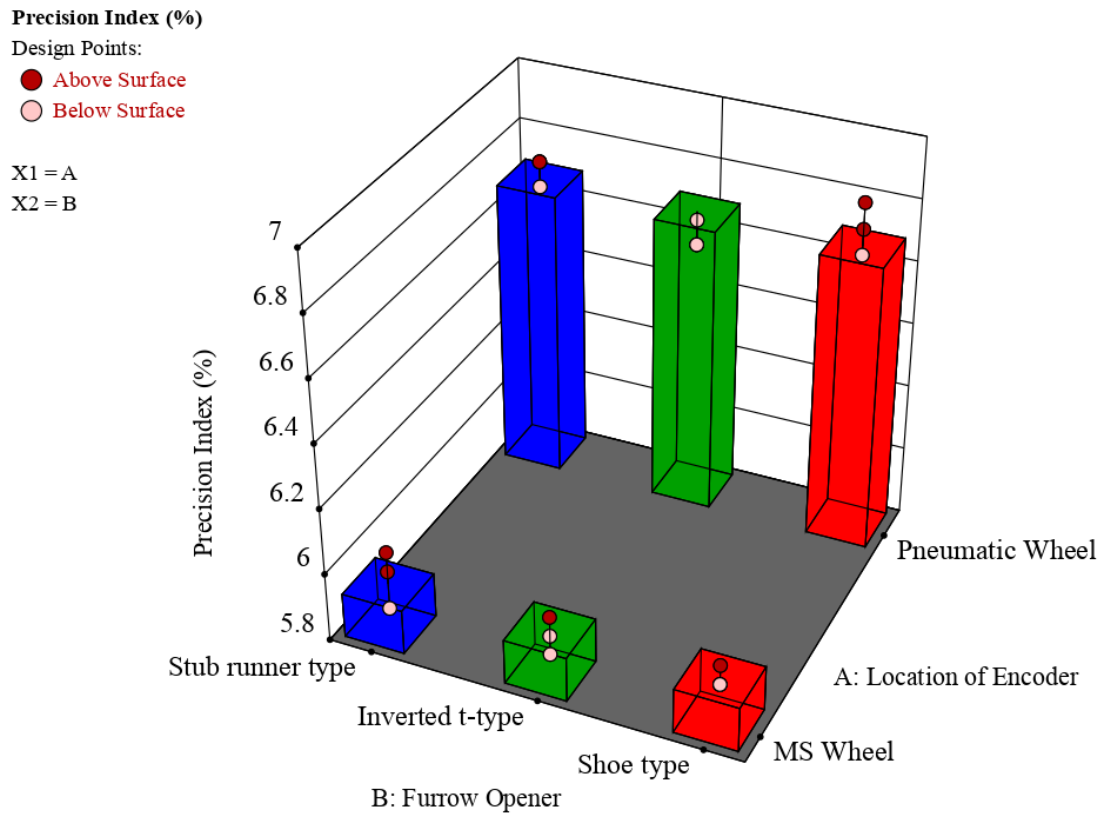


**Fig. 4.37 Effect of furrow opener and location of encoder on precision index for horse gram**

The precision of spacing, expressed as a per centage variation, Fig. 4.36 indicates that the precision of spacing is generally higher with the encoder located on the pneumatic wheel compared to the MS wheel. For performance quantification, a lower precision value indicates a better type of planter. When the encoder is on the steel wheel, the precision of spacing values ranges from 5.86 to 5.98 per cent. The shoe type furrow opener shows precision values of 5.92 and 5.98 per cent, indicating consistent performance. The inverted T-type furrow opener exhibits precision values ranging from 5.86 to 5.98 per cent. The stub Runner type shows precision values from 5.86 to 6.04 per cent, suggesting slightly higher variability in spacing accuracy.

With the encoder on the pneumatic wheel, the precision of spacing values ranges from 6.6 to 6.84 per cent. The shoe type furrow opener demonstrates precision values ranging from 6.68 to 6.84 per cent, indicating superior performance compared to other

furrow opener types. The inverted T-type furrow opener shows precision values from 6.6 to 6.68 per cent, while the stub runner type exhibits values from 6.68 to 6.76 per cent.

These results suggest that the steel wheel provides lower precision of spacing, indicating better performance in terms of achieving uniform seed distribution. Among the furrow openers, the Shoe type exhibits the lowest precision of spacing when paired with the steel wheel encoder. The inverted T-type and stub runner types show slightly lower precision values, particularly with the steel wheel encoder.

#### 4.9.2.6 Germination

The ANOVA for germination revealed a highly significant model (F-value = 344.65, p-value < 0.0001), with 'Furrow Opener' being a significant term (F-value = 344.65, p-value < 0.0001) as shown in Table 4.25. The residual error was 7.17, with a mean square of 0.47. The lack of fit was not significant (F-value = 1.37, p-value = 0.2976), suggesting a good fit. The model's R<sup>2</sup> was 0.97, with an adjusted R<sup>2</sup> of 0.97 and a predicted R<sup>2</sup> of 0.96. Adeq Precision was 36.61, indicating a robust signal-to-noise ratio.

**Table 4.25 Analysis of variance for germination of horse gram in the field testing**

Source	Sum of Squares	df	Mean Square	F-value	p-value	
<b>Model</b>	329.33	2	164.67	344.65	< 0.0001	significant
B-Furrow Opener	329.33	2	164.67	344.65	< 0.0001	
<b>Residual</b>	7.17	15	0.4778			
Lack of Fit	1.83	3	0.6111	1.37	0.2976	not significant
Pure Error	5.33	12	0.4444			
<b>Cor Total</b>	336.50	17				
<b>Std. Dev.</b>	0.691				R <sup>2</sup>	0.978
<b>Mean</b>	90.83				Adjusted R <sup>2</sup>	0.975
<b>C.V. %</b>	0.761				Predicted R <sup>2</sup>	0.969
					Adeq Precision	36.618

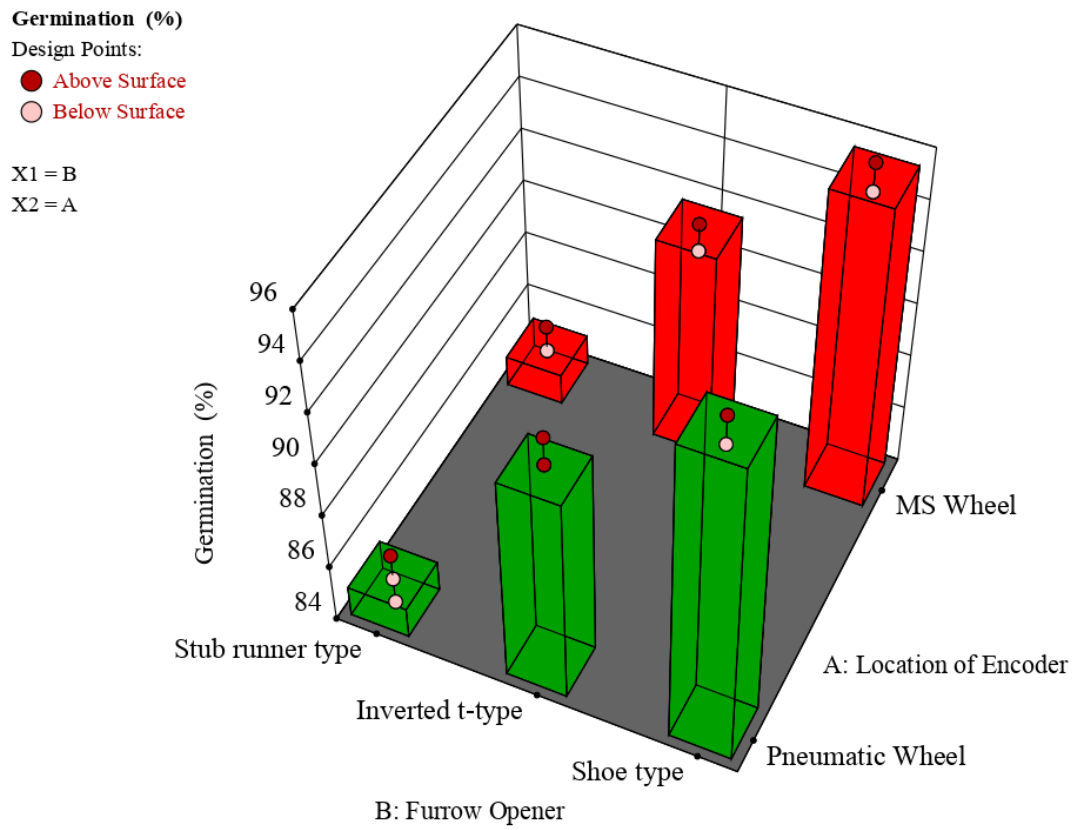


**Fig. 4.38 Effect of furrow opener and location of encoder on germination for horse gram**

The results show varying germination rates across different configurations. For horse gram, the highest germination per centages were achieved with the shoe type openers on both the steel wheel (95-96 per cent) and the pneumatic wheel (95-96 per cent). The inverted T-type openers also demonstrated good germination rates, ranging from 91 to 93 per cent, while the stub runner type openers showed slightly lower rates, ranging from 84 to 86 per cent.

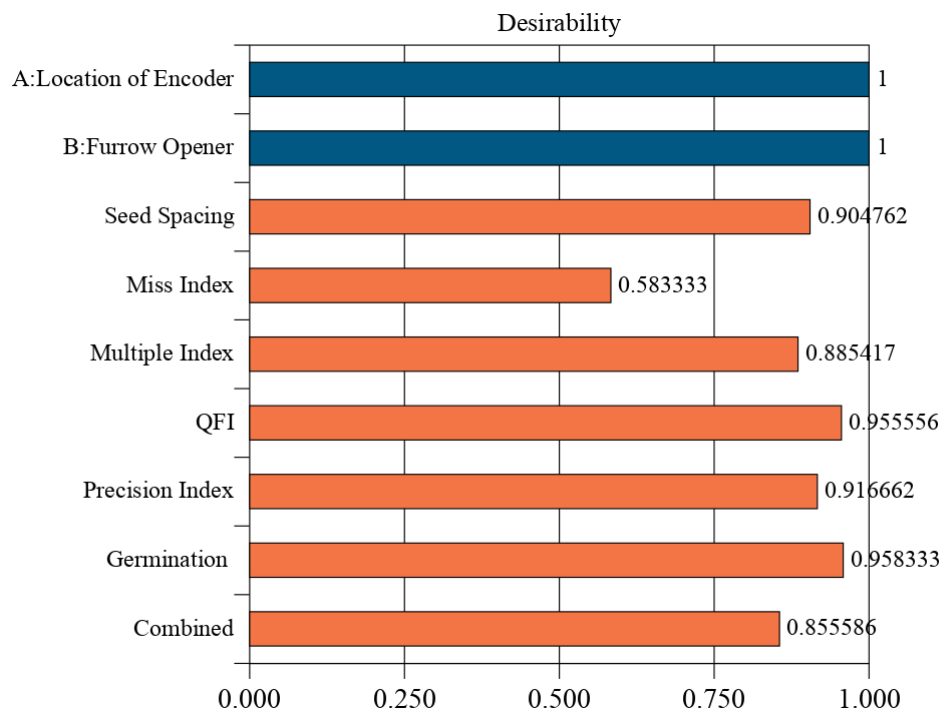


**Fig. 4.39 Desirability index for field testing of pneumatic planter with electronic control system for horse gram**

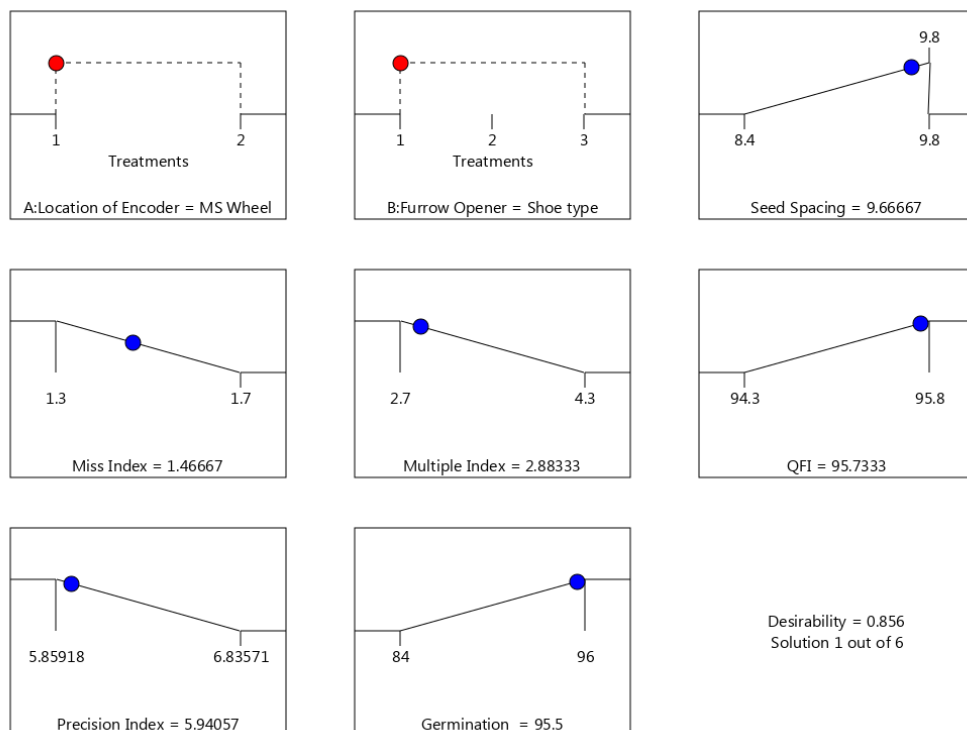


**Fig. 4.40 Optimum level of independent parameter on performance parameters for horse gram**

The analysis of results from various treatment combinations involving different furrow openers and encoder locations aimed to optimize several key performance indicators: seed spacing, miss index, multiple index, quality of feed index (QFI), precision index, and germination per centage. Optimization was based on a desirability index value of 0.856, as shown in Fig. 4.38. This indicating optimal performance for planting horse gram seeds with the encoder located at the steel wheel and using the furrow opener of shoe type.

The optimized values of the dependent parameters are as follows: seed spacing of 9.67 cm, miss index of 1.46 per cent, multiple index of 2.88 per cent, QFI of 95.73 per cent, precision index of 5.94 per cent, and germination per centage of 95.5 per cent, as illustrated in Fig. 4.39. These values represent the best performance achieved by the pneumatic planter under the specified conditions for horse gram seed planting. This configuration of independent parameters is recommended for achieving optimal performance tailored to the characteristics of horse gram seeds.

#### 4.10 FIELD PERFORMANCE TESTING OF THE DEVELOPED PROTOTYPE

Developed pneumatic planter with electronic control system was tested in the field by planting of seeds viz, black gram and horse gram as per standard procedure (IS: 6316-1971) and evaluated in terms of seed to seed distance, actual field capacity and germination per centage of seeds. The field experiments were conducted at the Instruction Farm, KCAEFT, Tavanur. Prior to the experiments, field was prepared for fine tilth which was suitable for seed planting. The soil and machine parameters were studied and recorded in Table 4.27.

Different plot of 50 × 50 m size was selected for planting black gram and horse gram seeds. The pneumatic planter prototype was mounted over 37 kW tractor as a power source and blower was operated from PTO drive. The engine speed was set to get desired PTO speed which rotates the blower fan at an optimum speed and maintains constant air flow. Black gram and horse gram seed respectively were used for planting operation with recommended seed spacing of 150 × 300 and 100 × 400 mm, respectively.

##### **4.9.1 Soil parameters**

The soil parameters such as soil type, moisture content, bulk density, cone index and shear strength were found before the sowing of seeds. These properties were determined as explained in section 3.9. The data was statistically analysed and the results are presented in Table 4.26.

###### ***4.9.1.1 Soil type***

The soil samples taken separately from the fields of experimental trials and were mechanically analysed for finding its textural composition. The per centage of different textures ranged between 61-62, 10-11 and 27-28 per cent sand, silt and clay in all these fields respectively. Hence, it was concluded that the type of soil was sandy clay loam soil in field.

###### ***4.9.1.2 Moisture content***

The soil moisture content was measured at different places of the experimental before sowing. The moisture content of the soil was determined and statistically

analysed. The moisture content varied from 12.11 to 13.49 per cent with mean of 12.78 per cent and a coefficient of variation of 7.52 per cent with standard deviation of 0.94. A favourable moisture level was chosen to sow the seeds for their optimal growth. It is recommended that the soil moisture content at the time of sowing is typically around 10-12% on a dry weight basis for pulses like black and horse gram. Maintaining this moisture level helps ensure that the seeds have enough water to germinate effectively and support early growth stages. Hence the experiments on performance study of the machine variables were conducted at this soil moisture level.

#### **4.9.1.3 Bulk density**

The soil bulk density was measured at different places of the experimental trial plot at the time of harvesting. Soil samples were collected for analysis. The bulk density of soil was determined and statistically analysed. The bulk density of the soil ranged from 1617 to 1813 kg cm<sup>-2</sup> with an average mean of 1760.0 kg cm<sup>-2</sup>. The coefficient of variation was found out as 6.02 per cent and standard deviation of 74.2. It shows the variations in soil bulk density at respective soil moisture. It was observed that bulk density of soil increased with increase in soil moisture content and had a linear relationship.

#### **4.9.1.4 Cone index**

The cone index of soil was determined and statistically analysed. The cone index varied from 1123 to 1569 kg cm<sup>-2</sup>. The mean value of the cone index was 1352 kg m<sup>-2</sup> at the soil moisture of 13.00 per cent. As the depth increased from surface, penetration resistance was also increased.

**Table 4.26 Soil parameters**

Parameter	Unit	Mean	Standard deviation	Coefficient of variation (%)
Moisture content	%	12.78	0.94	7.52
Bulk density	kg m <sup>-3</sup>	1760	74.2	6.02
Cone index	kg m <sup>-2</sup>	1352	376	8.03

**Table 4.27 Field performance of the developed pneumatic planter with electronic control system**

<b>Sl. No.</b>	<b>Particulars</b>	<b>Black gram</b>	<b>Horse gram</b>
1.	Size of plot, m	50 × 50	
2.	Location of plot	Instructional farm, KCAEFT, Tavanur	
3.	Source of power	Tractor (37 kW)	
4.	Type of soil	Sandy loam	
5.	Soil moisture, d. b. (%)	12.78	
6.	Bulk density, kg m <sup>-3</sup>	1760	
7.	Seed variety	VBN-6	KS-2
8.	Recommended plant geometry, mm	150 × 300	100 × 400
9.	Average depth of sowing, mm	37	40
10.	Speed of operation, km h <sup>-1</sup>	2.0	2.0
11.	Theoretical field capacity, ha h <sup>-1</sup>	0.24	0.32
12.	Effective field capacity, ha h <sup>-1</sup>	0.22	0.29
13.	Field efficiency (%)	91	90
14.	Draft of implement, N	572	572
15.	Wheel slip (%)	4.0	4.0
16.	Fuel consumption, L h <sup>-1</sup>	4.0	4.0
17.	Seed rate kg ha <sup>-1</sup>	9.8	9.6
18.	Germination, (%)	96	97
19.	Plant count per m <sup>2</sup>	17	18



#### 4.10 COMPARISON BETWEEN MECHANICAL AND DEVELOPED PNEUMATIC PLANTER

The comparative study between the mechanical pneumatic planter and the developed pneumatic planter with an electronic control system for black gram and horse gram seeds revealed distinct differences in performance across key parameters.

For black gram, the developed pneumatic planter demonstrated improved precision in seed placement. The range of seed spacing for the developed planter was between 13 to 15 cm, while the mechanical pneumatic planter exhibited a wider and less consistent range of 12 to 17 cm. The miss index for the developed planter was recorded at up to 1.3 per cent, significantly lower than the mechanical planter 3.5 per cent. The multiple index in the developed system was lower as well, reaching up to 4.3 per cent, compared to the mechanical planter's 8 per cent. The quality of feed index (QFI) was notably higher for the developed planter, achieving up to 96 per cent, while the mechanical planter QFI was limited to 88 per cent.

Similarly, for horse gram, the developed pneumatic planter also outperformed the mechanical planter. The seed spacing for the developed planter ranged from 8.5 to 10 cm, compared to the mechanical planter wider range of 7 to 12 cm, indicating greater consistency in seed placement. The miss index for the developed planter was up to 1.7 per cent, whereas the mechanical planter recorded a higher miss index of up to 4.8 per cent. The multiple index for the developed planter was lower, at 4.3 per cent, compared to the mechanical planter 9.2 per cent. The QFI for the developed planter was higher, reaching 95 per cent, while the mechanical planter's QFI was 86 per cent.

#### 4.11 COST ECONOMIC OF DEVELOPED PNEUMATIC PLANTER WITH ELECTRONIC CONTROL SYSTEM

The economic evaluation of the developed pneumatic planter with an electronic control system was conducted based on several assumptions, including the initial costs of the tractor and planter, their annual usage, and their total life span. The total cost of the developed planter with electronic control system was ₹1,80,000. The total fixed cost for operating the planter and tractor was calculated to be ₹224.58 per hour, while the variable cost was ₹635.97 per hour, leading to a combined operating cost of ₹860.55

per hour. The field capacity and field efficiency of planter was  $0.25 \text{ ha h}^{-1}$  and 90 per cent respectively. The cost per hectare for planting operations using the pneumatic planter was determined to be ₹3072. In comparison, manual sowing costs ₹4054 per hectare, resulting in a cost saving of ₹982 per hectare. The break-even point for the planter was calculated at 79.22 hours per year, indicating the minimum operational hours required to cover the fixed costs. Additionally, the payback period for the initial investment was found to be 1.13 years, demonstrating a quick return on investment. Overall, the developed pneumatic planter with electronic control system offers significant cost savings and efficiency improvements over traditional manual sowing methods. The detailed calculation is given in Appendix IV.

## CHAPTER V

### Summary and conclusion

The need for a tractor operated pneumatic no-till pulse planter with electronic control system arises from the demand for efficient and precise planting of pulse crops namely black gram and horse gram. Traditional planting methods often result in uneven seed distribution, inconsistent seed depth, and increased soil disturbance, resulting poor germination and crop yield. A pneumatic no-till planter minimizes soil disruption, preserves soil moisture, and enhances seed placement accuracy, leading to better germination and growth. The electronic control system further improves the planter performance by allowing adjustments and monitoring of critical parameters, such as seed spacing and metering rate, ensuring optimal planting conditions and higher crop productivity. This advanced technology addresses the challenges of traditional planting methods, providing a reliable solution for modern agriculture.

The research focused on optimizing planter performance by studying the influence of seed, soil properties, machine and operational parameters. Initially, a laboratory model was developed for controlled seeding, followed by the prototype development and was evaluated at the Instructional Farm, KCAEFT, Tavanur. The seed varieties used were VBN-6 (black gram) and KS-2 (horse gram). The vacuum disc type metering mechanism was selected for its precision in seed singulation, minimal seed damage, and adaptability to various seed sizes and shapes. The planter components included a hopper, vacuum-based metering mechanism, seed tube, furrow opener, frame, ground wheels and power source. The operation utilized a vacuum system for precise seed placement, with the metering mechanism involving a rotating disc with holes and an aspirator blower.

The detailed analysis of factors influencing the performance of an electronically controlled pneumatic planter, focusing on both seed and machine parameters were carried out. The investigation include laboratory experiments for seed metering mechanisms, calibration, testing, and field performance evaluation of the pneumatic planter for black gram and horse gram seeds. The optimal settings for vacuum pressure, plate hole size,

forward speed, and input sensors were identified through extensive trials and statistical analysis. Additionally, an economic analysis of the cost-effectiveness of the developed planter was also worked out.

**The laboratory studies on seeds and the pneumatic planter concluded with the following observations:**

- Black gram seeds have a length of 2.32-3.88 mm, width of 1.99-3.65 mm, and thickness of 1.56-2.07 mm, whereas horse gram seeds are larger, with a length of 6.02-6.27 mm, width of 4.10-4.35 mm, and thickness of 2.16-2.45 mm.
- The arithmetic mean diameter of black gram seeds was 2.62 mm, while horse gram seeds was 4.22 mm and the geometric mean diameter was 2.53 mm, and 3.86 mm respectively for black gram and horse gram.
- The aspect ratio of the black gram seeds, ranged were observed as 85.69 to 99.68 percent, while horse gram seeds ranged from 67.96 to 69.50 percent.
- Also, the sphericity of black gram and horse gram seeds were observed as of 83.61 percent and 63.68 percent respectively whereas, the roundness was 0.53, compared to horse gram seeds.
- The bulk density of black gram seeds ranged from 800.00 to 814.00 kg m<sup>-3</sup>, and its true density ranged from 1428.00 to 1440.00 kg m<sup>-3</sup>. Their porosity ranged from 43.08 to 44.17 percent.
- The bulk density of horse gram seeds ranged from 916.00 to 935.00 kg m<sup>-3</sup>, and its true density was ranged from 1380.00 to 1396.00 kg m<sup>-3</sup>.
- The porosity ranged from 43.08 to 44.17 percent for black gram and from 33.02 to 36.62 percent for horse gram. The angle of repose for black gram ranged from 25.01° to 25.31°, while it ranged from 23.41° to 25.06° for horse gram.
- The coefficient of friction for black gram seeds varied on different materials, with higher values for horse gram seeds, indicated greater resistance to its flowability.

- The terminal velocity of black gram seeds was  $8.21 \text{ m s}^{-1}$ , compared to  $8.68 \text{ m s}^{-1}$  for horse gram seeds and the drag coefficient for black gram seeds ranged from 0.63 to 0.68, while it ranged from 0.54 to 0.59 for horse gram.
- A tetrazolium test was conducted to find out the seed quality, which showed 95 percent viability for black gram seeds and 94 percent for horse gram seeds. The germination test revealed that the rate was 96 percent for black gram seeds and 92 percent for horse gram seeds.
- The pneumatic planter consisted of a vacuum disc-type precision seed metering mechanism, having rotating disc with holes oriented vertically and an aspirator blower to create vacuum which, ensured precise seed placement.
- Effective seed pickup and transport require vacuum pressure to overcome the seed weight which in turn for a balanced vacuum pressure, seed weight, gravity, and centrifugal forces during transport.
- Modifications to the planter from mechanical to electronically controlled systems, using a stepper motor regulated through a microcontroller resulted a precise seed plate rotation. The electronic system comprised of a stepper motor, rotary encoder, proximity sensor, Arduino Nano microcontroller, vacuum pressure sensor, micro-step drive, battery, and protective enclosure.
- The proximity sensor detected wheel spokes, and the rotary encoder provided accurate control of speed and position, while the vacuum sensor activated the system to operate under optimal conditions.

The study also investigated the optimization of a pneumatic seed metering mechanism for black and horse gram seeds, focused on various parameters influencing seed spacing, miss index, multiple index, quality of feed index, and precision of spacing. The experiment employed proximity and rotary encoder sensors with varied holes of 2.1 mm and 2.5 mm, vacuum pressures of 3.0 kPa, 4.0 kPa and 5.0 kPa, and planter speeds of 1.0 km h<sup>-1</sup>, 2.0 km h<sup>-1</sup>, 3.0 km h<sup>-1</sup> respectively.

**i. Black gram**

- The seed spacing for black gram ranged from 14.5 to 16 cm. using encoder sensor seed spacing close to 15 cm while with proximity sensor near to 16 cm. At forward speed of 1.0 km h<sup>-1</sup> the seed spacing close to 15 cm while at 2.0 km h<sup>-1</sup> it was near to 16 cm.
- Miss index increased from 1.0 to 3 percent with higher forward speed. Smaller hole sizes resulted in lower miss index. Encoder sensor had lower miss index compared to proximity sensor.
- Hole size, vacuum pressure, and forward speed were significantly affected multiple index, which was 3.38 percent. The larger hole sizes and increased vacuum pressure raised multiple index.
- QFI significantly affected all the independent factors; encoder sensor provided higher QFI compared to proximity sensor; smaller hole size of 2.1 mm resulted in higher QFI values while the optimal vacuum pressure was 4.0 kPa.
- The precision in seed spacing was 8.27 percent. Precision decreased with higher forward speeds but improved with increased vacuum pressure. Sensor type and forward speed significantly affected precision.
- Rotary encoder with hole size of 2.1 mm at 4.0 kPa and 1.0 km h<sup>-1</sup> speed was optimal for seed spacing, miss, and multiple indices; desirability of optimum parameters was 0.80.

**ii. Horse gram**

- Seed spacing was influenced by sensor type, hole size, vacuum pressure, and forward speed. The proximity sensors with a 2.1 mm hole size, 3.0 kPa vacuum pressure, and 1.0 km h<sup>-1</sup> forward speed, seed spacing was 9.2 cm which was increased to 12.9 cm at 3.0 km h<sup>-1</sup>. Encoder sensors provided consistent spacing between 9.8 cm and 11.1 cm.
- Miss index was lower with encoder sensors. At a 2.1 mm hole size and 3.0 kPa vacuum pressure. The encoder sensors had a miss index of 0.5 percent at 1.0 km h<sup>-1</sup>, while proximity sensors had 1.2 percent.
- Multiple index was higher for proximity sensors. At 2.5 mm hole size and 5 kPa vacuum pressure, proximity sensors had a multiple index of 5.2 percent at 1.0 km h<sup>-1</sup>, compared to 4.5 percent for encoder sensors; the multiple index increased with hole size and vacuum pressure but decreased with higher forward speeds.
- QFI was higher with encoder sensors. At 2.1 mm hole size, 3 kPa vacuum pressure, and 1.0 km h<sup>-1</sup> forward speed, QFI was 96.2 percent for encoder sensors and 95.4 percent for proximity sensors. Higher QFI values with encoder sensors suggested a more reliable seed metering process.
- Precision of spacing was higher at lower forward speeds. When used the proximity sensors, 2.1 mm hole size, and 3.0 kPa vacuum pressure, precision was 16.30 percent at 1.0 km h<sup>-1</sup> and 11.63 percent at 3.0 km h<sup>-1</sup>; encoder sensors provided consistent precision between 13.51 and 15.3 percent.
- Rotary encoder with a 2.1 mm hole size at 4 kPa and 1 km h<sup>-1</sup> speed was optimal for seed spacing, miss, and multiple index, with a desirability of 0.77.

The field evaluation of the pneumatic planter with an electronic control system tested the effect of furrow opener types and encoder locations on various performance parameters for black gram and horse gram.

**i. Black gram**

- Seed spacing results indicated that the steel wheel provided more accurate seed spacing. When used a shoe type furrow opener achieving an average spacing of approximately 14.8 cm, closer to the target of 15 cm, compared to the pneumatic wheel which showed high variability and lowered seed spacings.
- The miss index was low at all set ups, ranged from 1.2 to 1.3 percent. When a shoe type furrow opener was used a consistent miss index of 1.2 percent was obtained.
- The multiple index was lower when the encoder was fitted on a steel wheel, ranging from 2.5 to 2.7 percent, compared to 3.7 to 4.3 percent with the pneumatic wheel.
- The quality of feed index (QFI) was higher with the encoder on the steel wheel, ranging from 96 to 96.2 percent, indicated a superior seed metering performance.
- Precision index results showed that the steel wheel provided better precision, ranged from 6.12 to 6.24 percent. Lower the value of precision, the better was the type of metering performance.
- Germination rates were the highest when the shoe type furrow opener was used and the encoder was fitted on the pneumatic wheel, achieved 96 to 97 percent.
- Numerical optimization yielded an optimal desirability index of 0.870, with the best performance achieved when the encoder was fitted on the steel wheel and the shoe type furrow opener was used.
- The seed spacing of 14.76 cm, miss index of 1.24 percent, multiple index of 2.56 percent, QFI of 96.2 percent, precision index of 6.17 percent, and germination percentage of 96 percent was observed as the optimal values.



**ii. For horse gram**

- The encoder location significantly affected seed spacing for horse gram. When the encoder was fitted on a steel wheel and the shoe type furrow opener was used spacing of 9.6-9.7 cm was obtained which was close to the 10 cm. The pneumatic wheel encoder results in 8.4-8.7 cm spacing, which was below the required spacing. The location on the steel wheel was more effective for accurate spacing.
- The miss index was 1.4-1.7 percent with the encoder fitted on steel wheel and 1.3-1.6 percent when fitted on a pneumatic wheel. The inverted T-type furrow opener performed the best with the pneumatic wheel encoder, which showed a 1.3-1.4 percent miss index.
- The multiple index was lower with the steel wheel encoder of 2.7-3.2 percent than with the pneumatic wheel encoder of 3.9-4.3 percent. When operated with a shoe type furrow opener the lowest multiple index of 2.7-2.9 percent was obtained when used with the steel wheel.
- The QFI was the higher with the steel wheel encoder as 95.1-95.8 percent as compared to the pneumatic wheel encoder as 94.3-94.8 percent. The shoe type furrow opener achieved the highest QFI of 95.6-95.8 percent, when operated with the steel wheel.
- Precision of spacing was the higher with the pneumatic wheel encoder as 6.6-6.84 percent than the steel wheel encoder as 5.86-5.98 percent. The shoe type furrow opener showed the best precision of 6.68-6.84 percent with the pneumatic wheel. Lower the value of precision, the better was the type of metering performance.
- The highest germination rates for horse gram were observed with shoe type openers on both the steel wheel as 95-96 percent and the pneumatic wheel 95-96 percent. When used the inverted T-type openers, the germination rates were of 91-93 percent and 84-86 percent when operated with the stub runner type.
- The optimized values for seed spacing of 9.67 cm, miss index of 1.46 percent, multiple index of 2.88 percent, QFI of 95.73 percent, precision index of 5.94 percent, and germination percentage of 95.5 were obtained, Hence the best

configuration is selected as the steel wheel encoder with the shoe type furrow opener.

The field performance of the developed pneumatic planter was evaluated for black and horse gram seeds at the Instruction farm, KCAEFT, Tavanur. A plot size was  $50 \times 50$  m was selected in the form for trials. The planter mounted on a 37 kW tractor. The varieties such as VBN-6 and KS-2 of black gram and horse gram seeds were used. The recommended spacing of  $150 \times 300$  mm and  $100 \times 400$  mm were maintained in the field. The soil was sandy clay loam, with a moisture content of 12.78 percent. The bulk density and the cone index were  $1760 \text{ kg m}^{-3}$  and  $1352 \text{ kg m}^{-2}$ . The modified pneumatic planter with electronic control system with a encoder fitted on a steel with a inverted T-type furrow opener when operated in the field resulted a sowing depth of 37 mm for black gram and 40 mm for horse gram respectively. The operating speed was  $2.0 \text{ km h}^{-1}$  and fuel consumption of  $4.0 \text{ L h}^{-1}$ . The effective field capacity and field efficiency were  $0.22 \text{ ha h}^{-1}$  and 91 percent for black gram and  $0.29 \text{ ha h}^{-1}$  and 90 percent for horse gram. The germination rates recorded were of 96 and 97 percent, respectively for black gram and horse gram seeds.

The total cost of the developed planter with electronic control system was ₹1,80,000. The operating cost was calculated ₹860.55 per hour. The cost of operation per hectare was of ₹3072. As per the prevailing wage rates, the expenditure for manual sowing is ₹4054 per hectare. The break-even point is calculated 79.22 hours per year and the payback period is 1.13 years.

## REFERENCES

- AA, J. and Stover, J., 2023. Drivers of future population growth in six most populous countries: Effect of demographic components on the population growth using decomposition analysis. *Gates Open Res.* 7, p.118.
- Abdolahzare, Z. and Mehdizadeh, S.A., 2018. Nonlinear mathematical modeling of seed spacing uniformity of a pneumatic planter using genetic programming and image processing. *Neural Comput. Appl.*, 29(2), pp.363-375.
- Abdolahzare, Z. and Mehdizadeh, S.A., 2018. Real time laboratory and field monitoring of the effect of the operational parameters on seed falling speed and trajectory of pneumatic planter. *Comput. Electron. Agric.*, 145, pp.187-198.
- Afify, M., Z. El-Haddad, G. Hassan, and Y. Shaaban. 2009. Mathematical model for predicting vacuum pressure of onion seeds precision seeder. *J. of Agri. Eng.*, 26(4): 1776–1799.
- Ahmad, F., Adeel, M., Qui, B., Ma, J., Shoaib, M., Shakoor, A. and Chandio, F.A., 2021. Sowing uniformity of bed-type pneumatic maize planter at various seedbed preparation levels and machine travel speeds. *Int. J. Agric. Biol. Eng.*, 14(1), pp.165-171.
- Ahmad, O.T., Morad, M.M., Ali, M.M. and Abo-Elnaga, M.H., 2018. Development and performance evaluation of a new pneumatic precision metering device for planting medicinal and aromatic crops. *Zagazig J. Agric. Res.*, 45(1), pp.197-2011.
- Alchanatis, V., Kashti, Y. and Brikman, R., 2002. A machine vision system for evaluation of planter seed spatial distribution.
- Alhassan, E.A., Adewumi, A.D. and OKPODJAH, B., 2018. Development of a self-propelled multi-crop two rows precision planter: A new design concept for the metering mechanism. *Int. J. Mech. Eng. Technol.*

- AOAC. (2002). Official Methods of Analysis. Association of Official Analytical Chemists, Washington DC, USA.
- Arzu, Y. and Adnan, D., 2007. Optimization of the seed spacing uniformity performance of a vacuum type precision seeder using response surface methodology. *Biosyst. Eng.*, 97, pp.347-356.
- Bagherpour, H., 2019. Modeling and evaluation of a vacuum-cylinder precision seeder for chickpea seeds. *Agric. Eng. Int.: CIGR J.*, 21(4).
- Bahnasawy, A.H., 2007. Some physical and mechanical properties of garlic. *Int. J. Food Eng.*, 3(6).
- Bajaj, V. K., 1993, Mechanical year book new highlights. 1367/27, Hari Singh Nalwa Street, Karol Bagh, New Delhi, p. 1-230.
- Bakhtiari, M.R., 2015. Determining physical and aerodynamic properties of garlic to design and develop of a pneumatic garlic clove metering system. *Agric. Eng. Int.: CIGR J.*, 17(1).
- Balasubramanian, D., 2001. PH—Postharvest Technology. *J. Agric. Eng. Res.*, 3(78), pp.291-297.
- Barut, Z.B. and Özmerzi, A., 2004. Effect of different operating parameters on seed holding in the single seed metering unit of a pneumatic planter. *Turk. J. Agric. For.*, 28(6), pp.435-441.
- Bayhan, Y., Kayışoğlu, B., Ülger, P. and Akdemir, B., 2009. A research on the determination of sowing performance of pneumatic precision drill for cereals sowing. *J. Tekirdag Agric. Fac.*, 6(2), pp.131-136.
- Bilanski W K; Collins S H; Chu P Aerodynamic properties of seed grains. *Agri. Engg.*, 1962, 43(4), 216—219
- Borja, A.A., Amongo, R.M.C., Pabico, J.P. and Suministrado, D.C., 2021. Design and evaluation of a machine vision system and mechatronic drive for a pneumatic seed meter for corn. *Philipp. J. Agric. Biosyst. Eng.*, 17(1):49-69.

- Borja, A.A., Amongo, R.M.C., Suministrado, D.C. and Pabico, J.P., 2018, April. A machine vision assisted mechatronic seed meter for precision planting of corn. In 2018 3rd International Conference on Control and Robotics Engineering (ICCRE) (pp. 183-187). IEEE.
- Bozdogan, A.M., 2006. Uniformity of within-row distance in precision seeders: laboratory experiment. *Journal of Applied Sciences*, 6(10), pp.2281-2286.
- Cao, X., Wang, Q., Li, H., He, J., Lu, C., Xu, D. and Wang, X., 2023. Design and experiment of pneumatic pressure control device for no-till planter. *Int. J. of Agrl. and Bio. Engg.*, 16(3), pp.37-46.
- Cay, A., Kocabiyik, H. and May, S., 2018. Development of an electro-mechanic control system for seed-metering unit of single seed corn planters Part I: Design and laboratory simulation. *Comput. Electron. Agric.*, 144, pp.71-79.
- Cay, A., Kocabiyik, H. and May, S., 2018. Development of an electro-mechanic control system for seed-metering unit of single seed corn planters Part II: Field performance. *Comput. Electron. Agric.*, 145, pp.11-17.
- Cetin, M., Şimşek, E., Akbaş, T. and Özarlan, C., 2010. Physical properties of radish (*Raphanus sativus* L.) seed as a function of moisture content. *Philipp. Agric. Sci.*, 93(3), pp.291-298.
- Chen, Y., Tessier, S. and Irvine, B., 2004. Drill and crop performances as affected by different drill configurations for no-till seeding. *Soil Till. Res.*, 77(2), pp.147-155.
- Cherubin, M.R., Damian, J.M., Tavares, T.R., Trevisan, R.G., Colaço, A.F., Eitelwein, M.T., Martello, M., Inamasu, R.Y., Pias, O.H.D.C. and Molin, J.P., 2022. Precision agriculture in Brazil: The trajectory of 25 years of scientific research. *Agriculture* 12(11), p.1882.
- Coelho, A.L.D.F., de Queiroz, D.M., Valente, D.S. and Pinto, F.A., 2020. Development of a variable-rate controller for a low-cost precision planter. *Appl. Eng. Agric.*, 36(2), pp.233-243.

- Cujbescu, D., Matache, M. and Voicu, G., 2019. Mathematical model for sowing precision estimation of vacuum seed metering device. *UPB Sci. Bull., Series D: Mech. Eng.*, 81(3), pp.225-234.
- Dagar, V., Bansal, E., Murshed, M., Mishra, V., Alvarado, R., Kumar, A. and Anser, M.K., 2020. Stochastic frontier analysis to measure technical efficiency: Evidence from skilled and unskilled agricultural labour in India. *Int. J. Agric. Stat. Sci.* 16(2), pp.647-657.
- Deshpande, S.O., Bal, S., Ojha, T.P., 1993. Physical properties of soybean. *J. Agric. Eng. Res.* 56:89-98.
- Directorate of Pulses Development, 2022. Crop-wise area, production and productivity of pulses from 2010-11 to 2020-21.
- Dixit, A., Mahal, J.S., Manes, G.S., Khurana, R. and Nare, B., 2011. Comparative performance of tractor-operated inclined plate and pneumatic planters. *Agric. Eng. Today*, 35(1), pp.33-37.
- Dizaji, H.Z., Taheri, M.R.Y. and Minaei, S., 2010. Air-jet seed knockout device for pneumatic precision planters. *AMA-Agric. Mech. Asia Afr. Lat. Am.*, 41(1), pp.45-50.
- EL-Sheikha, A.M., Shabrawi, H., El-Salam, A. and Ghazy, M.E., 2019. Investigation an electronic device to complement the common planter feeding device. *J. Soil Sci. Agric. Eng.*, 10(11), pp.665-669.
- Emrah, K.U.Ş., 2021. Evaluation of some operational parameters of a vacuum single-seed planter in maize sowing. *J. Agric. Sci.*, 27(3), pp.327-334.
- Erenstein, O. and Laxmi, V., 2008. Zero tillage impacts in India's rice–wheat systems: a review. *Soil Tillage Res.*, 100(1-2), pp.1-14.
- Fangyan, W.A.N.G., Liang, Y.A.N.G. and Hongti, W.A.N.G., 2022. Design and test of electric driving pneumatic carrot planter in greenhouse. *Nongye Jixie Xuebao/Trans. Chin. Soc. Agric. Mach.*, 53(8).

- FAO et al., 2018. The state of food security and nutrition in the world 2018. Building climate resilience for food security and nutrition. Rome, FAO. Available from: <https://doi.org/10.1109/JSTARS.2014.2300145>
- FAO, 2013. The state of food and agriculture 2013. Rome, Italy. Available from: <https://www.fao.org/publications/sofa/2013/en/>.
- Findura, P., Malaga-Toboła, U., Kwaśniewski, D., Stasiak, M., Gugala, M., Sikorska, A. and Gancarz, M., 2023. Influence of physical properties of sugar beet seeds on the work quality of the seeding mechanism. *Int. Agrophys.*, 37(2), pp.171-178.
- Foqué, D., Biocca, M., Pochi, D., Pulcini, P. and Nuyttens, D., 2018. Comparing two dust drift mitigation strategies to the outcomes of a conventional vacuum based precision drill using in-field validated indoor static tests. *Aspects Appl. Biol.*, 137, pp.285-292.
- Fu, W., An, X. and Zhang, J., 2018. Study on precision application rate technology for maize no-tillage planter in North China Plain. *IFAC-Pap. OnLine*, 51(17), pp.412-417.
- Gao, Nana, Fu, Weiqiang, Meng, Zhijun, Wei, Xueli, Li, You, and Cong, Yue. 2016. Research and experiment on precision seeding control system of maize planter. In *Computer and Computing Technologies in Agriculture IX* (pp. 528-535). Springer International Publishing.
- Gautam, P.V., Kushwaha, H.L., Kumar, A., Khura, T.K. and Sarkar, S.K., 2023. Microcontroller-based low-cost seed metering module retrofit on cultivator.
- Gheorghe, G.V., Mateescu, M., Persu, C. and Gageanu, I., 2018. Theoretical simulation of air circulation inside cyclone mounted at exhaust outlet of pneumatic seed drill to optimize it. *Eng. Rural Dev.*, pp.813-817.
- Grover, D.K. and Sharma, T., 2011. Alternative resources conservative technologies in agriculture: impact analysis of zero-tillage technology in Punjab. *Indian J. Agric. Res.*, 45(4), pp.283-290.

- Gupta, P., Kapuriya Rohitkumar, L. and Yadav, R., 2017. Tractor air intake pressure use in pneumatic planter. *Int. J. of Advan. Scie. Res. and Manag.*, 2, pp 1-5.
- Harshavardhan, K., Sivakumar, S.S., Gunasekar, J.J., Albert, V.A. and Padmanathan, P.K., 2020. Design of seeder in relation to the physical and frictional properties of black gram varieties. *Curr. J. Appl. Sci. Technol.*, 39(36), pp.29-37.
- He, X., Cui, T., Zhang, D., Wei, J., Wang, M., Yu, Y., Liu, Q., Yan, B., Zhao, D. and Yang, L., 2017. Development of an electric-driven control system for a precision planter based on a closed-loop PID algorithm. *Comput. Electron. Agric.*, 136, pp.184-192.
- Hemathilake, D.M.K.S. and Gunathilake, D.M.C.C., 2022. Agricultural productivity and food supply to meet increased demands. In *Future Foods* (pp. 539-553). Academic Press.
- Heyns, A. J. (1989). Techniques for the evaluation of precision planters. In *Land and Water Use*, Dodd & Grace (Editors). Balkema, Rotterdam.
- Hoque, M.A., Hossain, M.M., Ziauddin, A.T.M., Krupnik, T.J. and Gathala, M.K., 2021. Furrow design for improving crop establishment of two-wheel tractor operated strip tillage planters in loam and clay loam soils.
- Ibrahim, E.J., Liao, Q., Wang, L., Liao, Y. and Yao, L., 2018. Design and experiment of multi-row pneumatic precision metering device for rapeseed. *Int. J. Agric. Biol. Eng.*, 11(5), pp.116-123.
- Innoti, I.K. and Namikawa, K., 1990. Electronically-controlled pneumatic precision planter (Part 1) Electronic seed sensing and evaluation of metering uniformity. *J. Japan Soc. Agric. Mach.*, 52(6), pp.35-43.
- Inoti, I.K. and Namikawa, K., 1991. Electronically-controlled pneumatic precision planter (Part 2) Solenoid operated seed metering. *J. Jpn. Soc. Agric. Mach.*, 53(3), pp.67-73.



- Ismail, Z.E., 2008. Developing the metering unit of the pneumatic planter 2-The injection planting seed. *J. Soil Sci. Agric. Eng.*, 33(10), pp.7317-7330.
- Jayan, P.R. and Kumar, V.J.F., 2006. Planter design in relation to the physical properties of seeds. *J. Trop. Agric.*, 42, pp.69-71.
- Jiajia, Y., Yitao, L., Jinling, C., Song, Y. and Qingxi, L., 2014. Simulation analysis and match experiment on negative and positive pressures of pneumatic precision metering device for rapeseed. *Int. J. Agric. Biol. Eng.*, 7(3), pp.1-12.
- Jin, X., Li, Q., Zhao, K., Zhao, B., He, Z. and Qiu, Z., 2019. Development and test of an electric precision seeder for small-size vegetable seeds. *Int. J. Agric. Biol. Eng.*, 12(2), pp.75-81.
- Jing, H., Zhang, D., Wang, Y., Yang, L., Fan, C., Zhao, H., Wu, H., Zhang, Y., Pei, J. and Cui, T., 2020. Development and performance evaluation of an electro-hydraulic downforce control system for planter row unit. *Comput. Electron. Agric.*, 172, p.105073.
- Johnson, G.R., Slocombe, J.W., Domann, T.A. and Hofmeister, K.M., 1991. Laboratory equipment for teaching planter technology. *Appl. Eng. Agric.*, 7(1), pp.21-24.
- Kamel, O.M., El-Iragi, M. and Metwaly, M., 2003. Operating factors affecting using pneumatic seed drill for sowing wheat. *Misr J. Ag. Eng.*, 20(3), pp.767-782.
- Kamgar, S. and Eslami, M.J., 2012. Design, development and evaluation of a mechatronic transmission system for upgrading performance of a row crop planter. In 2012 Dallas, Texas, July 29-August 1, 2012 (p. 1). *Am. Soc. Agric. Biol. Eng.*
- Karayel, D. and Özmerzi, A., 2008. Evaluation of three depth-control components on seed placement accuracy and emergence for a precision planter. *Appl. Eng. Agric.*, 24(3), pp.271-276.

- Karayel, D. and Šarauskis, E., 2011. Effect of down force on the performance of no-till disc furrow openers for clay-loam and loamy soils. *Agric. Eng. Res. Pap.*, 43(3), pp.16-24.
- Karayel, D., 2009. Performance of a modified precision vacuum seeder for no-till sowing of maize and soybean. *Soil Till. Res.*, 104(1), pp.121-125.
- Karayel, D., Barut, Z.B. and Özmerzi, A., 2004. Mathematical modelling of vacuum pressure on a precision seeder. *Biosyst. Eng.*, 87(4), pp.437-444.
- Karayel, D., Hacıyusufoğlu, A.F., Çanakci, M. and Topakci, M., 2020. Performance of a large seed vacuum planter for bare and pelleted onion seeds. *Mediterr. Agric. Sci.*, 33(2), pp.253-258.
- Kaspar, T.C. and Erbach, D.C., 1998. Improving stand establishment in no-till with residue-clearing planter attachments. *Trans. ASAE-Am. Soc. Agric. Eng.*, 41(2), pp.301-306.
- Katchman and Smith, 1995, Alternative measures of accuracy in plant spacing for planter using single seed metering. *Trans. American Soc. Agril. Engg.*, 38(2): 379-387.
- Kaur, B., Dimri, S., Singh, J., Mishra, S., Chauhan, N., Kukreti, T., Sharma, B., Prakash, S., Arora, S., Uniyal, D. and Agrawal, Y., 2023. Insights into the harvesting tools and equipment's for horticultural crops: From then to now. *J. Agric. Food Res.*, p.100814.
- Kepner, R. A., Bainer, R. and Barger, E. L., 1987, Principles of farm machinery. CBS Publishers and Distributors, New Delhi. p. 1-340.
- Khambalkar, V.P., Karale, D.S. and Kankal, U.S., 2014. Evaluation of self propelled pneumatic planter for rain fed crops. *Int. J. Agric. Eng.*, 7(1), pp.225-228.
- Khura, T.K., Lande, S.D., HLKushwaha, P.K.S., Parray, R.A., & Chandra, R., 2018. Improved equipment and technologies for lentil cultivation in India. In

*Scientific Lentil Production* (pp. 579-597). Satish Serial Publishing House, New Delhi.

Khurmi, R. S. and Gupta, J. K., 2003, Text book of machine design. Eurasian publishing House (Pvt.) Ltd., Ram Nagar, New Delhi, India. p. 1-280.

Kiani Deh Kiani, M., Minaei, S., Maghsoudi, H., Ghasemi Varnamkhashti, M., (2008). Moisture dependent physical properties of red bean (*Phaseolus vulgaris* L) grains. *Int. Agrophysics* 22: 231-237.

Koley, S., Bhatt, Y.C., Singh, G., Joshi, S. and Jain, H.K., 2017. Development of electronic metering mechanism for precision planting of seeds. *Int. J. Curr. Microbiol. Appl. Sci.*, 6, pp.3481-3487.

Krishna, K.R., 2010. Agroecosystems of South India: nutrient dynamics, ecology and productivity. Universal-Publishers.

Krutz, G., Thompson, L., and Paul, C. 1984. Design of agricultural machinery. John Wiley and Sons. Singapore. pp 245-255.

Kryuchin, N.P. and Gorbachev, A.P., 2021, November. Improvement of the technological process of sowing sunflower seeds with a pneumatic seed planter. In *IOP Conf. Ser.: Earth Environ. Sci.* (Vol. 845, No. 1, p. 012136). IOP Publishing.

Kumar, R., Adamala, S., Rajwade, Y.A. and Singh, H.V., 2015. Performance evaluation of a tractor-mounted pneumatic planter for sorghum in dryland. *Afr. J. Agric. Res.*, 10(39), pp. 3767-3772.

Kumar, S. T., Sankaranarayanan, K. and Annamalai, S.J.K., 2020. Optimization of functional components of the developed planters for high-density cotton.

Kumar, S., Gopinath, K.A., Sheoran, S., Meena, R.S., Srinivasarao, C., Bedwal, S., Jangir, C.K., Mrunalini, K., Jat, R. and Praharaj, C.S., 2023. Pulse-based cropping systems for soil health restoration, resources conservation, and nutritional and environmental security in rainfed agroecosystems. *Front. Microbiol.* 13, p.1041124.

- Kuş, E. and Yıldırım, Y., 2021. Optimization of the shoe furrow openers designed in different heights for vacuum single-seed planter. *Pak. J. Agric. Sci.*, 58(2).
- Kuş, E., 2021. Field-scale evaluation of parameters affecting planter vibration in single seed planting. *Meas.*, 184, p.109959.
- Lahai, M.K., Kabba, V.T. and Mansaray, L.R., 2022. Impacts of land-use and land-cover change on rural livelihoods: Evidence from eastern Sierra Leone. *Appl. Geogr.* 147, p.102784.
- Li, B., Ahmad, R., Qi, X., Li, H., Nyambura, S.M., Wang, J., Chen, X. and Li, S., 2021. Design evaluation and performance analysis of a double-row pneumatic precision metering device for brassica chinensis. *Sustainability*, 13(3), p.1374.
- Li, H., He, J., Wang, C., Yang, W., Lin, H., Wang, Q., Yang, H. and Tan, L., 2023. Research progress on the development of the planter unit for furrowing control and the depth measurement technology. *Appl. Sci.*, 13(21), p.11884.
- Li, H., He, J., Wang, C., Yang, W., Lin, H., Wang, Q., Yang, H. and Tan, L., 2023. Research Progress on the Development of the Planter Unit for Furrowing Control and the Depth Measurement Technology. *Applied Sciences*, 13(21), p.11884.
- Li, H., Liu, H., Zhou, J., Wei, G., Shi, S., Zhang, X., Zhang, R., Zhu, H. and He, T., 2021. Development and first results of a no-till pneumatic seeder for maize precise sowing in Huang-Huai-Hai plain of China. *Agriculture*, 11(10), p.1023.
- Li, K., Li, S., Ni, X., Lu, B. and Zhao, B., 2023. Analysis and experimental of seeding process of pneumatic split seeder for cotton. *Agriculture*, 13(5), p.1050.
- Li, Y., Bai, Y., Zhang, X. and Xie, F., 2023. Structural design and simulation analysis of a dual-row pneumatic vegetable precision planter. *Processes*, 11(6), p.1803.

- Li, Y., Xiantao, H., Tao, C., Dongxing, Z., Song, S., Zhang, R. and Mantao, W., 2015. Development of mechatronic driving system for seed meters equipped on conventional precision corn planter. *Int. J. Agric. Biol. Eng.*, 8(4), pp.1-9.
- Li, Z., Wu, J., Du, J., Duan, D., Zhang, T. and Chen, Y., 2023. Experimenting and optimizing design parameters for a pneumatic hill-drop rapeseed metering device. *Agronomy*, 13(1), p.141.
- Liang, Z., Zhang, D., Yang, L., Cui, T. and Hao, Y., 2015. Experimental study on motor driven pneumatic precision seed-metering device for maize. In 2015 ASABE Annual International Meeting (p. 1). *Am. Soc. Agric. Biol. Eng.*
- Lijing, L., Hui, Y. and Shaochun, M., 2016. Experimental study on performance of pneumatic seeding system. *Int. J. Agric. Biol. Eng.*, 9(6), pp.84-90.
- Liny, P., Manish, S.K. and Shashikala, M., 2013. Geometric and gravimetric characteristics of black gram. *Int. J. of Develop. Res.*, 3(9), pp.13-16.
- Liu, Q., Cui, T., Zhang, D., Yang, L., Wang, Y., He, X. and Wang, M., 2018. Design and experimental study of seed precise delivery mechanism for high-speed maize planter. *Int. J. Agric. Biol. Eng.*, 11(4), pp.81-87.
- Liu, R., Liu, Z., Zhao, J., Lu, Q., Liu, L. and Li, Y., 2022. Optimization and experiment of a disturbance-assisted seed filling high-speed vacuum seed-metering device based on DEM-CFD. *Agriculture*, 12(9), p.1304.
- Liu, W., Zhao, M., Wang, W. and Zhao, S., 2010. Theoretical analysis and experiments of metering performance of the pneumatic seed metering device. *Trans. Chin. Soc. Agric. Eng.*, 26(9), pp.133-138.
- Liu, Z., Liu, L., Yang, X. and Zhao, Z., 2016. Design and experiment of no-till precision planter for corn. *Trans. Chin. Soc. Agric. Eng.*, 32(1), pp.1-6.
- Losavio, G., 2010. MA/AG extends pneumatic precision planter range with Precisa. *Mondo Macchina*, 19(3/4), pp.32-33.

- Madhu Kumar, D.M. 2017. Design, development and testing of a tractor drawn semi-automatic rhizome planter for ginger and turmeric. M.Tech. (Ag. Engg.) thesis, Kerala Agricultural University.
- Maduako JN, Hamman M. Determination of some physical properties of three groundnut varieties. *Nigerian J. Technol.* 2005;24(2):12-28.
- Maheshwari, T.K. and Varma, M.R., 2007. Performance study of pneumatic planter for pea. *Agric. Eng. Today*, 31(3and4), pp.39-42.
- Maleki, M., Hosein Minekhati, H. and Zareei, S., 2020. Design, development and evaluation of a pneumatic planter for sunflower and sugar beet intercropping. *Iranian J. Biosyst. Eng.*, 51 Borja (2), pp.273-283.
- Mandal, S., Kumar, G.P., Tanna, H. and Kumar, A., 2018. Design and evaluation of a pneumatic metering mechanism for power tiller operated precision planter. *Curr. Sci.*, 115(6), pp.1106-1114.
- Mangus, D.L., Sharda, A., Flippo, D., Strasser, R. and Griffin, T., 2017. Development of high-speed camera hardware and software package to evaluate real-time electric seed meter accuracy of a variable rate planter. *Comput. Electron. Agric.*, 142, pp.314-325.
- Manoharan, M., 2018. A comprehensive study on physical properties of black gram and green gram for developing a planter. *Int. J. Agric. Sci. Res.*, 8(6), pp.71-74.
- Meena, B.P., Shirale, A.O., Dotaniya, M.L., Jha, P., Meena, A.L., Biswas, A.K. and Patra, A.K., 2016. Conservation agriculture: a new paradigm for improving input use efficiency and crop productivity. In *Conservation agriculture: an approach to combat climate change in Indian Himalaya* (pp.39-69).
- Miller, A., 2005. 15 Tetrazolium Testing for Flower Seeds. *Flower Seeds: Biology and Technology*, p.299.
- Mohsenin, N.N. 1970. *Physical Properties of Plant and Animal Materials*. Gordon and Breach Science Publishers, New York.

- Mohsenin, N.N., (1986). *Physical Properties of Plant and Animal Materials*, 2nd Edition. Gordon and Breach Science Publishers, New York.
- Molin, J.P., Bashford, L.L., Von Bargen, K. and Leviticus, L.I., 1998. Design and evaluation of a punch planter for no-till systems. *Trans. ASAE*, 41(2), pp.307-314.
- Molotoks, A., Smith, P. and Dawson, T.P., 2021. Impacts of land use, population, and climate change on global food security. *Food Energy Secur.* 10(1), p.e261.
- Moreno, F.G., Zimmermann, G.G., Jasper, S.P., da Silva Ferraz, R. and Savi, D., 2023. Sensors installation position and its interference on the precision of monitoring maize sowing. *Smart Agric. Technol.*, 4, p.100150.
- Munde, A. V. 1999. Effect of moisture content on gravimetric properties of black gram. *J. Maharashtra Agric. Univ.*, 22(3): 833-835.
- Nag, P.K., Gite, L.P., Nag, P.K. and Gite, L.P., 2020. Farm mechanization: Nature of development. In *Human-Centered Agriculture: Ergonomics and Human Factors Applied* (pp.149-171).
- Nath, C.P., Kumar, N., Dutta, A., Hazra, K.K., Praharaj, C.S., Singh, S.S. and Das, K., 2023. Pulse crop and organic amendments in cropping system improve soil quality in rice ecology: Evidence from a long-term experiment of 16 years. *Geoderma* 430, p.116334.
- Nithiyanandham, T., Rajasankar, M., Suresh, S. and Dinesan, D., 2018. Pulses separator machine. *Manage. Int. J. Plant Tech. Manage.* 9(2), pp.95-104.
- Nunes, M.R., van Es, H.M., Schindelbeck, R., Ristow, A.J. and Ryan, M., 2018. No-till and cropping system diversification improve soil health and crop yield. *Geoderma*, 328, pp.30-43.
- Osadare, T. and Manuwa, S.I., 2019. Performance evaluation of a pulse planter developed for conservation agriculture. *J. Agric. Vet. Sci.*, 12(6), pp.15-21.

- Pandey, M.M., 2004. Present status and future requirements of farm equipment for crop production. Central Institute of Agricultural Engineering, Bhopal, 24, pp.69-113.
- Panning, J.W., Kocher, M.F., Smith, J.A. and Kachman, S.D., 2000. Laboratory and field testing of seed spacing uniformity for sugarbeet planters. *Appl. Eng. Agric.*, 16(1), pp.7-13.
- Pareek, C.M., Tewari, V.K. and Machavaram, R., 2023. Multi-objective optimization of seeding performance of a pneumatic precision seed metering device using integrated ANN-MOPSO approach. *Engineering Applications of Artificial Intelligence*, 117, p.105559.
- Pradhan, N.C., Sahoo, P.K., Kushwaha, D.K., Mani, I., Srivastava, A., Sagar, A., Kumari, N., Sarkar, S.K. and Makwana, Y., 2021. A novel approach for development and evaluation of LiDAR navigated electronic maize seeding system using check row quality index. *Sensors*, 21(17), p.5934.
- Pradhan, R.C., Said, P.P. and Singh, S., 2013. Physical properties of bottle gourd seeds. *Agr. Engg. Int.: CIGR J.*, 15(1), pp.106-113.
- Qinghui, L., Wenpeng, M., Wei, S., Ziwu, H. and Jinlong, X., 2016. Design and experiment of pneumatic disc seed-metering device for mini-tuber. *Trans. Chin. Soc. Agric. Mach. (Nongye Jixie Xuebao)*, 47(12).
- Rahmati, M.H., Mohammadi Gol, R., Saracheh, H. and Ruhi, A.V., 2005. Modification and comparison of tomato pneumatic planter with mechanical planter.
- Rajaiah, P., Mani, I., Parray, R.A., Lande, S.D., Kumar, A. and Vergese, C., 2020. Design and development of precision planter for paddy direct seeding. *J. Agric. Eng.*, 57(4), pp.302-314.
- Rajan, P. and Sirohi, N.P.S., 2012, July. A low-cost precision pneumatic planter for vegetables studies and development. In *Proceedings of International Conference of Agricultural Engineering, Valencia, Spain* (pp. 8-12).



- Ramesh, M.B., Veerangouda, M., Reddy, B.S., Anantachar, M. and Sharanagouda, H., 2017. Simulation of design and operational parameters of pneumatic seed planter for cotton using ANSYS software. *Agric. Eng. Today*, 41(4), pp.37-45.
- RNAM. 1991. *Agricultural machinery design data handbook, seeders and planter*. Ec. and Soci. Commis. Asia and the Pacific: 17-20.
- Sani, A., Mohammed, U., Saleh, A. and Yunusa, S., 2021. Development and performance evaluation of a single-row manually operated grain planter. *Niger. J. Sci. Res.*, 20(5), pp.582-588.
- Sarauskis, E., Vaiciukevicius, E., Romaneckas, K., Sakalauskas, A. and Barauskaite, R., 2009. Economic and energetic evaluation of sustainable tillage and cereal sowing technologies in Lithuania. *Rural Dev.*, 4(1), pp.280-285.
- Satti, Y.H., Liao, Q., Yu, J. and He, D., 2013. Dynamic analysis for kernel picking up and transporting on a pneumatic precision metering device for wheat. *Agricultural Engineering International: CIGR Journal*, 15(2), pp.95-100.
- Senger, S. M., 2002, *Design and development of animal drawn seeder for rice cum green manure crops for cultivation system*. M. Tech. Thesis, Indira Gandhi Agric. Uni. Raipur, Chhattisgarh.
- Shah, K., Alam, M.S., Nasir, F.E., Qadir, M.U., Haq, I.U. and Khan, M.T., 2022. Design and performance evaluation of a novel variable rate multi-crop seed metering unit for precision agriculture. *IEEE Access*, 10, pp.133152-133163.
- Sharma, D.N., and Mukesh, S., 2008. *Principles and problems, Farm Machinery Design*. Jain brothers publications.
- Sharon, M.E.M., Abirami, C.K., Alagusundaram, K. and RPS, J.A., 2015. Moisture dependent physical properties of black gram. *Agric. Eng. Int.: CIGR J.*, 17(1).

- Shearer, S.A. and Pitla, S.K., 2013. Precision planting and crop thinning. In *Automation: The Future of Weed Control in Cropping Systems* (pp. 99-124). Dordrecht: Springer Netherlands.
- Shi, L., Zhao, W., Sun, W., Li, R. and Sun, B., 2017. Parameters optimization of speed compensation mechanism of electric driving maize planter with dibbling on membrane. *Trans. Chin. Soc. Agric. Mach. (Nongye Jixie Xuebao)*, 48(8).
- Shi, L., Zhao, W., Sun, W., Li, R., Xin, B. and Dai, F., 2017. Development and experiment of electric driving insert hill-drop planter on film for plot corn. *Trans. Chin. Soc. Agric. Eng.*, 33(4), pp.32-38.
- Shi, Y., Wang, X., Hu, Z., Gu, F., Wu, F. and Chen, Y., 2021. Optimization and experiment on key structural parameters of no-tillage planter with straw-smashing and strip-mulching. *Int. J. Agric. Biol. Eng.*, 14(3), pp.103-111.
- Shinde, G.U., Mandal, S., Ghosh, P.K., Bhalerao, S., Kakade, O., Motapalukula, J. and Das, A., 2023. Farm mechanization. In *Trajectory of 75 Years of Indian Agriculture After Independence* (pp. 475-496). Singapore: Springer Nature Singapore.
- Shinde, P.R., Lende, A.B., Rane, S.V., Nawale, S.A., Patwardhan, M.S. and Gharate, L.V., 2009. Development and functional test of electronic metering mechanism for bullock drawn Jyoti Multicrop planter. *Int. J. Agric. Environ. Biotechnol.*, 2(3), pp.305-309.
- Sial, F. S., and S. P. E. Persson. 1984. Vacuum nozzle design for seed metering. *Transactions of the ASAE*, 27(1): 688–696.
- Siddique, K.H., Johansen, C., Turner, N.C., Jeuffroy, M.H., Hashem, A., Sakar, D., Gan, Y. and Alghamdi, S.S., 2012. Innovations in agronomy for food legumes. A review. *Agron. Sustain. Dev.*, 32, pp.45-64.
- Singh, A.K., 2014. Probable agricultural biodiversity heritage sites in India: XXI. The Malabar region. *Asian Agri-Hist.*, 18(4), pp.311-341.

- Singh, K.K. and Goswami, T.K., 1996. Physical properties of cumin seed. *J. Agric. Eng. Res.*, 64(2), pp.93-98.
- Singh, R. C., Singh, G. and Saraswat, D. C., 2005, Optimization of design and operational parameters of a pneumatic seed metering device for planting cotton seeds. *Biosys. Engg.*, 92(4): 429-438.
- Singh, R.P., 2013. Status paper on pulses. Government of India Ministry of Agriculture, Department of Agriculture & Cooperation, Bhopal, Madhya Pradesh, 215.
- Singh, S.N., Sah, A.K., Prakash, O., Singh, R.K. and Singh, V.K., 2010. Assessing the impact of zero tilled wheat growing in rice (*Oryza Sativa L.*)–wheat (*Triticum Aestivum L.*) cropping systems: the case of central Uttar Pradesh in the Indo-Gangetic Plain. *Outlook Agric.*, 39(3), pp.197-202.
- Singh, S.P. and Singh, S., 2021. Farm power availability and its perspective in Indian agriculture. *RASSA J. Sci. Soc.*, 3(2), pp.114-126.
- Singh, T.P. and Mane, D.M., 2011. Development and laboratory performance of an electronically controlled metering mechanism for okra seed. *AMA-Agric. Mechanization Asia Africa Lat. Am.*, 42(2), p.63.
- SK, P., JB, B. and BK, Y., 2021. Optimization of the design and operational parameters of planter for vegetable pigeon pea (*Cajanus cajan L. Millsp.*) seed. *INMATEH-Agric. Eng.*, 63(1).
- Sonawane, A.V., Rajwade, Y.A., Singh, D., Desai, S. and Rajurkar, G.B., 2014. Moisture dependent physical properties of horse gram. *Int. Agric. Eng. J.*, 23(2), pp.7-14.
- Song, S., Dongxing, Z., Li, Y., Tao, C., Rui, Z. and Xiaowei, Y., 2014. Design and experiment of pneumatic maize precision seed-metering device with combined holes. *Trans. Chin. Soc. Agric. Eng.*, 30(5).
- Soyoye, B.O., 2020. Design and fabrication of an electrically powered maize planter. *J. Eng. Stud. Res.*, 26(3), pp.204-211.

- Soyoye, B.O., 2020. Development of the instrumentation unit of a motorized precision planter. *Eur. J. Eng. Technol. Res.*, 5(4), pp.403-407.
- Srivastava, A. K., Carroll, E. G. and Roger, P. R., 2003, Engineering principles of agricultural machines. ASAE Text book No. 6. American Soc. Agril. Engg., 2950, Viles Road, St. Joseph Michigan-4, USA, p. 1-190.
- Strasser, R., Badua, S., Sharda, A., Mangus, D. and Haag, L., 2019. Performance of planter electric-drive seed meter during simulated planting scenarios. *Appl. Eng. Agric.*, 35(6), pp.925-935.
- Tang, H., Xu, F., Xu, C., Zhao, J. and Wang, Y.J., 2023. The influence of a seed drop tube of the inside-filling air-blowing precision seed-metering device on seeding quality. *Comput. Electron. Agric.*, 204, p.107555.
- Theertha, D.P., Sujeetha, J.A.R.P., Abirami, C.K. and Alagusundaram, K., 2014. Effect of moisture content on physical and gravimetric properties of black gram (*Vigna mungo* L.). *Int. J. Advancements Res. Technol.*, 3(3), pp.97-104.
- Thiet, N.X. and Thong, N.C., 2023. Effects of the main operating parameters on seed holding in a seeder-pneumatic metering device with an inclined plate for maize. *Vietnam J. Agric. Sci.*, Vol. 21, No. 2: 197-206.
- Topakci, M., Karayel, D., Canakci, M., Furat, S. and Uzun, B., 2011. Sesame hill dropping performance of a vacuum seeder for different tillage practices. *Appl. Eng. Agric.*, 27(2), pp.203-209.
- Vaishnavi, D., Carolin Rathinakumari, G. Senthil Kumaran, and Edukondalu Lingathoti, 2018. "Physical and engineering properties of vegetable seeds relevant for development of protray vacuum seeder for vegetable nursery." In National Conference on Digital and Engineering Technologies for Precision Agriculture and Value Addition.
- Varshney, A.C., 2005. Data book for agricultural machinery design.

- Vashishth, R., Semwal, A.D., Pal Murugan, M., Govind Raj, T. and Sharma, G.K., 2020. Engineering properties of horse gram (*Macrotyloma uniflorum*) varieties as a function of moisture content and structure of grain. *J. Food Sci. Technol.*, 57(4), pp.1477-1485.
- Vasylykivska, K., Vasylykivskyi, O., Leshchenko, S., Sviren, M. and Moroz, M., 2020. Identification of parameters of pneumatic and mechanical seeding device under the influence of vacuum. *Bulg. J. Agric. Sci.*, 26(5), pp.1091-1094.
- Verma, S.R., 2006. Impact of agricultural mechanization on production, productivity, cropping intensity income generation and employment of labour. *Status of Farm Mechanization in India*, 2006, pp.133-53.
- Vivek, P., Duraisamy, V.M. and Kavitha, R., 2019. Development of a gripper for robotic picking and transplanting operation of protrait grown vegetable seedlings. *Innovative Farming*, 4(2), pp.097-104.
- Wang, C., Yang, H., He, J., Kang, K. and Li, H., 2023. The influence of seed variety and high seeding speed on pneumatic precision seed metering. *Eng. Agric.*, 43, p.e20220183.
- Wang, G., Sun, W., Zhang, H., Liu, X., Li, H. and Yang, X., 2020. Research on a kind of seeding-monitoring and compensating control system for potato planter without additional seed-metering channel. *Comput. Electron. Agric.*, 177, p.105681.
- Wang, L., Liao, Y., Wei, Y. and Liao, Q., 2014. Seed-grain sucking and metering test based on pneumatic precision metering device. *J. Hunan Agric. Univ.*, 40(6), pp.655-659.
- Wang, W., Wu, K., Zhang, Y., Wang, M., Zhang, C. and Chen, L., 2022. The development of an electric-driven control system for a high-speed precision planter based on the double closed-loop fuzzy PID algorithm. *Agronomy*, 12(4), p.945.

- Wei, S., Fu-lin, W., Hai-tao, C. and Qing-hui, L., 2013. Vacuum and air flow for 2QXP-1 vacuum precision seed metering. *J. Northeast Agric. Univ. (English Ed.)*, 20(2), pp.61-64.
- Xia, H., Zhen, W., Liu, Y. and Zhao, K., 2021. Optoelectronic measurement system for a pneumatic roller-type seeder used to sow vegetable plug-trays. *Meas.*, 170, p.108741.
- Xia, L., Wang, X., Geng, D. and Zhang, Q., 2011. Performance monitoring system for precision planter based on MSP430-CT171. In *Computer and Computing Technologies in Agriculture IV: 4th IFIP TC 12 Conference, CCTA 2010, Nanchang, China, October 22-25, 2010, Selected Papers, Part II 4* (pp. 158-165). Springer Berlin Heidelberg.
- Xiaohui, Z.H.A.N.G., Yongzhen, W., Li, Z., Chuanjie, P.E.N.G. and Guiju, F.A.N., 2018. Design and experiment of wheat pneumatic centralized seeding distributing system. *Nongye Jixie Xuebao/Transactions of the Chinese Society of Agri. Mach.*, 49(3).
- Xing, H., Wang, Z., Luo, X., He, S. and Zang, Y., 2020. Mechanism modeling and experimental analysis of seed throwing with rice pneumatic seed metering device with adjustable seeding rate. *Comput. Electron. Agric.*, 178, p.105697.
- Xu, J., Hou, J., Wu, W., Han, C., Wang, X., Tang, T. and Sun, S., 2022. Key structure design and experiment of air-suction vegetable seed-metering device. *Agronomy*, 12(3), p.675.
- Yan, B., Gao, N. and Meng, Z., 2020, June. Design and test of a gravity-assisted vacuum seed-meter for maize. In *IOP Conf. Ser.: Earth Environ. Sci.* (Vol. 512, No. 1, p. 012093). IOP Publishing.
- Yanni, S.F., De Laporte, A., Rajsic, P., Wagner-Riddle, C. and Weersink, A., 2021. The environmental and economic efficacy of on-farm beneficial management practices for mitigating soil-related greenhouse gas emissions in Ontario, Canada. *Renew. Agric. Food Syst.*, 36(3), pp.307-320.

- Yasir, S.H., Liao, Q., Yu, J. and He, D., 2012. Design and test of a pneumatic precision metering device for wheat. *Agric. Eng. Int.: CIGR J.*, 14(1), pp.16-25.
- Yazgi, A. and Degirmencioglu, A., 2007. Optimisation of the seed spacing uniformity performance of a vacuum-type precision seeder using response surface methodology. *Biosystems engineering*, 97(3), pp.347-356.
- Yu, X., Geng, D., Wang, Q., Liu, Y., Tan, D., Su, G. and He, K., 2019. Design and experiment of pneumatic conveying seeder with no-tillage for simultaneous seeding of wheat seed and fertilizer. In 2019 ASABE Annual International Meeting (p. 1). Am. Soc. Agric. Biol. Eng.
- Yuvaraj, M., Pandiyan, M. and Gayathri, P., 2020. Role of legumes in improving soil fertility status. In *Legume Crops-Prospects, Production and Uses* (pp.16-27).
- Zaidi, M.A., Amjad, N., Mahmood, H.S. and Shah, S.U.S., 2019. Performance evaluation of pneumatic planter for peas planting. *Pak. J. Agric. Sci.*, 56(1).
- Zaki, D.H., Minaei, S. and Yousefzadeh, T.M., 2008. Improvement of vacuum-precision planter by development and application of a pneumatic seed knockout device. pp:219-230.
- Zhan, Z., Yaoming, L., Jin, C. and Lizhang, X., 2010. Numerical analysis and laboratory testing of seed spacing uniformity performance for vacuum-cylinder precision seeder. *Biosyst. Eng.*, 106(4), pp.344-351.
- Zhang, C., Zhang, X., Zheng, Z., Xie, X., Liu, L. and Chen, L., 2022. Numerical simulation and test of the disturbance air suction garlic seed metering device. *Machines*, 10(12), p.1127.
- Zhang, K., Sun, Y., Liu, L., Liu, X. and Zhao, X., 2020. Design and test of variable diameter pneumatic drum type bean seed metering device. *INMATEH-Agric. Eng.*, 60(1).

Zhao, J., Zhang, J., Nian, Y. and Zheng, C., 2020. Design and test of wheat seeder with suction and metering device with cone surface of circular tube. Trans. Chin. Soc. Agric. Mach. (Nongye Jixie Xuebao).

Zulin, Z., Upadhyaya, S. K., Shafii, S. and R. E. Garrett (1991). A hydropneumatic seeder for primed seeds. Trans. ASAE. 34(1): 21–26. Am Soc. Agr. Eng. St Joseph, MI.



### APPENDIX-I

#### Physical properties of black gram (VBN-6) and horse gram (KS-2) seeds

Sl. No.	Parameter	Measurement	Black Gram (VBN-6)	Horse Gram (KS-2)
1.	Length (mm)	Min	2.32	6.02
		Max	3.88	6.27
		Mean	3.12	6.14
		Var	0.234	0.006
		Std Dev	0.484	0.074
2.	Width (mm)	Min	1.99	4.10
		Max	3.65	4.35
		Mean	2.90	4.23
		Var	0.283	0.006
		Std Dev	0.532	0.077
3.	Thickness (mm)	Min	1.56	2.16
		Max	2.07	2.45
		Mean	1.85	2.31
		Var	0.022	0.008
		Std Dev	0.148	0.089
4.	Arithmetic Mean D (mm)	Min	1.95	4.09
		Max	3.20	4.36
		Mean	2.62	4.22
		Var	0.149	0.006
		Std Dev	0.386	0.079
5.	Geometric Mean D (mm)	Min	1.92	3.71
		Max	3.05	4.00
		Mean	2.53	3.86
		Var	0.122	0.008
		Std Dev	0.349	0.087
6.	Aspect Ratio (%)	Min	85.69	67.96
		Max	99.68	69.50

	Mean	92.62	68.88
	Var	16.978	0.215
	Std Dev	4.120	0.464
<b>7. Sphericity (%)</b>	Min	78.34	61.43
	Max	85.12	67.86
	Mean	83.61	63.68
	Var	2.851	3.121
	Std Dev	1.688	1.793
<b>8. Roundness</b>	Min	0.45	0.33
	Max	0.57	0.42
	Mean	0.53	0.38
	Var	0.001	0.001
	Std Dev	0.033	0.035
<b>9. Thousand seed weight (g)</b>		44.2	38.4

## APPENDIX-II

### Engineering properties of black gram (VBN-6) and horse gram (KS-2) seeds

Sl.	Parameter	Black gram (VBN-6)			Horse gram (KS-2)		
		Min	Max	Mean	Min	Max	Mean
1.	<b>Bulk Density</b>	800.00	814.00	806.93	916.00	935.00	925.80
2.	<b>True Density</b>	1428.00	1440.00	1433.50	1380.00	1396.00	1387.93
3.	<b>Porosity</b>	43.08	44.17	43.71	33.62	33.02	33.297
4.	<b>Angle of Repose</b>	25.01	25.31	25.18	23.41	25.06	24.45
5.	<b>Coefficient of friction</b>						
	a) <b>Wood</b>	0.49	0.53	0.52	0.58	0.63	0.61
	b) <b>Galvanized Iron</b>	0.45	0.51	0.47	0.39	0.45	0.42
	c) <b>Aluminium</b>	0.35	0.41	0.38	0.51	0.62	0.58
	d) <b>Mild Steel</b>	0.32	0.37	0.35	0.38	0.49	0.45
	e) <b>Stainless Steel</b>	0.27	0.32	0.29	0.26	0.35	0.31
6.	<b>Terminal Velocity</b>	8.13	8.26	8.21	8.6	8.79	8.68
7.	<b>Drag coefficient</b>	0.63	0.68	0.64	0.54	0.59	0.55

**Appendix- III**

**Filed performance evaluation of the developed planter**

<b>Black gram</b>							
<b>location of encoder</b>	<b>furrow opener type</b>	<b>seed spacing, cm</b>	<b>miss index, %</b>	<b>multiple index, %</b>	<b>QFI, %</b>	<b>precision of spacing, %</b>	<b>Germination %</b>
MS Wheel	Shoe type	14.8	1.2	2.6	96.2	6.16	96
MS Wheel	Shoe type	14.7	1.3	2.5	96.2	6.20	96
MS Wheel	Shoe type	14.8	1.2	2.6	96.2	6.16	95
MS Wheel	Inverted t-type	14.9	1.3	2.7	96	6.12	92
MS Wheel	Inverted t-type	14.8	1.2	2.6	96.2	6.16	92
MS Wheel	Inverted t-type	14.9	1.3	2.7	96	6.12	91
MS Wheel	Stub runner type	14.6	1.3	2.7	96	6.25	87
MS Wheel	Stub runner	14.8	1.2	2.6	96.2	6.16	86
MS Wheel	Stub runner	14.7	1.3	2.7	96	6.20	85
Pneumatic Wheel	Shoe type	12.9	1.2	4	94.8	7.07	96
Pneumatic Wheel	Shoe type	12.8	1.2	3.9	94.9	7.13	97
Pneumatic Wheel	Shoe type	12.8	1.2	4	94.8	7.13	96
Pneumatic Wheel	Inverted t-type	13.2	1.2	4.2	94.6	6.91	93
Pneumatic Wheel	Inverted t-type	13.1	1.3	4.2	94.5	6.96	94
Pneumatic Wheel	Inverted t-type	13.2	1.2	4.3	94.5	6.91	93
Pneumatic Wheel	Stub runner	13.1	1.3	3.7	95	6.96	86
Pneumatic Wheel	Stub runner	13	1.2	3.8	95	7.02	85
Pneumatic Wheel	Stub runner	13.1	1.3	3.7	95	6.96	86

<b>Horse gram</b>							
<b>location of encoder</b>	<b>furrow opener type</b>	<b>seed spacing, cm</b>	<b>miss index, %</b>	<b>multiple index, %</b>	<b>QFI, %</b>	<b>precision of spacing, %</b>	<b>germination %</b>
MS Wheel	Shoe type	9.7	1.5	2.9	95.6	5.92	95
MS Wheel	Shoe type	9.7	1.4	2.8	95.8	5.92	96
MS Wheel	Inverted t-type	9.7	1.6	3.1	95.3	5.92	91
MS Wheel	Stub runner	9.8	1.6	3	95.4	5.86	85
MS Wheel	Inverted t-type	9.6	1.7	3.2	95.1	5.98	92
MS Wheel	Shoe type	9.6	1.5	2.7	95.8	5.98	95
MS Wheel	Inverted t-type	9.8	1.7	3.2	95.1	5.86	91
MS Wheel	Stub runner	9.5	1.5	3.1	95.4	6.04	86
MS Wheel	Stub runner	9.6	1.5	3.2	95.3	5.98	85
Pneumatic Wheel	Shoe type	8.6	1.6	4.1	94.3	6.68	95
Pneumatic Wheel	Inverted t-type	8.7	1.4	4.2	94.4	6.60	92
Pneumatic Wheel	Shoe type	8.4	1.5	4.1	94.4	6.84	96
Pneumatic Wheel	Stub runner	8.6	1.5	4.1	94.4	6.68	85
Pneumatic Wheel	Shoe type	8.5	1.5	4	94.5	6.76	96
Pneumatic Wheel	Stub runner	8.5	1.3	3.9	94.8	6.76	86
Pneumatic Wheel	Inverted t-type	8.6	1.3	4.3	94.4	6.68	93
Pneumatic Wheel	Inverted t-type	8.7	1.4	4.3	94.3	6.60	92
Pneumatic Wheel	Stub runner	8.5	1.3	4.1	94.6	6.76	84

### Appendix- IV

#### Cost economics of developed pneumatic planter with electronic control system

The cost of operation has been worked out based on the following assumptions.

##### Assumptions made,

Initial cost of tractor, ₹.	= 8, 00,000
Initial cost of planter, ₹	= 1,80,000
Annual usage for tractor, h	= 1,000
Annual usage of planter, h	= 250
Total life of tractor, year	= 10
Total life of Planter, year	= 10

---

Average purchase price of a machine = (purchase price + Residual value)/2

#### A. Fixed cost of tractor operated pneumatic no-till pulse planter with electronic control system

Sl. No.	Annual fixed cost	Tractor		Planter	
		Annual	Per hour	Annual	Per hour
1	Depreciation, ₹	$(800000 - 80000) / 10 = 72000$	72.00	$(180000 - 200) / 10 = 16200$	64.8
2	Interest, ₹	$(800000 + 80000) / 2 \times 7 / 100 = 30800$	30.80	$(180000 + 1800) / 2 \times 7 / 100 = 6930$	27.72
3	Housing, @ 1.5% of average purchase price, ₹.	6600	6.6	1485	5.94
4	Taxes @ 1 % of average purchase price, ₹	4400	4.40	990	3.96
5	Insurance, @ 1 % of average purchase price, ₹	4400	4.40	990	3.96
6	Total fixed cost, ₹ h <sup>-1</sup>	118200	118.2	26595	106.38

**Total Fixed Cost Calculation:**

- Tractor: ₹118.2 per hour
- Pneumatic Planter: ₹106.38 per hour
- Combined Fixed Cost: ₹118.2 + ₹106.38 = ₹224.58 per hour

**B. Variable cost of tractor operated pneumatic no-till pulse planter with electronic control system**

Sl. No.	Variable cost	Tractor	Planter
		Per hour	Per hour
1	Fuel, ₹	$5 \times 95.34 = 476.7$	-
2	Oil, ₹ (2.5 % of fuel)	11.92	-
3	Repair and maintenance, ₹	(4 % of the purchase price) = 32	(3 % of the purchase price) = 21.6
4	Wages and labour charges	$750/8 = 93.75$ (@ ₹. 750 per day of 8 h)	-
5	Total Variable cost, ₹ h <sup>-1</sup>	614.37	21.6

**Total Variable Cost Calculation:**

- Tractor: ₹614.37 per hour
- Pneumatic Planter: ₹21.6 per hour
- Combined Variable Cost: ₹614.37 + ₹21.6 = ₹635.97 per hour

**Total Operating Cost Calculation:**

- Total Fixed Cost: ₹224.58 per hour
- Total Variable Cost: ₹635.97 per hour
- Combined Operating Cost: ₹224.58 + ₹635.97 = ₹860.55 per hour

**Planting Operation Cost Using Pneumatic Planter:**

- Operating Cost: ₹860.55 per hour
- Field Capacity: 0.28 hectares per hour

- Cost per Hectare: ₹860.55 / 0.28 = ₹3072 per hectare

### Manual Sowing Cost:

- Cost per Hectare: ₹4054 (Source: Directorate of Economics and Statistics, Department of Agriculture and Farmers Welfare, 2022)

### Cost Savings:

- Saving per hectare: ₹4054 - ₹3072 = ₹982 per hour

### C. Break-even point

$$BEP = \frac{AFC}{CC - OC}$$

Where,

BEP = Break-even point, h yr<sup>-1</sup>

AFC = Annual fixed cost for the machine, ₹. yr<sup>-1</sup>

CC = Custom hiring charge, ₹. h<sup>-1</sup>

OC = Operating cost, ₹. h<sup>-1</sup>

Annual fixed cost for the machine, AFC (₹. yr<sup>-1</sup>)

$$\begin{aligned} &= \text{Annual fixed cost of tractor} + \text{Annual fixed cost of machine} \\ &= (118.2 + 106.38) \times 250 \\ &= 56145 \end{aligned}$$

Custom hiring charges, CC (₹. h<sup>-1</sup>)

$$\begin{aligned} &= (\text{Total operating cost per h} + 25 \text{ per cent overhead} \\ &\quad \text{charges}) \times 25 \text{ per cent profit over new cost} \\ &= (860.55 + (0.25 \times 860.55)) \times 1.25 \\ &= 1344.61 \end{aligned}$$

Variable operating cost, OC (₹. h<sup>-1</sup>) = 614.37 + 21.6 = 635.97

$$BEP = \frac{AFC}{CC - OC} = \frac{56145}{1344.61 - 635.97}$$

**Break-even point = 79.22 h yr<sup>-1</sup>**



#### D. Payback Period

$$PBP = \frac{IC}{ANP}$$

Where,

PBP = Payback period, yr

IC = Initial cost of the machine, ₹.

ANP = Average net annual profit, ₹. yr<sup>-1</sup>

ANP = (CC - OC) × AU

AU = Annual use, h yr<sup>-1</sup>

$$\begin{aligned} \text{Average net annual profit (ANP)} &= (\text{CC} - \text{OC}) \times \text{Annual usage of the machine} \\ &= (1344.61 - 635.97) \times 250 \\ &= ₹. 177160 \end{aligned}$$

Initial cost of the machine (IC) = operational cost of tractor for 250 h + Initial cost of machine

$$\begin{aligned} &= \frac{8,00,000 \times 250}{1000 \times 10} + 1,80,000 \\ &= 2,00,000 \end{aligned}$$

$$PBP (yr) = \frac{IC}{ANP} = \frac{200000}{177160} = 1.13$$

**Payback period = 1.13 year**

Appendix- V

Programming for the electronic control system

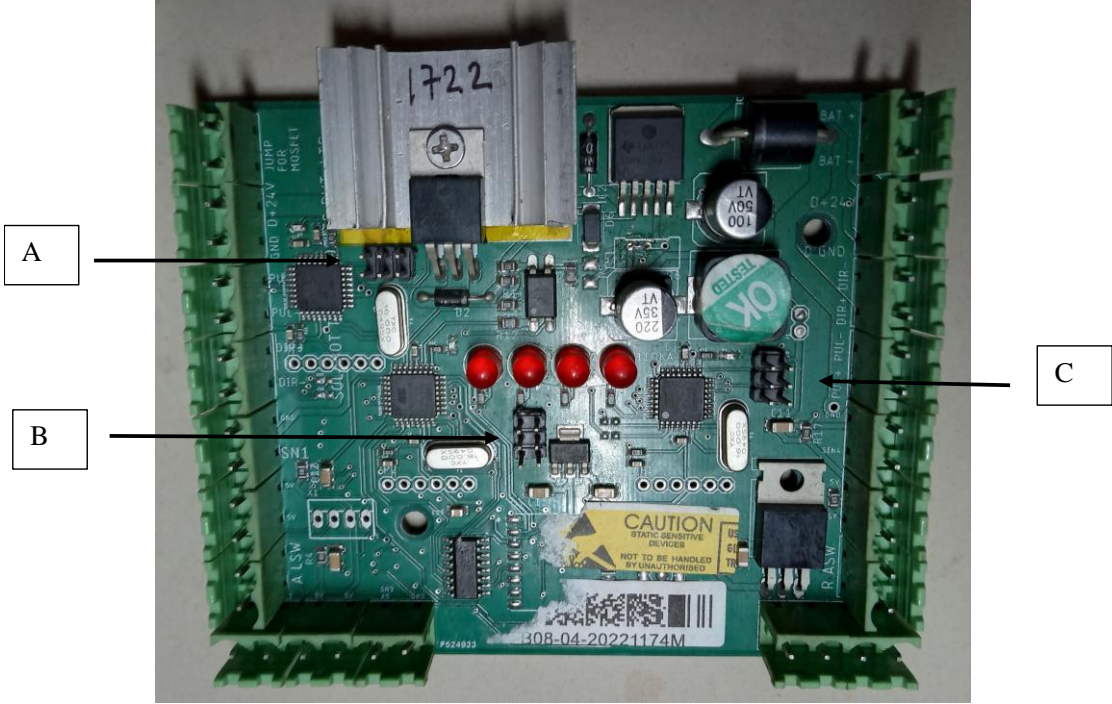


**Fig. I. PCB microcontroller**

Microchip ‘A’ – Brush motor program

Microchip ‘B’ – Main program control

Microchip ‘C’ - Drive motor program

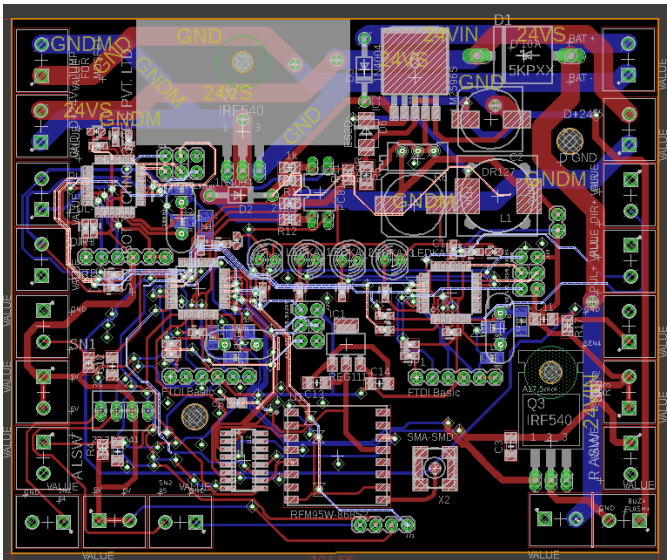


**Fig. II. Design layout of PCB**

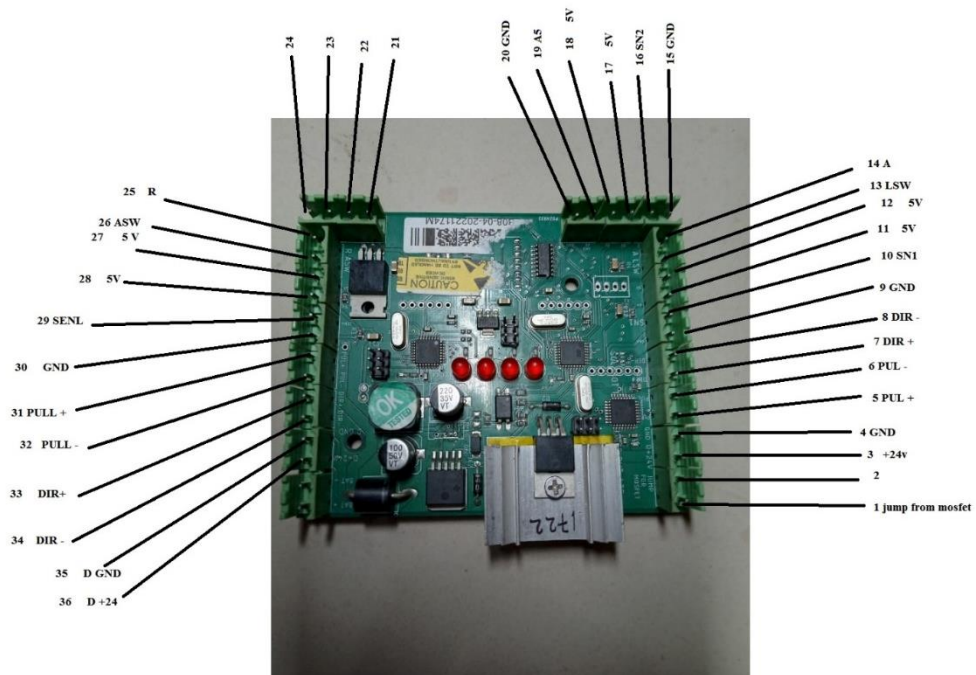


**Fig. III. Pins layout of PCB microcontroller**

### A. I2C Motor Control using Arduino (Upload to microchip 'A')

```

#include <Wire.h>
#define PULS 7
#define DIR_PIN 8
char c;int x;
//float cal=0.01744;//0.01779;
float val;

void setup() {
  Wire.begin(1);
  Wire.onReceive(receiveEvent);
  pinMode(PULS, OUTPUT);
  pinMode(DIR_PIN, OUTPUT);
}

void loop() {
  y:
  while (1 < Wire.available()) {
    c = Wire.read();
    x= Wire.read();
  }
  int cc=485; //385 //609=120 //355=200 //480=150
  //408=175 //407v2s----- speed change
  if(c=='L' || c=='R')
  {
    if(c=='L')

```

```

    {digitalWrite(DIR_PIN, HIGH);

digitalWrite(PULS,HIGH);
delayMicroseconds(1);
digitalWrite(PULS,LOW);
delayMicroseconds(cc);

}
if(c=='R')
    {digitalWrite(DIR_PIN, LOW);

digitalWrite(PULS,HIGH);
delayMicroseconds(1);
digitalWrite(PULS,LOW);
delayMicroseconds(cc);

}
while(c!='z')
    {
    if (1 < Wire.available()) {
c = Wire.read();
x= Wire.read();
if(c=='S')
    {

digitalWrite(PULS,HIGH);
delayMicroseconds(1);
digitalWrite(PULS,LOW);
delayMicroseconds(cc);

c='z';x='z';
goto y;}
    }
digitalWrite(PULS,HIGH);
delayMicroseconds(1);
digitalWrite(PULS,LOW);
delayMicroseconds(cc);
    }
}}

void receiveEvent(int howMany) {
    (void)howMany; // cast unused parameter to void to avoid compiler warning
}

```

In summary, this code controls a stepper motor using I2C commands received from a master device. The motor can be rotated clockwise or counter clockwise, and the speed can be adjusted by changing the value of 'cc'.

## **B. Arduino program to control the complete system with proximity sensor ((Upload to microchip 'B')**

```
#include <Wire.h>
#include <EEPROM.h>
#include <SPI.h>          // include libraries
# define BRUSHCTRL 1
# define DRIVCTRL 2
#define PAYLOAD_SIZE 2
int spd=800;    //previous 275
int spb=275;   //Previous 800
#define FLASH 10
int count,countx,gap;
int p=0;
int q=0;
int spc;
char speedx = 'b';
float vout = 0.0;
float vin = 0.0;
float R1 = 92.5; // resistance of R1 (330K) -see text!
float R2 = 10; // resistance of R2 (10K) - see text!
int value = 0;
#define LEFT true
#define RIGHT false
boolean machine_direction = LEFT;
boolean machine_running = false;
const int timer_rst_time = 3100;
double distance;
float mtr=0;
float mtr1=0;
int seconds = 0;
int updated_minutes;
int updated_hours1;
int updated_hours2;
int updated_seconds;
unsigned long meter1;
unsigned long time;
int total_hours;
void setup() {
  Wire.begin();
  Serial.begin(9600);
  pinMode(FLASH, OUTPUT);
  pinMode(A3, INPUT);
  pinMode(A2, INPUT);
```

```

    pinMode(5, INPUT_PULLUP);
    pinMode(6, INPUT_PULLUP);
    // pinMode(10, INPUT);
    pinMode(7, OUTPUT);
    pinMode(13, OUTPUT);
    digitalWrite(7, LOW);
timer1_init();
    updated_hours1 = EEPROM.read(3);
    updated_hours1 = EEPROM.read(2);
    updated_minutes = EEPROM.read(1);
    updated_seconds = EEPROM.read(0);
    EEPROM.get(10,meter1);
    seconds = 0;
    Serial.write(17);
    delay(100);
    Serial.write(24);
    delay(100);
    Serial.write(12);
    Serial.write("Pneumatic");
    delay(50);
    Serial.write(148);
    Serial.write("Planter");
for (int i=0;i<3;i++)
    {
        digitalWrite(FLASH, 1);digitalWrite(13, 1);
        delay(20);
        digitalWrite(FLASH, 0);digitalWrite(13,0);
        delay(20);
        digitalWrite(FLASH, 1);digitalWrite(13, 1);
        delay(20);
        digitalWrite(FLASH, 0);digitalWrite(13,0);
        delay(20);
    }
delay(1500);
    Serial.write(18);
    delay(10);
    Serial.write(21);
    machine_running = false;
    delay(200);
    Serial.write(17);
    delay(100);
    Serial.write(24);
    delay(100);
    Serial.write(12);;
int total_hours = updated_hours2 * 254 + updated_hours1;
meter1=meter1+((mtr+mtr1)*10);
    value = analogRead(A7);
    delay(200);

```

```

    value = analogRead(A7);
    vout = (value * 5.6) / 1024.0;
    vin = vout / (R2/(R1+R2));
for (int i=0;i<5;i++)
    {
        digitalWrite(FLASH, 1);digitalWrite(13, 1);
        delay(20);
        digitalWrite(FLASH, 0);digitalWrite(13, 0);
        delay(20);
        digitalWrite(FLASH, 1);digitalWrite(13, 1);
        delay(20);
        digitalWrite(FLASH, 0);digitalWrite(13, 0);
        delay(20);}
        delay(2500);
    Serial.write(18);
    delay(10);
    Serial.write(21);
}
void loop()
{ digitalWrite(7, LOW);
delay(50);
autoswitch();
/* if (digitalRead(A2) !=1 && digitalRead(6) != 0 &&machine_running==false )
{
    delay(500);
    if (digitalRead(A2) !=1 && digitalRead(6) != 0 &&machine_running==false)
    {leftw();}}
if (digitalRead(A3)!=1 && digitalRead(5) != 0 &&machine_running==false)
{
    delay(500);
    if (digitalRead(A3)!=1 && digitalRead(5) != 0 &&machine_running==false)
    {rightw();}}*/
if(machine_running==true)
{if(digitalRead(A2)!=1||digitalRead(A3) != 1 )
{
    for(int i=0;i<=50;i++)
    {}
if(digitalRead(A2)!=1||digitalRead(A3) != 1)
{
    stopblink();
    stopmsg();
    machine_running==false;
    delay(1400);digitalWrite(7, HIGH);
    }}}
}
int sec;
ISR(TIMER1_OVF_vect) {
    TCNT1 = timer_rst_time;

```

```

    if(machine_running == true)
    {
seconds++;
    if(seconds >15)
    {
        digitalWrite(FLASH, 1);digitalWrite(13, 1);
    }
    if(seconds >16)
    {
        digitalWrite(FLASH, 0);digitalWrite(13, 0);
        seconds=0;
    }
        updated_seconds++;
    if(updated_seconds>59)
    {
        updated_seconds =0;
        updated_minutes++;
        if(updated_minutes>59)
        {
            updated_minutes =0;
            updated_hours1++;
            if(updated_hours1 > 254)
            {
                updated_hours1 = 0;
                updated_hours2++;
            }
        }
    }
}
//run any if logic here
}
}
void timer1_init() {
    noInterrupts();
    TCCR1A = 0;
    TCCR1B = 0;
    TCNT1 = timer_rst_time;
    TCCR1B |= (1 << CS12);
    TIMSK1 |= (1 << TOIE1);
    sei();
}
void leftw()
{
    digitalWrite(7, LOW);
    startbkink();
    startmsgleft();
    delay(500);
    machine_direction = LEFT;
    machine_running = true;
}

```



```

    delay(50);
    Wire.beginTransmission(BRUSHCTRL);
    Wire.write("L");Wire.write(spb);
    Wire.endTransmission();;
    delay(1500);
    Wire.beginTransmission(DRIVECTRL);
    Wire.write("L");Wire.write(spd);
    Wire.endTransmission();
}
void rightw()
{
    //digitalWrite(7, LOW);
    //startbkink();
    //startmsgright();
    // delay(500);
    machine_direction = RIGHT;
    machine_running = true;
    delay(10);
    Wire.beginTransmission(BRUSHCTRL);
    Wire.write("R");Wire.write(spb);
    Wire.endTransmission();;
    //delay(1500);
    Wire.beginTransmission(DRIVECTRL);
    Wire.write("R");Wire.write(spd);
    Wire.endTransmission();;
}
void autoswitch()
{xxx:
    if(machine_running==false)
    {
        /*if(digitalRead(6)!=1&&machine_direction == LEFT)
        {
            while(digitalRead(6)!=1&&machine_direction == LEFT)
            {
                stopmsg();
                delay(1400);digitalWrite(7, HIGH);
                autostopblink();
                goto xxx;
            }
        }*/
        if(digitalRead(5)!=1)//&&machine_direction == RIGHT)
        {delay(10);
        if(digitalRead(5)!=1)//&&machine_direction == RIGHT)
        {
            rightw();
            delay(151); // decide the run time angle 140==13.8 degree for distance between 2 holes
            stopmsg();
            delay(5); //for instant stop

```

```

    //digitalWrite(7, HIGH);
    //autostopblink();
    goto xxx;
}}
if(digitalRead(5)!=0)//&&machine_direction == RIGHT)
{
    //delay(10);
if(digitalRead(5)!=0)//&&machine_direction == RIGHT)
{
    //rightw();
    //delay(70);
    // decide the run time angle 70==13.8 degree for distance between 2 holes
    stopmsg();
    delay(5); //for instant stop
    //digitalWrite(7, HIGH);
    //autostopblink();
    goto xxx;
}}
}
}
/*void autoe()
{
    for (int i=0;i<5;i++)
        {
            digitalWrite(FLASH, 1);digitalWrite(13, 1);
            delay(200);
            digitalWrite(FLASH, 0);digitalWrite(13, 0);
            delay(80);
            digitalWrite(FLASH, 1);digitalWrite(13, 1);
            delay(200);
            digitalWrite(FLASH, 0);digitalWrite(13, 0);
            delay(80);}
}*/
void startbkink()
{
    digitalWrite(FLASH, 1);digitalWrite(13, 1);
    delay(600);
    digitalWrite(FLASH, 0);digitalWrite(13, 0);
}
void stopblink()
{
    digitalWrite(FLASH, 1);digitalWrite(13, 1);
    delay(100);
    digitalWrite(FLASH, 0);digitalWrite(13, 0);
    delay(80);
    digitalWrite(FLASH, 1);digitalWrite(13, 1);
    delay(500);
    digitalWrite(FLASH, 0);digitalWrite(13, 0);
}

```

```

    machine_running = false;
}
void autostopblink()
{
    for (int i=0;i<15;i++)
    {
        digitalWrite(FLASH, 1);digitalWrite(13, 1);
        delay(100);
        digitalWrite(FLASH, 0);digitalWrite(13, 0);
        delay(80);
        digitalWrite(FLASH, 1);digitalWrite(13, 1);
        delay(100);
        digitalWrite(FLASH, 0);digitalWrite(13, 0);
        delay(80);}
        digitalWrite(FLASH, 1);digitalWrite(13, 1);
        delay(400);
        digitalWrite(FLASH, 0);digitalWrite(13, 0);
        machine_running = false;
    }
}
void batteryvolt()
{
    value = analogRead(A7);
    vout = (value * 5.6) / 1024.0; // see text
    vin = vout / (R2/(R1+R2));
}
}
void startmsgleft()
{
    batteryvolt();
}
}
void startmsgright()
{
    batteryvolt();
}
}
void stopmsg()
{
    batteryvolt();
    machine_running = false;
    //delay(1000);
    Wire.beginTransmission(BRUSHCTRL);
    Wire.write("S");Wire.write(1);
    Wire.endTransmission();
    Wire.beginTransmission(DRIVECTRL);
    Wire.write("S");Wire.write(1);
    Wire.endTransmission();
    /*EEPROM.write(0,updated_seconds);
    EEPROM.write(1,updated_minutes);
    EEPROM.write(2,updated_hours1);
    EEPROM.write(3,updated_hours2);

```

```

EEPROM.put(10,meter1);
delay(50);*/
}

```

This program provides comprehensive control over a machine operation, including motor control, direction switching, battery voltage monitoring, and time tracking. It uses I2C communication to send commands, EEPROM to store state information, and timers/interrupts for precise timing control. The program is robust, ensuring the machine operates correctly under various conditions and stops safely when necessary.

## C. Program for rotary encoder sensor

### I. Motor program

```

//these pins can not be changed 2/3 are special pins
int encoderPin1 = 2;
int encoderPin2 = 3;
//white pin 2
//green pin 3
//red vcc
//black gnd
volatile int lastEncoded = 0;
volatile long encoderValue = 0;

long lastencoderValue = 0;
int lastMSB = 0;
int lastLSB = 0;
int m;

void setup() {
  Serial.begin (9600);

  pinMode(encoderPin1, INPUT);
  pinMode(encoderPin2, INPUT);
  digitalWrite(encoderPin1, HIGH); //turn pullup resistor on
  digitalWrite(encoderPin2, HIGH); //turn pullup resistor on

  //call updateEncoder() when any high/low changed seen
  //on interrupt 0 (pin 2), or interrupt 1 (pin 3)
  attachInterrupt(0, updateEncoder, CHANGE);
  attachInterrupt(1, updateEncoder, CHANGE);
}

void loop()
{
  //Do stuff here

```

```

updateEncoder();
if(encoderValue%500< 10 && encoderValue<50)
{
    m=1;//fail
}
else if (encoderValue%500< 10 && encoderValue>50)
{
    m=0; //successs
}
else
{
    m=1;//fail
}
Serial.print(encoderValue);
Serial.print(" , ");
Serial.println(m);
delay(10); //just here to slow down the output, and show it will work even
during a delay
}

```

```

void updateEncoder()
{
    int MSB = digitalRead(encoderPin1); //MSB = most significant bit
    int LSB = digitalRead(encoderPin2); //LSB = least significant bit
    int encoded = (MSB << 1) |LSB; //converting the 2 pin value to single number
    int sum = (lastEncoded << 2) | encoded; //adding it to the previous encoded
value
    if(sum == 0b1101 || sum == 0b0100 || sum == 0b0010 || sum == 0b1011)
encoderValue ++;
    if(sum == 0b1110 || sum == 0b0111 || sum == 0b0001 || sum == 0b1000)
encoderValue --;
    lastEncoded = encoded; //store this value for next time
}

```

## II. Main program with rotary encoder

```

#include <Wire.h>
#include <EEPROM.h>
#include <SPI.h> // include libraries
# define BRUSHCTRL 1
# define DRIVCTRL 2
#define PAYLOAD_SIZE 2
int spd=800; //previous 275
int spb=275; //Previous 800
#define FLASH 10
int count,countx,gap;
int p=0;
int q=0;

```

```

int spc;
char speedx = 'b';
float vout = 0.0;
float vin = 0.0;
float R1 = 92.5; // resistance of R1 (330K) -see text!
float R2 = 10; // resistance of R2 (10K) - see text!
int value = 0;
#define LEFT true
#define RIGHT false
boolean machine_direction = LEFT;
boolean machine_running = false;
const int timer_rst_time = 3100;
double distance;
float mtr=0;
float mtr1=0;
int seconds = 0;
int updated_minutes;
int updated_hours1;
int updated_hours2;
int updated_seconds;
int encoderPin1 = 2;
int encoderPin2 = 3;
volatile int lastEncoded = 0;
volatile long encoderValue = 0;
long lastencoderValue = 0;
int lastMSB = 0;
int lastLSB = 0;
int m;
unsigned long meter1;
unsigned long time;
int total_hours;
void setup() {
  Wire.begin();
  Serial.begin(9600);
  pinMode(FLASH, OUTPUT);
  pinMode(A3, INPUT);
  pinMode(A2, INPUT);
  //pinMode(5, INPUT_PULLUP);
  // pinMode(6, INPUT_PULLUP);
  // pinMode(10, INPUT);
  pinMode(7, OUTPUT);
  pinMode(13, OUTPUT);
  pinMode(encoderPin1, INPUT);
  pinMode(encoderPin2, INPUT);
  digitalWrite(encoderPin1, HIGH); //turn pullup resistor on
  digitalWrite(encoderPin2, HIGH); //turn pullup resistor on
  digitalWrite(7, LOW);
  attachInterrupt(0, updateEncoder, CHANGE);
}

```

```

    attachInterrupt(1, updateEncoder, CHANGE);
timer1_init();
updated_hours1 = EEPROM.read(3);
updated_hours1 = EEPROM.read(2);
updated_minutes = EEPROM.read(1);
updated_seconds = EEPROM.read(0);
    EEPROM.get(10,meter1);
seconds = 0;
    Serial.write(17);
    delay(100);
    Serial.write(24);
    delay(100);
    Serial.write(12);
    Serial.write("Pneumatic");
    delay(50);
    Serial.write(148);
    Serial.write("Planter");
for (int i=0;i<3;i++)
    {
        digitalWrite(FLASH, 1);digitalWrite(13, 1);
        delay(20);
        digitalWrite(FLASH, 0);digitalWrite(13,0);
        delay(20);
        digitalWrite(FLASH, 1);digitalWrite(13, 1);
        delay(20);
        digitalWrite(FLASH, 0);digitalWrite(13,0);
        delay(20);
    }
delay(1500);
    Serial.write(18);
    delay(10);
    Serial.write(21);
    machine_running = false;
    delay(200);
    Serial.write(17);
    delay(100);
    Serial.write(24);
    delay(100);
    Serial.write(12);;
int total_hours = updated_hours2 * 254 + updated_hours1;
meter1=meter1+((mtr+mtr1)*10);
    value = analogRead(A7);
    delay(200);
    value = analogRead(A7);
    vout = (value * 5.6) / 1024.0;
    vin = vout / (R2/(R1+R2));
for (int i=0;i<5;i++)
    {

```

```

    digitalWrite(FLASH, 1);digitalWrite(13, 1);
    delay(20);
    digitalWrite(FLASH, 0);digitalWrite(13, 0);
    delay(20);
    digitalWrite(FLASH, 1);digitalWrite(13, 1);
    delay(20);
    digitalWrite(FLASH, 0);digitalWrite(13, 0);
    delay(20);}
    delay(2500);
    Serial.write(18);
    delay(10);
    Serial.write(21);
}
void loop()
{
    digitalWrite(7, LOW);
    delay(50);
    autoswitch();
    updateEncoder();
    if(machine_running==false)
    {
        /*if(digitalRead(6)!=1&&machine_direction == LEFT)
        {
            while(digitalRead(6)!=1&&machine_direction == LEFT)
            {
                stopmsg();
                delay(1400);digitalWrite(7, HIGH);
                autostopblink();
                goto xxx;
            }
        }*/
        if(encoderValue%1000< 300 && encoderValue>300)//&&machine_direction
        == RIGHT)
        {delay(10);
        if(encoderValue%1000< 300 && encoderValue>300)//&&machine_direction
        == RIGHT)
        {
            rightw();
            delay(151); // decide the run time angle 140==13.8 degree for distance between
            2 holes
            stopmsg();
            delay(5); //for instant stop
            //digitalWrite(7, HIGH);
            //autostopblink();
            //goto xxx;
        }
    }

    //if we will talk about the circumference then we need to change the 500 value

```



```

//10000/circumference partition and that value will decide the change in 500
//according to machine calibration including machinery error we will change the
delay(151); value
//to avoid the continuous running of motor for single response we will decrease
the remainder value
if(encoderValue%1000< 300 && encoderValue<300)//&&machine_direction
== RIGHT)
{
if(encoderValue%1000< 300 && encoderValue<300)//&&machine_direction
== RIGHT)
{
//rightw();
//delay(70);
// decide the run time angle 70==13.8 degree for distance between 2 holes
stopmsg();
delay(5); //for instant stop
//digitalWrite(7, HIGH);
//autostopblink();
//goto xxx;
}}
else
{ //rightw();
//delay(70);
// decide the run time angle 70==13.8 degree for distance between 2 holes
stopmsg();
delay(5); //for instant stop
//digitalWrite(7, HIGH);
//autostopblink();
//goto xxx;
}
}
/* if (digitalRead(A2) !=1 && digitalRead(6) != 0 &&machine_running==false
)
{
delay(500);
if (digitalRead(A2) !=1 && digitalRead(6) != 0
&&machine_running==false)
{leftw();}}
if (digitalRead(A3)!=1 && digitalRead(5) != 0 &&machine_running==false)
{
delay(500);
if (digitalRead(A3)!=1 && digitalRead(5) != 0 &&machine_running==false)
{rightw();}}*/
if(machine_running==true)
{if(digitalRead(A2)!=1||digitalRead(A3) != 1 )
{
for(int i=0;i<=50;i++)

```

```

    {}
    if(digitalRead(A2)!=1||digitalRead(A3) != 1)
    {
        stopblink();
        stopmsg();
        machine_running==false;
        delay(1400);digitalWrite(7, HIGH);
    }}
}
int sec;
ISR(TIMER1_OVF_vect) {
    TCNT1 = timer_rst_time;
    if(machine_running == true)
    {
seconds++;
        if(seconds >15)
        {
            digitalWrite(FLASH, 1);digitalWrite(13, 1);
        }
        if(seconds >16)
        {
            digitalWrite(FLASH, 0);digitalWrite(13, 0);
            seconds=0;
        }
        updated_seconds++;
        if(updated_seconds>59)
        {
            updated_seconds =0;
            updated_minutes++;
            if(updated_minutes>59)
            {
                updated_minutes =0;
                updated_hours1++;
                if(updated_hours1 > 254)
                {
                    updated_hours1 = 0;
                    updated_hours2++;
                }
            }
        }
    }
}
//run any if logic here
}
}
void timer1_init() {
    noInterrupts();
    TCCR1A = 0;
    TCCR1B = 0;
    TCNT1 = timer_rst_time;
}

```

```

TCCR1B |= (1 << CS12);
TIMSK1 |= (1 << TOIE1);
sei();
}
void leftw()
{
    digitalWrite(7, LOW);
    startbkink();
    startmsgleft();
    delay(500);
    machine_direction = LEFT;
    machine_running = true;
    delay(50);
    Wire.beginTransmission(BRUSHCTRL);
    Wire.write("L");Wire.write(spb);
    Wire.endTransmission();;
    delay(1500);
    Wire.beginTransmission(DRIVECTRL);
    Wire.write("L");Wire.write(spd);
    Wire.endTransmission();
}
void rightw()
{
    //digitalWrite(7, LOW);
    //startbkink();
    //startmsgright();
    // delay(500);
    machine_direction = RIGHT;
    machine_running = true;
    delay(10);
    Wire.beginTransmission(BRUSHCTRL);
    Wire.write("R");Wire.write(spb);
    Wire.endTransmission();;
    //delay(1500);
    Wire.beginTransmission(DRIVECTRL);
    Wire.write("R");Wire.write(spd);
    Wire.endTransmission();;
}
void autoswitch()
{xxx:
    if(machine_running==false)
    {
        /*if(digitalRead(6)!=1&&machine_direction == LEFT)
        {
            while(digitalRead(6)!=1&&machine_direction == LEFT)
            {
                stopmsg();
                delay(1400);digitalWrite(7, HIGH);

```

```

    autostopblink();
    goto xxx;
}
}*/
/*if(digitalRead(5)!=1)//&&machine_direction == RIGHT)
{delay(10);
if(digitalRead(5)!=1)//&&machine_direction == RIGHT)
{
    rightw();
delay(151); // decide the run time angle 140==13.8 degree for distance between
2 holes
    stopmsg();
    delay(5); //for instant stop
    //digitalWrite(7, HIGH);
    //autostopblink();
    goto xxx;
}}*/
/*if(digitalRead(5)!=0)//&&machine_direction == RIGHT)
{
    //delay(10);
if(digitalRead(5)!=0)//&&machine_direction == RIGHT)
{
    //rightw();
    //delay(70);
    // decide the run time angle 70==13.8 degree for distance between 2 holes
    stopmsg();
    delay(5); //for instant stop
    //digitalWrite(7, HIGH);
    //autostopblink();
    goto xxx;
}}*/
}
}
}
/*void autoe()
{
    for (int i=0;i<5;i++)
    {
        digitalWrite(FLASH, 1);digitalWrite(13, 1);
        delay(200);
        digitalWrite(FLASH, 0);digitalWrite(13, 0);
        delay(80);
        digitalWrite(FLASH, 1);digitalWrite(13, 1);
        delay(200);
        digitalWrite(FLASH, 0);digitalWrite(13, 0);
        delay(80);}
}*/
void startbkink()
{

```

```

digitalWrite(FLASH, 1);digitalWrite(13, 1);
    delay(600);
    digitalWrite(FLASH, 0);digitalWrite(13, 0);
}
void stopblink()
{
digitalWrite(FLASH, 1);digitalWrite(13, 1);
    delay(100);
    digitalWrite(FLASH, 0);digitalWrite(13, 0);
    delay(80);
    digitalWrite(FLASH, 1);digitalWrite(13, 1);
    delay(500);
    digitalWrite(FLASH, 0);digitalWrite(13, 0);
    machine_running = false;
}
void autostopblink()
{
    for (int i=0;i<15;i++)
    {
        digitalWrite(FLASH, 1);digitalWrite(13, 1);
        delay(100);
        digitalWrite(FLASH, 0);digitalWrite(13, 0);
        delay(80);
        digitalWrite(FLASH, 1);digitalWrite(13, 1);
        delay(100);
        digitalWrite(FLASH, 0);digitalWrite(13, 0);
        delay(80);}
        digitalWrite(FLASH, 1);digitalWrite(13, 1);
        delay(400);
        digitalWrite(FLASH, 0);digitalWrite(13, 0);
        machine_running = false;
    }
}
void batteryvolt()
{
    value = analogRead(A7);
    vout = (value * 5.6) / 1024.0; // see text
    vin = vout / (R2/(R1+R2));
}
void startmsgleft()
{
    batteryvolt();
}
void startmsgright()
{
    batteryvolt();
}
void stopmsg()
{

```

```

batteryvolt();
machine_running = false;
//delay(1000);
Wire.beginTransmission(BRUSHCTRL);
Wire.write("S");Wire.write(1);
Wire.endTransmission();
Wire.beginTransmission(DRIVECTRL);
Wire.write("S");Wire.write(1);
Wire.endTransmission();
/*EEPROM.write(0,updated_seconds);
EEPROM.write(1,updated_minutes);
EEPROM.write(2,updated_hours1);
EEPROM.write(3,updated_hours2);
EEPROM.put(10,meter1);
delay(50);*/
}
void updateEncoder()
{
int MSB = digitalRead(encoderPin1); //MSB = most significant bit
int LSB = digitalRead(encoderPin2); //LSB = least significant bit
int encoded = (MSB << 1) |LSB; //converting the 2 pin value to single number
int sum = (lastEncoded << 2) | encoded; //adding it to the previous encoded
value
if(sum == 0b1101 || sum == 0b0100 || sum == 0b0010 || sum == 0b1011)
encoderValue ++;
if(sum == 0b1110 || sum == 0b0111 || sum == 0b0001 || sum == 0b1000)
encoderValue --;
lastEncoded = encoded; //store this value for next time
}

```

**TRACTOR OPERATED PNEUMATIC NO-TILL PULSE PLANTER  
WITH ELECTRONIC CONTROL SYSTEM**

*by*

**Amit Kumar  
(2020-28-005)**

**ABSTRACT**

**Submitted in partial fulfilment of the  
requirements for the degree of**

**DOCTOR OF PHILOSOPHY**

**IN**

**AGRICULTURAL ENGINEERING**

**(Farm Machinery and Power Engineering)**

**Faculty of Agricultural Engineering and Technology**

**Kerala Agricultural University**



**DEPARTMENT OF FARM MACHINERY AND POWER ENGINEERING**

**KELAPPAJI COLLEGE OF AGRICULTURAL ENGINEERING AND**

**FOOD TECHNOLOGY, TAVANUR - 679 573**

**KERALA, INDIA**

**2024**





## ABSTRACT

Addressing the global population surge expected to reach 10.4 billion by the mid-2080s, especially in densely populated regions like India, poses significant agricultural challenges. Integrating pulses into sustainable agriculture is crucial for food security due to their benefits in enhancing soil fertility and resilient ecosystems. This study focuses on developing a tractor operated pneumatic no-till pulse planter with electronic control system for black gram and horse gram, essential pulses in Kerala. Traditional planting methods are labor-intensive, inefficient and costly. The proposed planter ensures accurate seed placement, uniform emergence, and minimal soil disturbance. An electronic control system enhances precision in seed spacing placement and improves overall efficiency.

The objectives of the study include determining seed properties, developing planter with electronic control system, and evaluating the planter performance. A vacuum disc-type metering mechanism was chosen for its precision in seed singulation, minimal damage, and adaptability to various seed sizes and shapes. The investigation included laboratory experiments for seed metering mechanisms, calibration, testing, and field performance evaluation of the pneumatic planter for the black gram (VBN-6) and horse gram (KS-2) seeds. Optimal settings for vacuum pressure, plate hole size, forward speed, and the location of sensors were identified through extensive trials and statistical analysis. The study observed that black gram seeds have a length of 2.32-3.88 mm, width of 1.99-3.65 mm, and thickness of 1.56-2.07 mm, whereas horse gram seeds are larger, with a length of 6.02-6.27 mm, width of 4.10-4.35 mm, and thickness of 2.16-2.45 mm. The mean diameter of black gram seeds is 2.62 mm, and for horse gram, it is 4.22 mm. The optimum terminal velocity is  $8.21 \text{ m s}^{-1}$  for black gram and  $8.68 \text{ m s}^{-1}$  for horse gram. The pneumatic planter uses a vacuum disc-type precision seed metering mechanism with a vertically oriented rotating disc and an aspirator blower to ensure precise seed placement. The planter was modified using electronically controlled system using a stepper motor, which was regulated by a microcontroller for precise seed plate rotation. The electronic system includes a stepper motor, rotary encoder, proximity sensor, Arduino Nano microcontroller, vacuum pressure sensor, micro-step drive, battery, and protective enclosure. The proximity sensor detects wheel spokes, the rotary encoder provides speed and position feedback, and the vacuum sensor activates the system under optimal conditions.

Laboratory experimental results on the pneumatic seed metering mechanism for black gram and horse gram showed optimal seed spacing and reduced miss and multiple indices with specific settings. The use of encoder sensor ensured the required spacing of 15.0 cm with a lower miss index of 1-3 percent compared to the proximity sensor. Smaller hole sizes and higher vacuum pressures improved seed placement accuracy. The optimal spacing for horse gram was achieved with a 2.1 mm hole size, 4.0 kPa vacuum pressure, and 1.0 km h<sup>-1</sup> speed, resulted the required spacing of 9.2-12.9 cm and with the lower miss index of 0.5 percent with encoder sensor. Encoder sensor, forward speed of 2 km h<sup>-1</sup> and vacuum pressure of 4 kPa were selected for field evaluation. Field evaluation of a pneumatic planter with electronic controls for black gram and horse gram assessed impact with different type of furrow opener and locations of the encoder. When the location of encoder on steel wheel with shoe type furrow opener was used a spacing of 14.8 cm was obtained a consistent miss index of 1.2 percent for black gram. The encoder on the steel wheel lowered the multiple index to 2.5-2.7 percent and improved quality of feed index from 96-96.2 percent for black gram. Similar type of result showed with horse gram. The location of the encoder on the steel wheel showed better results compared to its location on the pneumatic wheel due to reduced slippage. Inverted t-type furrow opener work well in no-till field. Germination rates were optimal at 95-96 percent in both black and horse gram. The study recommended the location of encoder on steel wheel with shoe-type furrow opener showed best performance. The field capacity and field efficiency of planter was 0.25 ha h<sup>-1</sup> and 90 percent respectively.

The total cost of the developed planter with electronic control system was ₹1,80,000. The pneumatic planter with electronic controls incurred an operating cost as ₹860.55 per hour and ₹3072 per hectare. As per the prevailing wage rates, the cost for manual sowing is ₹4054 per hectare, the planter saved ₹982 per hectare. Hence, the 24 percent saving in cost of operation is found out ensured by using this developed planter. Break-even point of 79.22 hours per year and a payback period of 1.13 years are expected. It is concluded that the pneumatic planter with electronic control significantly improves planting performance for black gram and horse gram by ensuring precise seed placement, reducing misses and multiples, and enhancing quality and precision indices. Economic analysis confirms its cost-effectiveness and potential to increase crop productivity and profitability for farmers.